THESE

Présentée pour obtenir le titre de

DOCTEUR DE L'UNIVERSITE LOUIS PASTEUR DE STRASBOURG

(Option Physico-Chimie Macromoléculaire)

par

Isabelle COUILLET

PROPRIETES DYNAMIQUES EN MILIEU AQUEUX DE SYSTEMES MIXTES MICELLES VERMICULAIRES-POLYMERES ASSOCIATIFS D'ORIGINE NATURELLE

*Soutenue le **7 Novembre 2005** devant la Commission d'Examen:*

Mme Annie Audibert-Hayet	Invitée
Mme Françoise Candau	Directeur de thèse
M. Georges Hadzioannou	Rapporteur
M. Trevor Hughes	Examinateur
M. Geoffrey Maitland	Co-Directeur de thèse
M. Lennart Piculell	Rapporteur
M. Brian Vincent	Rapporteur

REMERCIEMENTS

Je souhaiterais tout d'abord remercier le Centre de Recherche de Schlumberger à Cambridge ainsi que l'Institut Charles Sadron à Strasbourg pour m'avoir permis de réaliser ce travail. A cet égard, j'aimerais tout particulièrement remercier Monsieur Geoffrey Maitland, Professeur à Imperial College - Londres, pour m'avoir accordé sa confiance et apporté son soutien. Je souhaiterais également remercier Monsieur Jean-Claude Wittman, Directeur de l'Institut Charles Sadron, pour avoir accepté cette collaboration.

Je tiens à remercier vivement Madame Françoise Candau, Directeur de Recherche émérite au CNRS de Strasbourg, pour m'avoir dirigée tout au long de ces trois dernières années: ses conseils, sa disponibilité, son soutien constant m'ont permis d'accomplir cette thèse dans d'excellentes conditions.

Je remercie également Monsieur Jean Candau, Directeur de Recherche émérite au CNRS de Strasbourg, pour l'aide précieuse qu'il m'a apportée dans le domaine des surfactants.

Merci à Monsieur Trevor Hughes, Programme Manager au centre de Recherche Schlumberger Cambridge, pour l'aide permanente qu'il m'a prodiguée tout au long de ces années.

Je remercie Mme Annie Audibert-Hayet, Chef de Projets à l'Institut Français du Pétrole, Mme Françoise Candau, M. Georges Hadzioannou, Professeur et Directeur de l'ECPM, M. Trevor Hughes, M. Geoffrey Maitland, M. Lennart Piculell, Professeur à l'Université de Lund, et M. Brian Vincent, Professeur à l'Université de Bristol, d'avoir accepté de participer au jury de cette thèse.

Je voudrais remercier différents membres du centre de Recherche de Schlumberger, M. Sla Kefi, M. Gerry Meeten, M. Edo Boek, M. Carlos Abad, et de l'Institut Charles Sadron, M. Joseph Selb, Mme. Nicole Benoit, pour leurs aides scientifiques.

A tous ceux qui sont intervenus à un moment ou un autre dans le déroulement de cette thèse, j'adresse mes plus vifs remerciements. Philippe, Jian, merci de m'avoir convaincue de l'enrichissement que pourrait m'apporter l'aboutissement d'un tel projet. Gerry, je ne pouvais tomber sur plus agréable « office mate ». Merci à Loic, Sandra, Hedwige, Maddalena, Paolo, Benoît, Marco, Christian et mes amis en France, pour tous les bons moments passés. Merci à mes parents pour leur soutien moral, à ma sœur Séverine pour ses nombreux conseils. Gwen, merci de m'avoir supportée. David, merci d'avoir été là durant ces 3 années. Ma plus grande reconnaissance va à Valérie (« Suitcase »); ton aide, ton écoute, ta patience, et ton enthousiasme, m'ont énormément apporté.

RESUME

La fracturation hydraulique fait partie des méthodes permettant l'amélioration de la production des gisements pétroliers. Le procédé de fracturation hydraulique consiste à injecter un fluide visqueux dans le puits producteur. La forte pression engendrée par le pompage du fluide provoque la fracture de la roche et sa propagation dans la roche réservoir. Les propriétés viscoélastiques du fluide jouent un rôle fondamental; elles permettent le maintien en suspension du sable, dont le rôle est de maintenir la fracture ouverte quand la pression de pompage est arrêtée. Les propriétés du fluide doivent aussi lui permettre de limiter son infiltration dans la roche et de ne pas endommager sa perméabilité qui conduirait à une diminution de la productivité. Enfin, la température du réservoir ne doit pas altérer ses propriétés.

Les fluides de fracturation à base de polymères hydrosolubles sont aujourd'hui les fluides les plus utilisés du fait de leur coût modéré et de leur faible tendance à s'infiltrer dans la roche. Cependant ils présentent le désavantage, de par leur structure, d'endommager la perméabilité de la roche. Récemment, l'industrie pétrolière s'est intéressée à des fluides à base de tensioactif, car leurs changements de structure au contact de l'huile empêchent toute altération de la perméabilité. Cependant ces fluides s'infiltrent dans la roche beaucoup plus aisément qu'un polymère classique, perdent leurs propriétés rhéologiques avec la température et sont plus onéreux.

L'objectif de ce travail était de développer des gels aqueux viscoélastiques à base de polymères hydrophobiquement modifiés et de tensioactifs afin de combiner leurs avantages respectifs. Sous certaines conditions, les micelles de tensioactifs peuvent interagir avec les chaînes hydrophobes de polymères et conduire à des mélanges de viscosité élevée. Le réseau de polymères et de tensioactifs est détruit au contact de l'huile, pour conduire à un fluide de faible viscosité, ayant une faible aptitude à former une émulsion, ce qui limite l'endommagement de la perméabilité de la roche. De plus, ces fluides s'infiltrent beaucoup plus difficilement dans la roche du fait de la présence de polymères.

Afin de développer et d'optimiser la formulation de tels fluides, nous devions acquérir une meilleure compréhension, à l'échelle moléculaire, des interactions qui s'exercent entre les chaînes hydrophobes de polymères et les micelles de tensioactifs ainsi que de la structure du réseau formé par ces deux composants. Nous avons pour cela étudié dans un premier temps les propriétés rhéologiques linéaires et non linéaires de chacun des composants du mélange en fonction de la température et de la concentration avant d'analyser les propriétés rhéologiques des mélanges.

PROPRIETES STRUCTURALES ET DYNAMIQUES DE L'ERUCYL BIS-(HYDROXYETHYL)METHYLAMMONIUM CHLORIDE

Nous avons étudié les propriétés structurales et dynamiques d'un tensioactif cationique possédant une longue chaîne alkyle (C_{22}) mono-saturée, l'erucyl bis(hydroxyethyl)methylammonium chloride (EHAC). Dans des conditions appropriées de salinité et de concentration, ce tensioactif s'autoassemble en solution aqueuse pour former des micelles cylindriques géantes, ce qui confère à la solution une viscoélasticité marquée. Nous avons analysé le comportement rhéologique de ces systèmes en fonction de la température et de la concentration en présence de chlorure de potassium. Nous avons également réalisé une étude structurale par diffusion de lumière.

L'étude de la variation de la viscosité à gradient de vitesse nul de solutions aqueuses de EHAC en fonction de la concentration nous a permis de mettre en évidence l'existence de deux régimes délimités par la concentration de recouvrement des micelles vermiculaires C^* : le régime dilué où les chaînes micellaires sont isolées et la viscosité de la solution comparable à celle de l'eau ; le régime semi-dilué où les chaînes micellaires croissent continûment, se recouvrent et s'enchevêtrent. Nous observons en régime semi-dilué le comportement rhéologique en loi de puissance de la viscosité en fonction de la concentration prédit par les modèles théoriques. Nous avons également étudié la variation de C^* en fonction de divers paramètres tels que l'ajout d'isopropanol, la concentration en sel, et la température.

L’étude des propriétés viscoélastiques en régime linéaire a permis de déterminer selon trois méthodes différentes l’énergie de scission des micelles vermiculaires d'EHAC. Pour la première fois, tous les paramètres caractéristiques du spectre fréquenciel du module de cisaillement complexe ont été utilisés pour calculer cette énergie. La valeur obtenue s’est avérée élevée comparativement à d’autres tensioactifs classiques, ce qui explique la forte viscosité des solutions d'EHAC du fait de la formation de très longues micelles. L’existence d’un terme entropique dans l’énergie libre de scission, associé au réarrangement des contre-ions lors de la formation de bouts de chaînes hémisphériques est susceptible de rendre compte de la valeur de l’énergie libre calculée.

Nous avons réalisé une étude par diffusion statique de la lumière de solutions d'EHAC. Nous avons retrouvé qualitativement pour le rayon de giration et l'intensité diffusée les variations avec la concentration caractéristiques des régimes dilué et semi-dilué. Cependant, dans le régime dilué au voisinage de C^*, des déviations sont observées par rapport aux modèles théoriques avec en particulier la présence de larges agrégats de taille >100nm. Ce résultat a été confirmé par des expériences de diffusion dynamique de la lumière.

COMPARAISON DES PROPRIETES RHEOLOGIQUES DE POLYMERES MODIFIES HYDROPHOBIQUEMENT ET DE LEURS ANALOGUES NON MODIFIES.

Nous avons analysé le comportement rhéologique de solutions de polymères associatifs ayant un précurseur d’origine naturelle, l’hydroxypropyle guar hydrophobisé par une chaîne alkyle C_{22} (hm-HPG), et le chitosane hydrophobisé par une chaîne alkyle C_{10} (hm-chitosane), en présence de chlorure de potassium, dans un domaine de concentrations allant de 0.001 à 3% en poids selon les échantillons. Nous avons étudié l’influence de différents paramètres tels que la concentration en polymère, la teneur en groupes hydrophobes et la température, sur les propriétés rhéologiques de ces solutions.

Les courbes d’écoulement ont montré la présence d’un plateau newtonien dans le régime de bas cisaillement et un caractère rhéofluidifiant plus ou moins marqué selon la

concentration de la solution de polymère au-delà d'une valeur critique de la vitesse de cisaillement. Nous avons analysé la variation de cette valeur critique en fonction de la concentration en polymère, de la teneur en groupes hydrophobes et de la température. L'inverse de cette valeur correspondant au temps de relaxation terminal, de nombreuses conclusions ont pu être apportées concernant la dynamique des différents systèmes. La comparaison entre les comportements viscosimétriques des polymères modifiés hydrophobiquement et de ceux de leurs homologues linéaires révèle une diminution du nombre et/ou du temps de vie des associations intermoléculaires lorsque l'on augmente la température.

Les courbes représentatives de la variation de la viscosité en fonction de la contrainte de cisaillement ont permis d'identifier la contrainte à laquelle on observe la rupture des associations des chaînes hydrophobes ainsi que le temps de vie des associations. Nous avons étudié leurs variations en fonction de la température et de la concentration.

La variation de la viscosité du chitosane à gradient de vitesse nul en fonction de la concentration a montré un comportement différent de celui observé avec l'hydroxypropyle guar. La valeur anormalement haute de l'exposant reliant ces deux variables est due à la présence d'interactions intermoléculaires spécifiques entre les chaînes de polymères.

SYNERGIE ENTRE POLYMERES MODIFIES HYDROPHOBIQUEMENT ET TENSIOACTIFS

Nous avons étudié le comportement rhéologique de mélanges de hm-HPG ou de hm-chitosane et d'EHAC, à différentes compositions et températures.

L'addition du tensioactif à la solution de polymère ou inversement, entraîne une augmentation importante de la viscosité. Cet effet s'observe dès que les concentrations du polymère associatif et du tensioactif avoisinent leurs C^* respectifs, ce qui révèle une très grande synergie entre ces deux composants. Ce résultat s'observe dans tout le domaine de gradients étudiés ($\leq 100 s^{-1}$) et pour des températures comprises entre 20°C et 80ºC. La

synergie diminue, et peut même disparaître, aux concentrations et aux températures élevées.

Après avoir délimité le domaine de concentrations donnant lieu à une synergie optimale entre les deux composants, nous avons réalisé une étude complète à une concentration globale du mélange se situant dans ce domaine. Nous avons étudié les propriétés viscoélastiques en régime linéaire du mélange pour différents rapports polymère/tensioactif. Dans le domaine des basses fréquences, le comportement des modules de conservation et de perte suit le modèle de Maxwell. Dans le domaine des hautes fréquences, on observe une déviation par rapport à ce modèle avec un minimum de la valeur du module de perte à une fréquence ω_m. Nous avons étudié les variations du temps de relaxation terminal (défini par l'inverse de la fréquence à laquelle les modules de conservation et de perte se croisent), du module plateau et de la viscosité à gradient nul, en fonction de la composition du mélange. Le temps de relaxation terminal ainsi que le plateau module présentent un maximum pour une certaine composition du mélange qui est celle pour laquelle on observe également un minimum de la fréquence ω_m. Ces résultats permettent de déterminer les domaines de concentration et de composition pour lesquels il existe une forte synergie entre le polymère associatif et le tensioactif.

L'étude des propriétés rhéologiques en régime linéaire et non linéaire de mélanges de hm-HPG ou de hm-chitosane et d'EHAC, a permis de démontrer que la forte synergie observée pour une certaine composition du mélange provenait d'une augmentation du temps de vie des interactions entre les chaînes de polymères et de tensioactifs.

Les courbes d'écoulement obtenues pour la plupart des mélanges ont montré un comportement complexe suggérant des réarrangements successifs du réseau mixte transitoire de polymères associatifs et de micelles.

L'étude comparée des propriétés rhéologiques des deux systèmes, EHAC/hm-HPG et EHAC/hm-chitosane, a permis de généraliser les effets de synergie qui existent dans les mélanges de polymères hydrophobiquement modifiés et de micelles géantes. L'effet de synergie observé entre l'EHAC et le hm-chitosane, dont le poids moléculaire est inférieur a celui du hm-HPG, est plus important que celui obtenu avec le hm-HPG. Cependant,

pour la même viscosité, la concentration totale du mélange à base de hm-chitosane est supérieure à celle à base de hm-HPG. Ces résultats sont importants du point de vue des applications. Ils montrent qu'il est nécessaire de trouver le meilleur choix entre un polymère de haut poids moléculaire qui altère la perméabilité de la roche, et un polymère de poids moléculaire inférieur, moins endommageant, mais nécessitant des concentrations plus importantes pour obtenir la même viscosité et donc plus onéreux.

De nombreuses questions subsistent sur les propriétés fondamentales des mélanges de polymères hydrophobiquement modifiés et de micelles géantes. Le schéma proposé permettant d'expliquer le comportement rhéologique de ces mélanges demeure qualitatif et un modèle quantitatif décrivant leur écoulement fait encore défaut. Des méthodes de visualisation telles que la diffusion des neutrons et la microscopie électronique à transmission (cryoTEM) pourraient apporter des informations complémentaires sur la structure de ces mélanges.

Ce travail représente un point de départ pour l'étude des comportements de mélanges à base de polymères associatifs et de micelles géantes. L'influence de nombreux paramètres reste encore à explorer afin d'approfondir la compréhension du mécanisme des interactions. En particulier, la longueur, la distribution et la concentration des chaînes hydrophobes doivent jouer un rôle important. Du point de vue des applications, les mélanges de polymères hydrophobiquement modifiés et de micelles géantes ont montré des avantages certains, comparativement aux systèmes à base uniquement de polymères ou de tensioactifs et de nombreuses options restent ouvertes afin d'optimiser les propriétés de ces fluides complexes.

TABLE OF CONTENTS

Chapter I

POLYMER-LIKE SOLUTIONS
"CONVENTIONAL" POLYMERS, ASSOCIATING POLYMERS, WORMLIKE MICELLES

Chapter II

STRUCTURAL AND DYNAMIC PROPERTIES OF ERUCYL BIS-(HYDROXYETHYL)METHYLAMMONIUM CHLORIDE

Chapter III

SYNERGISTIC EFFECTS IN 0.4M KCl SOLUTIONS OF HYDROPHOBICALLY MODIFIED HYDROXYPROPYL GUAR/ ERUCYL BIS-(HYDROXYETHYL)METHYLAMMONIUM CHLORIDE MIXTURES

Chapter IV

SYNERGISTIC EFFECTS IN 0.4M KCl SOLUTIONS OF HYDROPHOBICALLY MODIFIED CHITOSAN/ ERUCYL BIS-(HYDROXYETHYL)METHYLAMMONIUM CHLORIDE MIXTURES

LIST OF SYMBOLS

a: size of a monomer.

$\boldsymbol{A_o}$: surface area occupied by the surfactant headgroup.

c(L): number density of elongated micelles of length *L*.

d: tube diameter

D: diffusion constant of the chain in real space.

D': curvilinear diffusion constant of a polymeric chain along its own contour.

$\boldsymbol{D_0}$: mobility constant.

$\boldsymbol{E_{sciss}}$**:** scission energy.

***F*:** total free energy per unit volume of micellar solution.

$\boldsymbol{G_0}$**:** plateau modulus.

***[H]*:** hydrophobic content.

***k*:** temperature-dependent rate constant.

k_H **:** Huggins coefficient.

$\boldsymbol{k_B}$: Boltzmann constant.

$\boldsymbol{l_p}$: length of a statistical unit, persistence length.

ℓ_e: entanglement length.

L: overall polymer chain length.

$\boldsymbol{L_H}$**:** extended length of the hydrophobic part of a surfactant.

$\overline{L}$: mean micellar length.

N: number of monomers in a polymeric chain.

$\tilde{N}$: number of statistical units per polymeric chain.

$\boldsymbol{N_H}$ **:** hydrophobic bloc length.

$\boldsymbol{N_e}$**:** number of monomers in an entanglement strand.

$\boldsymbol{N_s}$: average number of monomers along the chain between stickers.

p: average fraction of closed stickers.

P: packing parameter.

$\boldsymbol{R_G}$ **:** radius of gyration.

$\boldsymbol{S_c}$**:** section of the polymer chain.

S: number of stickers attached to a polymeric chain.

T_R**:** terminal relaxation time.

V: volume of the surfactant hydrophobic part.

V_0**:** excluded volume parameter.

ω_m**:** frequency corresponding to the minimum of G''.

χ **:** Flory's interaction parameter.

ϕ^***:** overlap volume fraction.

ϕ_e**:** entanglement volume fraction.

ϕ_η**:** overlap volume fraction of associating polymer.

ϕ_T**:** entanglement volume fraction of associating polymer.

η_s **:** viscosity of the solvent.

$[\eta]$ **:** intrinsic viscosity.

ξ**:** correlation length.

τ**:** average life-time of a sticker in the associated state.

τ_b**:** micellar breaking time.

τ_{rep}: reptation time.

τ_e**:** Rouse time.

τ_0**:** microscopic time.

$\mu(t)$**:** stress relaxation function.

$\sigma(t)$**:** time-dependent stress relaxation.

σ_c: *critical* shear stress

γ_0**:** step shear strain applied at time t=0.

$\dot{\gamma}$: shear rate

$\dot{\gamma}_c$: critical shear rate

GENERAL INTRODUCTION

The hydraulic fracturing of subterranean formations is a method used to increase oil recovery of low permeability natural hydrocarbons reservoirs by providing flow channels through the formation. These flow channels facilitate movement of the hydrocarbons to the wellbore so that the hydrocarbons may be pumped from the well. In such operations, a fracturing fluid is injected at very high rate into a wellbore penetrating the subterranean formation that is forced to crack and fracture. A proppant (sand or similar component) carried by the viscous fracturing fluid, is placed in the fracture to prevent its complete closure when the flow is reversed and maintain improved flow for the oil into the wellbore. So the fracturing fluid should have the ability to keep proppant in suspension during its tortuous path down the well, out through the perforations and to the end, or tip, of the fracture. This ability mainly depends on its viscosity. It should also be able to degrade after the fracture closes so as not to leave residual material in the formation or the proppant-filled fracture that will damage its permeability. This is referred as the fluid "clean-up" property. Finally, it should have the ability not to enter too easily the pore throats of the formation and so to have a limited "leak-off" or filtration rate.

Fracturing fluids have evolved significantly since the first fracture stimulation was performed in 1947[1]. Early stimulation treatments used surplus napalm added to gasoline to create a viscous fluid capable of initiating and propagating a fracture. Later on, engineers began pumping guar and guar derivatives based fluids. As fracturing grew in popularity, wells were being drilled deeper and hotter formations were encountered. So there was an increasing need for fluid viscosities greater than those offered by linear (non-crosslinked) gels. To attain sufficient viscosity and increased thermal stability in higher temperature reservoirs, linear gels were crosslinked with borate, zirconate or titanate ions. In the 1980s, foamed fracturing fluids grew more popular as engineers became more aware of the permeability damage caused by polymeric fluids. The use of foams decreased the amount of guar introduced into the fracture, thereby reducing the amount of residue and, hence, the extent of damage. In a foam fluid, the gas phase typically occupies more than half of the total fluid volume, so less liquid, and hence less guar, is pumped into the well. Foams also enhance clean-up after a fracturing treatment. The liquid volume is lower, and the entrained gas offers significantly more energy to

evacuate the fracturing fluid from the well. The quest for cleaner fluids continued into the 1990s, when advanced chemical breakers and lower polymer concentration became effective tools for reducing and limiting damage from guar.

The next evolution was the development of a "polymer-free" aqueous fracturing fluid. This fluid is different from guar or hydroxyethyl cellulose fluid systems; rather, it belongs to a new class of fracturing fluids, viscoelastic fluids based on surfactant, generally called "viscoelastic surfactant systems" (VES). The principal advantages of the VES approach are:

1. Simpler operation and field preparation: there is no need for polymer prehydration, no need for crosslinkers or breakers.
2. Improved fracture clean-up relative to the polymer-based systems. This is facilitated by the responsive nature of the VES-based fluids in that their worm-like micellar structure is broken on contact/mixing with produced hydrocarbon fluids, resulting in a low viscosity fluid and by the absence of any high molecular weight polymer which for polymeric-based fluids is retained and concentrated in the formation.

However, the current VES-based fracturing fluids have several limitations:

1. The cost of VES fluids is generally higher than the conventional polymer-based fluids. This is due both to the independent unit cost and the higher concentration of the components. The cost differential becomes considerable as the required VES dosage increases with temperature.
2. Unfavorable interactions with certain produced hydrocarbons. Compatibility issues with certain crude oil compositions lead to the formation of stable emulsions which may hinder clean up, particularly in the invaded matrix zone.
3. Health and safety (HSE) concerns: there is limited HSE acceptance of certain VES fluids in offshore oilfields, e.g. the North Sea.
4. The higher leak-off rate observed for VES systems (relative to polymeric fluids) restricts applications to reservoirs with low range permeability (<10mD).

An alternative approach has been to consider a fracturing fluid based on a blend of hydrophobically modified polymer (hm-polymer) and viscoelastic surfactant (VES), since this fluid is also responsive to hydrocarbons[2]. The responsivity of the fluid is due to

the hydrophobic interactions that are created between the hm-polymer and the VES, which can be broken by contact with oil. The fluid can reach appropriate rheology for fracture generation/propagation and proppant transport using a lower concentration of VES and polymer compared, respectively, to the pure VES-based fluid and the pure polymeric fluid. The polymer/surfactant network is broken by contact with hydrocarbon and the resultant mixture has a low tendency to form an emulsion. This explains the enhanced fluid clean-up from the invaded matrix zones. Moreover, the hm-polymer/VES blends should have a reduced leak-off rate as compared to pure VES fluids due to the presence of the polymer.

In order to develop and optimize such fluids, it is necessary to develop an in-depth understanding, at the molecular level, of the interactions between the hydrophobic groups on the polymer and the surfactant micelles, and of the blend structure in terms of the arrangement of the hm-polymer and VES networks. This understanding was the key point of this study and was achieved by first looking at the structural and dynamic properties of the individual components of the mixture before moving on to study the mixture properties.

Many studies on the interactions between surfactants and hydrophobically modified polymer have been reported[3-6]. They generally concern systems in which the surfactant concentration is close to the critical micellar concentration (CMC). Under these conditions, one observes an enhancement of the zero-shear viscosity due either to the formation of additional mixed plurifunctional aggregates or to an increase in the lifetime of the pre-existing crosslinks resulting from surfactant binding[7-17]. The first reported study on the rheological properties of mixtures of wormlike micelles and hydrophobically modified polymers focused on mixtures of cetyl trimethylammonium bromide (CTAB) and hm-hydroxyethylcellulose (with C_{12} and C_{16} hydrophobic substitution) or hm-polyacrylamide (with C_{12} hydrophobic substitution) in the presence of KBr[15]. Very recently, two others studies were published on the interaction between hm-polymers and VES or vesicles[18,19].

Water-soluble hydrophobically modified polysaccharide derivatives are commonly used as thickening and rheology-control agents in aqueous systems[20-23]. The specific rheological behaviour of such polymeric systems arises from their ability to give rise to weak intra- and inter-molecular interactions between the hydrophobic groups distributed along the polymer chains. In the semi-dilute entangled regime, which is the domain of interest for most industrial applications, the hydrophobic moieties build up a transitory tridimensional network interpenetrated with the entanglement network. Aqueous solutions of guar and its derivatives are the most widely used hydraulic fracturing fluids for hydrocarbon recovery from subterranean formations, mainly for economical reasons[7,24,25], and so was the polymer chosen for our study.

Under appropriate conditions (salinity, temperature, concentration, presence of counterions), surfactants molecules can self-assemble into long, flexible cylindrical structures, referred to as wormlike micelles. If the scission energy of a micelle (the energy required to create two end-caps from a semi-infinite cylinder) is large enough, then the semi-flexible linear micelles may become very long (several microns) and, similar to polymers, can form entangled networks in semi-dilute solutions, giving rise to highly viscoelastic fluids. Cationic surfactants with long mono-unsaturated tails (C_{22}) have been shown to be efficient fracturing fluids[26]. In particular, aqueous solutions of erucyl bis (hydroxyethyl) methyl ammonium chloride (EHAC) exhibit appropriate viscosities up to high temperatures (80°C)[27-29]. Consequently, this was the surfactant chosen for the study.

The analogy between wormlike micelles and polymers is a subject of debate; many similarities in the rheology and dynamics of the systems have been noted and are reported in the first chapter, which gives a general summary of the underlying chemistry and physics.

In the second chapter, we investigated the structural and dynamic properties of micellar solutions of the erucyl bis-(hydroxyethyl)methylammonium chloride (EHAC) surfactant mentioned above, blended with 2-propanol, in the presence of KCl, using light scattering and rheological experimental techniques. The results, that are reported in a published

paper[28], bring new information on the micellar growth induced by an increase of surfactant concentration and on the viscoelastic behaviour of wormlike micellar systems. The enthalpic part of the scission energy, in the semi-dilute regime, was determined through rheological measurements using three independent methods.

In the third chapter, we investigated the linear and non-linear rheological properties of aqueous solutions containing both the EHAC surfactant studied in the previous chapter, and the hydrophobically modified hydroxypropyl guar (hm-HPG). Results have been reported in a published paper[30]. The first part of the chapter presents a comparison of the flow behaviour of hydroxypropyl guar (HPG) and its hydrophobically modified analogue (hm-HPG) in the presence of salt and at various temperatures. These conditions are of primary importance in oil recovery processes. In the second part of the paper, a study is reported of the synergistic effects occurring in the viscoelastic behaviour of mixtures of aqueous solutions of EHAC surfactant and hm-HPG polymer in a concentration domain from 0.01wt% to 2.5wt% in the presence of 0.4M KCl and over a temperature range from 25°C to 80°C. Possible structures and models consistent with the reported results are also considered.

Finally, in the last chapter, we have generalised the synergistic effects observed between hm-HPG and EHAC surfactant by studying the linear and non-linear rheological properties of aqueous solutions of another hm-polymer, hydrophobically modified chitosan (hm-chitosan), and EHAC surfactant. A hm-chitosan with a lower molecular weight than the hm-HPG was chosen on purpose in order to study the effect of polymer molecular weight on the synergistic effects. This is an important issue from an applications point of view as it is thought that a low molecular weight polymer is required to limit the formation damage.

The thesis ends with a summary of the main conclusions and recommendations for further study.

REFERENCES

(1) Chase, B.; Chmilowski, W.; Marcinew, R.; Mitchell, C.; Dang, Y.; Krauss, K.; Nelson, E.; Lantz, T.; Parham, C.; Plummer, J. *Oilfield Review*, Autumn, **1997**, p.20.

(2) Couillet, I.; Hughes, T., GB Patent 2 383 355, **2003**; WO Patent 3 056 130, **2003**.

(3) *Interactions of Surfactants with Polymers and Proteins*, Eds.: Goddard, E.D.; Ananthapadmanabhan, K. P.; CRC Press, Boca Raton, FL **1993**.

(4) Hansson, P.; Lindman, B. *Curr. Opin. Colloid Interface Sci.* **1996**, *1*, 604.

(5) Winnik, F. M.; Regismond, S. T. A. *Colloids Surf. A, Physicochem. Eng. Aspects* **1996**, *118*, 1.

(6) *Polymers-Surfactants Systems*, Ed.: Kwak, J. C. T.; Surfactant Science Series, 77, Dekker, New York **1998**

(7) Aubry, T.; Moan, M. *J. Rheol.* **1996**, *40*, 441.

(8) Sau, A. C.; Landoll, L. M. In *Polymers in Aqueous Media: Performance through Association*, Ed.: Glass, J. E.; Advances in Chemistry Series 223, American Chemical Society, Washington, DC **1989**, p.343.

(9) Tanaka, R.; Meadows, J.; Phillips, G. O.; Williams, P. A. *Carbohydr. Polym.* **1990**, *12*, 443.

(10) Iliopoulos, L.; Wang, T. K.; Audebert, R. *Langmuir* **1991**, *7*, 617.

(11) Biggs, S.; Selb, J.; Candau, F. *Langmuir* **1992**, *8*, 838.

(12) Chang, Y.; Lochhead, R. Y.; McCormick, C. L. *Macromolecules* **1994**, *27*, 2145.

(13) Nyström, B.; Thuresson, K.; Lindman, B. *Langmuir* **1995**, *11*, 1994.

(14) Xie, X.; Hogen-Esch, T. E. *Macromolecules* **1996**, *29*, 1734.

(15) Panmai, S.; Prudhomme, R. K.; Peiffer, D. G. *Colloids Surf. A, Physicochem. Eng. Aspects* **1999**, *147*, 3.

(16) Piculell, L.; Guillemet, F.; Thuresson, K.; Shubin, V.; Ericsson, O. *Adv. Colloid Interface Sci.* **1996**, *63*, 1.

(17) Jimenez Regalado, E.; Selb, J.; Candau, F. *Langmuir* **2000**, *16*, 8611.

(18) Lee, J.-H.; Gustin, J. P.; Chen, T.; Payne, G. F.; Raghavan, S. R. *Langmuir* **2005**, *21*, 26.

(19) Shashkina, J. A.; Philippova, O. E.; Zaroslov, Y. D.; Khokhlov, A. R.; Pryakhina, T. A.; Blagodatskikh, I. V. *Langmuir* **2005**, *21*, 1524.

(20) *Polymers in Aqueous Media: Performance through Association*, Ed.: Glass, J. E.; Advances in Chemistry Series 223, American Chemical Society, Washington, DC **1989**.

(21) *Hydrophilic Polymers: Performance with Environmental Acceptability*, Ed.: Glass, J. E.; Advances in Chemistry Series 248, American Chemical Society, Washington, DC **1996**.

(22) *Associative Polymers in Aqueous Solution*, Ed.: Glass, J. E.; Advances in Chemistry Series 765, American Chemical Society, Washington, DC **2000**.

(23) Winnik, M. A.; Yelta, A. *Current Opinion in Colloid and Interface Science* **1997**, *2*, 424.

(24) Aubry, T.; Moan, M. *J. Rheol* **1994**, *38*, 1681.

(25) Caritey, J.-P. Relation entre la modification chimique de précurseurs hydrophiles d'origine naturelle et leurs propriétés en solution diluée et semi-diluée, Thèse Université de Rouen, **1994**.

(26) Qu, Q.; Nelson, E.; Willberg, D.; Samuel, M.; Lee, J.; Chang, F.; Card, R.; Vinod, P.; Brown, J.; Thomas, R., U.S. Patent 6 435 277 **2002**.

(27) Raghavan, S. R.; Kaler, E. *Langmuir* **2001**, *17*, 300.

(28) Couillet, I.; Hughes, T.; Maitland, G.; Candau, F.; Candau, S. J. *Langmuir* **2004**, *20*, 9541.

(29) Croce, V.; Cosgrove, T.; Maitland, G.; Hughes, T.; Karlsson, G. *Langmuir* **2003**, *19*, 8536.

(30) Couillet, I.; Hughes, T.; Maitland, G.; Candau, F. *Macromolecules* **2005**, *38*, 5271.

Chapter I

POLYMER-LIKE SOLUTIONS

"CONVENTIONAL" POLYMERS

ASSOCIATING POLYMERS

WORMLIKE MICELLES

In this chapter, we will discuss the structural and dynamical properties of the three kinds of polymer-like molecules that have been investigated in the framework of the present study, that is "conventional" polymers, associating polymers and wormlike micelles. By "conventional", we mean polymers obtained by covalent bonding of monomers. From the structural point of view, the three systems are characterized by the same parameters; the radius of gyration in the dilute regime, the correlation length in the semi-dilute regime and the crossover concentration between these two regimes. On the other hand, the dynamical properties are very specific of the type of polymer-like system investigated.

I. SINGLE CHAIN CONFORMATION

I.1. "Conventional" polymers

The polymeric chain consists of N monomers with size a. The statistical properties of the chain are described by means of wormlike chain models consisting of $\tilde{N}$ statistical units with length equal to the persistence length l_p. The latter is the contour length over which the chain can be considered as rigid.

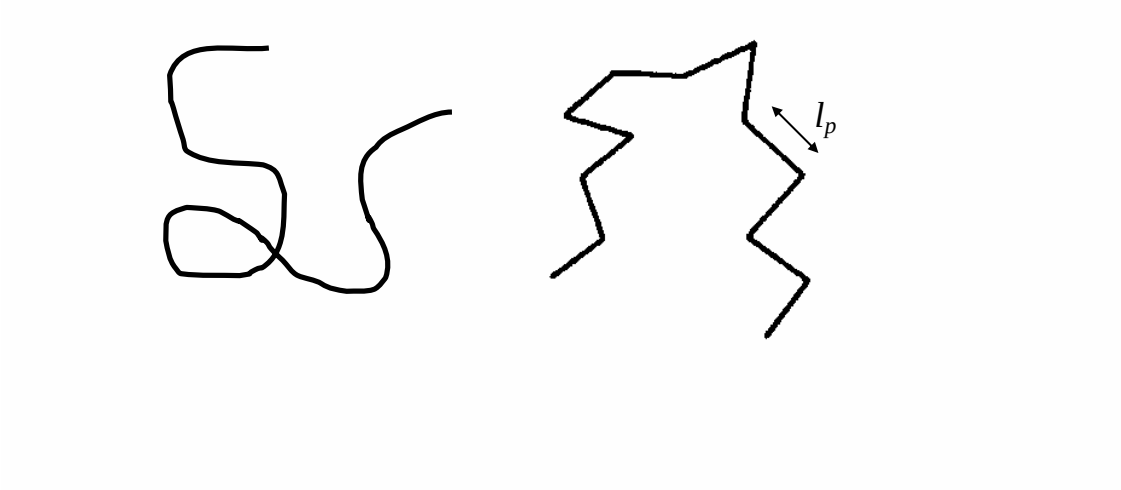

Figure 1: *Schematic representation of the wormlike polymeric model based on* $\tilde{N}$ *statistical units with length equal to the persistence length* l_p.

For most synthetic polymers, the statistical unit corresponds to a few monomeric units. The overall chain length L is given by[1]:

$$L = Na = \tilde{N} l_p \tag{1}$$

The dimensions of macromolecules in organic solvents depend crucially on the sign and magnitude of the interactions between the chain segments and the molecules of the surrounding liquid. In "good" solvents, the intra-chain repulsion or excluded volume between the segments tends to increase the polymer dimensions (e.g. the radius of gyration, R_G), as does the solvent-solute interaction. In less favourable solvents, however, the solvent-solute and solute-solute interactions have opposite signs, and when they are precisely balanced, the chain dimensions are independent of both segment-segment and solvent-solute interactions. This phenomenon occurs at a particular temperature (θ), where R_G adopts the dimensions of a volume-less non-interacting (i.e. "unperturbed") polymer coil. In the poor solvent regime, $T<<\theta$, the attractive and repulsive forces are no longer balanced, and R_G is dramatically reduced, as the polymer chain "collapses". This phenomenon is well understood and documented experimentally for dilute solutions where the macromolecules are widely separated and inter-chain effects can be neglected.
In this study we will only consider flexible chains in good solvent. Under these conditions, the radius of gyration, according to Flory's model, is given by[1]:

$$R_G = l_p^{2/5} V_0^{1/5} \tilde{N}^{3/5} \tag{2}$$

or

$$R_G = l_p^{-1/5} a^{3/5} V_0^{1/5} N^{3/5} \tag{3}$$

where V_0 is the excluded volume parameter given by

$$V_0 = a l_p^{\,2} (1/2 - \chi) \tag{4}$$

χ is Flory's interaction parameter[*].

The radius of gyration exhibits modest temperature and concentration dependences through mainly the interaction parameter but also possibly through the persistence length.

Water-soluble polymers are commonly used for their ability to increase the viscosity of a liquid, in which they are dissolved, even at low concentrations. The ability of a polymer to influence fluid rheology arises from the greater volume of a macromolecule in solution compared to the total volume of the molecular dimensions of the repeating units. The solution volume swept out by the polymer coil is known as the hydrodynamic volume, which is determined by polymer structural parameters (e.g., chain length and chain stiffness) and polymer-solvent interactions, as well as polymer associations or repulsions. The hydrodynamic volume also has temperature, concentration, molecular weight, and deformation-rate dependence.

I.2. Associating polymers

Associating polymers are hydrophilic long-chain molecules containing a small amount of hydrophobic groups. In aqueous solution they have a tendency to associate through hydrophobic interactions and build above a certain polymer concentration a temporary network that induces a strong increase in viscosity. Due to intra-chain and inter-chain associations, the solutions of associating polymers exhibit unique rheological properties.

As for conventional polymers, a persistence length l_p and a number of persistence lengths per chain can be defined. In addition, the nature and the spacing of the stickers along the chain play an important role, due to self-association. As a consequence, the radius of gyration of associating polymers in dilute solution cannot be expressed by the Eqs.(2) and (3) derived for conventional polymers. It was found to be smaller than that of the analogue polymer without the hydrophobic groups, due to intramolecular association.

[*] a model based on the renormalized group theory[2] gives for the exponent of the power law of R_G as a function of N a value of 0.5888. In the following of the study, we will take the value 3/5, which will also impose the values of the theoretical exponents in the different scaling behaviours encountered.

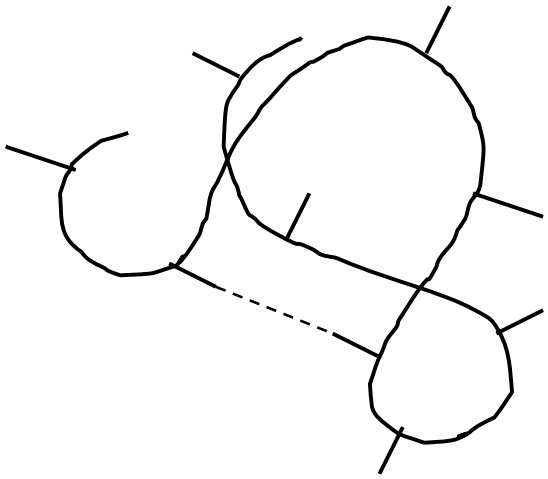

Figure 2: *Illustration of the self-association for a multisticker associating polymer chain.*

I.2.a. Classification of associating polymers

Associating polymers can be classified according to different criteria such as their origin (synthetic or natural), their chemical structure, their synthetic route….

I.2.a.1. Classification according to the localization of the hydrophobic groups

The associating polymers can be classified into two classes: (a) telechelic polymers, to which long alkyl chains (C_{12}-C_{18}) are incorporated as terminal groups, (b) multisticker polymers, in which the hydrophobic groups are randomly distributed (as single units or small blocks) along the water-soluble backbone.

Telechelic polymers have low molecular weights (<100,000) and are mostly derivatives of polyethylene oxide (PEO) with two alkyl chains at the end. This structure is rarely observed with other hydrophilic polymers such as polyacrylamide[3].

Multisticker polymers have generally much higher molecular weights (500,000 – 2,000,000). Typical examples are derivatives of natural polymers or polyacrylamide. The grafted hydrophobic groups are not necessary some long alkyl chains but can also be a group of small hydrophobic units (~2-10 units)[4-6].

I.2.a.2. Classification according to the chemical nature of the polymer backbone

One can distinguish four sub-categories in this classification:

Polyethylene oxide derivatives (PEO)[7-20]

They are also called hydrophobically ethoxylated urethane (HEUR) when there is a urethane junction between the polymer backbone and the hydrophobic chain, which is the case with mainly all the commercially available PEO. These polymers are mostly telechelic polymers.

Natural polymers

Most of the associating natural polymers are derivatives of cellulose, hydroxyethylcellulose[21-30], hydroxypropylcellulose[31,32], ethyl(hydroxyethyl)cellulose[33-37], carboxymethylcellulose[38], guar[39-45], pullulanes[46,47], chitosan[48-54], pectine[55],…
In our study, we only considered derivatives of natural polymers.

Polyacrylamide derivatives

They are mostly based on the acrylamide monomer [4-6,56-69] but also on other water soluble monomers such as N,N-dimethylacrylamide[70,71] or N-isopropylacrylamide[72,73]. They have a high molecular weight (1,000,000 – 3,000,000).

Associating polyelectrolytes

They are mostly based on carboxylic monomers such as the HASE (Hydrophobically Alkali Soluble or Swellable Emulsion) and are soluble in basic solution. They have found quite a lot of industrial applications[74-77].
Their behaviour is more complex than that of the equivalent non-charged polymer due to the competition between the attractive hydrophobic interactions and the repulsive

electrostatic interactions. The predominance of one effect onto the other will depend on molecular characteristics of the polymer, pH, salt presence, and will lead to different rheological properties.

I.2.a.3. Classification according to the synthetic route

There are two processes to synthesise associating polymers: either by modification of a preexisting polymer or by copolymerization of hydrophobic and hydrophilic monomers.

Chemical modification of pre-existing polymers

This process consists in the modification of a polymer by its chemical reaction with a hydrophobic group. By this method, it is possible to obtain series of associating polymers having for example, same molecular weight but different degrees of substitution of the hydrophobic group, or different types of hydrophobic groups. The distribution of the hydrophobic groups along the polymer backbone is usually random.

The chemical reaction can be processed in heterogeneous or homogeneous medium, the second one leading to a more homogeneous composition.

To obtain derivatives of polysaccharides or PEO, the hydrophobic groups are introduced by formation of ether, ester or urethane bonds from the hydroxyl, carboxylate or ester functions of the polymer[38,46,78]. The chemical modification is the only way to obtain amphiphilic compounds from a water-soluble natural polymer. During the synthetic process, some parallel reactions may occur that can lead to the breaking of the chemical backbone and so to a decrease of the polymer molecular weight[24,38]. Conversely, some coupling reactions that lead to an increase of the molecular weight can be observed with the HEUR[79].

Derivatives of polyacrylic acid are obtained by chemical reaction with aliphatic amines.

Recently hydrophobic groups have been introduced on polyacrylamides through N-alkylation[80,81].

The modification of polyacrylamide can be a simple hydrolysis of the polymer in order to increase its hydrophilic character[63,80].

Copolymerisation

There are different copolymerization processes: solution copolymerization, emulsion copolymerization and micellar copolymerization.

- copolymerisation in solution[70,72,73]

The difficulty in this synthesis process is to find a solvent that can solubilise both the hydrophilic and the hydrophobic monomers. Mixtures of solvents can sometimes be used. This leads to statistical polymers.

- emulsion copolymerisation

Direct emulsion polymerisation is the classical route to synthesise the HASE polymers (see I.2.a.2) but reverse emulsion and microemulsion polymerisation can also be used to synthesise associating polymers[82,83].

- micellar copolymerisation

This is the most efficient process for the copolymerisation of hydrophobic and hydrophilic monomers. It was first initiated by Dow Chemicals[84-87] and Exxon[66,88-93] before being extensively studied at the Institut Charles Sadron[4,5,56-58,61-63,94-97,129,130], in the team of McCormick [6,64,98-100,103,104,110,113] and in other laboratories[101,102]. In this process, the hydrophobe is solubilised within surfactant micelles (sodium dodecylsulfate) whereas the water-soluble monomer is dissolved in the aqueous continuous medium. Due to their high density in the micelles, the hydrophobic monomers are randomly distributed as small blocks in the hydrophilic backbone.

I.2.b. Characterisation of associating polymers

In order to compare the behaviour of associating polymers with their non-associating analogues, it is important to be able to characterize properly the polymers in terms of molecular weight, concentration of hydrophobic groups and monomer distribution.

I.2.b.1. Molecular weight

The determination of the molecular weight of copolymers is not as simple as that of homopolymers. Moreover, in the case of water-soluble polymers, this determination can be difficult and sometimes impossible due to some specific characteristics such as polarity and hydrogen bonding, that are responsible for aggregation and adsorption phenomena. The problem is even more difficult with amphiphilic copolymers due to the difference in solubility of the hydrophobic and hydrophilic parts. Besides water, only a limited number of solvents are able to solubilise the polymer at the molecular level without the formation of aggregates. Even when the polymer is fully soluble, the determination of the molecular weight can be altered by the presence of intramolecular interactions between the polymer chains that might change their conformation. This explains why many studies do not quote values of molecular weights or give inaccurate data.

It is often considered that the molecular weight of associating polymers is equivalent to that of the non-associating homologue[64,103].

Molecular weights can be obtained from the determination of the intrinsic viscosity of the aqueous polymer solution using the Mark-Houwink-Sakurada viscosity's law established for non-modified and modified polymers[6,67,100,104,105]. This method does not provide accurate values. The behaviour of the modified polymer in solution is different from that of the non-modified analogue. Its hydrodynamic volume is reduced due to the presence of hydrophobic interactions[4,22,24,29,58,71,106,107]. As a result, the molecular weight that is obtained by measurement of the intrinsic viscosity might be lower than the real value. Conversely, the presence of aggregates in dilute solution might alter the measurement and lead to a higher molecular weight value than the one expected[46,64,108].

Nevertheless, the viscosimetric method for the determination of molecular weights can be applied when a solvent capable of breaking the hydrophobic interactions is used[29,109].

For the same reasons, the determination of molecular weights by light scattering techniques provides accurate results only when using a solvent, in which the copolymer is dispersed at the molecular level. Some authors have also used static and dynamic light

scattering in the presence of an additive such as a cosolvent[110], a salt[111] or a surfactant[60,112,113].

As discussed above, the determination of the molecular weight of water-soluble associating polymers is not an easy task but it is even more difficult to determine its molecular weight polydispersity. Most of these polymers are only water soluble (except for the PEO that is also soluble in THF), and so, aggregation and adsorption phenomena on the columns occurring in aqueous media prevent the use of the classical size exclusion chromatography (SEC) technique[38,46,71,114]. Mixture of solvents such as water/acetonitrile/nitrate or lithium or sodium acetate, can be used in order to prevent the aggregation phenomena. But most of the time, the SEC technique cannot be used and so it is assumed that the molecular weight distribution is equivalent to that of the non-modified homologue for associating polymers obtained by chemical modification of a precursor, with the hypothesis that no degradation occurs during the synthesis process.

I.2.b.2. Molar composition

The determination of the exact content of substituted hydrophobic chains is quite difficult due to their very low concentration (usually a few %mol), which is close to the sensitivity limit of techniques such as elementary analysis or NMR. The determination of the molar composition by elementary analysis is easier when the hydrophobic comonomer contains a specific element such as nitrogen, fluor or silicium[114-116], which is not present in the hydrophilic monomer. The molar composition can also be determined precisely when the hydrophobic group contains a UV absorbent unit[4,6,59-61,63,69,100,104,112,113]. ^{1}H NMR, which gives less accurate results than the UV spectroscopy technique, can be used when the percentage of hydrophobic units is above 2%mol or in the case where the hydrophobic unit contains a large number of characteristic protons[5,58].

I.3. Wormlike micelles

Surfactants are amphiphilic molecules composed of two entities: a long hydrophobic tail that has a high affinity with oil or any apolar medium, and a hydrophilic head that has a

high affinity with water or any polar medium. In aqueous solution, such molecules assemble reversibly into a variety of spatially organized structures, whose common feature is the tendency for the hydrophobic tails to avoid any contact with water.

The shape of surfactant aggregates is determined by the packing parameter, $P=V/A_oL_H$, where V is the volume of the surfactant hydrophobic part, A_o is the surface area occupied by the surfactant headgroup, and L_H is the extended length of the hydrophobic part[117].

For P<1/3, spherical micelles are formed, for 1/3<P<1/2 cylindrical micelles are formed, and for 1/2<P<1, vesicles or bilayers are formed (Fig.3).

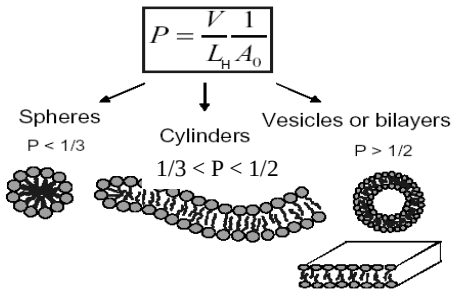

(5)

Figure 3: *Aggregate structures formed by surfactants molecules.*

In the case of charged surfactants, the area per polar head depends strongly on the nature of the counter ions and more specifically on their ability to bind to the surfactant molecules. An easy way to induce a morphological variation, for example, spherical micelles to cylindrical micelles, is to decrease the effective head-group area by adding salt, which screens the electrostatic repulsions between the headgroups and allows them to come closer. So, under appropriate conditions of concentration, salinity, temperature, presence of counter ion, etc., small aqueous spherical micelles can undergo uniaxial growth and become worm-like. If the energy required to break a wormlike micelle into smaller parts (scission energy) is large enough, the length of the rods can become longer

than their persistence length and they are then similar to semi-flexible linear polymer chains. In particular, these flexible wormlike micelles can become entangled, even at fairly low concentration.

The length of wormlike micelles has been shown to increase upon increasing the surfactant concentration and decreasing the temperature[118].

The wormlike micelles show a strong analogy with conventional polymer chains, the only differences being a thicker section (~2nm) and a longer persistence length (~20nm).

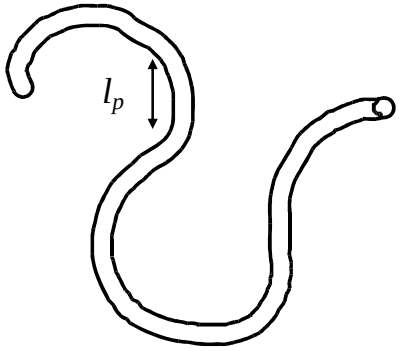

Figure 4: *Persistence length l_p of a wormlike micelle of contour length L.*

The radius of gyration in the limit $L>>l_p$ is given by the same expression as for conventional polymers

$$R_G = l_p{}^{2/5} V_0{}^{1/5} \tilde{N}^{3/5} \tag{6}$$

or in terms of the micellar contour length $L = \tilde{N} l_p$

$$R_G = l_p{}^{-1/5} V_0{}^{1/5} L^{3/5} \tag{7}$$

Unlike conventional polymers, the radius of gyration exhibits important temperature and concentration dependences through the contour length.

II. CROSSOVER BETWEEN DILUTE AND SEMI-DILUTE REGIMES

The properties of polymer-like solutions exhibit a drastic change at the overlap volume fraction ϕ^* defining the crossover between the dilute regime where the molecules are far apart from each other and the semi-dilute regime corresponding to solutions with overlapped chains. Figure 5 gives a schematic representation of the evolution of the system upon increasing the polymer concentration.

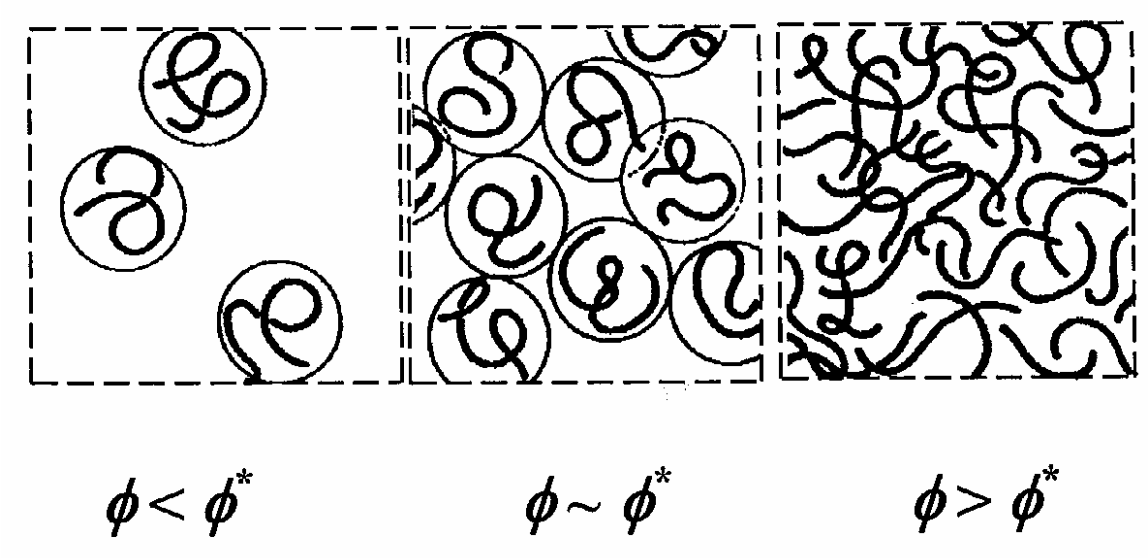

Figure 5: *Schematic representation of the state of a polymer solution with increasing polymer volume fraction.*

The expression of ϕ^* is obtained by stating that the volume fraction of the solution is that of a single chain given by the ratio of the volume of the polymer chain over the actual volume occupied by this chain

$$\phi^* \approx S_c l_p \tilde{N} / {R_G}^3 \quad (8)$$

where S_c is the section of the polymer chain.

The overlap volume fraction ϕ* of a polymeric chain can be determined by means of different techniques including static and dynamic light scattering[119-122], T-Jump (for wormlike micelles)[123] and rheological measurements[124-126]. Among these techniques, the rheology is particularly well adapted. In the dilute regime, the zero-shear viscosity is very low, of the order of that of the solvent. In the semi-dilute regime beyond the overlap volume fraction ϕ^*, the systems form an entangled mass of chains and the zero-shear viscosity increases sharply with the polymer volume fraction. This behavior is qualitatively observed for the three polymer-like systems investigated with however some specific features.

II.1. "Conventional" polymers

For these systems, the expression of ϕ^* is obtained from Eq.(8) by noting that $S_c \approx a^2$

$$\phi^* \approx a^2 l_p \tilde{N} / {R_G}^3 \quad (9)$$

or in terms of the true polymerization degree:

$$\phi^* \approx a^3 N / {R_G}^3 \quad (10)$$

The effect of temperature on ϕ^* is moderate in the case of conventional polymer, as it only results from the variation of R_G with temperature.

A typical schematic representation of the variation of the zero-shear viscosity with volume fraction for a "conventional" polymer is given in Fig.6.

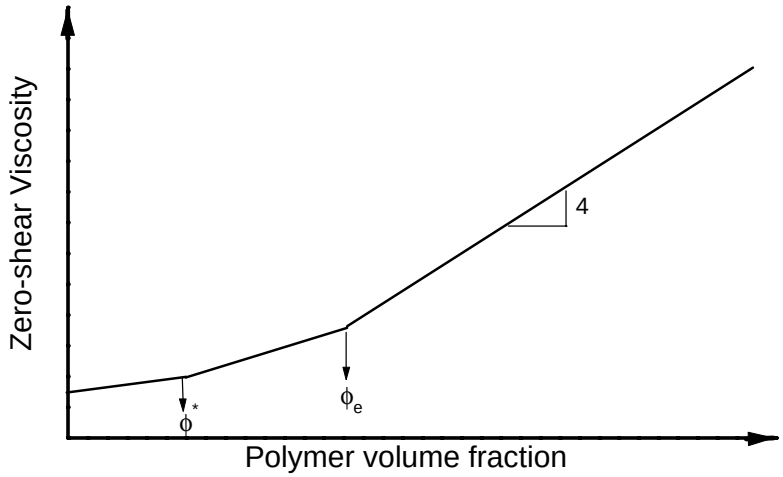

Figure 6: *Schematic diagram of the variation of the zero-shear viscosity with volume fraction for a "conventional" polymer and determination of the overlap volume fraction* ϕ^* *and of the entanglement volume fraction* ϕ_e.

In the dilute regime $\phi < \phi^*$, the zero-shear viscosity is of the same order as that of the solvent. It increases gently, according to[127]:

$$\eta = \eta_s[1 + [\eta]\phi + k_H[\eta]^2\phi^2] \qquad (11)$$

where η_s is the viscosity of the solvent, $[\eta]$ is the intrinsic viscosity, directly related to the hydrodynamic volume of the polymeric chain and k_H is the Huggins coefficient measuring the solvent-polymer interaction.

Above ϕ^*, two semi-dilute regimes are observed. The first one, which extends between ϕ^* and ϕ_e corresponds to a state of overlapped but un-entangled chains. In this regime, the dynamics of the system is described by the Rouse model. The viscosity scales with polymer volume fraction according to[128]:

$$\eta \approx (\frac{\phi}{\phi^*})^{1.3} \quad (12)$$

The second semidilute region, located beyond ϕ_e, is the entangled regime where the dynamics is described by the reptation model. The power law describing the variation of the zero-shear viscosity with volume fraction is:

$$\eta = \phi^{15/4} \quad (13)$$

In fact, the above behavior is only observed for polymers with molecular weight above 30,000. Below this limit, the behaviour of $\eta(\phi)$ remains Rouse-like.

II.2. Associating polymers

For these polymers, ϕ^* is also given by Eq.(10). The temperature dependence of ϕ^* might be more significant than for unmodified polymers because of possible breaking of the associations upon increasing temperature.
When studying the variation of the zero-shear viscosity of associating polymers with concentration, several regimes are also usually identified (see Fig.7)[129]:

(a) a dilute regime $\phi < \phi_\eta$. In this regime, the viscosity is slightly depressed, as compared to that of the corresponding unmodified polymer. This is due to the chain contraction resulting from intramolecular associations[4,67,107,108,130]. The volume fraction ϕ_η has been shown to be independent of the hydrophobic bloc length (N_H), the hydrophobic content ([H]) (ϕ_η is rather close to the overlap volume fraction ϕ^* of the corresponding unmodified polymer) and to decrease upon increasing the polymer molecular weight.

(b) a semidilute regime $\phi_\eta < \phi < \phi_T$. This regime is characterized by a fast viscosity increase, whose rate is enhanced upon increasing N_H and [H]. At the overlap volume fraction ϕ_η, intermolecular links form through hydrophobic associations, which lead to an

increase of the viscosity according to a mechanism that involves the disengagement of an associating sequence from a crosslink followed by Rouse relaxation[131-134].

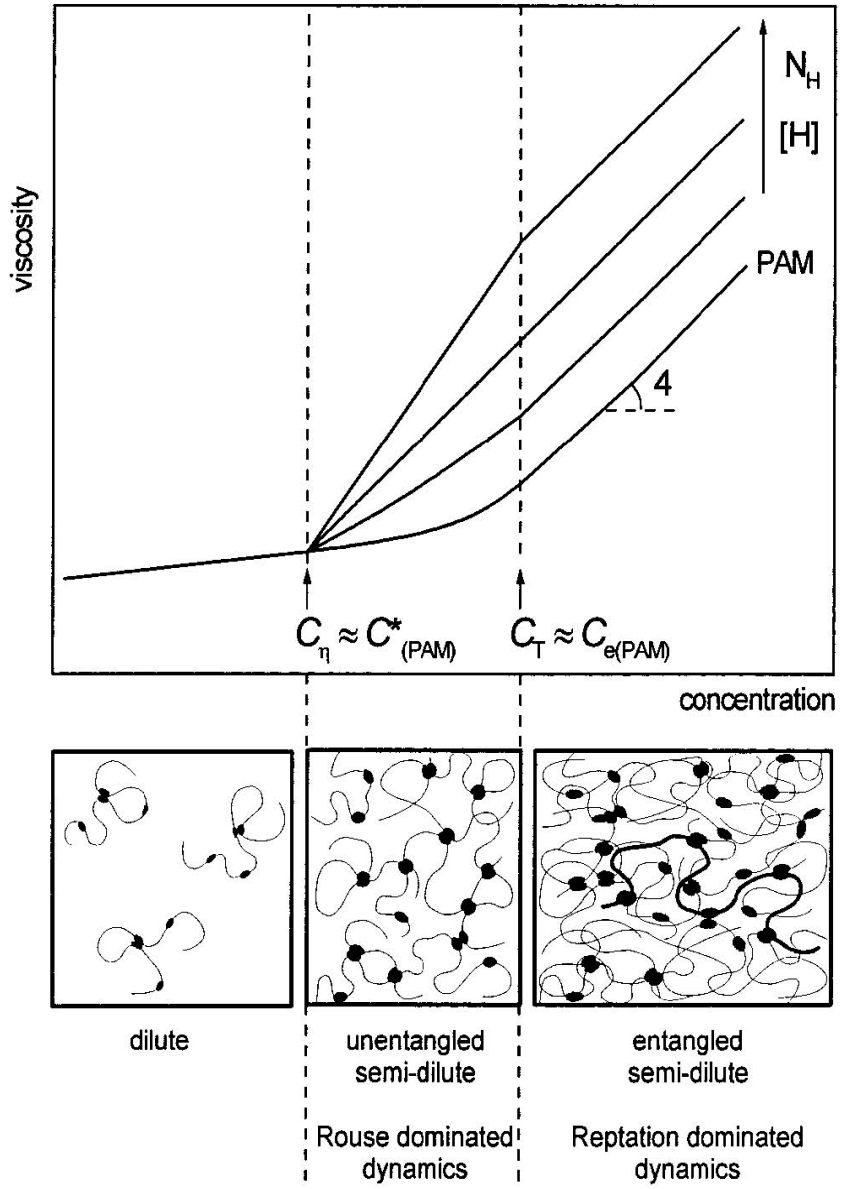

Figure 7: *Schematic diagram of the various concentration regimes for multisticker associating polymers (from ref.129)*

The rate of viscosity increase depends on the values of N_H and [H]. For multisticker chains, the disengagement of one hydrophobic block from a crosslink does not permit the relaxation of the entire chain, since the chain is still anchored by many other stickers even in the absence of entanglements. Therefore, the chain cannot diffuse very far between two consecutive sticker releases[135]. This slowing down of the relaxation can explain why the rate of viscosity increase with volume fraction becomes very large upon increasing the number of stickers per chain. This effect is also enhanced upon increasing the sticker size. (i.e., the hydrophobic block length $\approx N_H$), which controls the lifetime of an association.

(c) a concentrated regime $\phi > \phi_T$. In this regime, the viscosity follows a scaling behaviour of the polymer volume fraction with an exponent close to 4, whatever N_H and [H].
This scaling behaviour is similar to that of the unmodified polymers in the entangled regime as in this concentration range it can be assumed that the density of entanglements is much larger than that of the hydrophobic associations.

II.3. Wormlike micelles

For these systems, ϕ^* is given by Eq.(8), with R_G obeying Eqs.(6) and (7). As will be seen later, the micellar length decreases strongly upon increasing temperature. As a result, ϕ^* increases with temperature.
Figure 8 shows an example of the variation of the zero-shear viscosity with surfactant volume fraction. Again, one observes a dilute regime with a viscosity close to that of water and a sharp transition at ϕ^*. Generally, there is not a clear identifiable Rouse regime. This is partly due to the micellar growth resulting from the concentration increase.
An increase of micellar length can be promoted by addition of salt and as a consequence, the viscosity of the surfactant solution increases. The decrease in viscosity observed upon further addition of salt is more difficult to explain. Several authors[137-141] have proposed that this decrease at high salt concentrations may be due to the formation of branched micelles whose reptation is faster than that of linear micelles.

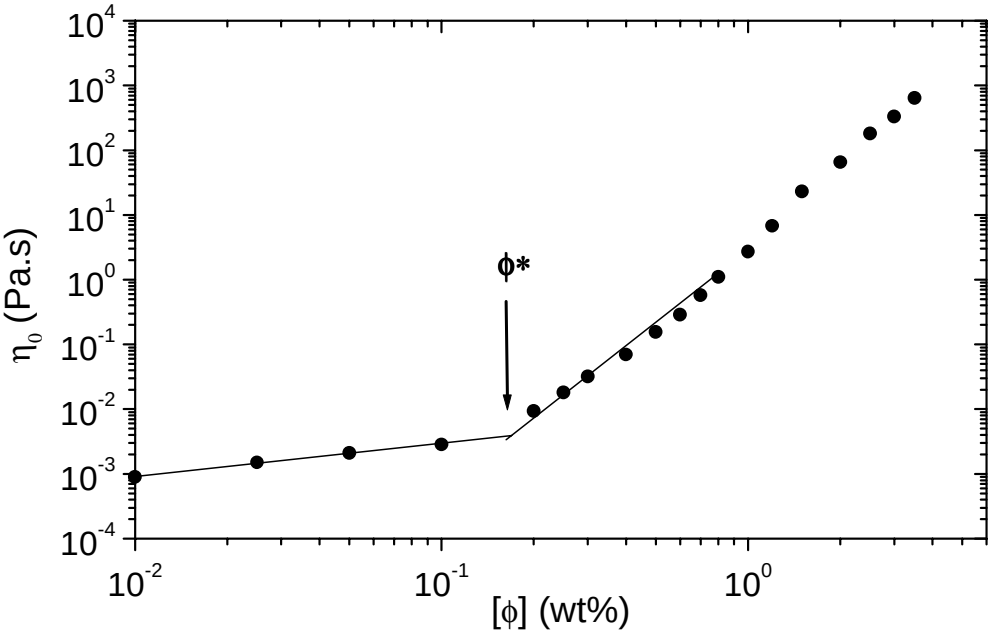

Figure 8: *Variation of the zero-shear viscosity as a function of surfactant volume fraction (from ref. 136).*

At very high salt content, the micelles eventually might form a multi-connected network, in which stress relaxation can occur by the sliding of cross-links along the wormlike micelles. Thus, the maximum in viscosity with increasing salt concentration would indicate a shift from linear to branched micelles, then to a network (Fig.9). Cryo-TEM is the only available technique suitable to give a direct evidence of branched micelles. However, one has to be cautious about the Cryo-TEM results because of possible artifacts due to mechanically-induced modification during the deposition of the sample on the grid.

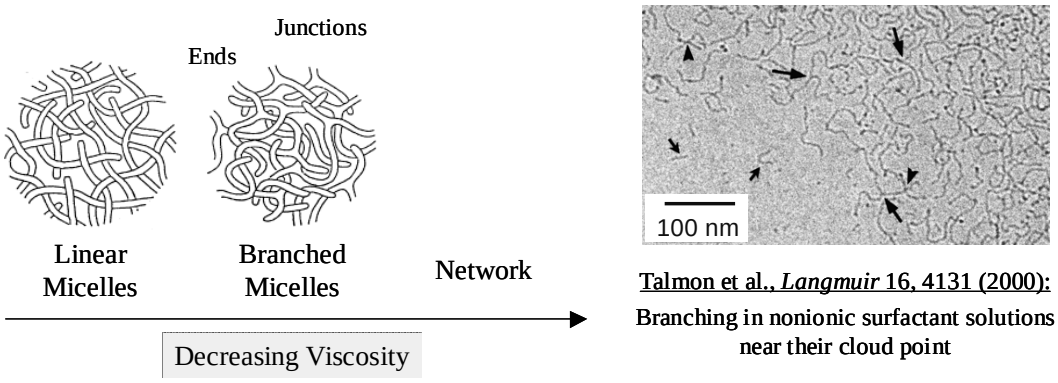

Figure 9: *Shift from linear to branched micelles by increasing salt concentration in surfactant solution and Cryo-TEM images of branched structures.*

III. THERMODYNAMICS

The notion of equilibrium is not the same for real polymers and for wormlike micelles. The latter are true equilibrium "living polymers" whose length distribution is fixed by thermodynamics conditions. For real polymers, the polymerization degree has been fixed by the chemistry and the equilibrium conditions apply to the remaining degrees of freedom.

The equilibrium properties of solutions are described by characteristic lengths, which in turn control the osmotic compressibility and, in the entangled regime, the shear-plateau modulus and the cooperative diffusion constant.

The properties of the dilute solutions are significantly different, depending on the type of system investigated, whereas in the entangled state, all the polymer-like solutions exhibit the same behaviour. The relevant length to describe the thermodynamic properties of semi-dilute systems is the correlation length ξ, defined as the mean distance between two inter-chain contact points between two distinct chains. It corresponds to the average mesh-size of the transient network. The expression of the correlation length in good solvent conditions has been derived by de Gennes[2]:

$$\xi = S_c^{3/4} l_p^{1/4} V_0^{-1/4} \phi^{-3/4} \qquad (14)$$

III.1. "Conventional" and associating polymers

For both the above systems, the section S_c is ~ a^2, so that Eq.(14) can be rewritten as:

$$\xi = a^{3/2} l_p^{1/4} V_0^{-1/4} \phi^{-3/4} \qquad (15)$$

In the dilute regime, the relevant length is the radius of gyration, which is, to the first approximation, independent of polymer concentration.
A schematic log-log representation of the variation of the correlation length with polymer volume fraction is given in Fig.10.

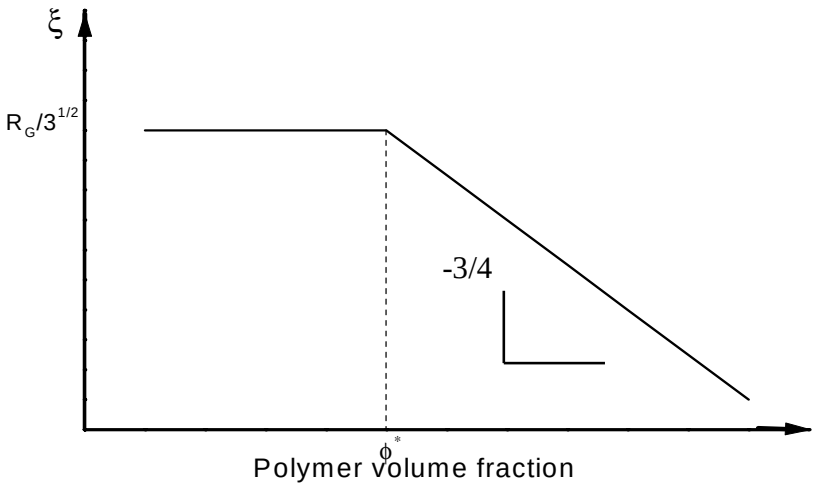

Figure 10: *Variation of the correlation length ξ with the polymer volume fraction.*

In the dilute range, ξ is equal to $R_G/\sqrt{3}$. The diagram $\xi(\phi)$ shown in Fig.10 is expected to be, to the first order, independent of temperature.

The osmotic pressure of the polymer solutions, which is proportional to the particle concentration in the dilute range, becomes controlled by the correlation length in the semi-dilute regime. It has been shown by de Gennes[2] that the osmotic pressure is proportional to the concentration of blobs, a blob being the part of the chain contained in between two consecutive contact points. The osmotic pressure scales with the concentration in the semidilute regime according to:

$$\pi \approx \frac{k_B T}{\xi^3} \approx k_B T \phi^{9/4} \tag{16}$$

where k_B is the Boltzmann constant.

The easiest way to investigate the osmotic behaviour of a solution is through light scattering experiments. A schematic representation of the concentration dependence of the scattered intensity at zero-wave vector $I_{q=0}$ is shown in Fig.11.

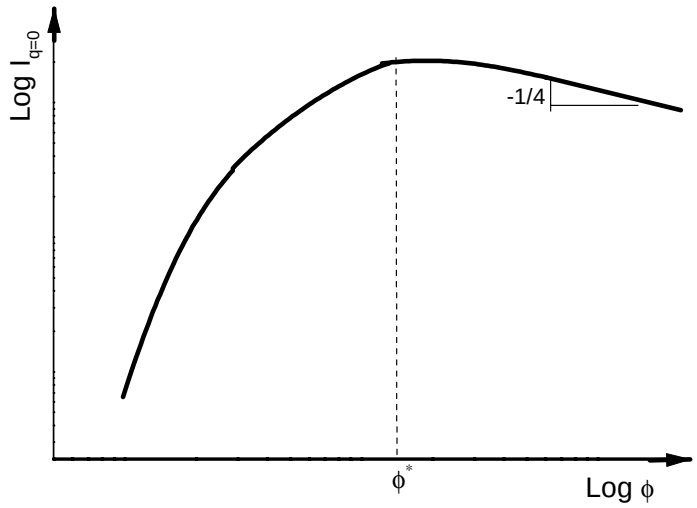

Figure 11: *Variation of the scattered intensity at zero-wave vector ($I_{q=0}$) with the polymer volume fraction.*

Up to ϕ^*, the scattered intensity increases due to the increase of concentration. The increase is not linear because of virial effects. In the semidilute regime, $I_{q=0}$ follows a scaling law of the volume fraction derived from Eq.(16)

$$I_{q=0} \approx \phi^{-1/4} \tag{17}$$

The plateau modulus G_0 obtained at high frequency in the linear viscoelasticity experiment is also proportional to the blob density and is given by the same power law as for the osmotic pressure:

$$G_0 \approx \frac{k_B T}{\xi^3} \approx \phi^{9/4} \tag{18}$$

III.2. Wormlike micelles

III.2.a. Micellar growth

The growth of cylindrical micelles is controlled by the competition between the entropy of mixing and the scission energy E_{sciss}[142,143]. For neutral micelles, the scission energy is equal to the end-cap energy that is the energy required to create two end-caps from a semi-infinite cylinder.

The length distribution in electrostatically screened solutions of wormlike micelles undergoing reversible scission can be obtained from the models derived for "conventional" polymers but taking into account the two specific features of equilibrium polymer solutions: i) the average length of the micelles is determined by the thermodynamical equilibrium of the solution. ii) the micelles continuously break and recombine. The length distribution of equilibrium polymers can be calculated using a mean-field approach. For an electrostatically neutral system of linear chains, the total free energy F per unit volume of micellar solution can be written as:

$$F = k_B T\left[\sum_L c(L)[\log c(L) + E_{sciss} / k_B T]\right] \tag{19}$$

where k_B is the Boltzmann constant, T is the absolute temperature and $c(L)$ is the number density of elongated micelles of length L. The first term in Eq.(19) corresponds to the entropy of mixing, and E_{sciss} is the energy of scission of the micelle. The total volume fraction is defined by

$$\phi = \sum_L c(L)L \tag{20}$$

The minimization of Eq.(19) with respect to $c(L)$ paying attention to the constraint of Eq.(20) leads to an exponential distribution of the micellar lengths and a mean micellar length $\overline{L}$ that increases as the square root of the surfactant volume fraction according to the following equations:

$$c(L) \approx \exp(-L / \overline{L}) \tag{21}$$

and

$$\overline{L} \approx \phi^{1/2} \exp(E_{sciss} / 2k_B T) \tag{22}$$

The above approach considers each polymer as a free random walk that is uncorrelated with itself and with its neighbours. It does not take into account correlations brought about by the mutual avoidance of the chains; such correlations are normally dealt with using a scaling approach. When the excluded volume repulsion of the chain is strong, the correlations are important in the dilute regime and also in the semi-dilute regime. At higher concentrations, or for weak repulsions, the mean-field results derived above are appropriate. A scaling approach of the equilibrium properties of semi-dilute solutions of wormlike micelles has been developed by Cates[142,143]. If the system consists only of

linear micelles, Eqs.(21) and (22) still apply, with however a slightly different value for the exponent of the variation of $\overline{L}$ with ϕ:

$$\overline{L} \approx \phi^{0.6} \exp(E_{sciss} / 2k_B T) \quad (23)$$

The scaling theory when rings are present is more complicated. The details have been worked out by Petschek et al.[144]. It is found that, for large E_{sciss} (20-30k_BT), micellar rings are invariably present below and around C^* [142,143]. The very long chains that would exist can gain entropy by fragmenting into numerous smaller rings, without having to pay a large free energy penalty to make linear chains of the same length. In the limit of an infinite scission energy, the surfactant would form a cascade of micellar rings with a ring size distribution given by a power law times exponential, which is much broader than the exponential alone and a cut-off in the low size range, at a contour length of about twice the persistence length l_p. For a finite, but high value of the scission energy, both open chains and rings should be present in the system. The presence of such rings has been reported around the overlap threshold in a few systems[120,121]. In one of them, only rings were present, and their size distribution was found to agree with the theoretical prediction[120].

Around C^*, the size of the largest rings gives a correlation length ξ (the mesh size of the transient network of overlapping cylindrical micelles) that diverges smoothly, then the system transforms into a solution of entangled linear micelles, and the micellar growth behaviour described by Eqs.(21) and (22) or (23) is recovered. In that regime, the micellar system has similar properties to that of a semi-dilute polymer solution.

III.2.b. Analogy Polymer/Surfactant

The strongest evidence in favour of very flexible micelles was obtained in studies performed in the semi-dilute regime, i.e. at surfactant concentrations large enough so that the elongated micelles overlap, forming a transient network[145,146]. In this regime, the systems exhibit a viscoelastic behaviour, very reminiscent of that of entangled polymer solutions[125,141,147-160]. However, there are two major differences between polymer

solutions and wormlike micellar systems. The first difference is related to the self-assembling nature of the process of formation of elongated micelles, which leads to equilibrium polymers with a broad distribution of micellar sizes and an average micellar length $\bar{L}$ that has been defined previously. The second difference is due to the fact that the worm-like micelles can break and recombine on a time scale, which is dependent on the system and on the physicochemical conditions.

One expects then a solution of semi-dilute wormlike micelles to behave as an entangled network of polymer molecules, if observations are made on a time scale shorter than the time τ_b for scission or recombination. In this case, the properties of the system only depend on the correlation length ξ that represents the mesh size of the transient network of overlapping cylindrical micelles. These properties can be characterized through the measurement of the intensity of scattered light at zero wavevector $I_{q=0}$, the determination of correlation length ξ, and the measurement of the high frequency elastic moduli. All these parameters are insensitive to the overall length of the micelles and to the micellar kinetics. Experimental studies have shown that $I_{q=0}$ and ξ obey power laws of the surfactant volume fraction with exponents close to those predicted for semi-dilute polymer solutions[119,161-163]:

$$I_{q=0} \approx \phi^{-1/4} \tag{24}$$

$$\xi \approx \phi^{-3/4} \tag{25}$$

The volume fraction dependence of ξ is illustrated in Fig.12. The only difference with the behaviour of conventional polymers appears in the dilute regime where $\xi = R_G/\sqrt{3}$ increases with concentration, due to the micellar growth.

As for the scattered intensity, its variation with the volume fraction is qualitatively the same as that shown in Fig.11 for polymers.

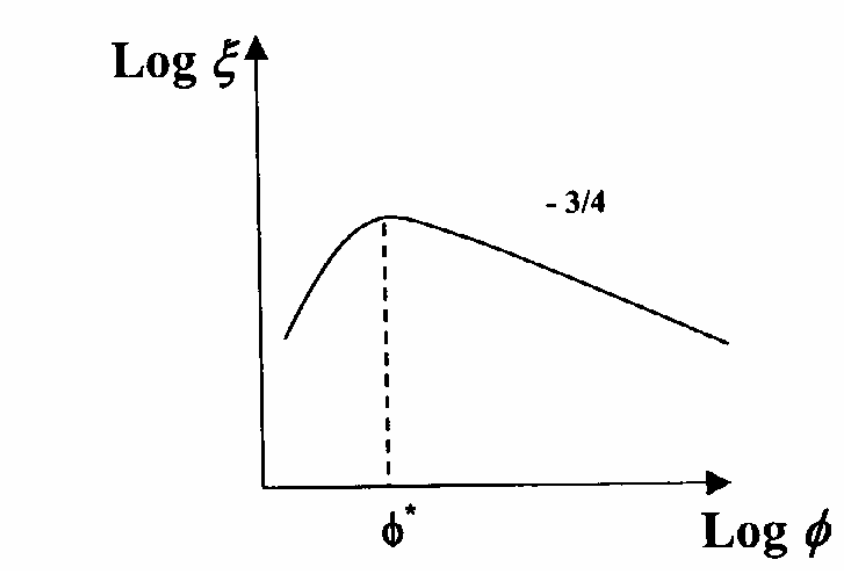

Figure 12: *Variation of the correlation length with the surfactant volume fraction.*

IV. LINEAR DYNAMIC PROPERTIES

IV.1. "Conventional" polymers

IV.1.a. Reptation and Rouse models

De Gennes suggested that the predominant relaxation mechanism for long linear polymers in the melt, is that of reptation[164]. This process consists in the gradual disengagement of any given chain, by curvilinear diffusion along its own contour, from a tube-like environment. The tube is made up of neighbouring chains; these present a set of topological obstacles to diffusion normal to the chain contour (Figs.13-15).

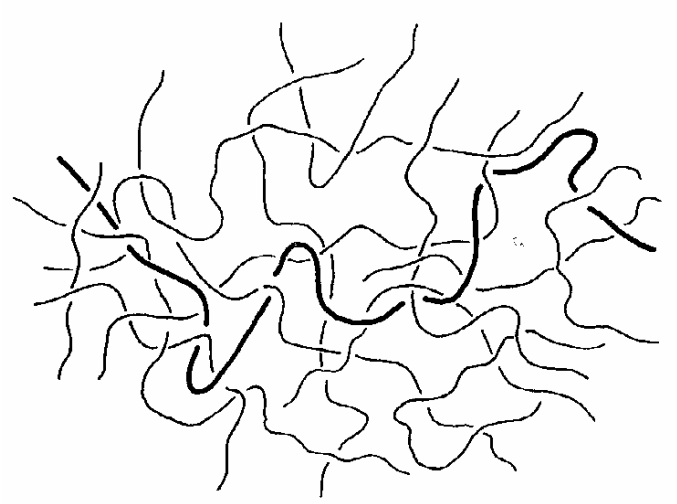

Figure 13: *A polymer molecule entangled in a mesh of other polymer chains (From Graessley 1982[165]).*

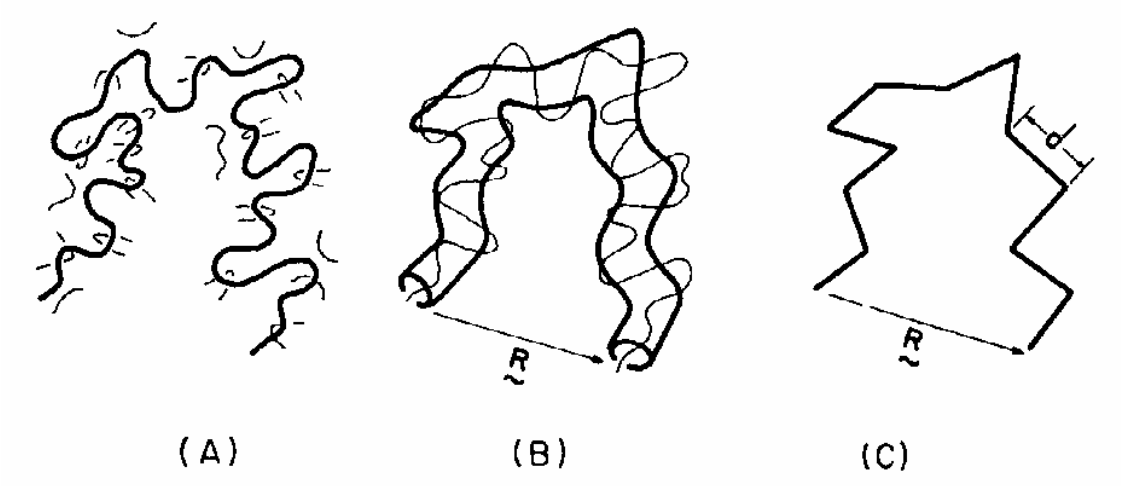

Figure 14: *(A) A polymer molecule entangled with neighbouring molecules that delimits the contour tube (B) in which the polymer molecule is confined. (C) The tube contour is roughly that of a random walk with a step size equal to the tube diameter d (From Graessley 1982[165]).*

.

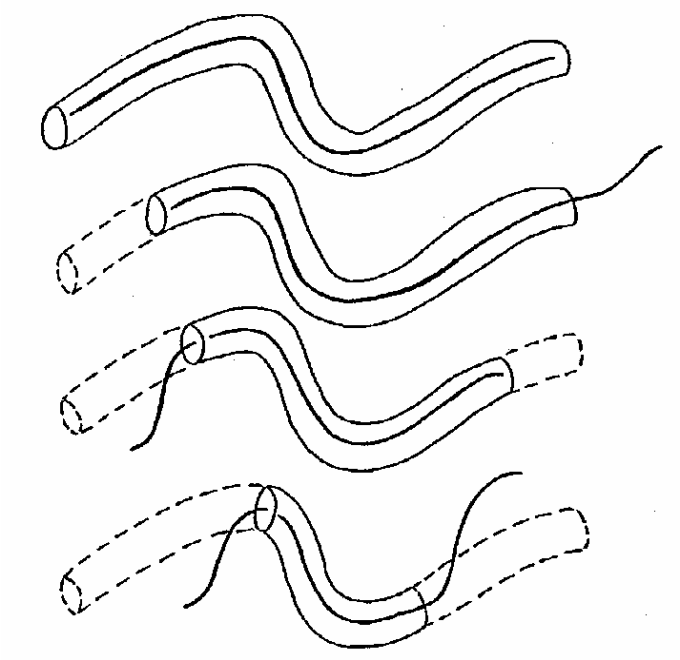

Figure 15: *Reptation of a polymer molecule out of its tube.*

The diffusion constant of the chain in real space is:

$$D \cong R_G^{\,2} / \tau_{rep} \cong D_0 l_p \bar{L}^{-2} \tag{26}$$

where R_G represents the radius of gyration ($R_G = (\bar{L} l_p)^{1/2}$), τ_{rep} is the reptation time, and D_0 is a mobility constant, independent of the average chain length $\bar{L}$.

The prediction of Eq.(26) is confirmed experimentally for chains longer than the entanglement length ℓ_e. For shorter chains, the topological obstruction of one chain by another is much less important; the dominant relaxation mechanism is not reptation but a Rouse-like motion.

The Rouse relaxation modes[166,167] correspond to the internal relaxation modes of the chain. Rouse described the chain as a succession of "beads" separated by "springs" (Fig.16).

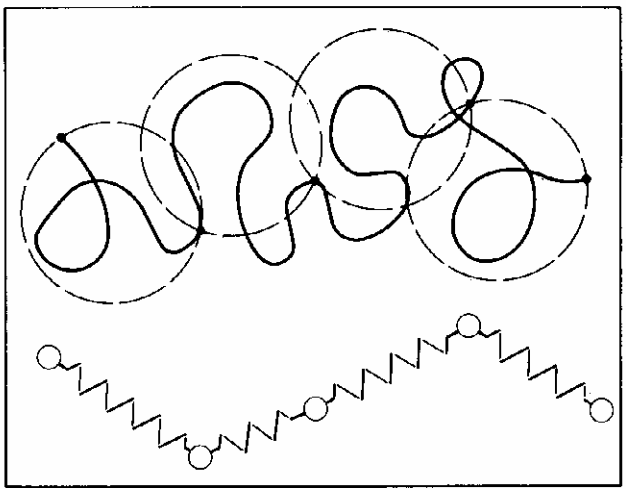

Figure 16: *Representation of a flexible randomly coiled macromolecule by the bead-spring model.*

In the Rouse model[166,167], the excluded volume interactions and the hydrodynamic interactions are disregarded and the relaxation modes involve only the rigidity of the springs and the friction of the beads with solvent, both chain-ends being fixed.
The Rouse relaxation modes are observed in the case of fast relaxations (high frequencies).

IV.1.b. Stress relaxation

Doi and Edwards[168] examined in detail the consequences of the reptation hypothesis, and constructed a constitutive equation based on the reptation model that describes the linear and nonlinear viscoelastic response of polymer melts under a variety of deformation conditions. In the Doi-Edwards theory, the stress relaxation function $\mu(t)$, which describes the fraction of imposed stress remaining at time t is simply the average fraction of tube that has not been lost by disengagement by time *t*:

$$\mu(t) = \frac{8}{\pi^2} \sum_{p=odd} \frac{1}{p^2} \exp\left[-\frac{tp^2}{\tau_{rep}} \right] \tag{27}$$

where τ_{rep}, the reptation time, which represents the requested time for a chain to lose total link with its initial tube, is equal to:

$$\tau_{rep} = \frac{\overline{L}^2}{D^{'}\pi^2} \tag{28}$$

where $D^{'}$ represents the curvilinear diffusion constant of a chain along its own contour

$$D^{'} = D_0 / \overline{L} \tag{29}$$

This result is found by observing that the parts of the original tube remaining at time t are those, through which neither end has passed.

The scaling approach of de Gennes[2] leads to the following expression of τ_{rep} for solutions in good solvent:

$$\tau_{rep} \approx \overline{L}^3 \phi^{3/2} \tag{30}$$

The zero-shear viscosity η_0 is then given by:

$$\eta_0 = G_0 \int_0^{\infty} \mu(t) dt \tag{31}$$

In deriving $\mu(t)$, an important assumption is that the tube constraint imposed on any given chain by its neighbours remains intact on the time scale τ_{rep} of the disengagement. The zero-shear viscosity can also be written as:

$$\eta_0 = G_0 \tau_{rep} \tag{32}$$

By combining Eqs.(18) and (32), one gets:

$$\eta_0 \approx \overline{L}^3 \phi^{15/4} \tag{33}$$

The relaxation times characteristic of the Rouse modes or the Reptation modes, are not in the same scale range: at short time, the relaxation is controlled by the Rouse modes and is observed at a scale smaller than the correlation length ξ. For longer times, the relaxation is controlled by the reptation modes at a scale larger than the correlation length ξ.

IV.2. Associating polymers

IV.2.a. Sticky reptation[135,169-171]

Associating polymers can be represented as linear flexible monodisperse chains of *N* monomers with *S* stickers attached to each chain that can associate to form reversible crosslinks. The stickers are considered as being at fixed positions along the chains. The average number of monomers along the chain between stickers is:

$$N_s = N/(S+1) \tag{34}$$

A given sticker can exist in one or two states: either it is free (an open sticker) or it is associated and forms a crosslink with other stickers (a close sticker). The simplest description on a microscopic level requires two parameters: the average fraction *p* of stickers that are closed and the average life-time τ of a sticker in the associated state.

The motion of chain molecules, in general, is controlled by their conformation and topological constraints.

On time scales shorter than the average lifetime of a sticker in the associated state τ, the reversible gel is indistinguishable from a permanent network. However, for times longer than τ, the structure of this network changes as stickers break away from one tie point (on time scale τ) and re-associate at another tie point (on time scale τ_1). Thus, contrary to the permanent network, chains can diffuse in the reversible network and the stress can relax.

In analogy with polymers, the topological constraints due to surrounding chains can be modeled by a confining tube. Therefore, the chain can move only along its own contour length. In the case of associating polymers and as shown by Leibler et al.[135], this scheme is modified by the possibility for the hydrophobic blocks to stick to other chains that comprise the wall of the tube (Fig.17).

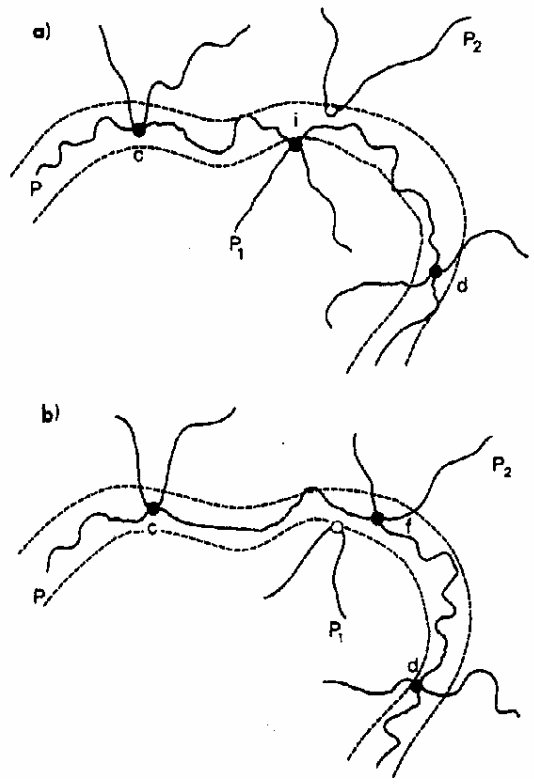

Figure 17: *Schematic representation of an elementary step of chain diffusion. (a) Initial situation where the chain P has a crosslink i with chain P_1. (b) Final situation where the sticker forms a new crosslink f with another chain P_2.(From ref. 135).*

This results in a hindered reptation with a slowing down of the system dynamics and consequently a much higher viscosity. This model was derived under the assumption that the number of entanglements is much larger that the density of stickers and of binary associations between stickers. Another interesting prediction concerns the variation of the zero-shear viscosity which is found to obey the following relationship as a function of polymer concentration:

$$\eta_0 \propto C^{33/8} N^{3.5} [S]^2 \tau(f(p)) \quad (35)$$

where N is the degree of polymerisation.

IV.2.b. Stress relaxation

The linear viscoelastic response of associating polymers has been calculated under the assumption that the tube diameter is fixed by the density of entanglements and that the number of monomers in an entanglement strand, N_e, is much smaller than the average number N_s of monomers along the chain between stickers[135].
Consider a step shear strain γ_0 applied to a reversible gel at time t=0. The time-dependent stress relaxation $\sigma(t)$ is described by the shear relaxation modulus, that is defined as:

$$G(t) = \sigma(t)/\gamma_0 \quad (36)$$

At times shorter than the Rouse time of an entanglement strand τ_e, the relaxation is indistinguishable from that in the polymer without stickers. Since only the case $N_s > N_e$ is considered, Rouse motions of the entanglement strands are unaffected by the presence of the stickers. On time scale $\tau_e < t < \tau$, there will be a plateau analogous to that observed in permanently crosslinked networks[172], with a modulus which has contributions from both crosslinks and entanglements. Making the assumption that the number densities of entanglements and crosslinks add together without synergistic effects, the shear modulus is equal to:

$$G_1 \approx Ck_BT\left[\frac{p}{N_s}+\frac{1}{N_e}\right] \tag{37}$$

where C is the polymer concentration.

On the time scale τ where the stickers open, the stress held by the stickers relaxes, and the modulus drops to the level of the identical linear chain without stickers:

$$G_2 \approx Ck_BT\left(\frac{1}{N_e}\right) \tag{38}$$

This second plateau ends up at the terminal relaxation time of the reversible gel, T_R, which depends strongly on the chain length, the density of stickers and τ:

$$T_R \approx \left(\frac{N}{N_e}\right)^{3/2} \frac{2S^2\tau}{1-9/p+12/p^2} \tag{39}$$

This second plateau modulus can be rewritten by taking into account the scaling of N_e with polymer concentration, i.e., $N_e \propto C^{-5/4}$ in good solvent[2,173]:

$$G_2 \approx k_BTC^{9/4} \tag{40}$$

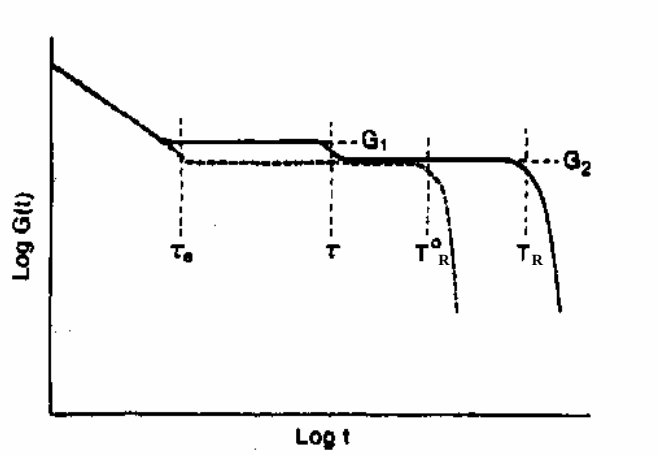

Figure 18: *Schematic comparison of the time-dependent relaxation moduli for reversible networks comprising linear chains with stickers (solid line) and linear chains without stickers (dashed line) (From ref. 135).*

IV.3. Wormlike micelles

IV.3.a. Micellar kinetics

Cates et al. have considered two types of kinetic micellar processes for living polymers[174-176]:

(i) One process considered was the reversible uni-micellar scission (Fig.19), characterized by a temperature-dependent rate constant, k per unit time per unit arc length, which is the same for all elongated micelles and is independent of time and volume fraction. Such assumptions are strictly valid in the entangled regime when reaction rates are determined by the local motion of chain sub-sections and not by diffusion of polymers over distances that are large compared to their gyration radii. The micelle breaking time τ_b is found to be given by:

$$\tau_b = (k\bar{L})^{-1} \tag{41}$$

Equations (22) and (41) predict that τ_b should decrease upon increasing ϕ as $\phi^{1/2}$ in the limit of high ionic strength, according to:

$$\tau_b \approx k^{-1}\phi^{-1/2}\exp(-E_{sciss}/2k_BT) \tag{42}$$

The derivation of Eq.(42) assumed fully screened electrostatic effects and no excluded volume effect. Cates has accounted for the excluded volume effect and obtained an equation identical to Eq.(42), where the $\phi^{1/2}$ term is replaced by $\phi^{0.6}$. In Equation (42), k is found experimentally to be strongly temperature dependent (it increases with temperature) and both k and E_{sciss} vary with the nature and the content of added salt.

(ii) The other process is the bimolecular end interchange process (Fig.20) where a free micellar end brings about the rupture of a micelle away from its ends and combine simultaneously with one of the two free ends resulting from the rupture, the other end remaining free. The associated breaking time is given by:

$$\tau_b \approx (k'\phi)^{-1} \tag{43}$$

where *k'* is the rate constant for the end interchange process.

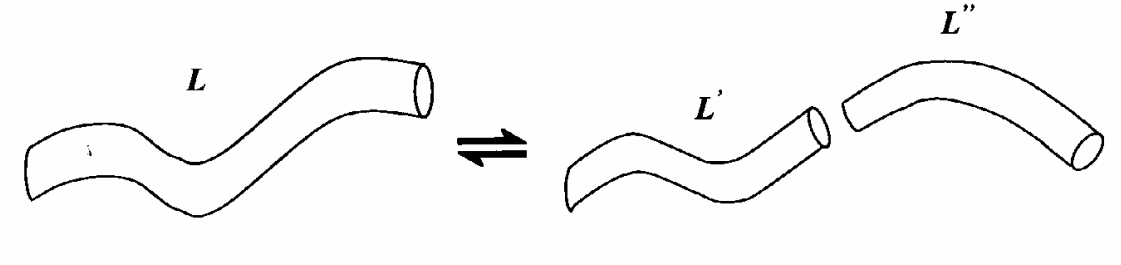

***Figure 19**: Scheme of the reversible uni-micellar scission process of rod-like micelles.*

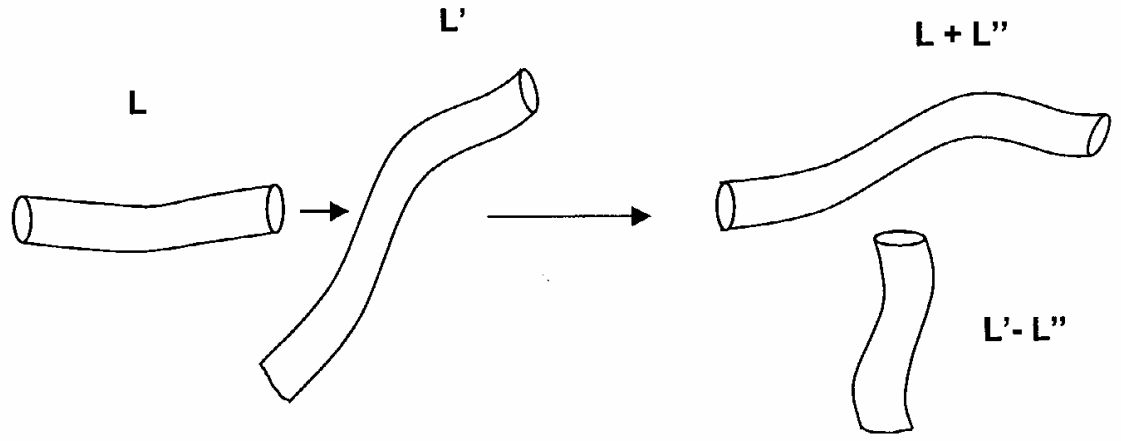

***Figure 20:** Scheme of bimolecular end interchange process of rod-like micelles.*

Another possible bimolecular reaction scheme involves an inter-bond exchange (Fig.21). The associated breaking time is given by:

$$\tau_b \approx (k''\phi)^{-1} \tag{44}$$

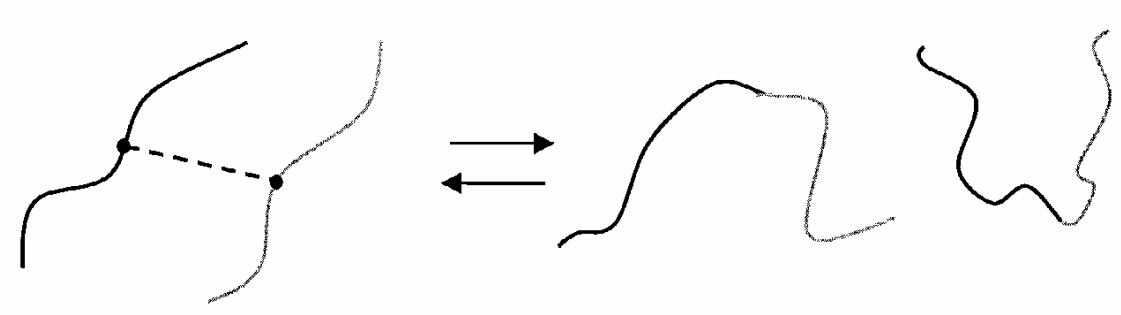

Figure 21: ***Scheme of the interbond exchange process of rod-like micelles.***

IV.3.b. Stress relaxation

In the semi-dilute range, i.e. at surfactant concentrations large enough so that the elongated micelles overlap, the systems exhibit a viscoelastic behaviour very reminiscent of that of transient polymeric networks. It has been previously presented (paragraph IV.1) that in polymeric systems, the viscoelastic properties are described by a model based on the reptation theory[164]. However the "living" character of the micelles provides additional pathways for disentanglement; as a consequence, a speeding up of the relaxation process is observed. In Fig.22 is represented the relaxation process when reptation and reversible breaking process are combined.

Several behaviors are predicted depending on the relative values of τ_b, breaking time of a polymeric micelle with a length equal to the average micellar length $\overline{L}$ and τ_{rep}, reptation time.

It was found that if the breaking time is long compared to the reptation time ($\tau_b >> \tau_{rep}$), the theory of reptation of polydisperse polymers should apply; a stress relaxation function $\mu(t)$ can be defined by

$$\mu(t) \approx \exp[-const(t/\tau_{rep})^{1/4}] \qquad (45)$$

In this regime, the terminal relaxation time T_r equals τ_{rep}.

In the opposite case where $\tau_b << \tau_{rep}$, the micelle breaking plays an important role in the viscous flow process as first stressed by Hoffmann et al.[149,154]. The Cates model predicts an almost pure exponential form of the stress relaxation function with the terminal time:

$$T_R \approx (\tau_b \tau_{rep})^{1/2} \tag{46}$$

In this regime, breakage and recombination of the chain will occur before the chain reptates out of the tube segment.

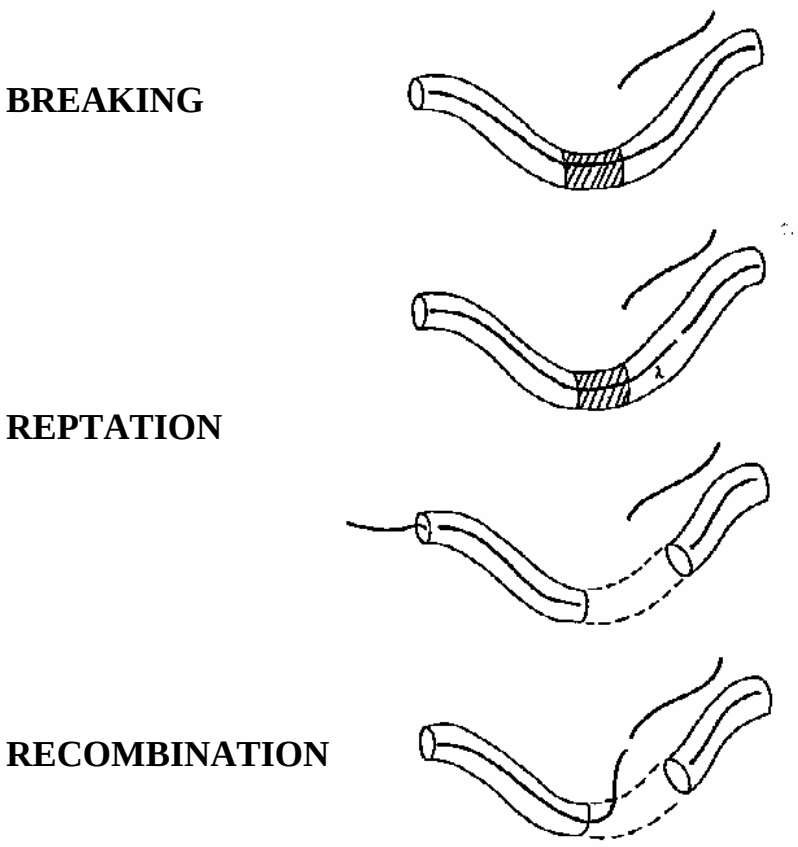

Figure 22: *Relaxation process of "living polymers".*

Such a viscoelastic system is generally identified as a Maxwell element[172] that is described by:

$$G'(\omega) = G_0(\omega T_R)^2/(1+\omega^2\ T_R^{\ 2}) \quad (47)$$

$$G''(\omega) = G_0\omega T_R/(1+\omega^2\ T_R^{\ 2}) \quad (48)$$

where G_0 is the plateau modulus and the relaxation time $T_R = \eta_o/G_o$. The Cole-Cole representations, in which the imaginary part $G''(\omega)$, of the frequency-dependent shear modulus is plotted against the real part $G'(\omega)$, can be used to get an estimate of the relaxation time T_R. The Maxwellian behavior is ascertained by a semicircular shape of the Cole-Cole plot $G''(G')$, but deviations from the half circle occur at a circular frequency, ω, of the order of the inverse of the breaking time of the micelles (Fig.23).

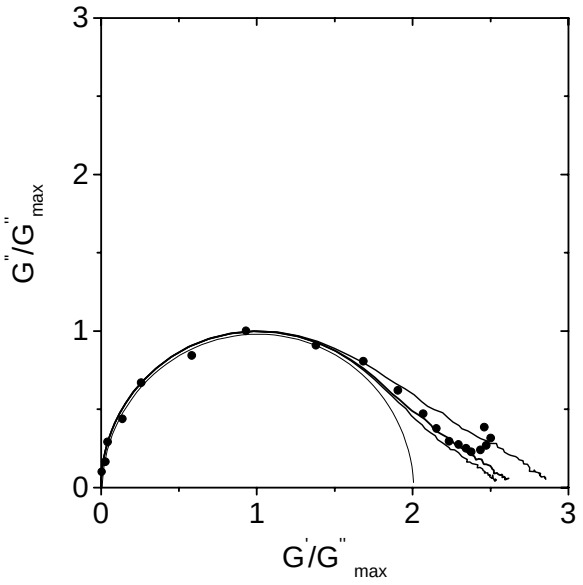

Figure 23: *Typical normalized Cole-Cole plot for a 14.4mM viscoelastic surfactant (erucyl bis-(hydroxyethyl)methylammonium chloride) solution, with KCl, at 15°C. The lines are the calculated Cole-Cole plots for different values of the parameter ζ. (*$\zeta = \tau_b/\tau_{rep}$*). The solid line represents the osculating semicircle at the origin*[136].

Detailed results were obtained from a computer simulation by Turner and Cates[176] and from a Poisson renewal model by Granek and Cates[177] for various values of the ratio $\zeta = \tau_b/\tau_{rep.}$ including the intermediate regime $\tau_b \approx \tau_{rep}$. The calculated Cole-Cole plots give the correspondence between the values of ζ and $\bar{\zeta} = \tau_b/T_R$, which provides a measurement of τ_b by a comparison procedure between experimental and calculated Cole-Cole plots. Equation (46) can be rewritten under the form:

$$T_R = (\zeta^{1/2}/\bar{\zeta})(\tau_b\ \tau_{rep})^{1/2} \tag{49}$$

with $(\zeta^{1/2}/\bar{\zeta}) \rightarrow 1$ as τ_b/τ_{rep} is decreasing. The Poisson renewal model was also applied to study the regimes that arise for a small breaking time, and/or small time scales when the dominant polymer motion is not reptation but either breathing (which arises from the tube length fluctuations) or the local Rouse-like motion (arising from regions of chains shorter than the entanglement length ℓ_e).

A typical signature of the latter effect is a turn-up of both $G'(\omega)$ and $G''(\omega)$ at high frequency, whereas the simple reptation picture predicts a constant for $G'(\omega)$ and a decreasing $G''(\omega)$. This results in a minimum in the Cole-Cole representation of the dynamic modulus, whose depth can be used to estimate the number of entanglements per chain in the system. The above model applies strictly to systems of entangled wormlike micelles with an entanglement length (i.e. the contour length ℓ_e between two successive entanglements) much larger than the persistence length l_p and in a regime where the breaking time is much larger than the Rouse time τ_e of a chain with the entanglement length.

Under these conditions, the dip in the Cole-Cole plot was found theoretically to obey the relationship[177]:

$$\frac{G''_{\min}}{G_0} \approx \frac{\ell_e}{\bar{L}} \tag{50}$$

The frequency ω_m corresponding to the minimum of G'' was assumed to be:

$$\omega_m \approx \tau_e^{-1} \approx \tau_o^{-1} \ell_e^2 \approx \eta_s l_p \ell_e \tag{51}$$

where τ_o is a microscopic time, proportional to the solvent viscosity η_s and the persistence length l_p [2].

Later on, the scaling behaviour of the dip was reexamined by Granek, using both an analytical and a numerical procedure[178]. This analysis leads to different expressions of $G''_{\min} / G_0$, and ω_m in the regime $\tau_b \gg \omega_m^{-1}$ usually encountered.

$$G''_{\min} / G_0 \approx (\ell_e / \overline{L})^{4/5} \tag{52}$$

$$\omega_m \approx (\frac{\ell_e}{\overline{L}})^{4/5} \tau_e^{-1} \tag{53}$$

Note that the above expressions are the same as for regular polymers and are valid in the case generally encountered where the dip occurs in a range of frequencies much higher than τ_b^{-1}. For associating polymers, it can be speculated that the same expressions hold if ω_m is much higher than the inverse of the lifetime of the associations.

An interesting consequence of Eq.(46) concerns the effect of temperature. The three characteristic times involved in Eq.(46) are expected to follow Arrhenius laws of the form $\exp(E/k_B T)$. This leads to the following relationship of T_R in terms of the activation energies, E_b and E_{rep} corresponding respectively to the temperature dependences of τ_b and τ_{rep}:

$$T_R \sim \exp\left(\frac{E_b + E_{rep}}{2k_B T} \right) \tag{54}$$

The above expression is valid under the condition τ_b « τ_{rep} or $\zeta/\bar{\zeta}^2$ being temperature independent.

The reptation theory predicts that $\tau_{rep} \sim \bar{L}^3 \tau_o$. The temperature dependence of η_s, characterized by an activation energy, E_{η_s}, is generally neglected in the analysis of the data. In fact, as seen later, it turns out that it is not negligible when determining the scission energy T_R is then given by:

$$T_R \sim \exp\frac{E_b}{2k_BT}\exp\frac{3E_{sciss}}{4k_BT}\exp\frac{E_{\eta_s}}{2k_BT} \tag{55}$$

Equation 55 has been used to obtain E_{sciss} for wormlike micelles from rheological and T-jump data[145,179].

The modified reptation model developed by Cates can also be used to predict the dependence of the terminal time T_R on the surfactant volume fraction. The reptation theory of semi-dilute polymer solutions in good solvents predicts that[2]:

$$\tau_{rep} \cong \bar{L}^3 \xi^{-6} \phi^{-3} \tau_o \tag{56}$$

Combining Eq.(22) with Eqs.(25) and (56) yields:

$$\tau_{rep} \cong \phi^3 \tag{57}$$

Then inserting Eqs.(57) and (42) in Eq.(46), using the mean field exponent 0.5 gives:

$$T_R \cong \phi^{5/4} \tag{58}$$

The zero-shear viscosity η_0 is related to the terminal time and to the plateau modulus G_0 through:

$$\eta_0 = G_0 T_R \tag{59}$$

For semi-dilute polymer solutions in good solvents, it has been shown that[180]:

$$G_0 \cong k_B T \phi^{9/4} \tag{60}$$

This relation has been shown to hold for polymer-like surfactant systems[124,146,159]. The combination of Eqs.(58-60) gives:

$$\eta_0 \cong \phi^{3.5} \tag{61}$$

In the scaling approach with $L \cong \phi^{0.6}$, one obtains:

$$\eta_0 \cong \phi^{3.6} \tag{62}$$

V. NON LINEAR RHEOLOGICAL PROPERTIES

The non-linear rheology of entangled polymer solutions has attracted the attention of many theoreticians and experimentalists in recent years. Quite different behaviors were observed for the three kinds of polymer systems considered here:

V.1. "Conventional" polymers

The models derived for these systems predict that the steady shear stress decreases with shear rate $\dot{\gamma}$ when $\dot{\gamma}$ is large enough and that the polymers are aligned along the flow direction[173,181-183]. This behavior cannot persist to indefinitely high shear rate and eventually, short relaxation-time processes become important, causing the stress to increase again. The nonmonotonic variation of the steady shear stress versus the shear rate is schematically represented in Fig.24[183,184].

Nonmonotonic means here that there exists a $\dot{\gamma}$-range over which the stress is multivalued. A schematic representation is shown in Fig.24. If the applied shear rate lies in the region of decreasing stress (dotted part of the curve in Fig.24, $\dot{\gamma}_1 < \dot{\gamma} < \dot{\gamma}_2$), an initially homogeneous flow becomes mechanically unstable. As a result, the solution evolves up to a stationary state of shearing where bands of highly sheared liquid of low viscosity coexist with a more viscous part supporting a lower rate. In the banded regime, changes in shear rate essentially alter the proportions of the low-and high- viscosity bands. The stress upturn occurring at high shear rate ($\dot{\gamma} > \dot{\gamma}_2$) is due to the contribution of the solvent viscosity and of the high frequency relaxation modes.

Such a behaviour has not been observed experimentally for ordinary polymers. Some shear-thinning occurs at higher shear rates but the shear stress continues to rise gently.

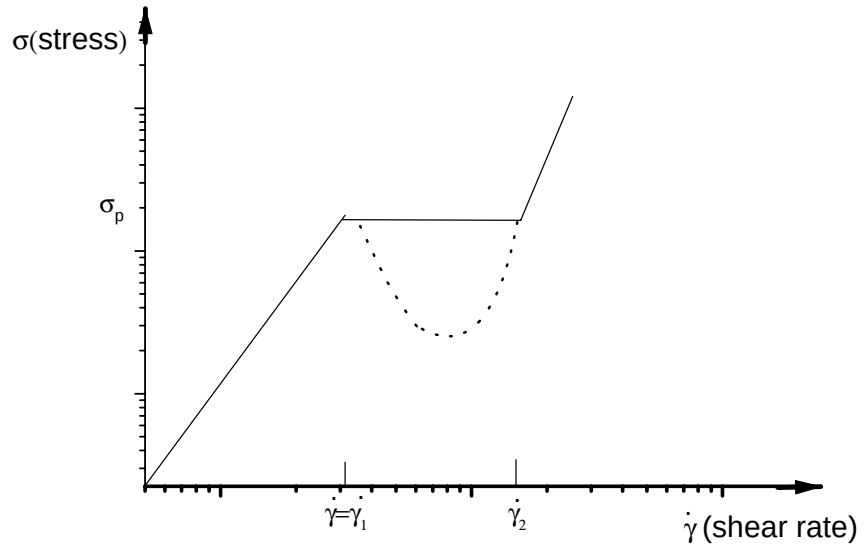

Figure 24: *A nonmonotonic stress versus shear rate curve; the dotted part is unstable. In a banded flow, regions of shear rate* $\dot{\gamma}_1$, $\dot{\gamma}_2$ *coexist to give a macroscopic mean shear rate* $\dot{\gamma}$ *which is fixed (under controlled shear rate conditions).*

V.2. Wormlike micelles

An extension of the linearised model presented in the previous section to describe nonlinear phenomena has been derived by Cates et al.[182-184]. As a starting point, it is argued that, while strong flows have important effects on the chain dynamics, they do not at a first approximation have any effects on the scission/recombination reaction rates themselves. With this assumption, a nonlinear viscoelastic constitutive equation for the regime where τ_b is much shorter than τ_{rep} but long compared to τ_e has been derived by adapting the nonlinear theories of Doi and Edwards[173,185] and Marrucci[186,187], relative to unbreakable polymers. However, for breakable polymers, the retraction affects all tube segments equally at time scale larger than τ_b. The equivalence of all tube segments, which leads to a single exponential behavior in the linear relaxation spectrum is maintained in the nonlinear regime. As a result, the nonlinear behavior is very close to that predicted for monodisperse unbreakable polymers by the Doi and Edwards model except that the terminal time is not τ_{rep} but the shorter time given by Eq.(46).

A nonlinear viscoelastic constitutive equation has been derived for the case of the steady shear flow by Cates et al.[182-184]. It predicts that at a critical shear rate $\dot{\gamma}_c$, an instability appears that triggers the isotropic phase to a new state oriented parallel to the velocity. To $\dot{\gamma}_c$ corresponds a maximum value σ_c of σ. When performing the experiments by gradually increasing the stress σ and measuring the shear rate $\dot{\gamma}$, one should observe a plateau in the curve $\sigma(\dot{\gamma})$. The value of σ_c is related to the plateau modulus G_0 by:

$$\sigma_c \approx 0.67 G_0 \tag{63}$$

As for the critical shear rate $\dot{\gamma}_c$ which corresponds to the sharp corner in the stress-shear-rate curve, it is of the order of T_R^{-1} ($\dot{\gamma}_c T_R \approx 2.6$).

The existence of a well defined stress plateau in the stress-shear rate curves has been observed for several systems. The occurrence of shear bands for micellar systems undergoing flow both in cylindrical Couette and cone-plate geometries, is established by experiments. The evidence comes from birefringence microscopy[188,189] and NMR

velocimetry[190,191]. Furthermore, good quantitative agreement was found between the predictions of the reptation-reaction model. Some deviations were observed concerning the values of σ_c / G_0 and $\dot{\gamma}_c T_R$ with respect to the theoretical values, mostly in relatively concentrated systems. However, one always experimentally observes that the stress plateau occurs at a shear rate of the order of T_R^{-1} and has a value of the order of G_0.

V.3. Associating polymers

A stress plateau was also reported in the stress-shear-rate curves obtained for solutions of associating polymers[43,56,82,192]. As a matter of fact, the results were presented as plots showing the variation of the viscosity with stress. The representative curves showed an abrupt drop of the viscosity at a critical stress σ_c. However, and contrary to the case of wormlike micelles, the occurrence of this drop followed a gradual shear-thinning regime. The value of σ_c was more than 10 times larger than the plateau modulus G_0. It was suggested by Aubry and Moan[43] that this abrupt drop resulted from the breaking of the associations. The corresponding $\dot{\gamma}_c$ was assumed to be the inverse of the life-time of the associations. Up to now, no theoretical model has been proposed to describe the non-linear rheology of these systems.

REFERENCES:

(1) Flory, P. J. *Principles of Polymer Chemistry,* Cornell University Press, Ithaca, N.Y. **1953**.

(2) de Gennes, P. G. *Scaling Concepts in Polymer Physics,* Cornell Univesity Press, Ithaca, N.Y. **1979**.

(3) Corpart, J.-M.; Boutevin, B.; Collete, C.; Ciampa, R. US Patent 5 798 421 **1998**.

(4) Hill, A.; Candau, F.; Selb, J. *Macromolecules* **1993**, *26*, 4521.

(5) Volpert, E.; Selb, J.; Candau, F. *Macromolecules* **1996**, *29*, 1452.

(6) Ezzell, S. A.; McCormick, C. L. *Macromolecules* **1992**, *25*, 1881.

(7) Maechling-Strasser, C.; Francois, J.; Clouet, F.; Tripette, C. *Polymer* **1992**, *33*, 627.

(8) Dai, S.; Tam, K. C.; Jenkins, R. *J. Phys. Chem. B.* **2001**, *105*, 10189.

(9) Xu, B.; Yekta, A.; Winnik, M. A.; Sadeghy-Dalivand, K.; James, D. F.; Jenkins, R.; Bassett, D. *Langmuir* **1997**, *13*, 6903.

(10) Zhang, K.; Xu, B.; Winnik, M. A.; Macdonald, P. M. *J. Phys. Chem*. **1996**, *100*, 9834.

(11) Hulden, M. *Colloids Surf. A, Physicochem. Eng. Aspects* **1994**, *82*, 263.

(12) Walderhaug, H.; Hansen, F. K.; Abrahmsen, S.; Persson, K.; Stilbs, P. *J. Phys. Chem*. **1993**, *97*, 8336.

(13) Karunasena, A.; Brown, R.G.; Glass, J.E. in *Polymers in Aqueous Media: Performance through Association,* Ed.: Glass J.E., Advances in Chemistry Series; American Chemical Society, Washington, DC **1989,** Vol. 223, p.495.

(14) Eisenbach, C. D.; Reimann, H.; Joos-Muller, B.; Scmidtchen, M.; Schauer, T. *Polym. Mater.Sci.Eng.* **2002**, *87*, 32.

(15) Jenkins, R. D.; Silebi, C. A.; El-Aasser, M. S. *Polym. Mater.Sci.Eng.* **1989**, *61*, 629.

(16) Xu, B.; Yekta, A.; Li, L.; Masoumi, Z.; Winnik, M. A. *Colloids Surf. A, Physicochem. Eng. Aspects* **1996**, *112*, 239.

(17) May, R.; Kaczmarski, J. P.; Glass, J. E. *Macromolecules* **1996**, *29*, 4745.

(18) Alami, E.; Almgren, M.; Brown, W. *Macromolecules* **1996**, *29*, 5026.

(19) Vorobyova, O.; Lau, W.; Winnik, M. A. *Langmuir* **2001**, *17*, 1357.

(20) Yekta, A.; Duhamel, J.; Adiwidjaja, H.; Brochard, P.; M.A., W. *Langmuir* **1993**, *9*, 881.

(21) Tanaka, R.; Meadows, J.; Phillips, G. O. *Macromolecules* **1992**, *25*, 1304.

(22) Tanaka, R.; Meadows, J.; Phillips, G. O.; Williams, P. A. *Carbohydrate Polym.* **1990**, *12*, 443.

(23) Panmai, S.; Prudhomme, R. K.; Peiffer, D. G.; Jockusch, S.; Turro, N. J. *Langmuir* **2002**, *18*, 3860.

(24) Picton, L.; Merle, L.; Muller, G. *Int.J.Polym.Anal.Charact.* **1996**, *2*, 103.

(25) Guillemet, F.; Piculell, L. *J.Phys.Chem.* **1995**, *99*, 9201.

(26) Guillemet, F.; Piculell, L.; Nilsson, S.; Djabourov, M.; Lindman, B. *Prog. Colloid Polym. Sci.* **1995**, *98*, 47.

(27) Kastner, U.; Hoffmann, H.; Donges, R.; Ehrler, R. *Prog. Colloid Polym. Sci.* **1995**, *98*, 57.

(28) Goddard, E. D.; Leung, P. S. *Langmuir* **1992**, *8*, 1499.

(29) Nishikawa, K.; Yekta, A.; Pham, H. H.; Winnik, M. A.; Sau, A. C. *Langmuir* **1998**, *14*, 7119.

(30) Panmai, S.; Prudhomme, R. K.; Peiffer, D. G. *Colloids Surf. A, Physicochem. Eng. Aspects* **1999**, *147*, 3.

(31) Landoll, L. M. *J. Polym. Sci., Polym. Chem. Ed.* **1982**, *20*, 443.

(32) Winnik, F. M. *Macromolecules* **1987**, *20*, 2745.

(33) Joabsson, F.; Lindman, B. *Prog. Colloid Polym. Sci.* **2000**, *116*, 74.

(34) Zou, S.; Zhang, W.; Zhang, X.; Jiang, B. *Langmuir* **2001**, *17*, 4799.

(35) Tsianou, T.; Thuresson, K.; Piculell, L. *Colloid Polym. Sci.* **2001**, *279*, 340.

(36) Joabsson, F.; Thuresson, K.; Blomberg, E. *Langmuir* **2001**, *17*, 1506.

(37) Kjoniksen, A. L.; Nilsson, S.; Thuresson, K.; Lindman, B.; Nystroem, B. *Macromolecules* **2000**, *33*, 877.

(38) Charpentier, D.; Mocanu, G.; Carpov, A.; Chapelle, S.; Merle, L. *Carbohydrate Polym.* **1997**, *33*, 177.

(39) Aubry, T.; Bossard, F.; Moan, M. *Polymer* **2002**, *43*, 3375.

(40) Cheng, Y.; Brown, K. M.; Prudhomme, R. K. *Biomacromolecules* **2002**, *3*, 456.

(41) Kastner, U.; Zana, R. *J. Colloid Interface Sci.* **1999**, *218*, 468.

(42) Aubry, T.; Moan, M.; Argillier, J. F.; Audibert, A. *Macromolecules* **1998**, *31*, 9072.

(43) Aubry, T.; Moan, M. *J. Rheol.* **1994**, *38*, 1681.

(44) Aubry, T.; Moan, M. *J. Rheol.* **1996**, *40*, 441.

(45) Aubry, T.; Moan, M. *Rev, Inst. Fr. Petr.* **1997**, *52*, 129.

(46) Bataille, I.; Huguet, J.; Muller, G.; Mocanu, G. *Int. J. Biol. Macromol.* **1997**, *20*, 179.

(47) Deguchi, S.; Kuroda, K.; Akiyoshi, K.; Lindman, B.; Sunamoto, J. *Colloids Surf. A, Physicochem. Eng. Aspects* **1999**, *147*, 203.

(48) Desbrieres, J. *Polymer* **2004**, *45*, 3285.

(49) Philippova, O. E.; Volkkov, E. V.; Sitnikova, N. L.; Khokhlov, A. R.; Desbrieres, J.; Rinaudo, M. *Biomacromolecules* **2001**, *2*, 483.

(50) Nystrom, B.; Kjoniksen, A. L.; Iversen, C. *Adv. Colloid Interface Sci.* **1999**, *79*, 81.

(51) Lee, J.; Gustin, J. P.; Chen, T.; Payne, G. F.; Raghavan, S. R. *Langmuir* **2005**, *21*, 26.

(52) Brugnerotto, J.; Desbrieres, J.; Roberts, G.; Rinaudo, M. *Polymer* **2001**, *42*, 9921.

(53) Esquenet, C.; Terech, P.; Boue, F.; Buhler, E. *Langmuir* **2004**, *20*, 3583.

(54) Esquenet, C. *Propriétés Structurales et Dynamiques des Solutions de Polyelectrolytes Rigides et Semi-Rigides et de Polysaccharides Associatifs*, Thèse Université Joseph Fourier-Grenoble I Sciences et Geographie, **2003**.

(55) Miralles-Houzelle, M. C.; Hubert, P.; Dellacherie, E. *Langmuir* **2001**, *17*, 1384.

(56) Kujawa, P.; Audibert-Hayet, A.; Selb, J.; Candau, F. *J. Polym. Sci: Part B: Polym. Phys.* **2004**, *42*, 1640.

(57) Caputo, M. R. *Etude de la Structure et des Propriétés de Polymères Hydrosolubles associatifs Synthétisés par Copolymerisation Micellaire*, Thèse Université Louis Pasteur, Strasbourg, **2003**.

(58) Volpert, E.; *Copolymères d'Acrylamide et d'Alkylacrylamides: Synthèse, Propriétés Associatives en Solution et Adsorption sur des Silicates*, Thèse Université Louis Pasteur, Strasbourg, **1996**.

(59) Grassl, B.; Francois, J.; Billon, L. *Polym. Int.* **2001**, *50*, 1162.

(60) Branham, K. D.; Davis, D. L.; Middleton, J. C.; McCormick, C. L. *Polymer* **1994**, *35*, 4429.

(61) Bigg, S.; Hill, A.; Selb, J.; Candau, F. *J.Phys.Chem.* **1992**, *96*, 1505.

(62) Bigg, S.; Selb, J.; Candau, F. *Langmuir* **1992**, *8*, 838.

(63) Bigg, S.; Selb, J.; Candau, F. *Polymer* **1993**, *34*, 580.

(64) McCormick, C. L.; Nonaka, T.; Johnson, C. B. *Polymer* **1988**, *29*, 731.

(65) Schulz, D. N.; Bock, J. *J. Macromol. Sci., Chem.* **1991**, *A28*, 1235.

(66) Bock, J.; Pace, S. J.; Schulz, D. N., U.S. Patent 4 709 759 **1987**.

(67) Schulz, D. N.; Kaladas, J. J.; Maurer, J. J.; Bock, J.; Pace, S. J.; Schulz, D. N. *Polymer* **1987**, *28*, 2110.

(68) Chang, Y.; Lochhead, R. Y.; McCormick, C. L. *Macromolecules* **1994**, *27*, 2145.

(69) Vittadello, S. T.; Bigg, S. *Macromolecules* **1998**, *31*, 7691.

(70) Guillaumont, L.; Bokias, G.; Iliopoulos, I. *Macromol. Chem. Phys.* **2000**, *201*, 251.

(71) Vasiliadis, I.; Bokias, G.; Mylonas, Y.; Staikos, G. *Polymer* **2001**, *42*, 8911.

(72) Poncet-Legrand, C.; Winnik, F.M. *Polym. J.* **2001**, *33*, 277.

(73) Kujawa, P.; Ester Goh, C. C.; Winnik, F.M. *Macromolecules* **2001**, *34*, 6387.

(74) Prazeres, T. J. V.; Beingessner, R.; Duhamel, J.; Olesen, K.; Shay, G. D.; Bassett, D. *Macromolecules* **2001**, *34*, 7876.

(75) Tirtaatmadja, V.; Tam, K. C.; Jenkins, R. D. *Macromolecules* **1997**, *30*, 3271.

(76) Tirtaatmadja, V.; Tam, K. C.; Jenkins, R. *AlChe J.* **1998**, *30*, 2756.

(77) English, R. J.; Gulati, H. S.; Jenkins, R.; Khan, S. A. *J. Rheol.* **1997**, *41*, 427.

(78) Caritey, J.-P. *Relation entre la modification chimique de precurseurs hydrophiles d'origine naturelle et leurs propriétés en solution diluée et semi-dilué*, Thèse Université de Rouen, **1994**.

(79) Cathebras, N.; Collet, A.; Viguier, M.; Berret, J.-F. *Macromolecules* **1998**, *31*, 1305.

(80) Feng, Y.; Billon, L.; Grassl, B.; Khoukh, A.; Francois, J. *Polymer* **2002**, *43*, 2055.

(81) Deguchi, S.; Lindman, B. *Polymer* **1999**, *40*, 7163.

(82) Pabon, M.; Corpart, J.-M.; Selb, J.; Candau, F. *J. Appl. Polym. Sci.* **2002**, *84*, 1418.

(83) Pabon, M.; Corpart, J.-M.; Selb, J.; Candau, F. *J. Appl. Polym. Sci.* **2004**, *91*, 916.

(84) Evani, S. Eur. Patent 057 875 **1982**.

(85) Evani, S. U.S. Patent 4 432 881 **1984**.

(86) Evani, S.; Kien, V. P. PCT Int. Appl. WO 85/3510 **1985**.

(87) Kien, V. P.; Evani, S. Eur. Pat. EU 226 097 **1987**.

(88) Bock, J.; Valint, P. L.; Pace, S. J. U.S. Patent 4 702 319 **1987**.

(89) Bock, J.; Siano, D. B.; Turner, S. R. U.S. Patent 4 694 046 **1987**.

(90) Turner, S. R.; Siano, D. B.; Bock, J. U.S. Patent 4 528 348 **1985**.

(91) Turner, S. R.; Siano, D. B.; Bock, J. U.S. Patent 4 520 182 **1985**.

(92) Bock, J.; Siano, D. B.; Kowalik, R. M.; Turner, S. R. Eur. Patent 115 213 **1984**.

(93) Bock, J.; Valint, P. L. U.S. Patent 4 730 028 **1988**.

(94) Hill, A. *Synthèse, Caractérisation et Propriétés de Polyacrylamides s'associant par Interactions Hydrophobes,* Thèse Université Louis Pasteur, Strasbourg, **1991**

(95) Jimenez-Regalado, E.; Selb, J.; Candau, F. *Langmuir* **2000**, 16, 8611.

(96) Jimenez-Regalado, E.; Selb, J.; Candau, F. *Macromolecules* **2000**, 33, 8720.

(97) Volpert, E.; Selb, J.; Candau, F. *Polymer* **1998**, *39*, 1025.

(98) McCormick, C.L.; Johnson, C.B. *Polymers in Aqueous Media: Performance through Association*, Ed.: Glass J.E., Advances in Chemistry Series; American Chemical Society, Washington, DC **1989,** Vol. 223, p.437.

(99) *Stimuli-Responsive Water-Soluble and Amphiphilic Polymers*, Ed.: McCormick, C.L.; ACS Symposium Series 780, American Chemical Society, Washington, DC **2001**.

(100) Ezzell, S.A.; McCormick, C.L. in *Water-Soluble Polymers: Synthesis, Solution Properties and Applications*, Eds.: Shalaby, S.W.; McCormick, C.L.; Butler,

G.B., ACS Symposium Series; American Chemical Society, Washington, DC **1991,** Vol. 467, Chap. 8, p.130.

(101) Camail, M.; Margaillan, A.; Martin, I.; Papailhou, A. L.; Vernet, J. L. *Eur. Polym. J.* **2000**, *36*, 1853.

(102) Meyer, V. *Synthèse et Caractérisation de Polymères Associatifs porteurs de Groupes Siloxanes*, Thèse Université Louis Pasteur, Strasbourg, **1999**.

(103) McCormick, C. L.; Middleton, J. C.; Cummins, D. F. *Macromolecules* **1992**, *25*, 1201.

(104) Ezzell, S. A.; Hoyle, C. E.; Creed, D.; McCormick, C. L. *Macromolecules* **1992**, *25*, 1887.

(105) Flynn, C. E.; Goodwin, J. W. *Polm. Mater. Sci. Eng.* **1989**, *61*, 522.

(106) Guo, L.; Tam, K. C.; Jenkins, R. *Macromol. Chem. Phys.* **1998**, *199*, 1175.

(107) Senan, C.; Meadows, J.; Shone, P. T.; Williams, P. A. *Langmuir* **1994**, *10*, 2471.

(108) Magny, B.; Iliopoulos, I.; Audebert, R. *Polym. Commun.* **1991**, *32*, 456.

(109) Jenkins, R.; Bassett, D.; Silebi, C. A.; El-Aasser, M. S. *J. Appl. Polym. Sci.* **1995**, *58*, 209.

(110) Chang, Y.; McCormick, C. L. *Macromolecules* **1993**, *26*, 6121.

(111) Argillier, J. F.; Audebert, R.; Lecourtier, J.; Moan, M.; Rousseau, L. *Colloids Surf. A, Physicochem. Eng. Aspects* **1996**, *113*, 247.

(112) Branham, K. D.; McCormick, C. L. in *Multidimentional Spectroscopy of Polymers*, Eds.: Urban, M.W.; Provder, T.; ACS Symposium Series, American Chemical Society, Washington, DC **1995**, Vol. 598, Chap.32, p.551.

(113) Branham, K. D.; Snowden, H. S.; McCormick, C. L. *Macromolecules* **1996**, *29*, 254.

(114) Glinel, K.; Huguet, J.; Muller, G. *Polymer* **1999**, *40*, 7071.

(115) Sinquin, A.; Hubert, P.; Dellacherie, E. *Polymer* **1994**, *35*, 3557.

(116) Sinquin, A.; Hubert, P.; Dellacherie, E. *Langmuir* **1993**, *9*, 3334.

(117) Israelachvili, J.; Mitchell, D. J.; Ninham, B. W. *J. Chem. Soc. Faraday Trans.2* **1976**, *72*, 1525.

(118) *Surfactants and Polymers in Aqueous Solution*, Eds.: Lindman, B.; Jonsson, B.; John Wiley & Sons, **1998.**

(119) Candau, S.J.; Hirsch, E.; Zana, R. in *Physics of Complex and Supramolecular Fluids*, Eds.: Safran, S.A; Clark, N.A.; Wiley, N.Y. **1987,** p.569.

(120) In, M.; Aguerre-Chariol, O.; Zana, R. *J. Phys. Chem.* **1999**, *103*, 7747.

(121) Bernheim-Groswasser, A.; Zana, R.; Talmon, Y. *J. Phys. Chem. B* **2000**, *104*, 4005.

(122) Buhler, E. ; Munch, J.P. ; Candau, S.J. *J. Phys. II* **1995**, *5*, 765

(123) Faetibold, E.; Waton, G. *Langmuir* **1995**, *11*, 1972.

(124) Oda, R.; Narayanan, J.; Hassan, P.A.; Manohar, C.; Salkar, R.A.; Kern, F.; Candau, S.J. *Langmuir* **1998**, *14*, 4364.

(125) Kern, F.; Lequeux, F.; Zana, R.; Candau, S.J. *Langmuir* **1994**, *10*, 1714.

(126) Hoffmann, H.; Herb, C.; Prud'homme, R. in *Structure and Flow in Surfactant Solutions*, Eds.: Holland, P.M.; Rubing, D.N.; ACS Symposium Series 578, American Chemical Society, Washington, DC **1994**, Chap.1.

(127) cf. for instance *Introduction to Polymers*, Eds.: Young, R.J.; Lovell, P.A.; Chapman and Hall, New York, **1991.**

(128) Adam, M. ; Lairez, D. ; Raspaud, E. *J. Phys. II France* **1992**, *2*, 2067.

(129) Jimenez-Regalado, E.; Selb, J.; Candau, F. *Macromolecules*, **1999**, *32*, 8580.

(130) Candau, F.; Selb, J. *Adv Colloid Interface Sci*. **1999**, *79*, 149.

(131) Tanaka, F.; Edwards, S.F. *Macromolecules* **1992**, *25*, 1516.

(132) Jenkins, R. D. *The Fundamental Thickening Mechanism of Associative Polymers in Latex Systems: A Rheological Study*, Thesis, Lehigh University, Bethlehem, PA, **1991.**

(133) Annable, T.; Buscall, R.; Ettelaie, R.; Whittlestone, D. *J. Rheol*. **1993**, *37*, 695.

(134) Annable, T.; Buscall, R.; Ettelaie, R. *Colloids Surf. A, Physicochem. Eng. Aspects* **1996**, *112*, 97.

(135) Leibler, L.; Rubinstein, M.; Colby, R. H. *Macromolecules* **1991**, *24*, 4701.

(136) Couillet, I. ; Hughes, T. ; Maitland G. ; Candau, F. ; Candau S.J. *Langmuir* **2004**, *20*, 9541.

(137) Croce, V.; Cosgrove, T. *Langmuir* **2003**,*19*, 8536-8541.

(138) Magid, L.J. *J.Phy. Chem. B* **1998**, *102*, 4064.

(139) Cappelaere, E.; Cressely, R. *Colloid Polym. Sci.* **1998**, *276*, 1050.

(140) Lin, Z. *Langmuir* **1996**, *12*, 1729.

(141) Khatory, A.; Lequeux, F.; Kern, F.; Candau, S. J. *Langmuir* **1993**, 1456.

(142) Cates, M.E. *J. Phys. (Paris)* **1988**, *49*, 1593.

(143) Cates, M.E. *Macromolecules* **1987**, *20*, 2289.

(144) Petschek, R. G.; Pfeuty, P.; Wheeler, J.C. *Phys. Rev.* **1986**, *A34*, 2391.

(145) Cates, M.E.; Candau, S.J. *J. Phys. Condens. Matter* **1990**, *2*, 6869

(146) Rehage, H.; Hoffmann, H. *Mol. Phys.* **1991**, *74*, 933

(147) Hoffmann, H.; Platz, G.; Rehage, H.; Schorr, W. *Adv. Colloid Interface Sci.* **1982**, *17*, 275.

(148) Lobl, M.; Thurn, H.; Hoffmann, H. *Ber Bunsenges Phys. Chem.* **1984**, *88*, 1102.

(149) Hoffmann, H.; Lobl, H.; Rehage, H.; Wunderlich, I. *Tenside Deter* **1985**, *22*, 290.

(150) Thurn, H.; Lobl, H.; Hoffmann, H. *J. Phys. Chem.* **1985**, *29*, 517.

(151) Shikata, T.; Hirata, H.; Kotaka, T. *Langmuir* **1987**, *3*, 1081; **1988**, *4*, 354; **1989**, *5*, 398.

(152) Shikata, T.; Hirata, H.; Takatori, E.; Osaki, K. *J. Non-Newtonian Fluid. Mech.* **1988**, *28*, 171.

(153) Imae, T.; Abe, A.; Ikeda, S. *J. Phys. Chem.* **1988**, *92*, 1548.

(154) Rehage, H.; Hoffmann, H. *J. Phys. Chem.* **1988**, *92*, 4712

(155) Candau, S. J.; Hirsch, E.; Zana, R.; Adam, M. *J. Colloid Interface Sci.* **1988**, *122*, 430.

(156) Candau, S. J.; Hirsch, E.; Zana, E.; Delsanti, M. *Langmuir* **1989**, *5*, 1525.

(157) Messager, R.; Ott, A.; Chatenay, D.; Urbach, W.; Langevin, D. *Phys. Rev. Lett.* **1988**, *60*, 1410.

(158) Kern, F.; Zana, R.; Candau, S.J. *Langmuir* **1991**, *7*, 1344.

(159) Kern, F.; Lemarechal, P.; Candau, S.J.; Cates, M.E. *Langmuir* **1992**, *8*, 437.

(160) Candau, S. J.; Khatory, A.; Lequeux, F.; Kern, F. *J. Phys.IV France* **1993**, *3*, 197

(161) Candau, S.J.; Hirsch, E.; Zana, R. *J. Phys. (Paris)* **1984**, *45*, 1263.

(162) Candau, S.J.; Hirsch, E.; Zana, R. *Colloid Interface Sci.* **1985**, *105*, 521.

(163) Appell, J.; Porte, G.; Poggi, Y. *J. Colloid Interface Sci.* **1982**, *87*, 492.

(164) de Gennes, P.G. *J. Chem. Phys.* **1971**, *55*, 572.

(165) Graessley, W. W. *Adv. Polym. Sci.* **1982**, *47*, 68.

(166) Rouse, Jr. P. E. *J. Chem. Phys.* **1953**, *21*, 1272.

(167) de Gennes, P.G. *Macromolecules* **1976**, *9*, 587.

(168) Doi, M.; Edwards, S. F. *J. Chem. Soc., Faraday Trans. 2* **1979**, *75*, 78.

(169) Semenov, A. N.; Rubinstein, M. *Macromolecules*, **1998**, *31*, 1373.

(170) Rubinstein, M.; Semenov, A.N.; *Macromolecules*, **1998**, 31, 1386.

(171) Rubinstein, M.; Semenov, A. N. *Macromolecules*, **2001**, *34*, 1058.

(172) Ferry, J.D. *Viscoelastic Properties of Polymers*, 3rd Ed.; Wiley, New York, **1980**

(173) Doi, M.; Edwards, S. *The Theory of Polymer Dynamics*, Clarendon Press: Oxford, **1986**.

(174) Turner, M.S.; Cates, M.E. *J. Phys. France*. **1990**, *51*, 307.

(175) Cates, M.E.; Turner, M.S. *Europhys. Lett.* **1990**, *7*, 681.

(176) Turner, M.S.; Cates, M.E. *Langmuir* **1991**, *7*, 1590.

(177) Granek, R.; Cates, M.E. *J. Chem. Phys.* **1992**, *96*, 4758.

(178) Granek, R. *Langmuir* **1994**, *10*, 1627.

(179) Candau, S.J.; Merikhi, F.; Waton, G.; Lemaréchal, P. *J. Phys. France* **1990**, *51*, 977.

(180) Adam. M.; Delsanti. M. *J. Phys. (Paris)* **1985**, *44*, 1760.

(181) Larson, R. G.; *Constitutive Equations of Polymer Melts and Solutions*, Butterworth, Stoneham, **1988.**

(182) Spenley, N. A.; Cates, M. E. *Macromolecules* **1994**, *27*, 3850.

(183) Spenley, N. A.; Cates, M. E.; MacLeish, T. C. B. *Phys. Rev. Lett.* **1993**, *71*, 939.

(184) Spenley, N. A.; Yuan, X. F.; Cates, M. E. *J. Phys. II* **1996**, *6*, 551.

(185) Doi, M.; Edwards, S. F. *J. Chem. Soc. Faraday Trans. 2* **1979**, *74*, 1789, 1802, 1818.

(186) Marrucci, G. *J. Non-Newtonian Fluid Mech.* **1986**, *21*, 329.

(187) Marrucci, G. J.; Grizzuti, N. *Non-Newtonian Fluid Mech.* **1986**, *21*, 319.

(188) Makhloufi, R.; Decruppe, J. P.; Ait-Ali, A.; Cressely, R. *Europhys. Lett.* **1995**, *32*, 253.

(189) Decruppe, J. P.; Cressely, R.; Makhloufi, R.; Cappelaere, E. *Colloid Polym. Sci.* **1995**, *273*, 346.

(190) Mair, R. W.; Callaghan, P. T. *Europhys. Lett.* **1996**, *65*, 241.

(191) Callaghan, P. T.; Cates, M. E.; Rofe, C. J.; Smeulders, J. B. A. F. *J. Phys. II France* **1996**, *6*, 375.

(192) Caputo, M. R.; Selb, J.; Candau, F. *Polymer* **2004**, *45*, 231.

Chapter II

STRUCTURAL AND DYNAMIC PROPERTIES OF ERUCYL BIS-(HYDROXYETHYL)METHYLAMMONIUM CHLORIDE

INTRODUCTION

Under appropriate conditions (salinity, temperature, concentration, presence of counterions), surfactants molecules can self-assemble into long, flexible chains referred to as wormlike micelles[1-3]. If the scission energy of a micelle (the energy required to create two end-caps from a semi-infinite cylinder) is large enough, then the semi-flexible linear micelles may become very long and, similarly to polymers, can form entangled networks in semidilute solutions, giving rise to highly viscoelastic fluids.

The analogy between wormlike micelles and polymers is a subject of debate; many similarities in the rheology and dynamics of the systems have been noted and are reported in the previous chapter.

Unlike polymers, wormlike micelles can break and recombine reversibly, and so are in equilibrium with respect to their molecular weight distribution (this contrasts with ordinary polymers, for which the molecular weight distribution is fixed by the conditions prevailing at the time of the synthesis). The kinetics of micelle breakage and reconnection depends on the surfactant type and the salinity.

In the semi-dilute regime, the osmotic compressibility and the correlation length follow the same power laws with the volume fraction of surfactant, as those observed for classical polymers[1,4-6], while the dynamic properties are more complex. A model derived by Cates[7,8] is commonly used to describe the dynamics of such living polymers. It is based on the reptation model of polymer dynamics but includes the effect of reversible scission kinetics on the viscoelastic behaviour.

In this chapter, we investigate the structural and dynamic properties of the micellar solutions of a cationic surfactant having a long (C_{22}) mono-unsaturated tail, the erucyl bis-(hydroxyethyl)methylammonium chloride (EHAC), blended with 2-propanol, in the presence of KCl, using light scattering and rheological experimental techniques.

The rheological properties of the pure surfactant (not blended with 2-propanol) has been intensively studied by Raghavan and Kaler[9]. Their studies demonstrate that this surfactant has the property to self-assemble into giant wormlike micelles in the presence of either sodium salicylate (binding counterion) or sodium chloride (nonbinding counterion). The solutions exhibit very high relative viscosity ($\eta_r \sim 10^7$) or a gel-like behavior at room temperature, and they retain appreciable viscosity (($\eta_r > 10^4$) for temperatures up to 90°C.

However, much higher concentrations of NaCl are required to produce high viscosities as compared to those obtained by addition of NaSal. In the later case, the salicylate counterions are incorporated between the headgroups and penetrate into the hydrophobic core of the micelles, whereas the Cl^- counterions only exhibit a screening effect. These results make this surfactant a good "fracturing fluid" candidate for which a high temperature resistance is required. In their analysis of the rheological behavior, Raghavan and Kaler have considered surfactant concentrations well above the overlap concentration C^*.

The abnormally high viscosity observed compared to other conventional viscoelastic surfactants is due to the enormous length of the wormlike micelles resulting from a huge end-cap energy ($E_{sciss} = 65 k_B T$ for a 60mM, 30mM NaSal solution, at 25°C). The end-cap energy was determined from the Arrhenius relationship for the total contour length $\bar{L}$ (cf. Chap. I., IV.3.b):

$$\bar{L} \approx \phi^{1/2} \exp(E_{sciss} / 2k_B T) \qquad (1)$$

and from the expression of Granek and Cates[10]:

$$\frac{G''_{\min}}{G_0} \approx \frac{\ell_e}{\bar{L}} \qquad (2)$$

These authors showed that this high value could not be explained by the nature of the headgroup, as they demonstrated that changing the headgroup from EHAC to ETAC (that is from bis(hydroxyethyl)methyl ammonium to trimethylammonium) did not alter the main rheological features but by the nature of the hydrophobic tail. EHAC contains a cis-double bound, which yields a very low Krafft point (<0°C)[11] and leads therefore to a good water solubility. The long (C_{22}) tail is also at the origin of the low C^* value observed for this surfactant.

Some reservations were however made concerning the calculated value of the scission energy that was found far above those reported for C_{16} surfactant micelles ($\cong 20\ k_B T$)[12,13]. Equation (1) is only valid for electrostatically screened micelles. When electrostatic repulsions persist between the surface charges, the E_{sciss} value thus obtained must be

considered as a lower estimate, since it was determined at a low concentration of NaSal, probably insufficient for complete screening.

Contrary to Raghavan and Kaler, we focused our investigation of the rheological behaviour of the EHAC surfactant both in the dilute and semi-dilute regime. We determined the scission energy of EHAC in the semi-dilute regime, at high salt concentrations (KCl), through rheological experiments, using for the first time all the features of the complex shear modulus spectrum, including the Rouse modes, thus providing three independent methods of measurement of the scission energy. We also tried to explain the inconsistency between the high value of the E_{sciss} determined by Raghavan and Kaler and the lower values we obtained, by considering that the free energy of scission could contain a large entropic term, possibly associated with the rearrangement of counterions upon formation of an end-cap[15,16].

A theoretical model of Cates[17] describes the dynamics of living polymers in the semidilute regime taking into account the presence of closed rings that form around C^* in the case of large E_{sciss} values and that affects the excluded volume statistics as well as the scaling exponents for the concentration dependence of the viscosity and monomer diffusion constant. In this chapter, we present a study on the micellar growth induced by an increase of surfactant concentration by comparing for the first time, quantitatively, the experimentally measured concentration dependence of the radius of gyration of the micelles with the mean-field and scaling models derived for linear micelles. We conclude to the presence of large aggregates, possibly rings or microgels, in the vicinity of C^* as already observed for low-ionic strength micellar solutions of surfactants with a large scission energy[8,17].

Aqueous solutions of ionic surfactants can undergo uniaxial growth upon the addition of salt and form an entangled network with a concomitant increase of the solution viscosity. However, a maximum of viscosity is generally observed upon further addition of salt. Several authors[8,18-20] have proposed that the decrease in viscosity observed with further addition of salt might be due to the formation of branched micelles and eventually a multiconnected network in which stress relaxation can occur by the sliding of crosslinks along the wormlike micelles. Thus, the maximum in viscosity with increasing salt concentration may indicate a shift from linear to branched micelles. Branching is expected to occur when the free energy cost associated with the crosslink formation

becomes comparable to that needed for the formation of end caps. A multiconnected micellar network and an entangled micellar network cannot be distinguished from each other directly by scattering techniques such as neutron or light scattering[19]. Cryogenic transmission electron microscopy (cryo-TEM) is a technique that allows a direct visualization of the surfactant aggregates in their aqueous environment. It is the only available technique to unambiguously distinguish between branched and unbranched micelles. Such a technique was recently used by Croce et al. to explore the effect of salt on the micellar shape of the EHAC surfactant[21], since Raghavan and Kaler previously showed[9] that the solutions of this surfactant present a viscosity maximum as a function of salt concentration. Spherical micelles were detected in the salt-free solutions and branched structures were observed above a certain salt concentration that corresponds to the maximum in the low shear viscosity. Croce et al. also observed the presence of loops at low surfactant concentrations (0.5wt%) and for a salt concentration (1wt%) much lower than the one corresponding to the maximum in the low shear viscosity (6wt%). This concentration (0.5wt%) might correspond to the C^* of this surfactant calculated for a 1wt% salt concentration and could confirm the conclusions drew in this chapter regarding the presence of rings in the vicinity of C^*.
The group of Kaler showed[22] that branched micelles may also develop with an increase of temperature and deterioration of the "solvent quality"[23].

The following paper will address all the issues mentioned above.

REFERENCES

(1) Cates, M.E.; Candau, S.J. *J. Phys.: Condens. Matter* **1990**, *2*, 6869.

(2) Cates, M.E. J., *J. Phys.Chem.* **1990,** *94*, 371.

(3) Cates, M.E. *J. Phys.: Condens. Matter* **1996**, *8*, 9167.

(4) Buhler, E.; Munch, J.P.; Candau, S.J. *J. Phys. II* **1995**, *5*, 765.

(5) Candau, S.J.; Hirsch, E.; Zana, R. *J. Phys. (Paris)* **1984**, *45*, 1263.

(6) Candau, S.J.; Hirsch, E.; Zana, R. In *Physics of Complex and Supramolecular Fluids;* Eds.: Safran, S.A.; Clark, N.A; Wiley, New York, N.Y. **1987,** p.509.

(7) Cates, M.E. *J. Phys (Paris)*. **1988**, *49*, 1593.

(8) Cates, M.E. *Macromolecules* **1987**, *20*, 2289.

(9) Raghavan, S.R.; Kaler, E. *Langmuir* **2001**, *17*, 300.

(10) Granek, R.; Cates, M.E. *J. Chem. Phys.* **1992**, *96*, 4758.

(11) Rose, G.D.; Foster, K.L. *J. Non-Newtonian Fluid Mech.* **1989**, *31*, 59.

(12) Candau, S.J.; Hirsch, E.; Zana, R.; Delsanti, M. *Langmuir* **1989**, *5*, 1225.

(13) Soltero, J.F.A.; Puig, J.E. *Langmuir* **1996**, *12*, 2654.

(14) Kern, F.; Lequeux, F.; Zana, R.; Candau, S.J. *Langmuir* **1994**, *10*, 1714.

(15) Kern, F.; Zana, R.; Candau, S.J. *Langmuir* **1991**, *7*, 1344.

(16) Oelschlaeger, Cl.; Waton, G.; Candau S.J. *Langmuir* , **2003**.

(17) Cates, M.E. *J. Phys (Paris)*. **1988**, *49*, 1593.

(18) Magid, L.J. *J. Phys. Chem. B* **1998**, *102*, 4064.

(19) Lin, Z. *Langmuir* **1996**, *12*, 1729.

(20) Khatory, A. ; Lequeux, F. ; Candau, S.J. *Langmuir* **1993**, *9*, 1456.

(21) Croce, V.; Cosgrove, T.; Maitland, G.; Hughes, T.; Karlsson, G. *Langmuir* **2003**, *19*, 8536.

(22) Raghavan, S.R.; Edlund, H.; Kaler. E. *Langmuir* **2002**, *18*, 1056.

(23) Schubert, B.A.; Wagner, N.J.; Kaler, E. *Langmuir* **2004**, *20*, 3564

GROWTH AND SCISSION ENERGY OF WORMLIKE MICELLES FORMED BY A CATIONIC SURFACTANT WITH LONG UNSATURATED TAILS

PUBLICATION 1

(*Langmuir* **2004**, *20*, 9541-9550)

GROWTH AND SCISSION ENERGY OF WORMLIKE MICELLES FORMED BY A CATIONIC SURFACTANT WITH LONG UNSATURATED TAILS

Isabelle Couillet[(*)]*, Trevor Hughes and Geoffrey Maitland*

Schlumberger Cambridge Research, High Cross, Madingley Road Cambridge, CB3 OEL, U.K.

Françoise Candau

Institut Charles Sadron, UPR 22 du CNRS, 6 rue Boussingault, F-67083 Strasbourg Cedex, France.

S. Jean Candau

Laboratoire de Dynamique des Fluides Complexes, U.M.R. n°7506, Université Louis Pasteur, C.N.R.S., 4 rue Blaise Pascal, 67070 Strasbourg Cedex, France.

*couillet@cambridge.oilfield.slb.com

ABSTRACT

The structural and dynamic properties of micellar solutions of erucyl bis(hydroxyethyl)methylammonium chloride (EHAC) blended with isopropanol, in the presence of KCl, have been investigated by means of light scattering and rheological experiments. In the dilute regime, the micellar growth is larger than expected from mean field or scaling models. The results obtained in the vicinity of the overlap concentration suggest the presence of large aggregates, with size >100 nm, possibly micellar rings or microgels. In the semi-dilute regime, the relationship between the zero shear viscosity and the surfactant concentration is described by a power law with an exponent in agreement with the mean field model of linear micelles. The methods based on the analysis of the temperature dependence of the complex shear modulus to provide a measure of the scission energy are discussed.

Introduction

Flexible elongated surfactant micelles can be considered as model systems for the study of reversibly breakable polymers[1,2]. If the scission energy of a micelle (the energy required to create two end-caps from a semi-infinite cylinder) is large enough, then the semi-flexible linear micelles may become very long and entangled at relatively low total volume fractions of surfactant. In this semi-dilute regime, the osmotic compressibility and correlation length follow the same power laws with the volume fraction of surfactant as is observed for classical polymers[1,3-5], while the dynamic properties are more complex. This is due to the self-assembling nature of the micelles that can be considered as equilibrium polymers undergoing a reversible breakdown. A model based on the reptation theory which describes the rheological properties of entangled polymeric chains but including the effects of reversible scission kinetics has been derived by Cates[6,7]. A wide range of viscoelastic data appears to support this model.

Worm-like micelles can be used as thickening and rheology-control agents in aqueous systems. Recently, they have been applied for drag reduction[8,9] or oil field fluids[10,11]. One advantage of these systems over the polymer solutions is that they reform after breaking under shear, making them stable in applications where high shear rates are used.

The recovery of hydrocarbons from subterranean formations can be accomplished by a fracturing process using wormlike micelles based fluids. Their main functions are to open the fracture and to transport the propping agent along the length of the fracture. The fluid should be highly viscous, but it should also exhibit low friction pressure during pumping, provide good fluid-loss control, clean-up rapidly once the treatment is over and be as economical as practical. Many different types of fluids have been developed to provide these properties. Polymer solutions are the most popular fracturing fluids but they offer some disadvantages. Recently a new class of fracturing fluids based on viscoelastic surfactants has been developed. Compared to conventional polymer-based treatment fluids, the viscoelastic surfactant fluids have the advantage that they do not clog the pore space in the proppant and so improve the fracture clean-up[12]. This is facilitated by the responsive nature of the VES-based fluids, in that their worm-like micellar structure is broken on contact/mixing with the produced fluids, resulting in a low viscosity fluid. Cationic surfactants with long (C_{22}) mono-unsaturated tails were shown to be efficient fracturing fluids[14]. In particular aqueous solutions of erucyl bis

(hydroxyethyl) methyl ammonium chloride (EHAC) in the presence of sodium or potassium chloride exhibit appreciable viscosities up to high temperatures (c.a. 80°C). In the presence of sodium salicylate, the effect is even enhanced[13].

In this paper, we report light scattering and rheology measurements on micellar solutions of a blend of EHAC and isopropanol, in the presence of KCl. The presence of isopropanol allows a storage of the surfactant under a liquid form, which is required for the applications. These experiments allowed us to investigate the connection between static and dynamic properties of the systems. Above the crossover concentration C^*, the viscoelastic properties of the entangled micellar network are well described by the Cates model[6,7]. From the temperature dependence of the complex modulus, we have determined the scission energy of the micelles using three different procedures that led to self-consistent results. Light scattering measurements show that in the semi-dilute regime, the scattered intensity and the correlation length obey the scaling behaviour observed for classical polymers. In contrast, below C^*, the scattering data are not consistent with the mean-field model of micellar growth. The results suggest the presence of very large aggregates, possibly micellar rings, that is predicted for systems with a large scission energy[6,7].

Theoretical background

The main features of the theoretical models describing both equilibrium and dynamic properties of wormlike micelles can be found in refs. 6 and 7. Here we simply recall the theoretical results that are needed to discuss our experiments, more specifically regarding the shape of the stress relaxation.

a) Equilibrium properties

The mean-field models[1,15] predict that *c(L)*, the number density of elongated micelles of length *L*, is exponential with some mean length, $\bar{L}$ (*L* being expressed in monomer units)

$$c(L) \sim \frac{1}{\bar{L}^2} \exp(-L/\bar{L}) \qquad (1)$$

With

$$\bar{L} = \Phi^{1/2} \exp(E_{sciss}/2k_BT) \qquad (2)$$

where Φ is the surfactant volume fraction and E_{sciss} is the scission energy of the micelle, that represents the excess free energy for a pair of hemispherical endcaps relative to a rodlike region containing an equal number of surfactants. The above relationships have been derived for nonionic micelles or ionic micelles at large ionic strength.

Benoit and Doty have calculated the unperturbed radius of gyration of wormlike chains in dilute solution as a function of the total contour length $\bar{L}$ and the persistence length l_p [16]:

$$R_G^2 = \frac{(\bar{L} l_p)}{3} - l_p^2 + \frac{2l_p^3}{\bar{L}} - \frac{2l_p^4}{\bar{L}^2}\left[1 - \exp\left(\frac{-\bar{L}}{l_P}\right)\right] \qquad (3)$$

The above expression serves as a bridge between the rod limit where $l_p \gg \bar{L}$ and $R_G^2 = \bar{L}^2/2$ and the random coil limit where $\bar{L} \gg l_p$ and $R_G^2 = \bar{L} l_p/3$.

The concentration dependencies of R_G for linear wormlike micelles in the two limits given above are obtained by using Eq.(2)

$$R_G \sim \Phi^{1/2} \quad \text{if} \quad \bar{L} \ll l_p$$
$$\qquad (4)$$
$$R_G \sim \Phi^{1/4} \quad \text{if} \quad \bar{L} \gg l_p$$

The above expressions are meant for the unperturbed radius of gyration. In the presence of excluded volume, the exponents of the power laws above are slightly modified (from 0.5 to 0.6 for $l_p \gg \bar{L}$ and from 0.25 to 0.3 for $\bar{L} \gg l_p$).

A scaling approach of the equilibrium properties of semi-dilute solutions of wormlike micelles has been developed by Cates[6,7]. If the system consists only of linear micelles, Eqs.(1) and (2) still apply, with however a slightly different value for the exponent of the variation of $\bar{L}$ with Φ:

$$\bar{L} \sim \Phi^{\sim 0.6} \exp(E_{sciss}/2k_BT) \quad (5)$$

According to the theory developed in ref. 6 and references therein, Eqs.(1) and (2) or (5) should apply in the concentration regime $\Phi \geq \sim 2\Phi^*$. It is found that, for large E_{sciss} (20-30 k_BT), micellar rings are invariably present below and around C^* [6,7]. The very long chains that would exist can gain entropy by fragmenting into numerous smaller rings, without having to pay a large free energy penalty to make linear chains of the same length. In the limit of an infinite scission energy, the surfactant would form a cascade of micellar rings with a ring size distribution given by a power law times exponential, which is much broader than the exponential alone and a cut off in the low size range, at a contour length of about twice the persistence length l_p. For a finite, but high value of the scission energy, both open chains and rings should be present in the system. The presence of such rings has been reported around the overlap threshold in a few systems[17,18]. In one of them, only rings were present, and their size distribution was found to agree with the theoretical prediction[17].

Around C^*, the size of the largest rings gives a correlation length that diverges smoothly, then the system transforms into a solution of entangled linear micelles, and the micellar growth behaviour described by Eqs.(1) and (2) or (5) is recovered. In that regime, the micellar system has similar properties to that of a semi-dilute polymer solution. In particular, the scattered intensity $I_{q\to 0}$ and the correlation length ξ, obey the following scaling laws to dilution[3-5,19]:

$$I_{q\to 0} \sim \Phi^{0.25}$$
$$\xi \sim \Phi^{0.75} \quad (6)$$

b) Dynamic properties

Cates et al. have considered two types of processes[20-22]:

(i) One process considered was the reversible unimicellar scission, characterized by a temperature-dependent rate constant, k per unit time per unit arc length, which is the same for all elongated micelles and is independent of time and volume fraction. Such assumptions are strictly valid in the entangled regime when reaction rates are determined

by the local motion of chain sub-sections and not the diffusion of polymers over distances large compared to their gyration radii. The micelle breaking time τ_b is found to be given by:

$$\tau_b = (k\bar{L})^{-1} \quad (7)$$

The temperature and volume fraction dependencies of τ_b are obtained by combining Eqs.(2) and (7):

$$\tau_b \approx k^{-1}\, \Phi^{-1/2} \exp(-E_{sciss}/2k_BT) \quad (8)$$

The derivation of Eq.(4) assumes fully screened electrostatic effects and no excluded volume effect. In Eq.(8), k is found experimentally to be strongly temperature dependent (it increases with temperature) and both k and E_{sciss} vary with the nature and the content of added salt.

(ii) The other process considered was the bimicellar end interchange process where a free micellar end brings about the rupture of a micelle away from its ends and combines simultaneously with one of the two free ends resulting from the rupture, the other end remaining free. The associated breaking time is given by:

$$\tau'_b \approx (k'\Phi)^{-1} \quad (9)$$

where k' is the rate constant for the end interchange process.

Another possible bimicellar reaction scheme involves an interbond exchange.

In systems where both bimicellar and unimicellar processes are simultaneously present, the breaking time which is relevant for the stress-relaxation experiments (see below) will be the fastest one.

c) Stress relaxation

In the linear regime, the model predicts several rheological regimes, depending on the relative rates of diffusive polymer motion and reversible breakdown processes.

In particular, a nearly single exponential stress decay function is predicted in the limit where the micelle breaking time is short, compared to the reptation time τ_{rep} of a micelle of length equal to the average micellar length.

The stress relaxation is then characterized by a new intermediate time scale, T_R,

$$T_R = (\tau_b \ \tau_{rep})^{1/2} \tag{10}$$

At low frequencies, the behaviour of the liquid is Maxwellian, which is described by the equations

$$G'(\omega) = G_0(\omega T_R)^2/(1+\omega^2 \ T_R^2)$$

$$G''(\omega) = G_0\omega T_R/(1+\omega^2 \ T_R^2) \tag{11}$$

where G_0 is the plateau modulus. The Cole-Cole representation in which the imaginary part $G''(\omega)$ of the frequency dependent shear modulus is plotted against the real part $G'(\omega)$ can be used to get an estimate of the relaxation time, T_R. The Maxwellian behavior is ascertained by a semicircular shape of the Cole-Cole plot $G''(G')$, but deviations from the half circle occur at a circular frequency, ω, of the order of the inverse of the breaking time of the micelles.

In the opposite limit $\tau_b \gg \tau_{rep}$, the stress relaxation is a stretched exponential with a terminal time $T_R = \tau_{rep}$. Detailed results were obtained from a computer simulation by Turner and Cates [20-22] and from a Poisson renewal model by Granek and Cates[23] for various values of the ratio $\zeta = \tau_b/\tau_{rep}$ including the intermediate regime $\tau_b \cong \tau_{rep}$. The calculated Cole-Cole plots give the correspondence between the values of ζ and $\bar{\zeta} = \tau_b/T_R$, which provides a measurement of τ_b by a comparison procedure between experimental and calculated Cole-Cole plots. The Eq.(10) can be rewritten under the form:

$$T_R = (\zeta^{1/2}/\bar{\zeta})(\tau_b \ \tau_{rep})^{1/2} \tag{12}$$

with $(\zeta^{1/2}/\bar{\zeta}) \rightarrow 1$ as τ_b/τ_{rep} decreases. The Poisson renewal model was also applied to study the regimes that arise for a small breaking time, and/or small time scales when the

dominant polymer motion is not reptation but either breathing (which arises from the tube length fluctuations) or the local Rouse-like motion (arising from regions of chain shorter than the entanglement length, ℓ_e).

A typical signature of the latter effect is a turnup of both $G'(\omega)$ and $G''(\omega)$ at high frequency, whereas the simple reptation picture predicts a constant asymptote for $G'(\omega)$ and a decreasing $G''(\omega)$. This results in a minimum in the Cole-Cole representation of the dynamic modulus, whose depth can be used to estimate the number of entanglements per chain in the system. The above model applies strictly to systems of entangled wormlike micelles with an entanglement length (i.e. the contour length ℓ_e between two successive entanglements) much larger than the persistence length l_p and in a regime where the breaking time is much larger than the Rouse time τ_e of a chain with the entanglement length.

Under these conditions the dip in the Cole-Cole plot was found theoretically to obey the relationship[23]:

$$\frac{G''_{\min}}{G_0} \sim \frac{\ell_e}{\bar{L}} \tag{13}$$

where G_0 is the plateau modulus. The frequency ω_m corresponding to the minimum of G'' was assumed to be:

$$\omega_m \cong \tau_e^{-1} \sim \tau_o^{-1} \ell_e^2 \sim \eta_s \ell_p \ell_e \tag{14}$$

where τ_o is a microscopic time, proportional to the solvent viscosity η_s and the persistence length l_p [19].

Later on, the scaling behaviour of the dip was reexamined by Granek, using both an analytical and a numerical procedure[24]. In the regime, usually encountered $\tau_b \gg \omega_m^{-1}$, his analysis leads to different expressions of $G''_{\min}/G_0$, and ω_m:

$$G''_{\min}/G_0 \sim (\ell_e/\bar{L})^{4/5} \tag{15}$$

$$\omega_m \sim (\frac{\ell_e}{\overline{L}})^{4/5} \tau_e^{-1} \quad (16)$$

Note that the above expressions are the same as for regular polymers. This is due to the fact that the dip occurs in a range of frequencies much higher than τ_b^{-1}.

An interesting consequence of Eq.(10) concerns the effect of temperature. The three characteristic times involved in Eq.(10) are expected to follow Arrhenian laws of the form $\exp(E/k_B T)$. This leads to the following relationship of T_R in terms of the activation energies, E_b, and E_{rep} corresponding respectively to the temperature dependences of τ_b and τ_{rep}:

$$T_R \sim \exp\left(\frac{E_b + E_{rep}}{2k_B T}\right) \quad (17)$$

The above expression is valid under the condition τ_b « τ_{rep} or $\zeta/\overline{\zeta}^2$ temperature independent.

The reptation theory predicts that $\tau_{rep} \sim \overline{L^3}\,\tau_o$. The temperature dependence of η_s, characterized by an activation energy E_{η_s} is generally neglected in the analysis of the data. In fact, as seen later, it turns out that it is not negligible when determining the scission energy T_R is then given by:

$$T_R \sim \exp\frac{E_b}{2k_B T} \exp\frac{3E_{sciss}}{4k_B T} \exp\frac{E_{\eta_s}}{2k_B T} \quad (18)$$

Equation 18 has been used to obtain E_{sciss} for wormlike micelles from rheological and T-jump data[1,25].

The modified reptation model developed by Cates can also be used to predict the dependence of the terminal time T_R on the surfactant volume fraction. The reptation theory of semi-dilute polymer solutions in good solvents predicts that[19]:

$$\tau_{rep} \cong \overline{L}^3 \xi^{-6} \phi^{-3} \tau_o \quad (19)$$

Combining Eq.(2) with Eqs.(6) and (19) yields:

$$\tau_{rep} \cong \phi^3 \tag{20}$$

Then inserting Eqs.(20) and (8) in Eq.(10), using the mean field exponent 0.5 gives:

$$T_R \cong \phi^{5/4} \tag{21}$$

The zero-shear viscosity η_0 is related to the terminal time and to the plateau modulus G_0 through:

$$\eta_0 = G_0 T_R \tag{22}$$

For semi-dilute polymer solutions in good solvents, it has been shown that[26]:

$$G_0 \cong k_B T \phi^{9/4} \tag{23}$$

This relation has been shown to hold for polymer-like surfactant systems[1,2,27]. The combination of Eqs.(21-23) gives:

$$\eta_0 \cong \phi^{3.5} \tag{24}$$

In the scaling approach with $\overline{L} \cong \phi^{0.6}$, one obtains:

$$\eta_0 \cong \phi^{3.6} \tag{25}$$

Materials and Methods

a) Materials

The erucyl bis-(hydroxyethyl)methylammonium chloride (EHAC) is a C_{22} surfactant with a cis unsaturation at the 13-carbon position. Its chemical structure is shown below. It is supplied by Akzo Nobel, Chicago, IL. It is used in the form of a liquid

blend of the quaternary ammonium salt with 25wt% isopropanol (I.P.A). Upon dilution, the ratio IPA/EHAC is maintained constant. Therefore the content of IPA in water varies from 0.014% for [EHAC] = 1 mM to 1.4% for [EHAC] = 100 mM.

The concentration of the EHAC samples reported in the text correspond to the active surfactant (i.e. after correction of the 25wt% I.P.A. added in the blend). Note that a few experiments were also performed with I.P.A.-free EHAC, denoted $EHAC_p$.

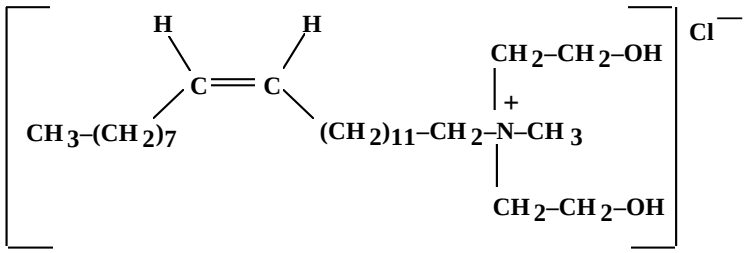

Potassium chloride was supplied from Aldrich.

Solutions containing surfactant and salt were prepared using deionised water.

b) Static Light scattering (SLS)

For light scattering experiments, all solutions were filtered through a 0.22µm Millipore (Sartorius) filter into the cylindrical scattering cells.

In the SLS experiments, the excess of scattered intensity *I(q)* was measured with respect to the solvent, where the magnitude of the scattered wave vector *q* is given by:

$$q = \frac{4\pi n}{\lambda} \sin\frac{\theta}{2} \qquad (26)$$

In Eq.(26), n is the refractive index of the solvent (1.34 for water at 25°C), λ is the wavelength of light in the vacuum, and θ is the scattering angle. In our experiments, the scattering angle θ was varied between 20° and 150°, which corresponds to scattering wave vectors q in the range from 6×10^{-3} to 3.2×10^{-2} nm^{-1}.

c) Dynamic Light scattering

Dynamic light scattering (DLS) experiments were performed on a standard setup by means of a spectrometer equipped with an argon ion laser (Spectra Physics model 2020) operating at λ 488 nm, an ALV-5000 correlator (ALV, Langen-Germany Instruments), a computer-controlled and stepping-motor-driven variable angle detection system, and a temperature-controlled sample cell. The temperature was 25 ± 0.1°C. The scattering spectrum was measured through a band-pass filter (488 nm) and a pinhole (200μm for the static experiments and 100μm for the dynamic experiments) with a photomultiplier tube (ALV).

In the dynamic light scattering experiments, the normalized time autocorrelation function $g^{(2)}(q,t)$ of the scattered intensity is measured.

$$g^{(2)}(q,t) = \frac{\langle I(q,0)I(q,t)\rangle}{\langle I(q,0)\rangle^2} \tag{27}$$

The latter can be expressed in terms of the field autocorrelation function or equivalently in terms of the autocorrelation function of the concentration fluctuations $g^{(1)}(q,t)$ through:

$$g^{(2)}(q,t) = A + \beta\left|g^{(1)}(q,t)\right|^2 \tag{28}$$

where A is the baseline and β is the coherence factor which in our experiments is equal to 0.7-0.9. The normalized dynamical correlation function $g^{(1)}(q,t)$ of polymer concentration fluctuations is defined as:

$$g^{(1)}(q,t) = \frac{\langle \delta c(q,0)\delta c(q,t)\rangle}{\langle \delta c(q,0)^2\rangle} \tag{29}$$

where $\delta c(q,t)$ and $\delta c(q,0)$ represent fluctuations of polymer concentration at time t and zero, respectively.

In the case of a diffusive process, $g^{(1)}(q,t)$ is given by:

$$g^{(1)}(q,t) = \exp(-t/\tau) \tag{30}$$

with $\tau = Dq^2$, where D is the diffusion coefficient.

The apparent hydrodynamic radius R_H of the diffusive particles is given by:

$$R_H = \lim_{q\to 0} \frac{k_B T}{6\pi\eta_0 D} \tag{31}$$

where η_0 is the viscosity of the solvent.

d) Rheology

Rheological experiments were performed with a Bohlin CVO rheometer. Steady state measurements were done under controlled stress or controlled rate depending on the sample viscosity using the cup and bob geometry (coaxial cup, 25mm diameter bob) or a double gap cell (inner diameter 40mm, outer diameter 50mm) depending on the sample viscosity. The shear rate was varied between 10^{-3} s^{-1} and 100 s^{-1}. Dynamic rheological experiments were carried out with the same rheometer using the coaxial cup cell. The frequency was varied between 10^{-3} Hz and 5 Hz under a maximum shear stress of 0.7 Pa. The cell was heated by a reservoir of fluid circulating from a high temperature bath. A metallic cover was placed on the top of the sample to minimize sample evaporation. The sample was equilibrated for at least 15 min at each temperature prior to conducting experiments. Both steady and dynamic rheological experiments were performed at different temperatures. The frequency spectra were conducted in the linear viscoelastic regime of the samples, as determined previously by dynamic stress sweep measurements.

e) Analysis of the complex modulus data

Figure 1 shows a typical Cole-Cole plot where *G'* and *G"* have been normalized by the value of *G"* at the maximum. The ratio $\zeta = \tau_b/\tau_{rep}$ can be obtained from the analysis of the very early departure from the osculating semicircle at the origin. This is done by superimposing to the experimental data the theoretical normalized Cole-Cole

plots that disregard nonreptative high-frequency effects, calculated numerically for different values of ζ [21,22,28]. This is illustrated in Figure 1 which shows the Cole-Cole plot obtained for a solution of EHAC at a 14.4 mM active concentration with 400mM KCl at T = 15°C, together with 3 calculated ones, the best fit being obtained for $0.13 < \bar{\zeta} < 0.3$. Note the departure in the high-frequency range, due to non-reptative effects. The low-frequency data or low-shear measurements yield the zero-shear viscosity.

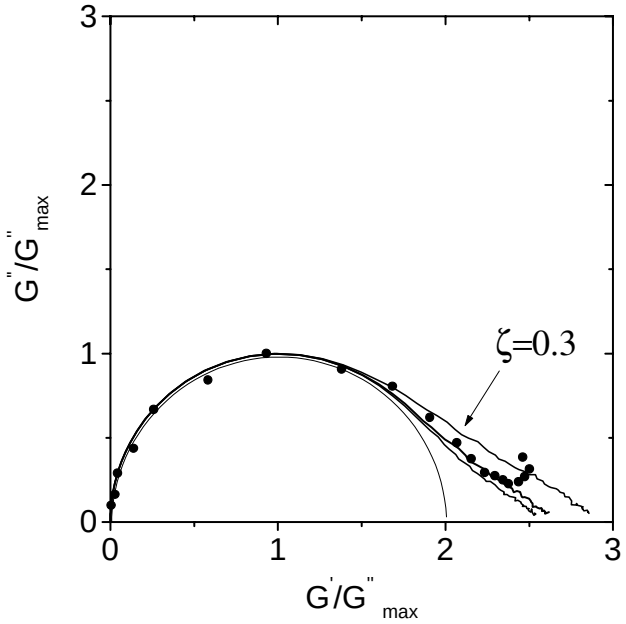

Figure 1: *Normalized Cole-Cole plot for a 14.4 mM EHAC solution, with 400mM KCl at T=15℃. The corresponding values of* $\bar{\zeta}$ *are (0.7, 0.8 and 1.2). The lines are the calculated Cole-Cole plots for different values of the parameter* ζ *(0.1, 0.13 and 0.3). The solid line represents the osculating semicircle at the origin.*

For quasi-Maxwellian systems, the plateau modulus and the terminal relaxation time can be estimated from $G'(\omega_R)$, where ω_R is the frequency at which $G'(\omega)$ and $G''(\omega)$ cross each other. $G_0 = 2G'(\omega_R) = 2G''_{max}$ and $T_R = (\omega_R)^{-1}$.

In all cases the zero-shear viscosity directly measured coincided within 10% with that obtained from $\eta_0 = G_0 T_R$.

The determination of τ_b was made by combining the measurements of T_R and $\bar{\zeta}$.

Results

a) Concentration regimes of wormlike micellar solutions

The overlap concentration C^* of the wormlike micelles, defining the crossover between the dilute and semi-dilute regimes, respectively, can be determined by means of different techniques including static and dynamic light scattering[3-5], T-Jump[29] and rheological measurements[28,30-33]. Among these techniques, the rheology is particularly well adapted. In the dilute regime, as the micelles are far apart from each other, the zero-shear viscosity is very low, of the order of that of water. In the semi-dilute regime beyond the overlap concentration C^*, the systems form an entangled mass of cylindrical micelles and the zero-shear viscosity increases sharply with concentration[28,30-33]. The zero-shear viscosity can be obtained both from the low frequency limit of the complex viscosity $\eta^*(\omega)$ and the zero-shear limit of the steady shear viscosity.

Figure 2 shows the comparison between the dynamical and the steady-shear viscosity for a EHAC sample at an active concentration of 8.8 mM, at a temperature T = 25°C and in the presence of 400 mM KCl. According to the Cox-Merz rule, these two functions were found to coincide for entangled solutions of polymers. For viscoelastic surfactant systems, dynamic and steady shear viscosities were reported to deviate from each other in the shear thinning regime, i.e. at $\dot{\gamma} T_R < 1$ [2]. These deviations seem to become more pronounced as the surfactant concentration is increased. They have been attributed to the occurrence of an isotropic-nematic transition induced by the flow[34]. The results reported in Fig.2 refer to highly diluted sample. No significant deviations within the experimental accuracy were observed in the $\dot{\gamma}$, ω range investigated. It is likely that at very low concentration, much larger shear rates are requested to produce an important effect of the orientation of the wormlike micelles.

Flow experiments were performed on EHAC as a function of surfactant concentration, temperature and KCl content. Also the behaviours of $EHAC_p$ and EHAC were compared.

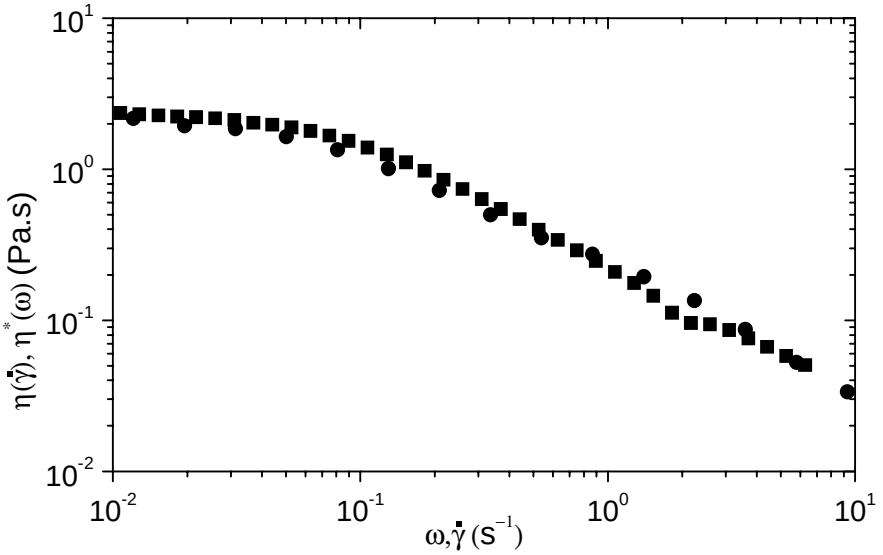

Figure 2: *Steady-state values of the shear viscosity $\eta(\dot{\gamma})$ as a function of shear rate ($\dot{\gamma}$) (●) and magnitude of the complex viscosity ($\eta^*(\omega)$) as a function of the angular frequency (ω) (■), for a 8.8 mM EHAC solution, with 400 mM KCl at T=25°C.*

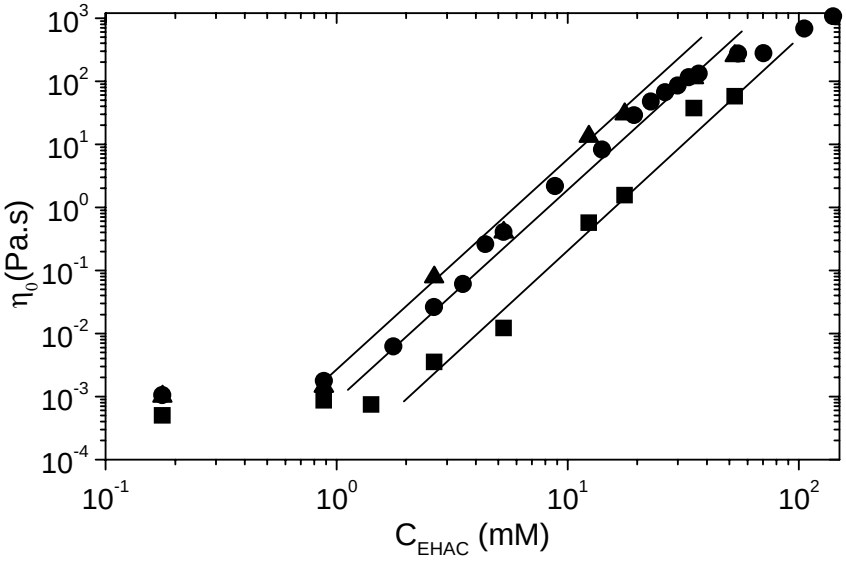

Figure 3: *Variation of the zero-shear viscosity versus EHAC concentration with 400mM KCl, at 15℃ (▲), 25℃ (●) and 50℃ (■). The straight lines are the best fits to the data.*

In Fig.3 are reported in log-log scales the variations of the zero-shear viscosity obtained from steady flow measurements with the total surfactant concentration for three EHAC solutions at different temperatures. One observes at each temperature a net break at a concentration C^* that increases with temperature.
Beyond C^*, the zero shear viscosity follows a power law with the concentration except at high concentrations ($C \geq 10\ C^*$) for which the variation of η_0 with C is less steep.

We have also investigated the effect of the salt concentration on C^*. The variations of C^* with 10^3/T for three potassium chloride concentrations are reported in Fig.4. The temperature dependence of C^* is much stronger for the low KCl content than for the systems with [KCl] ≥ 400 Mm. In correlation with this behaviour, it must be noted that the zero-shear viscosity measured at a given surfactant concentration exhibits a maximum in the vicinity of [KCl] = 400 mM (cf. Fig.5)[35,36]. Therefore, all the light scattering and the linear viscosity experiments reported below have been performed in the presence of 400 mM KCl.

It must also be noted that for pure EHAC, the maximum of the zero shear viscosity upon varying the salt concentration is obtained for a higher KCl concentration**,** namely 800mM. In Fig.6 are compared the variations of the zero-shear viscosity versus active surfactant concentration for both EHAC and $EHAC_p$ at salt concentrations corresponding to the maximum of η_0. Interestingly, the presence of I.P.A reduces the values of C^* (C^*_{EHAC}=1.2mM and C^*_{EHACp}=1.9mM). The localization of small amounts of I.P.A. at the micellar interface could be possibly the origine of this effect.

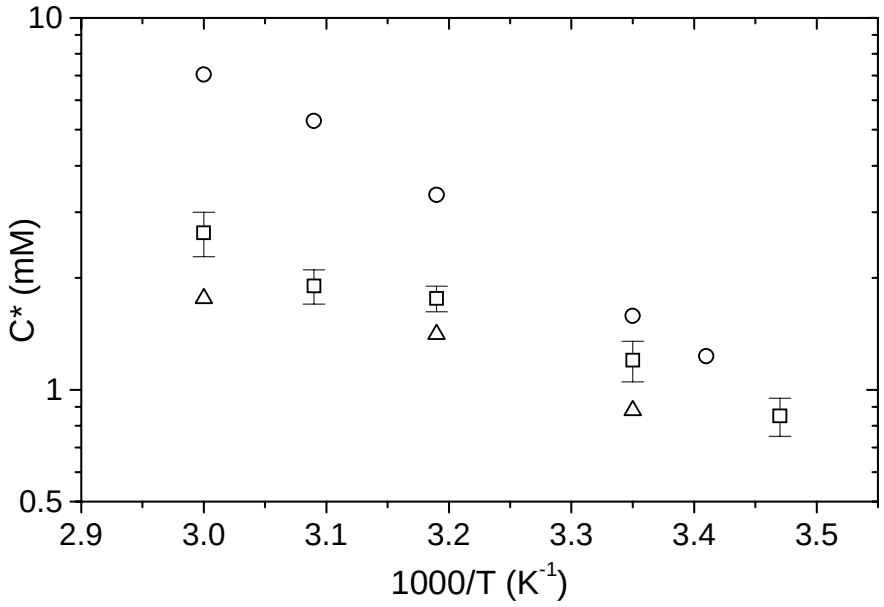

Figure 4: *Semi-log plots of C^* versus $10^3/T$ for EHAC solutions with 133.3 mM KCl (o), 400 mM KCl (□) and 666.6 mM KCl (Δ).*

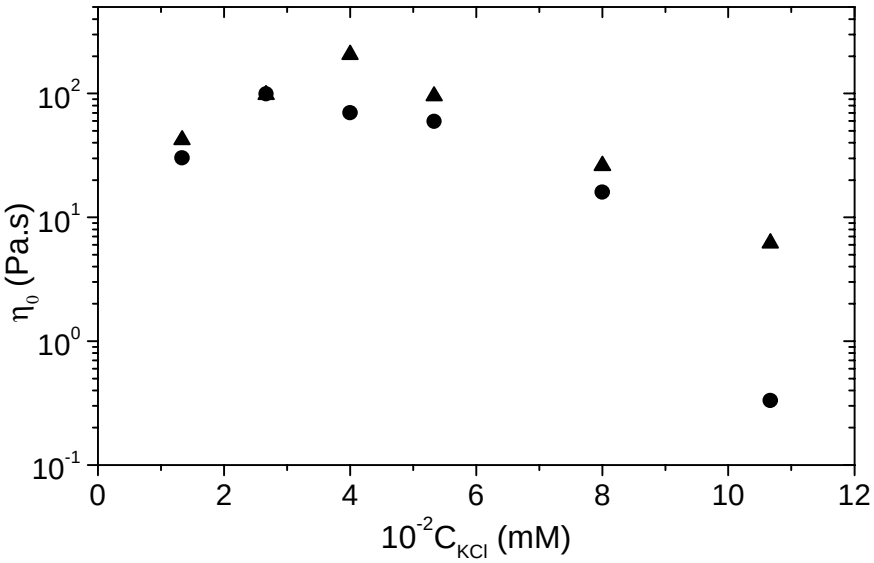

Figure 5: *Variation of the zero-shear viscosity versus KCl concentration for 105.6 mM (▲) and 70.4 mM (●) EHAC solutions at T = 25 ℃.*

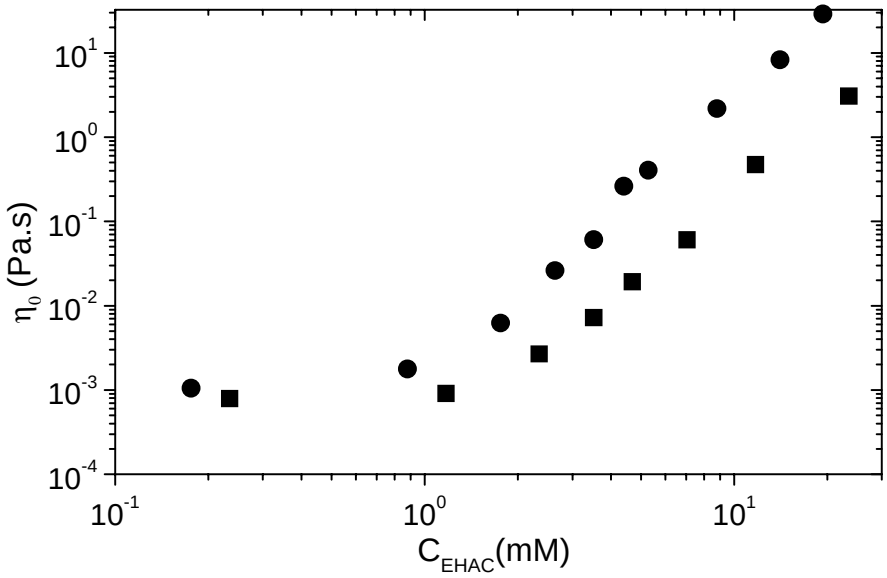

Figure 6: *Variations of the zero-shear viscosity versus active EHAC concentration for $EHAC_p$ (■) (800mM) and EHAC (●) (400mM) at T=25°C.*

b) Static light scattering

Plots of $I(q)^{-1}$ versus q^2 were extrapolated to q = 0 to give intercepts $I(0)^{-1}$. The average static correlation length ξ was determined from the slope of these plots using the Ornstein-Zernike law:

$$I(q)^{-1} = I(0)^{-1}[1 + q^2\xi^2] \tag{32}$$

In dilute solutions, the average radius of gyration of the micellar aggregates is given by:

$$R_G = \xi\sqrt{3} \tag{33}$$

Figure 7 shows typical scattering curves obtained for systems with active EHAC concentrations respectively equal to 0.35 mM ($C/C^* \cong 0.3$); 1.4mM ($C/C^* \cong 1$) and 14.4 mM ($C/C^* \cong 8$) in the presence of 400mM KCl. The downwards curvature displayed by the I^{-1} versus q^2 plots for the solution at C/C^* ~1, indicates a marked polydispersity of the

sample, with the presence of rather large scattering objects. Similar behaviours were reported for other wormlike micellar systems in the vicinity of C^*, where the micelles are expected to be the largest[4,5].

The curvature tends to disappear for systems whose concentrations are far apart on either side of C^*. This is due to the fact that, at high dilution, the particles are smaller and therefore the scattering curves are less sensitive to the polydispersity, whereas at concentrations $C \gg C^*$, the scattering is controlled by the correlation length that is independent of micellar length. From the slopes of the low q-range linear parts of the plots $I(q)^{-1}$vs q^2, one determines the correlation length ξ. The concentration dependences of ξ and of $I(0)$ are reported in Figs.8 and 9 respectively. Both parameters exhibit a maximum at a concentration of 1.75 mM, that is a value close to the crossover concentration C^* determined by viscosimetry.

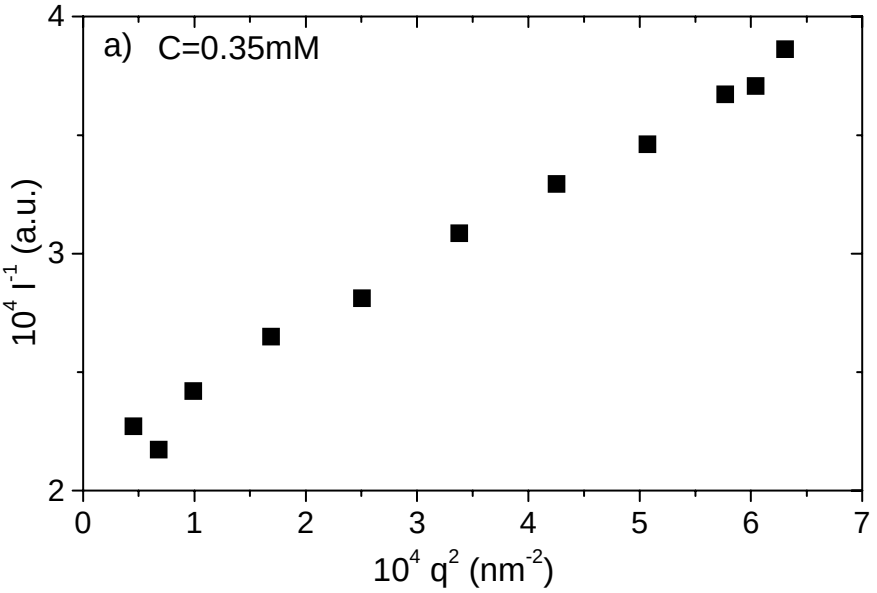

Figures 7: *Variations of the inverse scattered intensity versus q^2 for EHAC solutions with 400mM KCl at 3 different concentrations (a) C=0.35mM, b) C=1.4mM, c) C=14.4mM).*

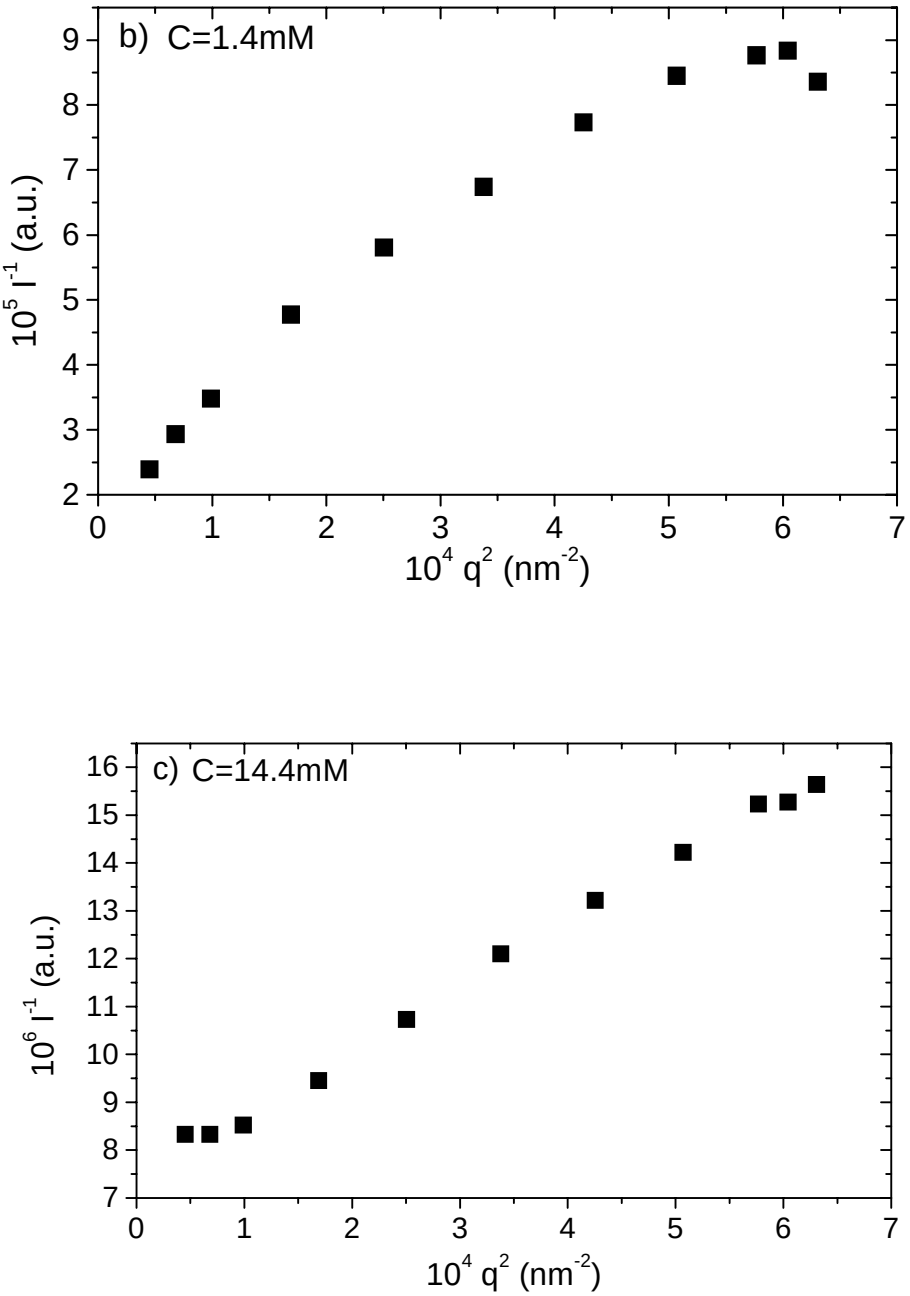

Figures 7: *Variations of the inverse scattered intensity versus q^2 for EHAC solutions with 400mM KCl at 3 different concentrations (a) C=0.35mM, b) C=1.4mM, c) C=14.4mM).*

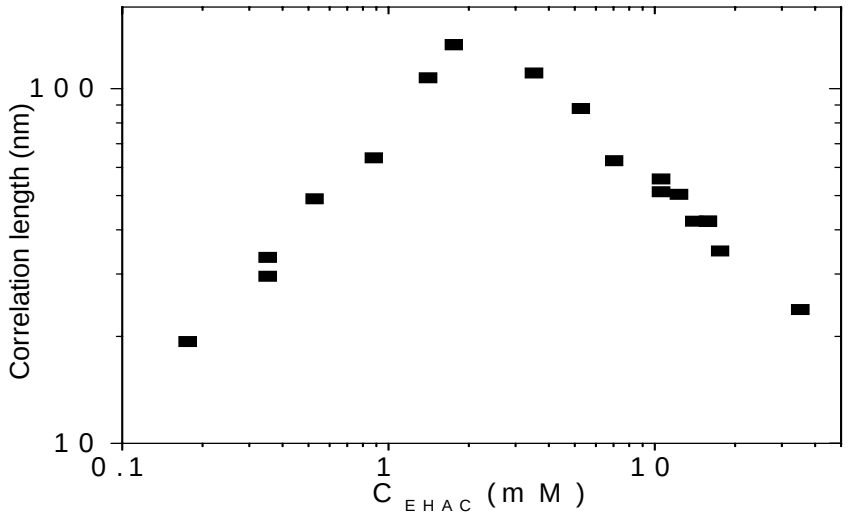

Figure 8: *Variation of the correlation length ξ versus EHAC concentration with 400mM KCl at T=25℃.*

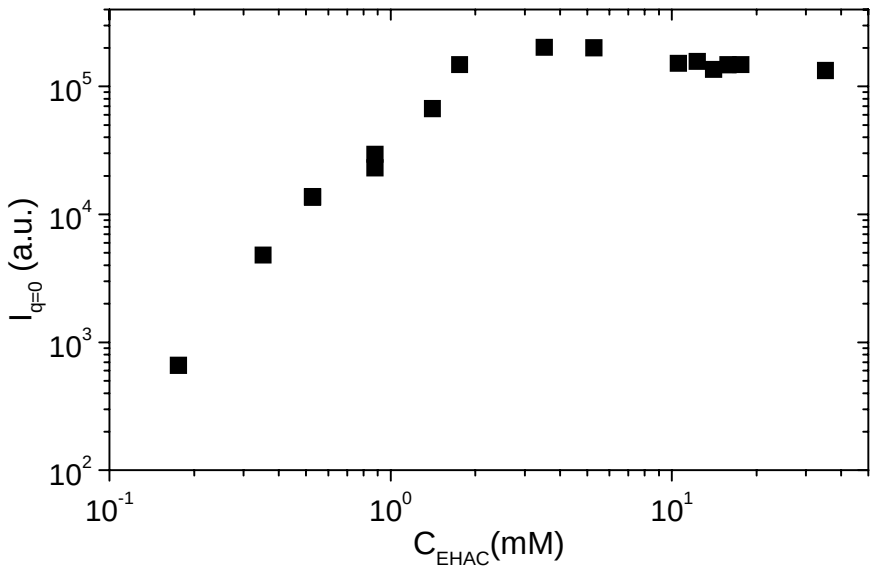

Figure 9: *Variation of the scattered intensity at zero scattering angle versus EHAC concentration with 400mM KCl at T=25℃.*

c) Dynamic light scattering

The normalized time autocorrelation functions of the scattered field, for a solution of EHAC with 1.75 mM active concentration were measured at different scattering angles. The analysis of $g^{(1)}(t)$ by means of the cumulant method yielded very large values of the variance that was found to increase upon decreasing scattering angle from 0.25 at θ = 120° to 0.38 at θ = 30°. One expects here a large polydispersity since the theoretically predicted length distribution is exponential (cf. Eq.(1)). However the value found here is still much higher than that previously reported ($v \cong 0.1$) for micellar solutions of cetyltrimethylammonium bromide in the presence of 0.5 M KBr [3].

Another method to analyze $g^{(1)}(\tau)$ is the Contin method, based on the Laplace transform of $g^{(1)}(q,t)$ that provides the distribution function of decay times $a(t)$ [37]. Figure10 shows the results obtained by applying this method. At large angles (θ = 120° and 90°), the distribution consists in a broad peak but as the angle is decreased, the distribution exhibits a shoulder, (θ = 60°) and becomes bimodal with well separated characteristic times at θ = 30°. At this scattering angle, the apparent hydrodynamic radii obtained from Eq.(31) yield R_{H1}= 37nm and R_{H2} = 175 nm. The latter value is rather close to that of the radius of gyration measured by static light scattering (cf. Fig.8). A similar behaviour is observed for a sample at C = 1.23mM. The Contin analysis of the solution at C = 0.35mM does not show a bimodal distribution, but a broad peak in the whole range of scattering angles investigated. The variance of this system is still very large (v = 0.32 at θ = 30°). The log-log variation of the average relaxation time $\bar{\tau}$ as a function of q, represented in Fig.11 is described by a slope of -2.5, whereas a q^{-2} dependence is expected for the collective diffusion process of particles.

All the above observations are the signatures of a very broad size distribution of particles with the presence of particles large as compared to the scattering vector ($q R_G < 1$).

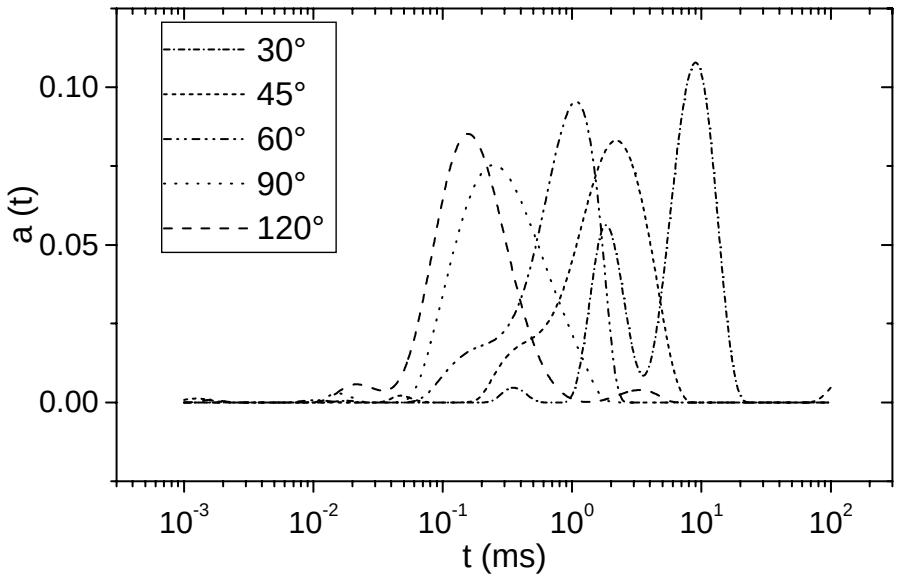

Figure 10: *Distribution function of decay times a(t) obtained by the Contin method at different scattering angles for a 1.75 mM EHAC solution with 400 mM KCl at T = 25°C.*

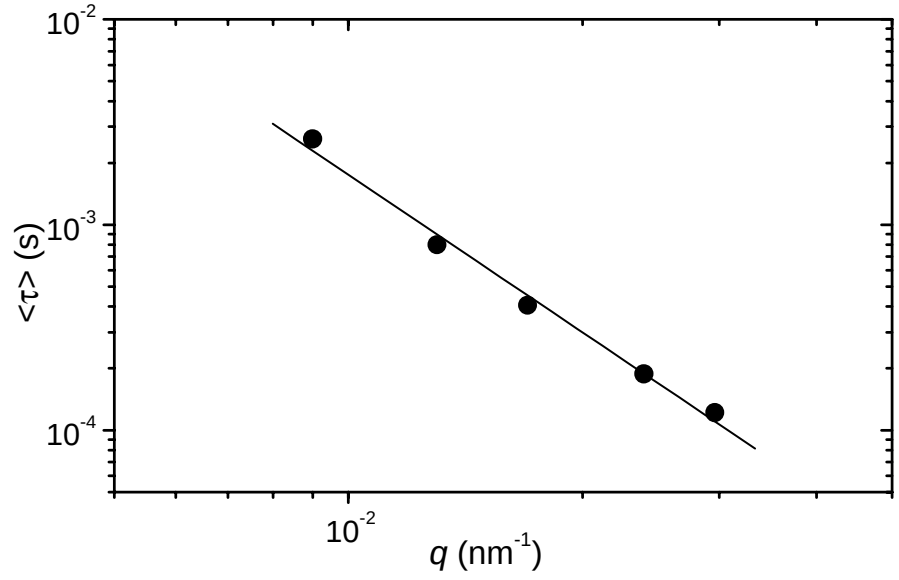

Figure 11: *Log-log variation of the average relaxation time as a function of q for a 0.35mM EHAC solution with 400mM KCl at T=25 ℃.*

d) Linear viscoelasticity

Figure 12 shows an example of the variations of the storage modulus G', and the loss modulus G'' as a function of the angular frequency for a sample with an active EHAC concentration C = 14.4mM (with 400mM KCL) at a temperature T = 25°C. The Maxwell Equations (11) fit the data in the low frequency range whereas at high frequencies one observes, first a deviation due to the effect of micellar breaking and the appearance of the breathing modes, then an upturn arising from the local Rouse modes as in the model of Turner and Cates[22].

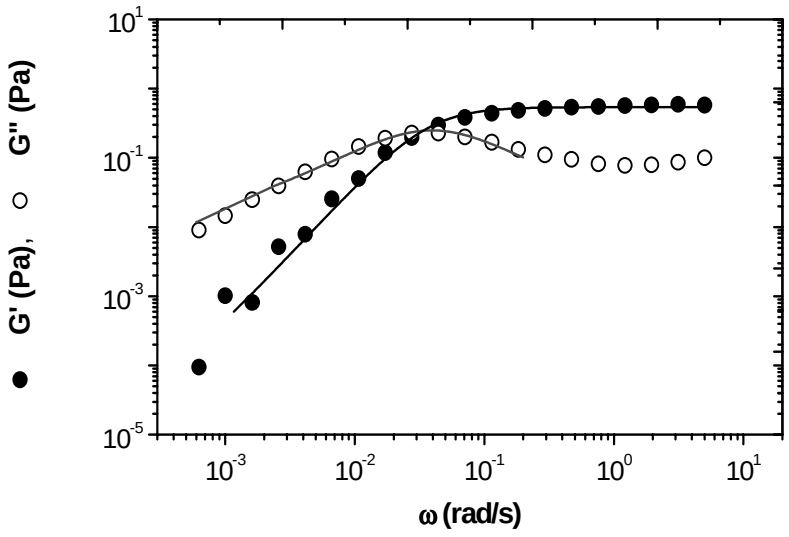

Figure 12: *Variations of G' and G" as a function of the angular frequency for a 14.4mM EHAC solution with 400mM KCL at T = 25°C. The lines are fits to the Maxwell model.*

Figure 13 shows a master curve where the data obtained at different temperatures have been plotted against the angular frequency scaled by the terminal time T_R. The low frequency data collapse onto single curves with slopes of 2 and 1. The high frequency plateau value G_0 of G' is constant with temperature within the experimental accuracy. This behaviour is in agreement with Eq.(23) that predicts a very small variation of G_0 with temperature. Beyond the maximum of G'', one observes deviations of $G''(\omega)$ from the master curve. This behaviour, previously observed for other systems[13], is due to the

fact that the different characteristic times of the stress relaxation scale differently with the average micellar length $\overline{L}$ and/or temperature:

$T_R \sim \overline{L}$; $\tau_b \sim k(T)\overline{L}^{-1}$; $\tau_r \sim \overline{L}^2$ where τ_r is the Rouse time of the micelle and τ_e, the Rouse time of the entanglement length ℓ_e which is independent of $\overline{L}$.

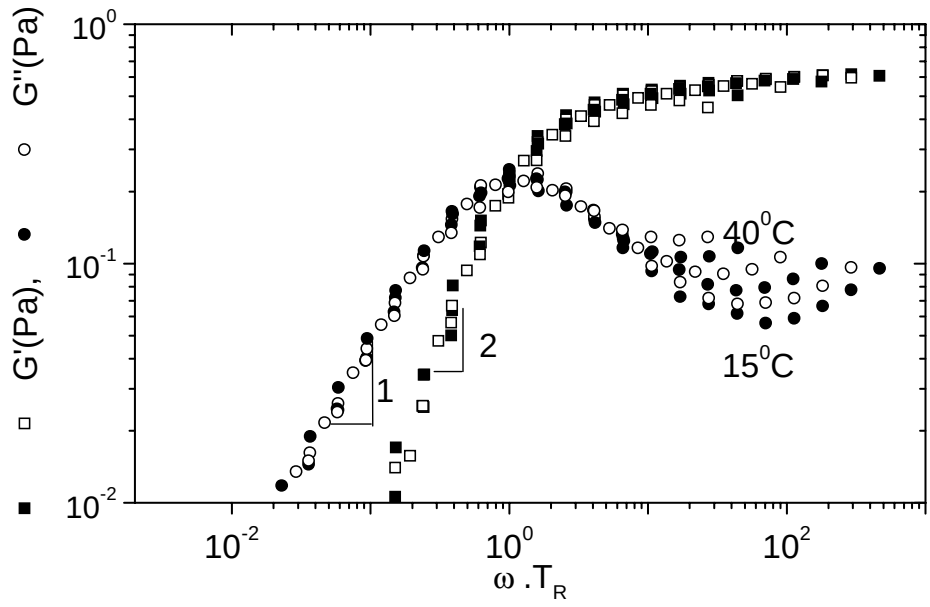

Figure 13: *Rheological master curves for dynamic shear for a 14.4 mM EHAC solution with 400mM KCl, obtained by scaling the data generated at various temperatures (15,20,25,30,35 and 40°C). For the clarity of the representation, filled and empty symbols have been used alternatively.*

This explains in particular that the minimum of *G"* is increasingly shifted in scaled frequencies as the temperature decreases, since the position of this minimum arises from the overlapping of the reptation and the local modes respectively as will be discussed later. It must also be stressed that the above behaviour differs strongly from that of conventional polymers for which a single master curve is expected in the whole frequency range upon varying the temperature.

The temperature dependence of T_R is found to follow an Arrhenius behaviour as illustrated in Fig.14 that shows the semi-log plot of T_R versus $10^3/T$. The slope of the obtained straight line gives an activation energy: $E_R = (34 \pm 1)\ k_B T$ (taking $T = 300°K$).

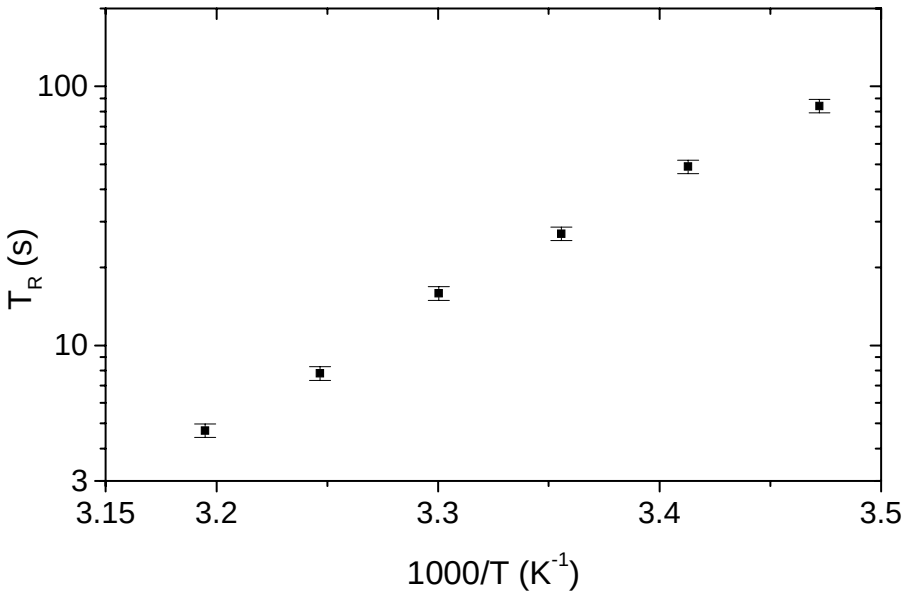

Figure 14: *Arrhenius plot of the relaxation time T_R versus $10^3/T$ for a 14.4 mM EHAC solution with 400mM KCl.*

Discussion

a) Micellar growth

Information on the micellar size and/or its variation with different parameters like surfactant concentration, salt concentration, temperature can be obtained by different experimental approaches. The light scattering experiments provide a direct measurement of the micellar size in the dilute regime. The C^* value is also directly related to the volume occupied by a micelle since at this concentration the micelles are in the verge of overlapping. In the semi-dilute regime, the rheological measurements provide an indirect test of the micellar growth.

In the dilute regime, the micellar growth induced by an increase of concentration is revealed by the increase of the radius of gyration $R_G = \xi\sqrt{3}$ shown in Fig.8. A least square fit to the data of Fig. 8 in the dilute regime yields a slope of ~0.8, that is a much larger value than the predictions of Eq.(4). This means that the classical mean field, or scaling models of micellar growth do not describe adequately the data. This is confirmed by the very large polydispersity observed both in static and dynamic light scattering. The exponential distribution of micellar lengths given in Eq.(1) yields a polydispersity index $\overline{L}_w/\overline{L}_N \cong 2$ where $\overline{L}_w$ and $\overline{L}_N$ are the weight and number averages of micellar lengths respectively. The variance for flexible chains with such a polydispersity index would be of the order of 0.2 [37,38]. Moreover the correlation functions of scattered field obtained at low angles in the vicinity of C^* are clearly bimodal. Such a behaviour has already been reported for low ionic strength micellar solutions of surfactants with a large scission energy[39,40].

The crossover concentration C^* is ill defined for polydisperse systems, and it slightly depends on the method of measurement. However, it is expected to be rather sensitive to the micellar structure. If the system contains only linear micelles with an exponential length distribution, then C^* should follow on Arrhenius behaviour with an activation energy E_{C^*}, obtained by combining the relationship $C^* \sim \overline{L}^{-0.8}$ derived for flexible polymeric chains in good solvent[19] with Eq.(2). This yields:

$$E_{C^*} \cong 0.28 E_{sciss} \tag{34}$$

On the opposite, if the rings are dominant, the volume fraction involved at C^* is dominated by the contribution of smaller rings[6,7]. In such a case, C^* should be only slightly sensitive to the temperature as the size of these smaller rings is only controlled by the persistence length that decreases weakly upon increasing temperature. The data of Fig.4 yields $E_{C^*} = (6.6 \pm 2)\ k_BT$ for the sample with 400 mM KCl. By using Eq.(34) one obtains $E_{\text{sciss}} = (23 \pm 6)\ k_BT$, that is a value comparable within the experimental accuracy to those previously obtained in other systems and that inferred from the present rheological measurements, as discussed later. This result indicates then that the linear micelles population is dominant in the dilute range.

The effect of the salt concentration is more complex. On lowering the salt concentration, the scission energy is expected to decrease, whereas one observes in Fig.4 an increase of E_{C^*}. Two effects can explain this behaviour. First, the scission energy is expected to increase with the ionic strength leading to longer micelles. At low ionic strength, the micelle contour length might not be much larger than the persistence length, and the radius of gyration of the micelle would be that of a semi-rigid polymer, given by Eq.(3). As a consequence the variation of C^* with temperature associated with that of the contour length would be increased. In the rigid rod limit $C^* \sim \bar{L}^{-2}$. It must also be noted that at very low ionic strength, the EHAC surfactant forms spherical micelles[35]. A second effect that might be relevant is the fact, discussed later on, in this paper, that the parameter actually measured in these experiments is the enthalpic part of the scission energy that might be quite sensitive to the ionic strength.

In the semi-dilute regime, the light scattering experiments suggest that the system consists of entangled linear micelles since the variations of ξ and of $I_{q=0}$ follow power laws of the concentration $\xi \sim C^{-0.66}$ and $I_{q=0} \sim C^{-0.2}$ in reasonable agreement with the prediction for entangled polymer solutions[19]. In this regime, the micelles should grow with the surfactant concentration, according to the mean field or scaling models (Eqs.2 to 5). This growth can be proved through the analysis of the variation of the zero-shear viscosity with surfactant concentration.

The best least square fits to the data of Fig.3 give the following values for the slopes: 3.1 for T = 15°C, 3.3 at T= 25°C and 3.5 at T = 40°C.

These values are in good agreement with the theoretical predictions for the power laws of the zero-shear viscosity with the surfactant concentration (cf. Eqs.24-25). The downward curvature observed at higher concentration has been observed in many other systems and often explained by the formation of branched micelles. The presence of such branched micelles has been revealed by recent Cryo-TEM experiments performed in solutions of the same surfactant at a concentration of 79mM and for salt concentrations $C_s \geq 66.6$mM [35].

The main information given by the results of this paragraph is that below C^*, the micellar growth does not follow the prediction of the mean field or scaling models, and exhibit a very large size polydispersity specially close to C^*. Above C^* the scaling behaviour characteristic of entangled linear micelles, already observed for other systems at high ionic strength, is observed. The temperature dependence of C^* seems to indicate

that the linear chains population is dominant in the dilute regime and that the possible presence of large micellar aggregates with a different topology do not produce a significant effect on the measurement of this parameter. On the other hand, such aggregates would contribute significantly to the scattering at low q.

Several light scattering experiments recently performed on low ionic strength micellar solutions of surfactants with a large scission energy gave evidence for a multimodal population of micellar aggregates below C^* [39-42]. This behaviour was qualitatively explained by assuming the presence in these systems of a broad distribution of interlinked micellar rings in equilibrium with linear chains or of microgels of multiconnected micelles[39,40]. Those systems exhibit a strong shear thickening effect in the vicinity of C^*. A ring driven mechanism was proposed[43]. This model can account for the experimental observations whereas the previous models based on a linear micelle structure failed.

b) Scission energy

The determination of the scission energy is a non trivial problem, and only few measurements were reported up to now[25,13,30,44-48]. The reported values of E_{sciss} range from 20 k_BT to 70 k_BT. As the micellar length is an exponential function of the scission energy (cf. Eq.(2)), very large values of E_{sciss} lead to unrealistic values of the micellar contour length $\overline{L}$. As an example, a micelle with E_{sciss} = 65 k_BT would be ~10^9 times longer than a micelle with E_{sciss} = 25 k_BT. Accordingly the ratio beween the C^* of the two systems would be 10^7. To explain the above inconsistency, it was suggested that the free energy of scission could contain a large entropic term, possibly associated with the rearrangement of counterions upon formation of an end-cap[44,45]. The scission free energy is then written:

$$E_{\text{sciss}} = H_{\text{sciss}} - T\,S_{\text{sciss}}$$

where H_{sciss} and S_{sciss} represent the enthalpic and entropic parts respectively of the scission free energy. Arrhenius plots would only measure H_{sciss}, whereas when calculating micellar lengths, a large positive S_{sciss}, may still lead to reasonable values.

The method first used to determine H_{sciss} consisted in measuring separately τ_b in the dilute regime by means of T-Jump experiments and the terminal relaxation time T_R in

the semi-dilute regime and applying Eq.(18) [25]. This method is reliable as both T-Jump and rheological date are accurate. However the T-Jump devices do not allow to measure breaking times longer than ~10 s [25,30]. Attempts performed on the systems investigated here showed that τ_b was longer than this upper limit, in agreement with the results obtained from the analysis of the viscoelastic spectra. Alternatively, H_{sciss} can be determined by combining the temperature dependences of the breaking time and of the terminal relaxation time obtained both from the viscoelastic spectra, through the procedure described p.91 and in ref.29. This method leads to less accurate values of H_{sciss} because of a larger uncertainty (± 20% on the average) on the τ_b measurements. The semi-log plot of τ_b versus 10^3/T is shown in Fig.15. In that range of temperature the ratio $\zeta^{1/2}/\bar{\zeta}$ was found to vary by less than 2%. From the slope of the best linear fit to the data, one obtains an activation energy for τ_b, $E_b \cong (24.5 \pm 4.5)\ k_BT$. By combining the values of E_R, obtained from the temperature dependence of the terminal time (cf. Fig.14), of E_b and of E_{η_s} (6.6 k_BT), one can determine H_{sciss} through Eq.(18).

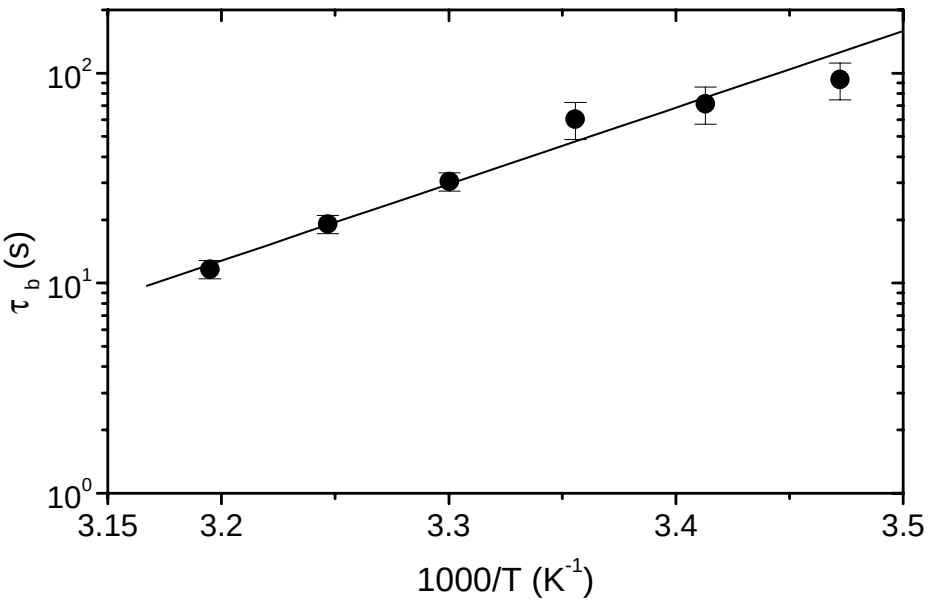

Figure 15: *Arrhenius plot of the breaking time τ_b versus $10^3/T$ for a 14.4mM EHAC solution with 400 mM KCl.*

One obtains

$H_{\text{sciss}} = (25 \pm 5)\ k_B T$

A priori, the most direct and accurate method to determine H_{sciss} should be through the analysis of the dip occurring in the high frequency part of the Cole-Cole representation, since $G''_{\min} / G_0$ is simply related to $\bar{L}$. Equation (13) has been commonly used to analyze the data. In particular, it was found that $G''_{\min} / G_0$ scales with the surfactant concentration with the expected exponent [49]. Furthermore, reasonable estimates of the contour length $\bar{L}$ were obtained from Eq.(13) [13,30,49]. However, as mentioned earlier, this expression has been calculated numerically by assuming $\omega_m \sim \tau_e^{-1}$. If the latter assumption is correct, then ω_m should depend on the temperature only through the variation of τ_o, that is of η_s. Fig.16 which shows in a semi-log representation the variation of ω_m with 10^3/T, gives E_{w_m} = (16.8 ± 3.3) $k_B T$, that is a much larger value than E_{η_s}. The Granek's prediction concerning the dip gives a slightly different scaling of $G''_{\min} / G_0$ with $(\bar{L} / \ell_e)$ (cf. Eq.(15)).

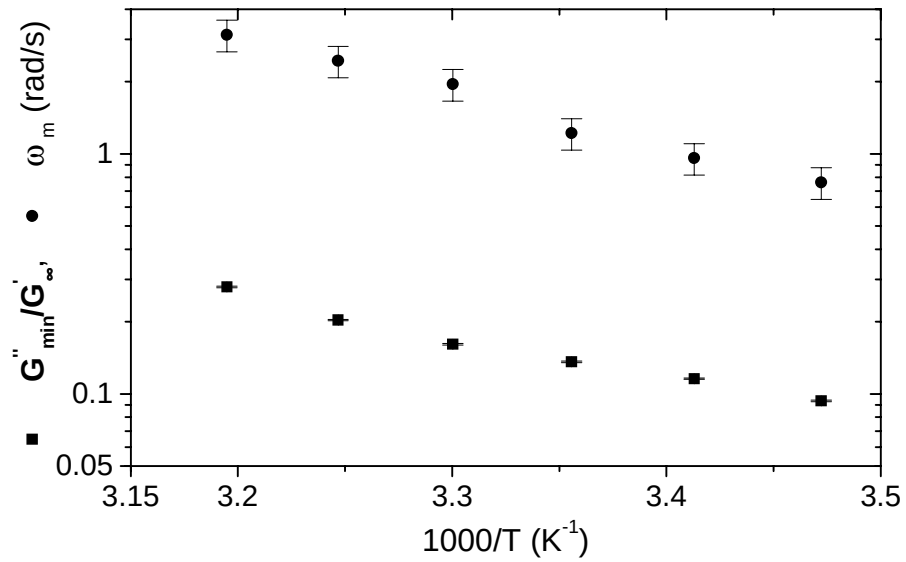

Figure 16: *Semi-log variations of G''_{min}/G'_{∞} (■) and ω_m (●) as a function of $10^3/T$ for a 14.4mM EHAC solution with 400 mM KCl.*

Using this equation one obtains from the variation of G''_{min}/G_0 with 10^3/T (cf. Fig.16)

$$H_{sciss} = (31 \pm 4)\ k_BT$$

The analysis of the temperature dependence of ω_m by using Eq.(16) leads to :

$$H_{sciss} = \frac{5}{2}(E_{\omega_m} - E_{\eta_s}) = (25.5 \pm 7.5)\ k_BT$$

The three methods of determination of H_{sciss} give concordant results, within the experimental accuracy. Examination of the results reported in the literature for H_{sciss} show that large scission enthalpies are generally obtained for low ionic strength systems[13,30,47]. Also, highly binding counterions like salycilate seem to increase H_{sciss} [13,44,45]. Highly screened systems with moderately binding counterions, like the one studied here are characterized by much lower values[25]. This suggests that in that case the entropy of scission is weak and the enthalpy of scission is close to the end-cap free energy. The average micellar length of a surfactant with an end-cap free energy of 25 k_BT at a volume fraction $\Phi = 10^{-2}$ can be estimated from the classical mean field model[15,50] to a reasonable value of the order of 1 μm.

Conclusion

The results reported in this paper bring new information on the micellar growth induced by an increase of surfactant concentration and on the viscoelastic behaviour of wormlike micellar systems. In particular, it is the first time to our knowledge that a quantitative comparison between the experimentally measured concentration dependence of the radius of gyration of the micelles with the mean field and scaling models derived for linear micelles is reported. It is found that the increase of the radius of gyration with surfactant concentration in the dilute regime is much larger than that theoretically expected. Also the distribution of micellar sizes, as probed by static and dynamic light scattering is much broader than the exponential distribution predicted by the mean field model.

The above observation was also made for several low ionic strength systems. In that case, the multimodal character of the micellar aggregates population was much more

visible[39-42]. These results, together with strong shear thickening effects observed for these systems led the authors to consider the possibility of the presence of micellar rings that is predicted by the theory[39,40,43].

These rings should also be present in the dilute solution of highly screened micelles. Some results of T-Jump studies were satisfactorily interpreted by assuming the law of micellar growth given by Eq.(2), inferred from statistical thermodynamics arguments[25,45]. Such a law is not obeyed for the surfactant investigated here. It must be noted that the light scattering is a very sensitive technique to detect the presence, even in small amount of large aggregates.

The second issue addressed in this paper concerns the determination of the enthalpic part of the scission energy, in the semi-dilute regime, through rheological experiments. For the first time, all the features of the complex shear modulus spectrum, including the Rouse modes were used, thus providing three independent methods of measurement of the scission energy.

Acknowledgments

The authors thank J. Selb, N. Benoit (ICS) and C. Oelschlaeger (LDFC) for their help in light scattering experiments.

References

(1) See for instance Cates, M.E.; Candau, S.J., *J. Phys.: Condens. Matter* **1990**, *2*, 6869.

(2) See for instance Rehage, H.; Hoffmann, H. *Mol. Phys*. **1991**,*74*, 933.

(3) Buhler, E.; Munch, J.P.; Candau, S.J. *J. Phys. II* **1995**, *5*, 765.

(4) Candau, S.J.; Hirsch, E.; Zana, R. *J. Phys. (Paris)* **1984**, *45*, 1263.

(5) Candau, S.J.; Hirsch, E.; Zana, R. In *Physics of Complex and Supramolecular Fluids*, Eds.: Safran, S.A; Clark, N.A.; Wiley, New York, N.Y. **1987,** p.509.

(6) Cates, M.E. *J. Phys (Paris)*. **1988**, *49*, 1593.

(7) Cates, M.E. *Macromolecules* **1987**, *20*, 2289.

(8) Lu, B.; Zheng, Y.; Davis, H.T.; Scriven, L.E.; Talmon, Y.; Zakin, J.L. *Rheol. Acta* **1998**, *37*, 528.

(9) Zakin, J.L.; Bewersdorff, H.W. *Rev. Chem. Eng.* **1998**, *14*, 253.

(10) Maitland, G.C. *Curr. Opin. Colloid Interface Sci.* **2000**, *5*, 301.

(11) Sullivan P.F.; Huang H.; Nelson E.; The Society of Rheology, Paper SM43, 75th Annual Meeting, Oct **2003**.

(12) Maitland, G.C. *Curr. Opin. Colloid Interface Sci.* **2000**, *5*, 301.

(13) Raghavan, S.R.; Kaler, E. *Langmuir* **2001**, *17*, 300.

(14) Qu Q., Nelson E., Willberg D., Samuel M., Lee J., Chang F., Card R., Vinod P., Brown J., Thomas R.; In *Compositions Containing Aqueous Viscosifying Surfactants and Methods for Applying Such Compositions in Subterranean Formations*, US patent US 6,435,277, 20/08/**2002**.

(15) Israelachvili, J.; Mitchell, D.J.; Ninham, B.W. *J. Chem. Soc. Faraday Trans. 2* **1976**, *72*, 1525.

(16) Benoît, H.; Doty, P. *J. Phys. Chem*. **1953**, *57*, 958.

(17) In, M.; Aguerre-Chariol, O.; Zana, R. *J. Phys. Chem.* **1999**, *103*, 7747.

(18) Bernheim-Groswasser, A.; Zana, R.; Thalmon, Y. *J. Phys. Chem. B* **2000**, *104*, 4005.

(19) De Gennes, P.G. *Scaling concepts in polymer physics*; Cornell University Press: Ithaca, NY, **1979**.

(20) Turner, M.S.; Cates, M.E. *J. Phys. France*. **1990**, *51*, 307.

(21) Cates, M.E.; Turner, M.S. *Europhys. Lett.* **1990**, *7*, 681.

(22) Turner, M.S.; Cates, M.E. *Langmuir* **1991**, *7*, 1590.

(23) Granek, R.; Cates, M.E. *J. Chem. Phys*. **1992**, *96*, 4758.

(24) Granek, R. *Langmuir* **1994**, *10*, 1627.

(25) Candau, S.J.; Merikhi, F.; Waton, G.; Lemaréchal, P. *J. Phys. France* **1990**, *51*, 977.

(26) Adam. M.; Delsanti. M. *J. Phys. (Paris)* **1985**, *44*, 1760.

(27) Oda, R.; Narayanan, J.; Hassan, P.A.; Manohar, C.; Salkar, R.A.; Kern, F.; Candau, S.J. *Langmuir* **1998**, *14*, 4364.

(28) Kern, F.; Lemaréchal, P.; Candau, S.J.; Cates, M.E. *Langmuir* **1992**, *8*, 437.

(29) Faetibold, E.; Waton, G. *Langmuir*. **1995**, *11*, 1972.

(30) Kern, F.; Lequeux, F.; Zana, R.; Candau, S.J. *Langmuir* **1994**, *10*, 1714.

(31) Candau, S.J.; Lequeux, F. in *Structure and Flow in Surfactant Solutions*, Eds.: Craig A. Herb; Robert, K.; ACS Symposium Series 578; American Chemical Society: Washington, DC **1994**, Chap.3.

(32) Hoffmann, H., Herb C., Prud'homme R.; In *Structure and Flow in Surfactant Solutions;* Eds.: Holland, P.M.; Rubing, D.N.; ACS Symposium Series 578; American Chemical Society: Washington DC, **1994**, Chap.1.

(33) Candau, S.J.; Oda, R. *Colloids and Surfaces A*: *Physicochem. Eng. Aspects* **2001**, *5*, 183.

(34) Berret, J.F.; Roux D.C.; Porte, G. *J. Phys. II France* **1994**, *4*, 1261.

(35) Croce, V.; Cosgrove, T.; Maitland, G.; Hughes, T.; Karlsson, G. *Langmuir* **2003**, *19*, 8536.

(36) Hughes, T. Private communication.

(37) Provencher, S.W. *Makromol. Chem*. **1985**, *82*, 632.

(38) Brown, J.C.; Pusey P.; Dietz R. *J. Chem. Phys.* **1975**, *62*, 1136.

(39) Oelschlaeger, C.; Waton, G.; Candau, S.J.; Cates, M.E. *Langmuir* **2002**, *18*, 7265.

(40) Oelschlaeger, C.; Waton, G. ; Buhler, E.; Candau, S.J; Cates, M.E. *Langmuir* **2002**, *18*, 3076.

(41) Weber, V.; Narayanan, T.; Mendes, E.; Schosseler, F. *Langmuir* **2003**, *19*, 992.

(42) Truong, M.T.; Walker, L.M. *Langmuir* **2002**, *18*, 2024.

(43) Cates, M.; Candau, S.J. *Europhys. Lett.* **2001**, *55*, 887.

(44) Kern, F.; Zana, R.; Candau, S.J. *Langmuir* **1991**, *7*, 1344.

(45) Oelschlaeger, Cl.; Waton, G.; Candau S.J. *Langmuir* , **2003**.

(46) Hassan, P. ; Valaulikar, B.S. ; Manohar, C. ; Kern, F. ; Candau, S.J. *Langmuir* **1996**, *12*, 4350.

(47) Oda, R.; Narayanan, J.; Hassan, P.; Manohar, C.; Salkar, R.A.; Kern, F.; Candau, S.J. *Langmuir* **1998**, *16*, 4364.

(48) Soltero, J.F.A.; Puig, J.E. *Langmuir* **1996**, *12*, 2654.

(49) Berret, J.F.; Appell, J.; Porte, G. *Langmuir* **1993**, 9, 2851.

(50) Mukerjee, P. *J. Phys. Chem.* **1972**, *76*, 565.

Chapter III

SYNERGISTIC EFFECTS IN 0.4M KCl SOLUTIONS OF HYDROPHOBICALLY MODIFIED HYDROXYPROPYL GUAR/ ERUCYL BIS-(HYDROXYETHYL)METHYLAMMONIUM CHLORIDE MIXTURES

INTRODUCTION

In this chapter, we investigate the linear and non linear rheological properties of aqueous solutions containing both wormlike micelles and associating polymer molecules. The polymer sample was a hydroxypropyl guar modified with a C_{22} n-alkyl chain (hm-HPG), supplied by Lamberti S.P.A. It is obtained by derivatisation of the guar gum, a natural polyssacharide that is extracted from the seeds / ground endosperm of the guar plant Cyamopsis tetragonolobus[1]. It is composed of a linear chain of D-mannose residues bonded together by (1→ 4)- β- glycosidic linkages, with D-galactosyl units randomly attached via (1→ 6)- α- glycosidic linkages along the backbone (Fig.1). The ratio of mannose to galactose units has been shown to be around 1.6:1 to 1.8:1 [2]. Guar exhibits one of the highest molecular weights of all naturally occurring biopolymers and is therefore used as a viscosifying agent in various industrial areas, including oil recovery, paints, pharmaceuticals, cosmetics, and food.

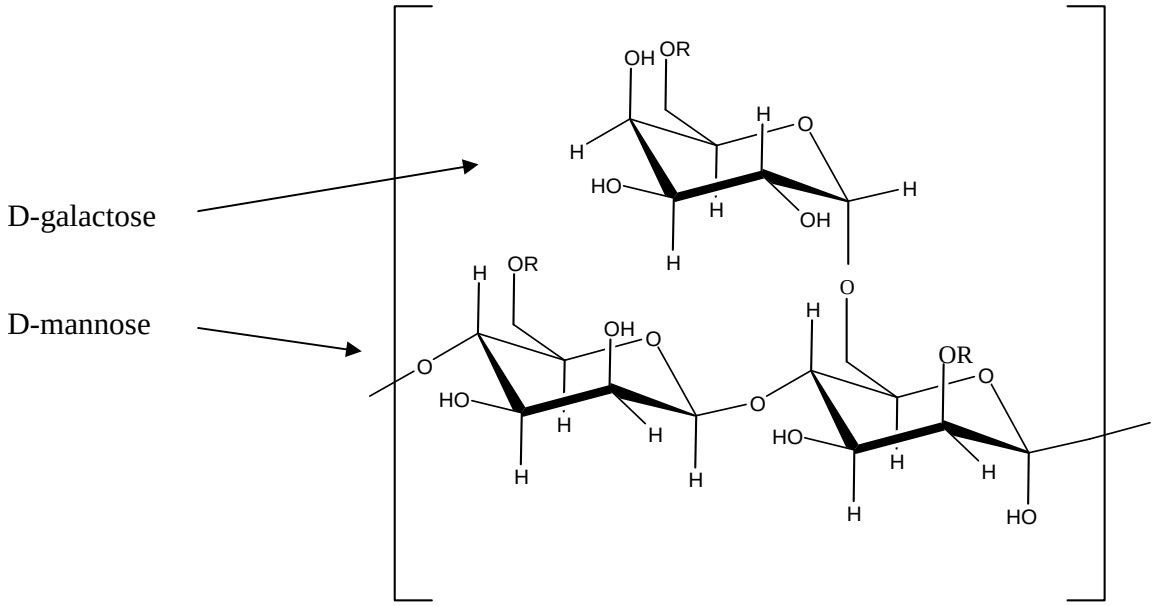

R= H for guar gum

R= C_3H_6OH for HPG

R= C_3H_6-O-CH_2-CHOH-$C_{(n-2)}H_{2n}$ for hm-HPG

Figure 1: Structure of Guar and guar derivatives

Treatment of guar with propylene oxide in an alkaline medium results in the formation of hydroxypropyl guar (HPG), which is more soluble in water than native guar. It is the most widely available derivative of natural guar. The various degrees of molar substitution (DS) measure the average number of moles of hydroxypropyl groups substituted per mole of anhydrous sugar units. The hydrophobically modified hydroxypropyl guar (hm-HPG) is obtained by reaction of HPG with $C_{(n-2)}$ *n*-alkyl epoxides (Fig.2).

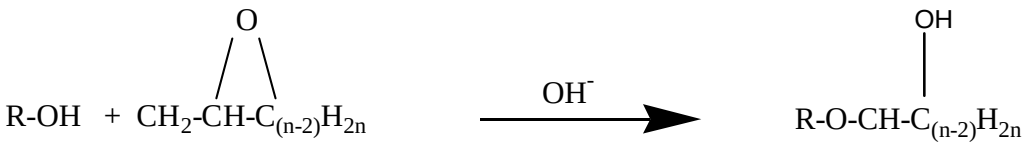

Figure 2: *Synthesis of hm-HPG*

The surfactant used was the erucyl bis-(hydroxyethyl)methylammonium chloride (EHAC), studied in the previous chapter.

Both the hm-HPG[2-4] and the EHAC[5-8] surfactant were found to be efficient thickeners and fracturing fluids[9,10]. The rheological behaviour of solutions of hm-HPG has been investigated by the group of Moan at T=25°C in the concentration range 0.01% and 1.5% (wt/wt)[3]. In the present study, we have considered solutions in the presence of 0.4M KCl at concentrations between 0.001% and 3% (wt/wt) and in the temperature range 25°C-80°C. It must be stressed that fracturing fluid applications are used at quite high temperatures[10].

Some differences can be observed when comparing the study of the Moan's group and ours. For instance the linear viscoelastic response obtained in the present work (Fig.3) appears to be better defined than that reported in literature where the $G'(\omega)$ and $G''(\omega)$ are quite smeared.

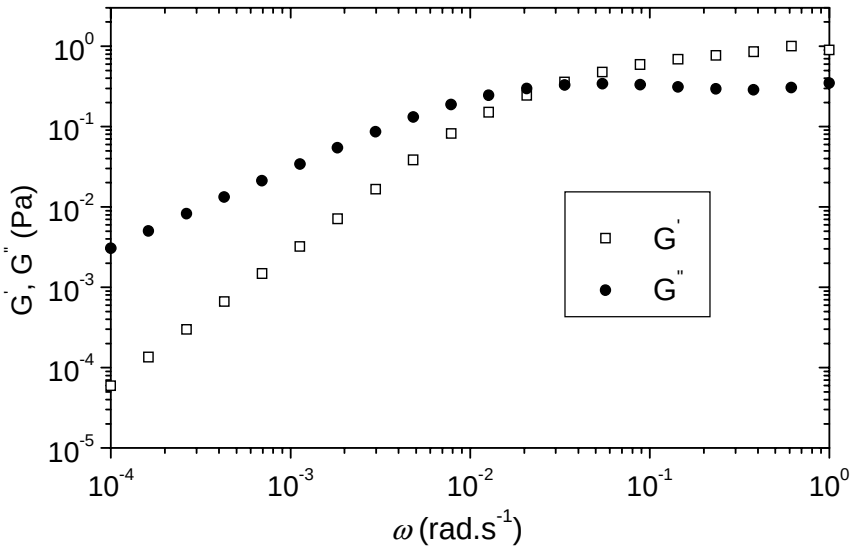

Figure 3: *Storage (G') and loss (G'') moduli as a function of frequency at 25°C for a solution of 0.35wt% hm-HPG and 3wt% KCl.*

We observed a behaviour characteristic of entangled systems, with a crossing of the $G'(\omega)$ and $G''(\omega)$ curves and a plateau modulus G_o at high frequencies. The relaxation time T_R and the plateau modulus G_o have been determined from the crossing point of the curves $G'(\omega)$ and $G''(\omega)$, according to $\omega_{max} T_R = 1$ and $G_o = 2\, G'(\omega_{max}) = 2\, G''(\omega_{max})$.

Aubry and Moan also reported that the response of the system to a shear stress was found to be time and history dependent. So, these authors established a protocol which consisted in preshearing at rather high shear stresses the sample during times of the order of 10 mins, in order to ensure the reproducibility of the results. In our system, we did not find it necessary to use any preshearing method and we obtained a good reproducibility, provided that the equilibrium time was respected.

Figure 4 shows a typical response of the shear viscosity as a function of time during the start-up of a shear flow. The applied shear rate is 0.5 s^{-1}.

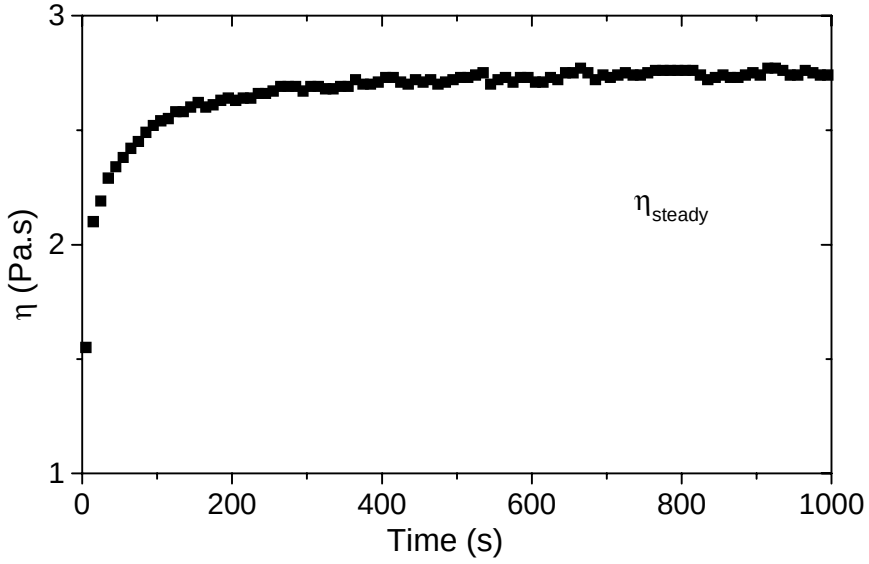

Figure 4: *Transient shear viscosity η as a function of time for a 0.45 wt% hm-HPG solution with an imposed shear rate of $\dot{\gamma} = 0.5\ s^{-1}$ ($\dot{\gamma}.T_R << 1$), at T=25°C.*

It can be observed that the time of equilibrium is quite long, of the order of 250 s for the example shown in Fig.4.

The transient response curves of the shear viscosity as a function of time, with an imposed shear rate in the vicinity of $\tilde{\dot{\gamma}}$, the crossover between the Newtonian plateau and the shear-thinning regime, is characterized by a large initial peak followed after some time by the steady-state value of the shear viscosity (Fig.5).

The importance of taking care in getting the equilibrium is illustrated in Fig.6 for a hm-HPG solution at C=0.45wt% and T=25°C. This Figure shows the comparison between the flow curves obtained under equilibrium and non equilibrium conditions.

In our study, all the experiments have been performed after waiting 200 s up to 1000 s, depending on the sample composition for each data point until the equilibrium is reached.

The presence of salt in the systems investigated in our study might be at the origin of the differences between our results and those of Aubry and Moan[3] concerning the shape of the viscoelastic spectra and the protocol used in the non linear rheological experiments.

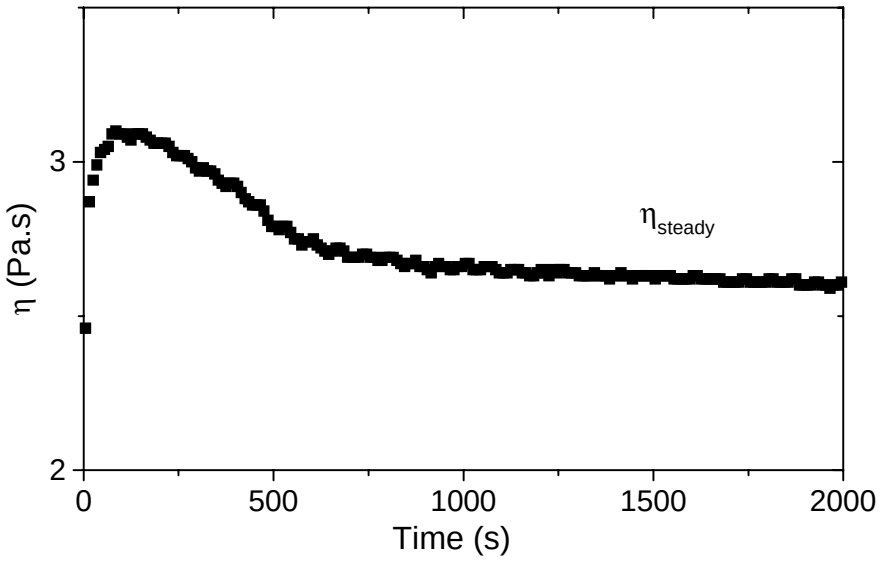

Figure 5: *Transient shear viscosity η as a function of time for a 0.45 wt% hm-HPG solution with an imposed shear rate of $\dot{\gamma} = 1\ s^{-1}$ ($\dot{\gamma}.T_R \approx 1$), at T=25°C.*

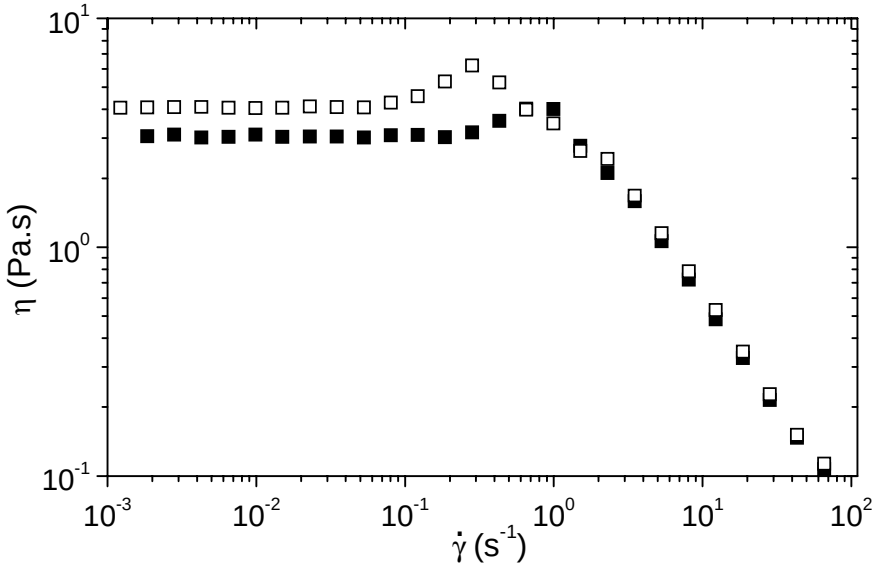

Figure 6: *Comparison of the flow curves obtained for a 0.45wt% hm-HPG solution at 25°C under equilibrium (□) and non equilibrium (■) conditions.*

Still and as discussed later, the overall behaviour of the measured rheological parameters with temperature and concentration was found to be qualitatively and in some cases quantitatively the same for the two sets of experiments.

The rheological properties of EHAC solutions have been described in the previous chapter. The linear viscoelasticity of these systems is quasi-Maxwellian. Figure 7 represents the circular frequency dependence of the complex shear modulus for a 3wt% (400mM) KCl aqueous solution at the concentration C=0.6wt% (14.4mM).

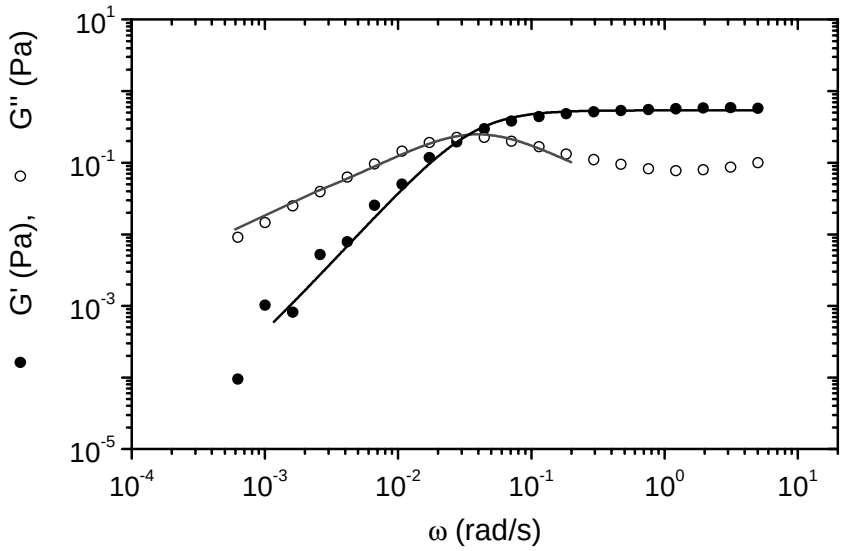

Figure 7: *Variations of G' and G" as a function of the angular frequency for a 14.4mM EHAC solution with 400mM KCL at T = 25°C. The lines are the fits to the Maxwell model.*

In the following paper, we address issues concerning the linear and non linear rheological properties of mixtures of the hm-HPG and the EHAC surfactant defined above, from both fundamental and applied points of view. Additional experimental results that do not figure in the paper will be presented in the Appendix I (Effect of temperature on the zero shear viscosity of HPG and hm-HPG solutions), Appendix II (Non linear rheological properties of hm-HPG solutions), and Appendix III (Rheological properties of hm-HPG/EHAC mixtures).

REFERENCES

(1) *Hydrogels, Elastic Latex and Resines*, Ed.: Wilson, H.D.; Plants and People-Botany, **1997**, p.328

(2) Caritey, J.-P. *Relation entre la modification chimique de precurseurs hydrophiles d'origine naturelle et leurs propriétés en solution diluée et semi-dilué*, Thèse Université de Rouen, **1994.**

(3) Aubry, T.; Moan, M. *J. Rheol.* **1994,** *38*, 1681.

(4) Aubry, T.; Moan, M. *J. Rheol.* **1996,** *40*, 441.

(5) Croce, V.; Cosgrove, T. ; Maitland, G. ; Hughes, T. ; Karlsson, G. *Langmuir* **2003**, *19*, 8536.

(6) Raghavan, S.R.; Kaler, E. *Langmuir* **2001**, *17*, 300.

(7) Raghavan, S.R.; Edlund, H.; Kaler. E. *Langmuir* **2002**, *18*, 1056.

(8) Schubert, B.A.; Wagner, N.J.; Kaler, E. *Langmuir* **2004**, *20*, 3564

(9) Sullivan P.F.; Huang H.; Nelson E.; The Society of Rheology, Paper SM43, 75th Annual Meeting, Oct **2003.**

(10) Maitland, G.C. *Curr. Opin. Colloid Interface Sci.* **2000**, *5*, 301.

SYNERGISTIC EFFECTS IN AQUEOUS SOLUTIONS OF MIXED WORMLIKE MICELLES AND HYDROPHOBICALLY MODIFIED POLYMERS

PUBLICATION 2

(Macromolecules,**2005**,*38*,5271-5282*)*

SYNERGISTIC EFFECTS IN AQUEOUS SOLUTIONS OF MIXED WORMLIKE MICELLES AND HYDROPHOBICALLY MODIFIED POLYMERS

Isabelle Couillet, Trevor Hughes, Geoffrey Maitland, Françoise Candau

ABSTRACT:

The linear and non linear rheological properties of a hydrophobically modified guar (hm-HPG) and a surfactant forming wormlike micelles, erucyl bis-(hydroxyethyl)methylammonium chloride, have been investigated in 0.4M KCl aqueous solution. The comparison between the zero-shear viscosity behaviours of the non-modified guar and the hm-HPG shows a decrease of the intermolecular associations upon increasing the temperature. Significant synergistic effects were observed between the modified polymer and the wormlike micelles in a range of concentrations extending from 0.1wt% to 1 wt% and for temperatures up to 60°C. The optimal synergy for the zero-shear viscosity is obtained for mixtures with an overall concentration ≈ 0.35wt% and a surfactant/polymer ratio equal to 1/4 (wt/wt). The terminal time of the stress relaxation, the zero-shear viscosity as well as the viscosity at a shear rate of 100 s^{-1} and the lifetime of the associations show a maximum at this composition. The experimental observations suggest the formation of very efficient crosslinks between the wormlike micelles and the polymer chains.

Introduction

Water-soluble hydrophobically modified polysaccharide derivatives are commonly used as thickening and rheology-control agents in aqueous systems.[1-4] The specific rheological behaviour of such polymeric systems arises from their ability to give rise to weak intra- and inter-molecular interactions between the hydrophobic groups distributed along the polymer chains. In the semi dilute entangled regime, which is the domain of interest for most industrial applications, the hydrophobic moieties build up a transitory tridimensional network interpenetrated with the entanglement network. This microstructure leads to a slowing down of the polymer diffusion and to an increase in the zero-shear viscosity when compared to the analogues without the hydrophobes.[5-9] A model based on a sticky reptation process of the polymer chains has been proposed to describe the viscoelastic properties of these systems.[10-11]

Aqueous solutions of guar and its derivatives are the most widely used hydraulic fracturing fluids for the hydrocarbon recovery from subterranean formations, mainly for economical reasons.[5,12,13] The main functions of hydraulic fracturing fluids are to initiate and propagate the fracture and to transport the proppant along the length of the fracture. However, polymer-based fracturing fluids present the disadvantage of at least partially clogging the pore space in the fracture, so that the fracture is not optimally cleaned up. Recently, a new class of fracturing fluids based on viscoelastic surfactants forming wormlike micelles has been developed.[14-16] During backflow, as the surfactant gel comes into contact with the produced hydrocarbons, the wormlike micelles break down forming spherical micelles, resulting in a low viscosity fluid which is more easily removed from the pore space in the propped fracture. Cationic surfactants with long mono-unsaturated tails (C_{22}) have been shown to be efficient fracturing fluids.[17] In particular, aqueous solutions of erucyl bis (hydroxyethyl) methyl ammonium chloride (EHAC) exhibit appropriate viscosities up to high temperatures (80°C).[18-20]

In view of the above, it seemed appealing to investigate the rheological behaviour of mixed surfactant/polymer aqueous solutions and particularly mixed viscoelastic

surfactant/hydrophobically modified polymer (HMWSP) aqueous solutions. Many studies on the interactions between surfactants and HMWSP have been reported.[21-24] They generally concern systems in which the surfactant concentration is close to the critical micellar concentration (CMC). Under these conditions, one observes an enhancement of the zero-shear viscosity due either to the formation of additional mixed plurifunctional aggregates or to an increase in the lifetime of the pre-existing crosslinks resulting from surfactant binding.[13,25-34] To our knowledge, only one study has been reported which investigates the rheological properties of mixtures of wormlike micelles and hydrophobically modified polymer; specifically, this study focussed on mixtures of cetyl trimethylammonium bromide (CTAB) and hm-hydroxyethylcellulose (with C_{16} hydrophobic substitution) in the presence of KBr.[35]

In the first part of this paper, we report a comparison of the flow behaviour of hydroxypropyl guar (HPG) and its hydrophobically modified analogue (hm-HPG). A rheological study on these polymers under salt-free conditions and at T=25°C has been previously reported.[5] In the present study, we have investigated the same systems in the presence of salt and at various temperatures. These conditions are of primary importance for applications, mainly in oil recovery processes. Concerning the effect of temperature, only a limited number of studies have been performed, with contradictory conclusions. Some authors claim that an increase in temperature favours hydrophobic interactions[36-38] while the reverse is suggested by others[39-40]. In fact, the effect of temperature might be strongly dependent on the nature of the polymer and of the quality of the diluent.

In the second part of the paper, we report a study on the synergistic effects occurring in the viscoelastic behaviour of mixtures of 0.4M KCl aqueous solutions containing EHAC surfactant and hm-HPG polymer in a concentration domain from 0.01wt% to 2.5wt% and in a temperature range from 25°C to 80°C. The micellar growth and the viscoelastic properties of EHAC surfactant were described in a recent paper.[20]

Experimental Section

Materials:

The HPG and hm-HPG polymers investigated here have been supplied by Fratelli Lamberti s.p.a. (Albizzate-Italy). The HPG sample is hydroxypropyl guar containing an average of one hydrophilic substituent (hydroxypropyl group) per monomer. Measurements by Caritey on the average molecular weight of the HPG sample lead to: M_w = 1.8 x 10^6 g/mol, that is an average degree of polymerisation of about 3000, with a polydispersity index of about 1.55.[12] As its native polymer, guar gum, hydroxypropyl guar is expected to be a slightly stiffened, random-coil polymer. The hydrophobically modified hydroxypropyl guar, hm-HPG, is obtained by reaction of the HPG with a C_{22} *n*-alkyl epoxide. The number of hydrophobic substituents per individual polymer chain is expected to be 10. The measurement of the mean molecular weight and the polydispersity of associating systems like hm-HPG is difficult and it is assumed that the hydrophobic modification of HPG does not produce chain degradation.[12] The purity index is 95% (by-products: propylene glycol, ethylene glycol, sodium acetate, open form of epoxide alkane).

The erucyl bis-(hydroxyethyl)methylammonium chloride (EHAC) is a C_{22} surfactant with a cis unsaturation at the 13-carbon position. Its chemical structure is shown below. It is supplied by Akzo Nobel, Chemicals, LLC, USA. It is used in the form of a liquid blend of the quaternary ammonium salt with 25wt% isopropanol (IPA). Upon dilution, the ratio IPA/EHAC is maintained constant. The concentrations of the EHAC samples reported in the text correspond to the active surfactant (i.e. after correction of the 25wt% IPA added in the blend).

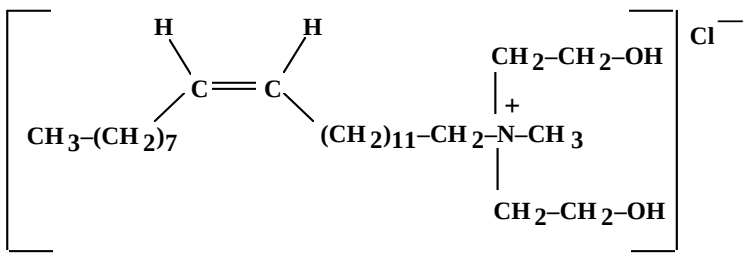

Potassium chloride was supplied from Aldrich.

Solutions containing surfactant and salt were prepared using deionised water. The concentration of polymer or surfactant will be expressed in wt%.

Methods:

Rheological experiments were performed with a Bohlin CVO rheometer. Steady state measurements were done under controlled stress or controlled rate depending on the sample viscosity, using the cup and bob geometry (coaxial cup, 25mm diameter bob) or a double gap cell (inner diameter 40mm, outer diameter 50mm). The shear rate was varied between 10^{-3} s^{-1} and 2000 s^{-1}. The response of the shear viscosity as a function of time during the start up of a shear flow is characterised by a rather long equilibrium time, from 200s up to 1000s, depending on the sample composition. A good reproducibility of the non linear rheological results was obtained without having to use a pre-shearing protocol.[5] Dynamic rheological experiments were carried out with the same rheometer using the coaxial cup cell. The frequency was varied between 10^{-3} Hz and 5 Hz under a maximum shear stress of 1 Pa. The frequency spectra were conducted in the linear viscoelastic regime of the samples, as determined previously by dynamic stress sweep measurements. The cell was heated by a reservoir of fluid circulating from a high temperature bath. A metallic cover was placed on the top of the sample to minimize sample evaporation. The sample was equilibrated for at least 15 min. at each temperature prior to conducting experiments. Both steady and dynamic rheological experiments were performed at different temperatures.

Results

Comparison of the Flow Rheology of Hydrophobically Modified and unmodified Hydroxypopyl Guars:

Figure 1. shows typical variations of the steady-state values of the relative viscosity η/η_s where η_s is the solvent viscosity, as a function of the shear rate $\dot{\gamma}$ for a HPG sample and its hm-HPG homologue at C = 1 wt% and at various temperatures ranging from 25° C to 80° C. The relative zero-shear viscosity of the HPG solution, determined from the Newtonian plateau, is found to decrease significantly as the temperature is increased (Fig.1a). Moreover, the crossover between the Newtonian plateau and the shear-thinning regime is shifted to higher values of $\dot{\gamma}$. This indicates a speeding up of the dynamics of the system since the inverse of the shear rate at the crossover, $\tilde{\dot{\gamma}}^{-1}$, can be roughly identified with the terminal time T_R of the stress relaxation. At high shear rates, the representative curves of $[\eta/\eta_s](\dot{\gamma})$ cross each other, so that the high shear value of the relative viscosity increases with temperature, that is the opposite behaviour of that of the zero-shear viscosity. The overall behaviour described above was observed over the concentration range investigated in this study (0.1wt% up to 3wt%).

The same effects are observed for solutions of the modified hm-HPG polymers, as shown in the example of Fig.1b. In that case, the decrease of the zero-shear viscosity as the temperature is increased is much more pronounced. The $[\eta/\eta_s](\dot{\gamma})$ curves also cross each other in the same range of $\dot{\gamma}$ as for the unmodified polymer of similar concentration.

The effect of the polymer modification on the flow behaviour is shown by comparing the data of Figs 1a and 1b respectively. The effect is that previously reported for systems in the entangled state.[5,8,41] In particular, the zero-shear viscosity is larger for the modified samples and the shear-thinning regime is shifted to lower values of $\dot{\gamma}$. This behaviour is well taken into account by the sticky reptation model meant for entangled networks made up of linear chains with many temporary crosslinks.[10-11] In this model, the

chain motion, governed by the reptation hindered by the hydrophobic interactions, is controlled by the concentration and the lifetime of the tie- points.

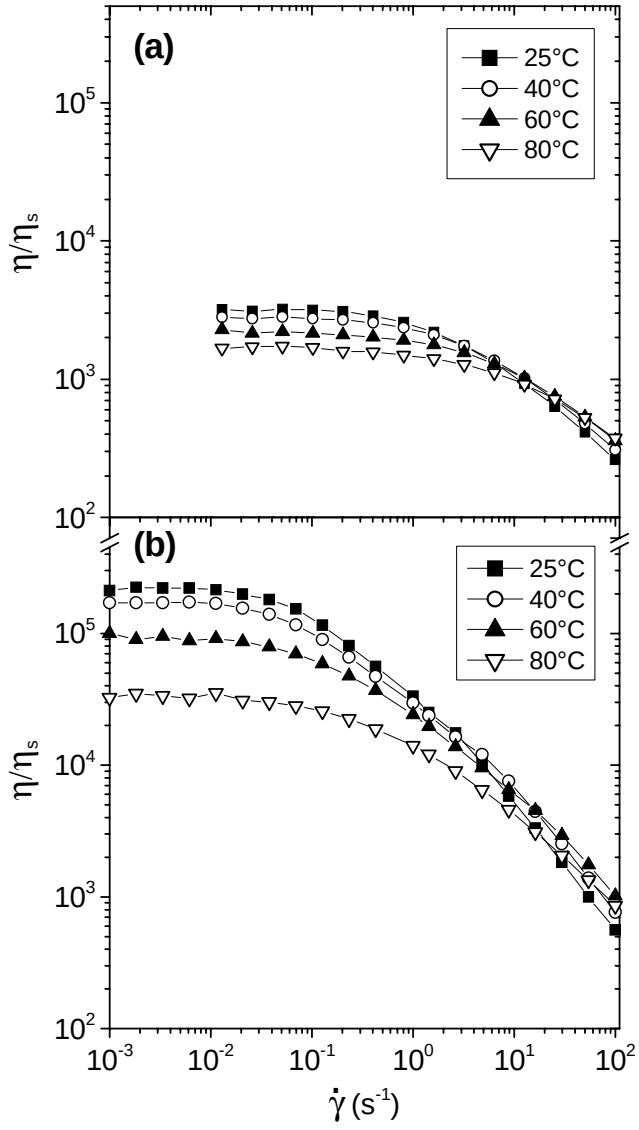

Figure 1: *Relative steady-state viscosity versus shear rate for HPG (a) and hm-HPG (b) solutions at C=1wt%, in the presence of 0.4M KCL, at various temperatures. The lines drawn through the data are guides for the eye.*

Previously reported rheological experiments, carried out with a stress-controlled rheometer on the same systems revealed the presence of a discontinuity in the flow curves of the modified hm-HPG, occurring at a critical shear stress, σ_c, which increased with the polymer concentration.[5] This discontinuity was attributed to a breaking of the temporary hydrophobically associating network. Beyond the discontinuity, the flow curves of the modified and unmodified polymers were found to coincide.

Typical variations of the steady-state shear viscosity versus shear stress, obtained in the present study, are represented in Fig.2. For the modified polymers, three regimes can be identified in the variation of the viscosity versus shear stress. At low shear stress, one observes the Newtonian plateau, followed by a shear-thinning regime beyond a shear stress $\tilde{\sigma} \approx \eta_0 T_R^{-1}$ where T_R represents the longest time of the stress relaxation and η_0 the Newtonian viscosity. The sharp viscosity drop, occurring at higher shear stress, defines the critical shear stress σ_c. The shear rate $\dot{\gamma}_c$, measured just before the sharp drop is, according to Aubry and Moan, the inverse of the lifetime of the associations.[5] An alternative representation is given in plotting the shear stress versus the shear rate, as illustrated in Fig.3, which shows the results obtained for 1wt% solution of hm-HPG at different temperatures. The determination of the shear rate at the crossovers between the different regimes provide estimates of $\tilde{\dot{\gamma}} = T_R^{-1}$ and $\dot{\gamma}_c$. The latter corresponds to the onset of the high shear plateau. It can be observed in Fig.3 that the critical shear stress is roughly independent of temperature at C=1wt%, whereas $\dot{\gamma}_c$ increases with temperature.

The variation of σ_c with concentration (not shown here) can be fitted at T= 25°C by a power law $\sigma_c \approx C^{1.62}$ in agreement with the previous findings of Aubry and Moan in the salt-free systems: $\sigma_c \approx C^{1.7}$ [5]. As for $\dot{\gamma}_c$, it is found to decrease slightly upon increasing concentration ($\dot{\gamma}_c \approx 12s^{-1}$ for C=0.35wt% and $\dot{\gamma}_c \approx 3s^{-1}$ for C=1wt% at T=25°C). It should be noted that, whereas σ_c can be determined with a good approximation, $\dot{\gamma}_c$ is less well defined. As mentioned in the experimental section, the equilibrium value of the stress upon applying a steady strain is reached after a long time. The transient response curves of the stress are characterised for shear rates in the vicinity

of $\tilde{\dot{\gamma}}$ by a large overshoot followed by a long relaxation. Such effects were reported for both wormlike micellar solutions[42-44] and hydrophobically modified polymers[5,45].

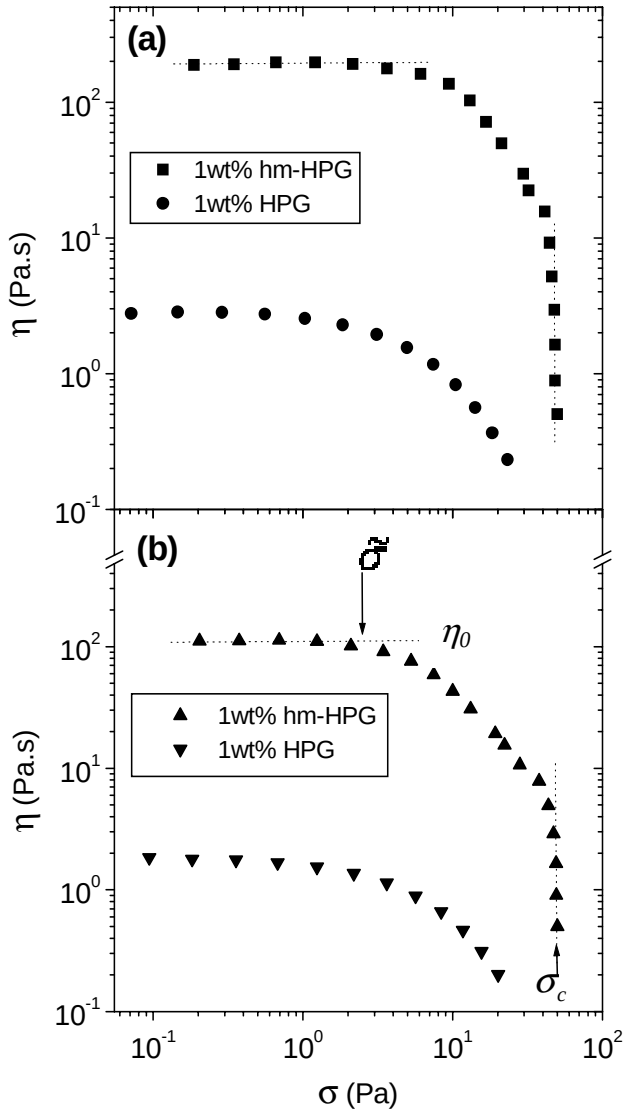

Figure 2: *Steady-state shear viscosity versus shear stress for HPG and hm-HPG solutions in the presence of 0.4M KCl at two different temperatures (a): 25 ℃; (b): 40 ℃. η_0 is the Newtonian viscosity, $\tilde{\sigma}$ is the shear at the onset of shear thinning, σ_c is the critical stress.*

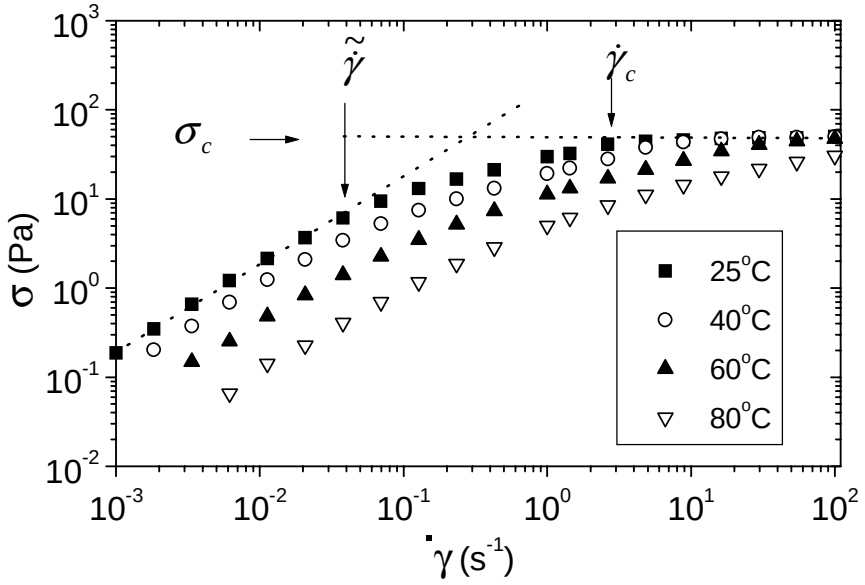

Figure 3: *Shear stress versus shear rate for a 1wt% hm-HPG solution at various temperatures. In the Newtonian regime at low shear rates, the data are fitted by a straight line of slope 1.*

It must also be remarked in Fig.1 that, in the whole shear rate range investigated, the steady-state viscosity of the modified sample remains larger than that of the unmodified one. This means that one does not reach the very short time scale where one probes local motions, insensitive to the presence of tie-points.

Figure 4 shows the comparison between the variations of the zero-shear viscosity versus polymer concentration measured at T= 25°C and T= 60°C for the HPG and hm-HPG samples respectively.

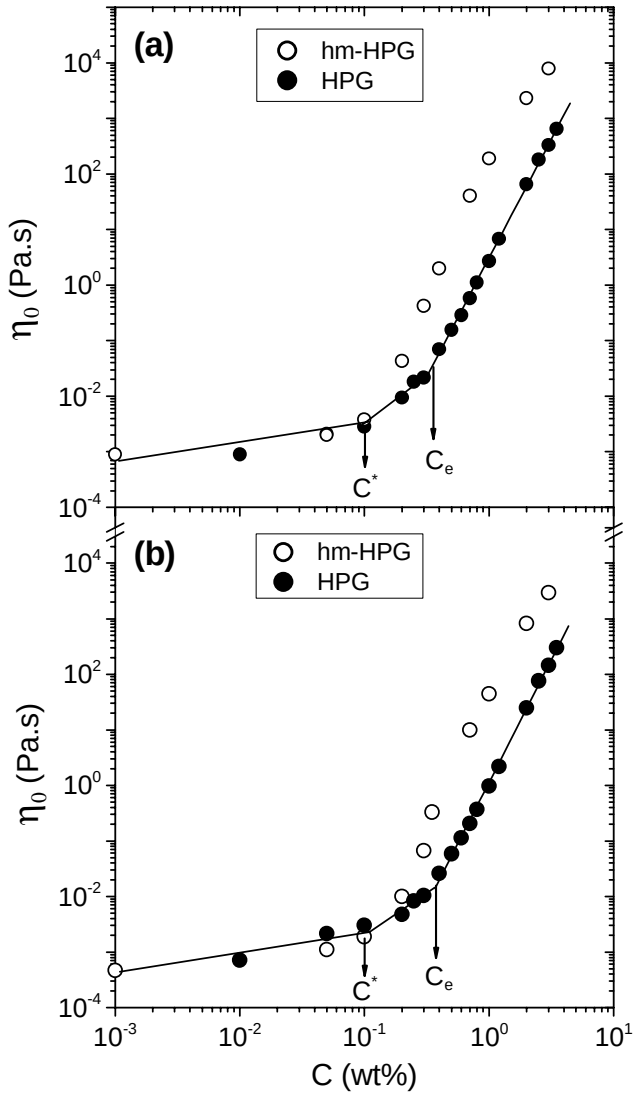

Figure 4: *Variation of the zero-shear viscosity with concentration for solutions of HPG and hm-HPG in the presence of 0.4M KCl, (a) T=25 °C, (b) T=60 °C.*

For the unmodified polymer, one observes the classical behaviour, with a first break at the concentration C^* at which the chains start to overlap and a second break at a higher concentration C_e corresponding to the onset of entanglements.[46-48] In this respect, it should be noted that a significant overlap of neighbouring chains is required in order for them to constrain each other's motion. As a consequence, the strand between two

consecutive entanglements in a chain is composed of a number $\tilde{N}$ of blobs with a size ξ [49,50]. Both C^*, C_e and the exponent α of the asymptotic law obtained for the HPG sample in the entangled regime were found quite independent of the temperature within the experimental accuracy. Their values are given in Table1. The ratio C_e/C^* is of the order of 3.5, that is a smaller value than those obtained for other systems, that range generally between 5 to 10 [47,48,50,51]. In fact, there is no theoretical model which allows one to predict this ratio, which is likely to depend on the nature of the polymer and in particular on its natural persistence length.

The rheological behaviour of the modified polymers is quite different. The viscosity of the solution rises steeply beyond a concentration which is of the same order of magnitude as the crossover concentration C^* of the unmodified polymer (Fig.4 and Table 1). Such a behaviour has already been reported for solutions of hydrophobically modified polyacrylamides[7]. In the latter case, clear Rouse regimes were observed and entanglement onsets could be determined. In the present case, there is no clear evidence of a Rouse regime in the curves of Fig.4, which display a sigmoidal shape.

Polymer	**C^* (wt%)**	**C_e (wt%)**	**C_e/C^***	**α**
HPG	0.10	0.35	3.5	4.4
Hm-HPG	0.15	—	—	—

Table 1: *Crossover concentrations, C^*, C_e and exponent α of the scaling law of the zero-shear viscosity versus concentration in entangled solutions of the modified and unmodified HPG samples.*

Note that experiments performed by Aubry and Moan on the same system at 25°C showed a behaviour quite similar to that represented in Fig.4, with α = 4.3 for the HPG polymers.[5]

Viscoelastic Behaviour of EHAC/hm-HPG Mixtures:

We have investigated the rheological behaviour of mixtures with different compositions. The latter are characterized by the ratio $R=C_{EHAC}/(C_{EHAC}+C_{hm\text{-}HPG})$ where the concentrations of the components are expressed in wt%.

Figure 5 represents typical frequency dependences of the storage (G') and loss (G'') moduli for a mixture at an overall concentration C_M = 0.35wt% and R=0.43. A behaviour, characteristic of entangled systems is observed, with a crossing of the $G'(\omega)$ and $G''(\omega)$ curves and a plateau modulus G_0 at high frequencies. The relaxation time T_R and the plateau modulus G_0 have been determined from the crossing point of the curves $G'(\omega)$ and $G''(\omega)$, according to $\omega_{max}T_R = 1$ and $G_0 = 2\,G'(\omega_{max}) = 2\,G''(\omega_{max})$.

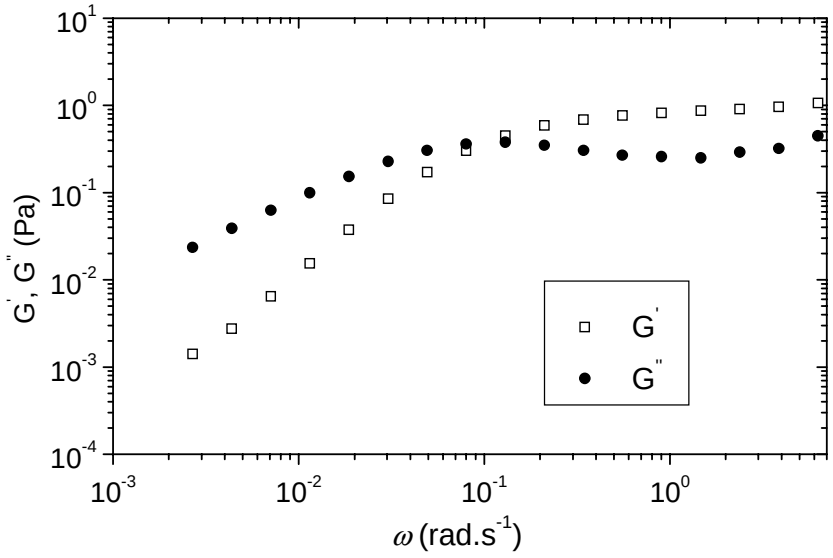

Figure 5 : *Storage (G') and loss (G'') moduli as a function of frequency at 25°C for a solution of 0.2wt% hm-HPG, 0.15wt% EHAC and 3wt% KCl (R=0.43).*

Figure 6 represents the variations of T_R and G_0 with the mixture composition, for samples with an overall concentration $C_M \approx 0.35$wt%. The compositions of the mixtures are the following:

R=0: 0.35wt% hm-HPG

R=0.2: 0.3wt% hm-HPG + 0.075wt% EHAC

R=0.43: 0.2wt% hm-HPG + 0.15wt% EHAC

R=0.69: 0.1wt% hm-HPG + 0.225wt% EHAC

R=1: 0.375 wt% EHAC

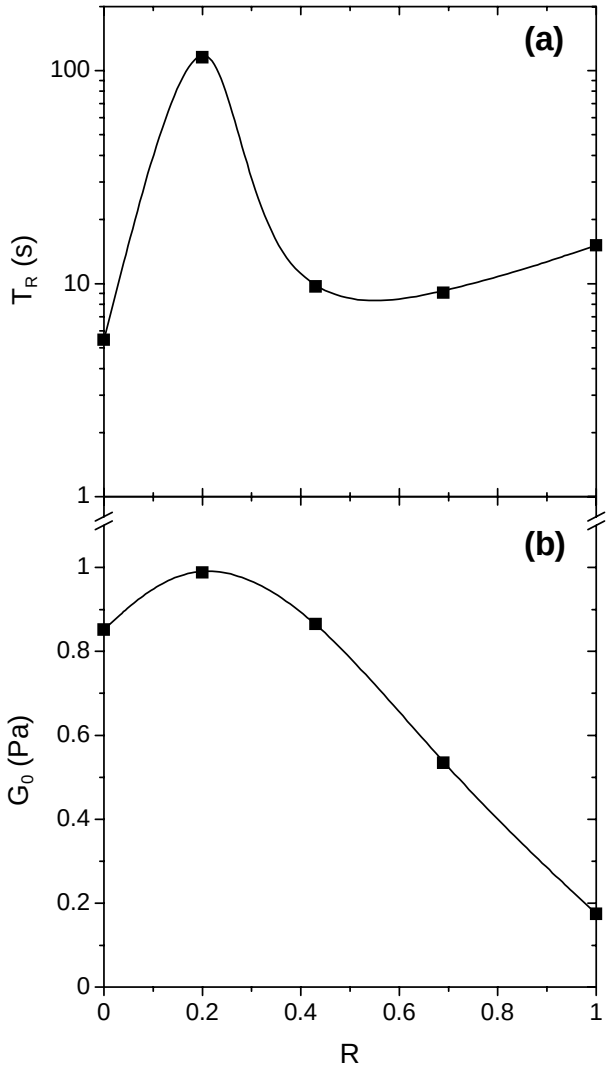

Figure 6: *Terminal relaxation time, (T_R), (a) and plateau modulus, (G_0), (b), versus R for systems with an overall concentration $C_M \approx 0.35$wt%.*

A maximum is observed in the relaxation time and to a lesser extent in the plateau modulus that is the signature of a pronounced synergy. The comparison between the plateau moduli of the EHAC and the hm-HPG solutions (R=1 and R=0 respectively) at about the same concentration shows that the density of the entanglements between the wormlike micelles is strongly reduced as compared with that of the crosslinks and/or the entanglements of the associating polymers. Another interesting feature concerns the high frequency range of the viscoelastic curves, which has never been analyzed before in associating polymer solutions. The minimum which is observed for G'' at the circular frequency ω_m corresponds to the crossover between the reptation controlled stress relaxation and the Rouse modes. The position and the normalized amplitude of the dip have been derived by Granek[52] and are given by:

$$G''(\omega_m)/G_0 \sim (\ell_e/\bar{L})^{4/5} \quad (1)$$

$$\omega_m \sim (\frac{\ell_e}{\bar{L}})^{4/5}\tau_e^{-1} \quad (2)$$

where $\bar{L}$ is the contour length of the chain, ℓ_e is the entanglement length and τ_e the Rouse time of the entanglement length. The above relations are valid for the regular polymers and the wormlike micelles, providing that the dip occurs at frequencies much higher than the inverse of their breaking time. This was found to be the case for EHAC solutions.[20] For associating polymers, it can be speculated that Eqs.(1) and (2) can be applied providing that ω_m is much larger than the inverse of the lifetime of the associations. Also, it should be kept in mind that the Rouse part of the spectrum may be modified by the breaking mechanism of the associations.

Table 2 gives the effect of the mixture composition on the values of ω_m and $G''(\omega_m)/G_0$ for systems with an overall concentration $C_M \approx$ 0.35wt%, at T= 25°C. The dependence of these parameters on R is rather complex but a clear minimum of both ω_m and $G''(\omega_m)/G_0$ is observed for R = 0.2, again suggesting a synergistic effect at this composition.

R	ω_m (rad. s^{-1})	$G''(\omega_m)/G_0$
0	2.3	0.33
0.2	0.6	0.16
0.43	1.2	0.29
0.69	1.9	0.17
1	1.1	0.35

Table 2: *Effect of the mixture composition on the dip coordinates ω_m and $G''(\omega_m)/G_0$ for solutions with overall concentrations $C_M \approx 0.35$wt% at 25 °C.*

The variations of the zero-shear viscosity of different EAHC/hm-HPG mixtures versus hm-HPG and EHAC concentrations, at 25°C, are plotted in Figs.7a and 7b respectively. A net zero-shear viscosity enhancement is observed in both representations by addition of one component to the other. Synergistic effects are best revealed by the plots of the zero-shear viscosity versus the total material concentration C_M (wt%), at various temperatures (Fig.8). At 25°C, there is a clear synergy for the zero-shear viscosity in a range of concentrations between 0.07wt% and 1wt% (Fig.8a). As an example, at a concentration C= 0.37%, for which both EHAC and hm-HPG solutions have the same viscosity ~ 2Pa.s, the viscosity of the mixtures is about 5 Pa.s for R=0.69, 9.2 Pa.s for R=0.43 and 83 Pa.s for R=0.2. The synergystic effect can also be expressed in the following way: to obtain a viscosity of 10 Pa.s, one can use either 0.6% solutions of pure EHAC or pure hm-HPG or 0.23wt% solutions of mixtures (for instance 0.18wt% of hm-HPG + 0.05wt% of EHAC). In the high concentration range, all the variations of η_0 with C_M tend to converge and there is no longer synergy. The results obtained at T= 40°C are quite similar, whereas at 60°C the viscosity enhancement with respect to the hm-HPG solutions is more limited. Finally at T= 80°C, mixtures with $R \leq 0.43$ exhibit the same viscosity as the hm-HPG for 0.15% < C_M < ~0.7% whereas at higher concentrations, the value of the zero-shear viscosity is in between those of the hm-HPG and the EHAC samples.

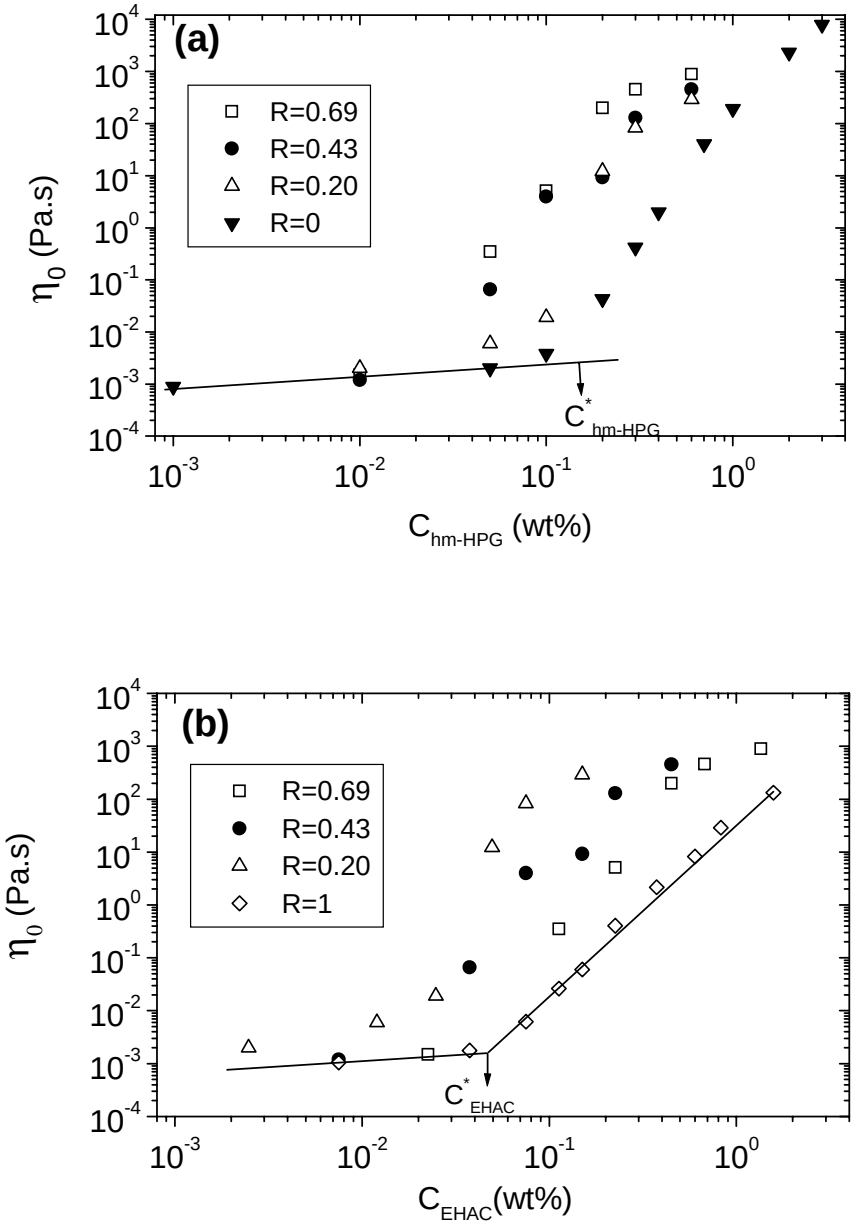

Figure 7: *Zero-shear viscosity versus hm-HPG (a) and EHAC (b) concentrations for various compositions of the mixtures at 25℃. Also are reported the variations corresponding to the single hm-HPG and EHAC components respectively.*

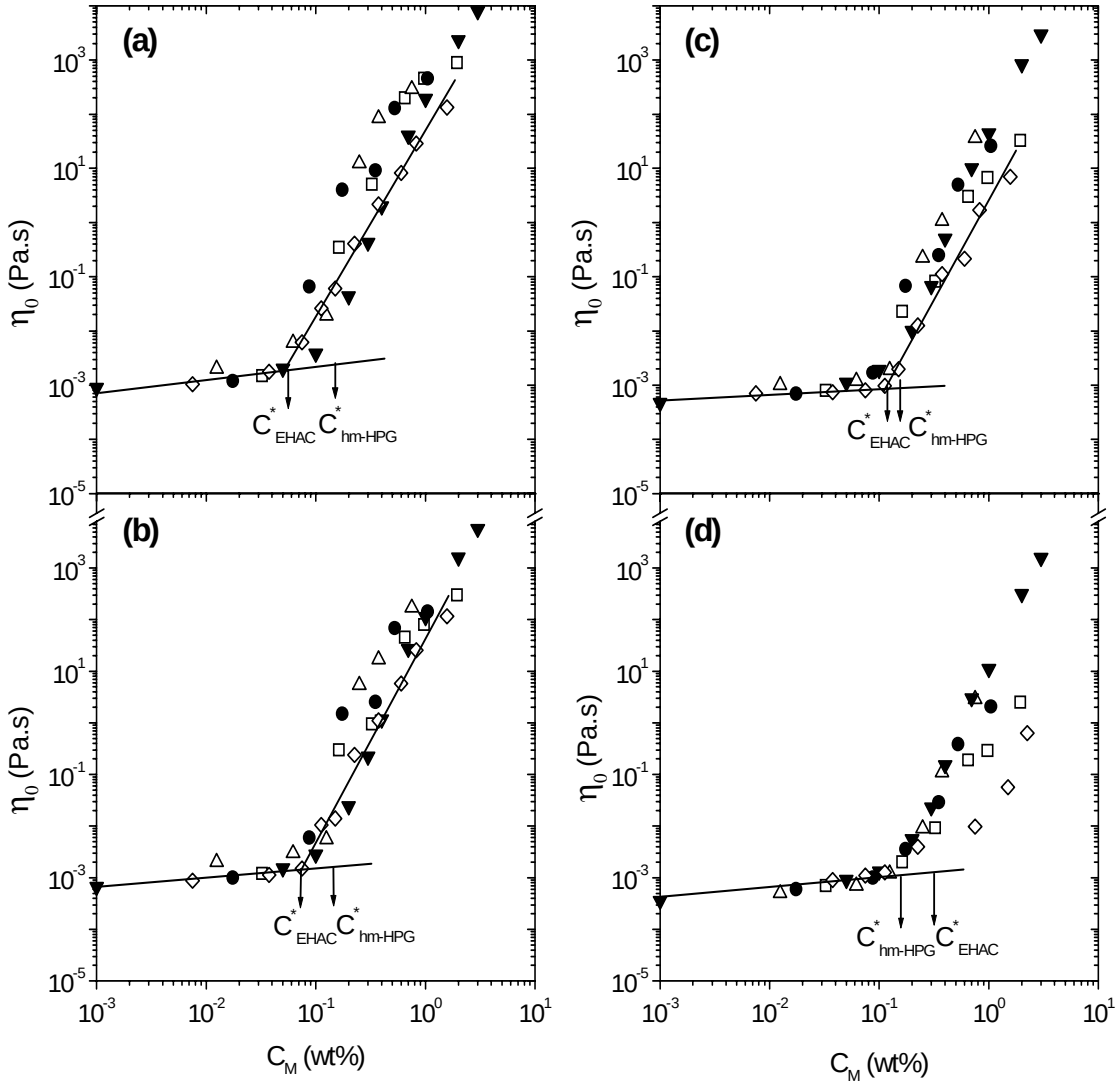

Figure 8: *Zero-shear viscosity versus overall concentration for various compositions of the mixtures (▼ R=0, Δ R=0.2, ● R=0.43, □ R=0.69, ◊ R=1) at various temperatures; (a) T=25°C; (b) =40°C; (c) T=60°C; (d) T=80°C.*

A more illustrative description of this synergistic effect is provided by Fig.9 where the zero-shear viscosity is plotted as a function of the composition *R*, for various

temperatures and for systems with an overall concentration $C_M \approx 0.35\%$, that is about 2.3 times the C^* of the modified polymer. The maximum which is observed for $R = 0.2$ at all temperatures up to 80°C is the signature of the synergy, the latter being more pronounced at low temperature.

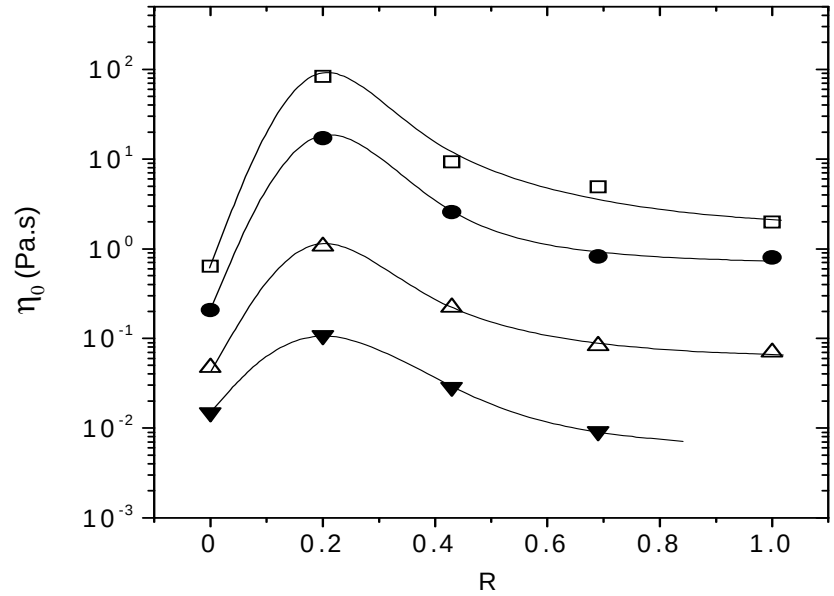

Figure 9: *Zero-shear viscosity versus R at various temperatures, □ 25℃, ● 40℃, Δ 60℃, ▼ 80℃, for systems with $C_M \approx 0.35$wt%. The lines drawn through the data are guides for the eye.*

Fig. 10 shows the flow curves obtained for systems with $C_M \approx 0.35\%$, which is the concentration in the optimal range with respect to the synergy. This synergy, which appears in the Newtonian plateau, is also reflected by the behaviour of $\tilde{\dot{\gamma}}$ that corresponds to the onset of the shear thinning and is of the order of T_R^{-1}. In fact, the values of $\tilde{\dot{\gamma}}$ observed in the curves of Fig.10 for T= 25°C correspond approximately to the values of T_R obtained from the linear viscoelasticity measurements and reported in Fig.6. The only exception concerns the hm-HPG sample for which one observes a Newtonian plateau much larger than what can be expected from the linear viscoelastic measurement ($\tilde{\dot{\gamma}}^{-1}$=0.1s as opposed to $T_R \approx$ 5s). Significant deviations from the

relationship $\tilde{\dot{\gamma}}^{-1} = T_R$ were also reported for other hydrophobically modified water soluble polymers.[7,40,53,54] In the present case, a close inspection of the flow curve obtained at T= 25°C for the hm-HPG solution reveals a weak shear-thickening. This effect which is commonly observed for associating polymers in the vicinity of C^* masks the real onset of shear thinning. [1,41,55,56]

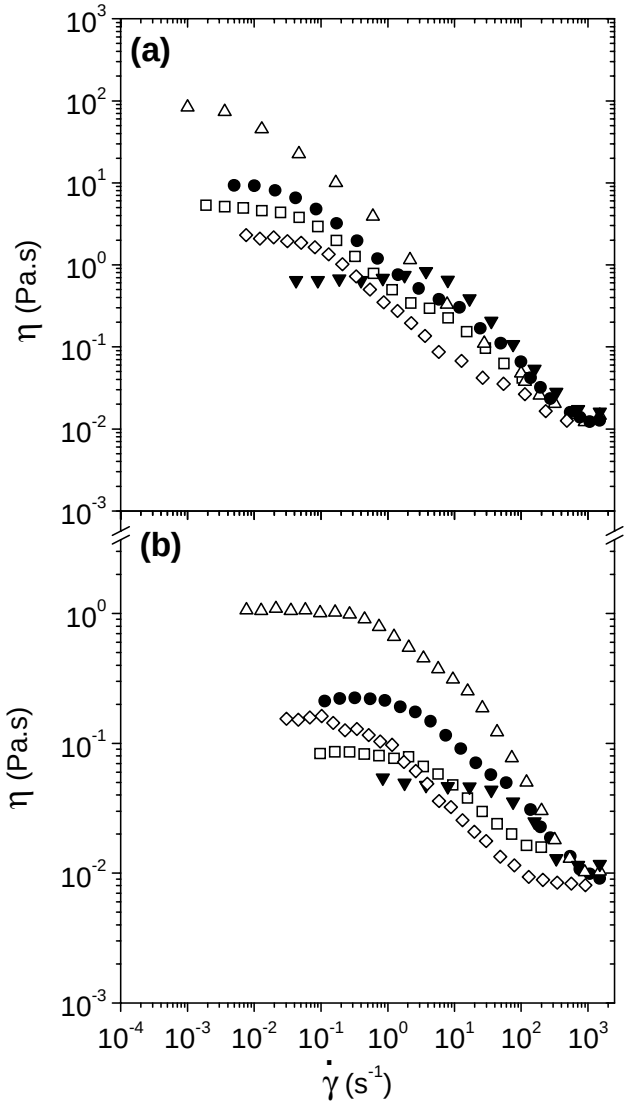

Figure 10: *Variation of the steady shear viscosity as a function of shear rate for different R values (▼ R=0, Δ R=0.2, ● R=0.43, □ R=0.69, ◊ R=1) with C_M≈0.35wt% at two temperatures (a) 25 ℃, (b) 60 ℃.*

The variation of $\eta(\dot{\gamma})$ for mixtures of different R also shows that the composition dependent synergistic effects are maintained at least up to $\dot{\gamma}$ =100s^{-1}. This is illustrated in Fig.11 where the viscosity at $\dot{\gamma}$ = 100 s^{-1} is plotted versus R for systems with an overall concentration $C_M \approx 0.35\%$ and at various temperatures. A maximum is observed for *R*=0.2, the amplitude of the maximum being roughly temperature independent. In fact, the viscosity at $\dot{\gamma}$ = 100 s^{-1} is only weakly temperature dependent, whatever the composition of the system. For instance, for the system with *R*= 0.2, the viscosity η_{100s}^{-1} drops by a factor of ~ 2 between 25°C and 80°C.

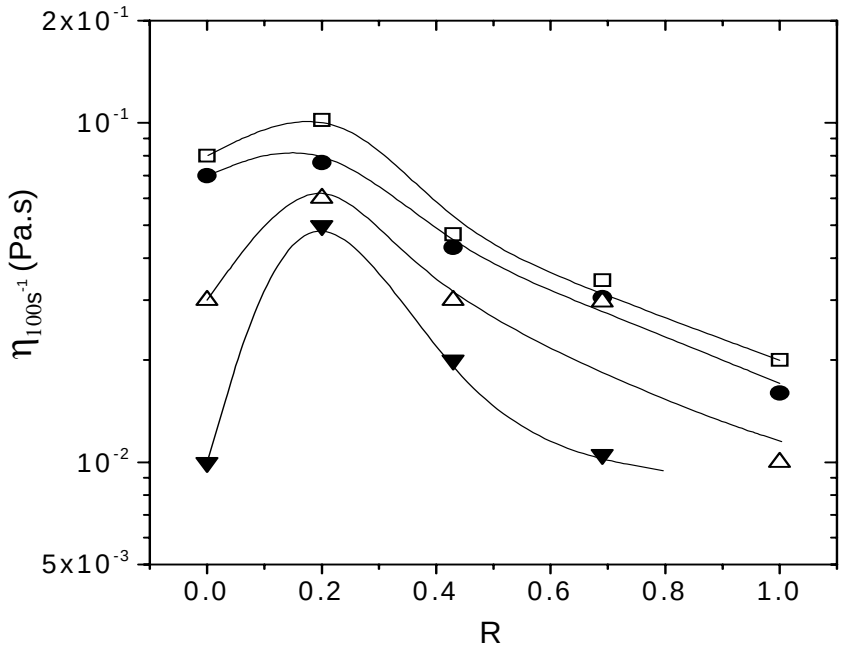

Figure 11: *High shear rate viscosity versus R at various temperatures, □ 25℃, ● 40℃, Δ 60℃, ▼ 80℃, for systems with $C_M \approx 0.35$wt%. The lines drawn through the data are guides for the eye.*

In Fig.12 are reported the same flow curves as those of Fig.10, in the representation $\eta = f(\sigma)$. The behaviour of the blends is more complex than for the single component EHAC or hm-HPG solutions. The high shear viscosity of mixtures still exhibits a more or less sharp drop, depending on the composition and the temperature.

For systems with a well defined plateau, one can determine the values of both σ_c and $\dot{\gamma}_c$. The values thus obtained are reported in Table 3.

R	T(°C)	σ_c (Pa)	$\dot{\gamma}_c$ (s^{-1})
0	25	8.5	12
	40	7.7	36
	60	4	150
0.2	25	2.5	1.6
	40	3.5	9
	60	5.5	27
0.43	25	5.8	39
	40	5.8	70

Table 3: *Effect of the mixture composition on the parameters σ_c and $\dot{\gamma}_c$ for solutions with an overall concentration $C_M \approx 0.35$wt% at various temperatures. The critical shear stress σ_c and critical shear rate $\dot{\gamma}_c$ are measured with an accuracy of +/- 10% and +/- 25% respectively.*

Inspection of this Table reveals several features. First, the decrease of σ_c upon increasing temperature for the hm-HPG solutions is much stronger than at higher concentration (cf. Fig.3). Secondly, whereas the behaviour of σ_c is rather complex, $\dot{\gamma}_c$ presents a pronounced minimum at the composition R= 0.2 corresponding to the optimal synergistic effect. If, as stated by Aubry and Moan, $\dot{\gamma}_c$ represents the inverse of the lifetime of the temporary crosslinks, this means that the lifetime of a EHAC/hm-HPG mixture with R = 0.2 is much larger (1.6s at 25°C) than that of the pure hm-HPG at the same concentration (0.08s at 25°C).[5]

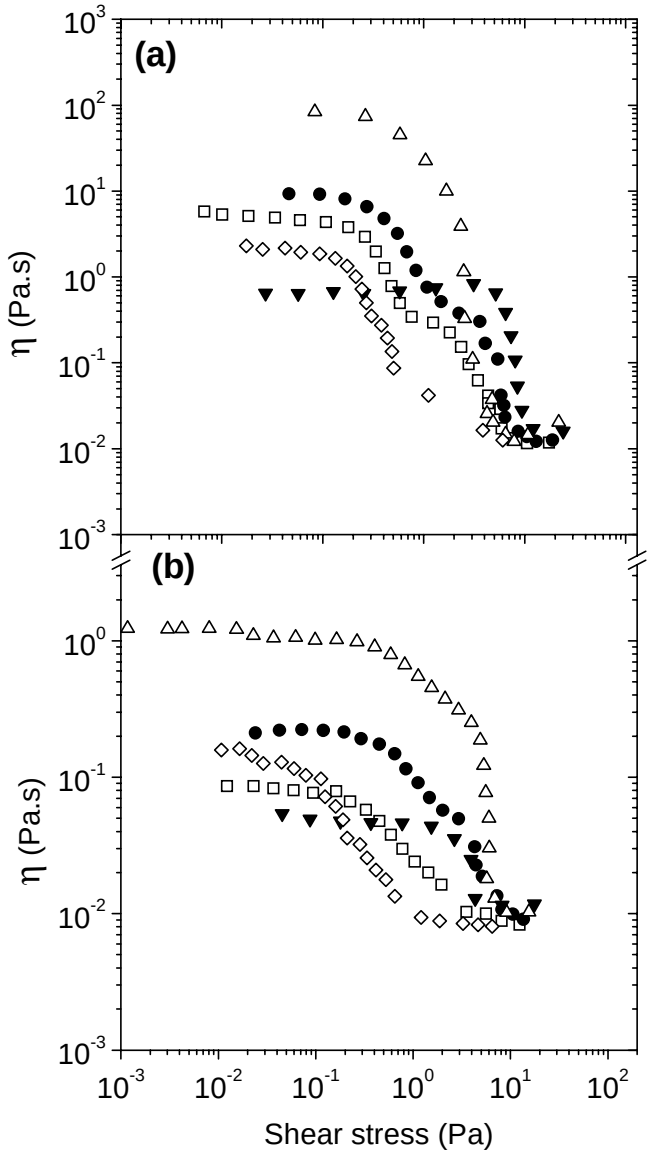

Figures 12: *Variation of the steady shear viscosity as a function of shear stress for different R values (▼ R=0, Δ R=0.2, ● R=0.43, □ R=0.69, ◊ R=1) with $C_M \approx 0.35$wt% at two temperatures (a) 25 ℃, (b) 60 ℃.*

Discussion

Unmodified and Modified Guars:

We discuss first the behaviour of the unmodified polymer. The guar is a slightly stiffened random coil polymer for which one can use the methods commonly employed in synthetic polymer studies.[57] In particular, the crossover volume fraction ϕ^* can be written as:

$$\phi^* \approx \frac{S_c L}{R_G{}^3} \tag{3}$$

where S_c is the section of the chain and R_G the radius of gyration. According to both the classical Flory's theory and the scaling model developed by de Gennes, the expression of ϕ^* for a flexible chain with N monomeric units of size a and a persistence length l_p, in good solvent conditions, is given by:[46]

$$\phi^* \approx S_c l_p{}^{3/5} v_0{}^{-3/5} L^{-4/5} \tag{4}$$

$$\phi^* \approx a^{6/5} l_p{}^{3/5} v_0{}^{-3/5} N^{-4/5} \tag{5}$$

where v_0 is the excluded volume parameter.

In the semi dilute regime, C ≥ C^*, the solution can be viewed as a melt of blobs whose size is the correlation length ξ, which, according to the scaling model of de Gennes is given by:[46]

$$\xi \approx a^{3/2} l_p{}^{1/4} v_0{}^{-1/4} \phi^{-3/4} \tag{6}$$

Based on the static picture outlined above, a dynamical scaling model has been proposed. In the entangled regime, the dynamical properties depend on the spatial scale. For length scales shorter than the correlation length, the hydrodynamic interactions control the dynamics and the motion within the blobs is Zimm-like, with a characteristic relaxation time τ_ξ proportional to the blob volume ξ^3

$$\tau_\xi \approx (\eta_s / kT)\xi^3 \tag{7}$$

On distance scales larger than ξ, the behaviour is that of a Rouse chain formed of $\tilde{N}$ blobs. Finally, the dynamics associated with the $N/(\tilde{N}\phi\xi)^3$ entanglement strands is reptation-like.

Under these assumptions, the longest relaxation time is given by:[46, 58]

$$T_R \approx \tau_\xi \tilde{N}^2 [N/(\tilde{N}\phi\xi^3)]^3 \tag{8}$$

$$T_R \approx (\eta_s kT)\tilde{N}^{-1} N^3 \phi^{-3} \xi^{-6} \tag{9}$$

The zero-shear viscosity is given by:

$$\eta_0 = T_R G_0 \tag{10}$$

where G_0 is the plateau modulus which is proportional to the entanglement density

$$G_0 = kT/(\tilde{N}\xi^3) \tag{11}$$

It follows:

$$\eta_0 \approx \eta_s \tilde{N}^{-2} N^3 \phi^{-3} \xi^{-9} \tag{12}$$

Equation (12) shows that, at a given concentration, the zero-shear viscosity varies oppositely to the correlation length.

The experimental observation of a decrease of the relative zero-shear viscosity η_0/η_s upon increasing the temperature (cf.Fig.1) suggests then an increase of the correlation length with temperature and correspondingly a decrease of the excluded volume parameter (cf. Eq.(6)), that is a decrease of the quality of solvent. The latter might result from the breaking of the hydrogen bonds present in most aqueous solutions of hydrophilic polymers. A decrease of v_0 upon increasing the temperature should lead to an increase of C^*, according to Eq.(4). However, this effect is much weaker for C^* that varies like $v_0^{-3/5}$ than for η_0/η_s that scales like $\xi^{-9} \sim v_0^{9/4}$ (Eqs.(6) and (12)). Experimentally no significant variation of C^* with temperature could be detected. Since η_0/η_s only decreases by a factor of ~ 2 when T varies from 25°C to 80°C, the expected variation of C^* remains in the limit of the experimental accuracy. Note that a possible effect of temperature on the persistence length may also be invoked.

The high shear results are also in agreement with the above observations. At high shear rate, the flow is controlled by the Zimm-like dynamics within a blob (cf. Eq.(7)). In that limit, for a system at a given concentration, the high shear viscosity should increase with ξ. This might explain the crossing of the curves $[\eta/\eta_s](\dot{\gamma})$ observed in Fig.1a, leading to an increase of the high shear rate viscosity with temperature.

Looking now at the concentration dependence of the zero-shear viscosity, one obtains power laws with an exponent of the order of 4 (Fig.4). This is the classical behaviour of random coils in good solvent and is in agreement with the scaling model that predicts:[46,58]

$$\eta_0 = \eta_s \tilde{N}^{-2} N^3 \phi^{15/4} \qquad (13)$$

The above equation is obtained by inserting the scaling law $\xi \approx \phi^{-3/4}$ in Eq.(12).

The behaviour of the modified polymer, as compared to that of the unmodified one, is quite similar to that reported for other systems. The enhancement of the zero-shear viscosity is accounted for by the sticky reptation model developed first by Leibler et al.[10]

and subsequently by Rubinstein and Semenov[11]. The prediction of the first version of the sticky reptation model, for the zero-shear viscosity is:

$$\eta_0 \approx \phi^{15/4} N^{7/2} [s]^2 \tau (1 - 9/p + 12/p^2)^{-1} \quad (14)$$

where [*s*] is the molar ratio of stickers with respect to the total number of monomers, *p* the average fraction of stickers engaged in an association and τ the average lifetime of a sticker in a crosslink. The temperature dependence observed in Fig.1 for η_0/η_s is stronger than for the HPG sample (decrease of 6.5 compared to 2) and can be mainly ascribed to a decrease of the lifetime of the associations, as shown by the $\dot{\gamma}_c$ values reported in Table 3.[40]

The above prediction was obtained within the assumption that after the breaking of an association, the search of a sticker for a new partner is restricted to a part of the tube confining entangled chains. Rubinstein and Semenov considered the effect associated with the increase of the fraction of the inter-chain associations at the expense of the intra chains ones with increasing the polymer concentration.[11] The model taking into account this effect predicts a very complex behaviour of the zero-shear viscosity for entangled systems in good solvent with four successive regimes of different extent where the zero-shear viscosity varies with concentration according to power laws with exponents 6.8, 8.5, 3.7, 4.7 respectively. This confers the representative curve of $\eta_0(C)$ a sigmoidal shape such as that observed experimentally in Fig.4.

In the high shear rate regime, the flow behaviour is qualitatively the same as for the unmodified polymers, as illustrated by the comparison between Figs.1a and 1b. A crossing of the curves $[\eta/\eta_s](\dot{\gamma})$ is again observed for the hm-HPG sample at about the same values of the crossing shear rates measured in Fig.1a.

EHAC/hm-HPG Mixtures:

The synergistic behaviour revealed by the rheological experiments is the signature of strong interactions between EHAC wormlike micelles and hm-HPG associating chains. These interactions are confirmed by the fact that the increase of the zero-shear

viscosity occurs at an overall concentration of the order of C^*_{EHAC} and, depending on the temperature, smaller or equal to $C^*_{hm\text{-}HPG}$. Looking separately at the two components in the mixtures, it can be observed in Figs. 7a and 7b that at T=25°C, the viscosity rise starts at EHAC and hm-HPG concentrations significantly lower than their respective C^*. Under these conditions, the EHAC micelles are shorter than at C^*, since their average length increases with concentration, in contrast with the polymer chains whose length remains unchanged. It should also be noted that the C^* of both hm-HPG and EHAC samples are of the same order of magnitude. It follows that the EHAC micelles, which are much thicker than the polymeric chains, are also longer in the vicinity of C^* according to Eq.(4).

The frequency dependences of the complex shear modulus provided by the linear viscoelasticity experiments are characteristic of entangled solutions, as ascertained by the presence of a plateau modulus and of a dip of $G''(\omega_m)$ in the high frequency range. Therefore, the stress relaxation is controlled by the chain reptation. The ratio C/C^* of the investigated systems are of about 2.3 for the hm-HPG solution and about 7 for the EHAC and mixtures solutions (T=25°C). It should be noted that the viscoelastic curves are not significantly smeared by the polydispersity of the samples containing micelles and chains with very different lengths. However, it must be reminded that the terminal time of the stress relaxation of wormlike systems does not only depend on their length but also on their breaking time. In the limit where the breaking time is much shorter than the reptation time, the stress relaxation is described by a single exponential.[59] As for the relaxation time of associating polymers, it also depends both on their length and the lifetime of the associations. In any case, the reptational mechanism of these mixtures must be very complex, but surprisingly the viscoelastic curves exhibit a quite simple behaviour.

The non linear behaviour of polymers and wormlike micelles submitted to a steady shear has been theoretically studied by Spenley et al..[60] The predictions of the model are the following: as the shear reaches a threshold value, $\dot{\gamma}_c = 2.6/T_R$, a mechanical instability of shear banding type occurs within the solutions. This instability is characterized above $\dot{\gamma}_c$ by a plateau of the shear stress $\sigma_c = \frac{2G_0}{3}$ (or a vertical variation in the representation

$\eta(\sigma)$). The plateau persists over a finite $\dot{\gamma}$ range, beyond which there is again a linear increase of σ. In the plateau regime, bands of highly sheared liquid of low viscosity coexist with a more viscous part supporting a lower rate. Such a behaviour does not seem to have been observed for ordinary polymers. Typically, some shear thinning occurs, but the shear stress continues to rise gently, reflecting a gradual stretching and orientation of the chains. This is what is observed in Fig 2 for the non-modified HPG polymer.

The occurrence of a stress plateau and of a shear banding at high shear has been reported for wormlike micelles.[42-44] However, a true discontinuity of the slope in the $\sigma(\dot{\gamma})$ or $\eta(\sigma)$ curves only occurs at relatively high concentrations (C/C^* ≥15). Below this value of C/C^*, the plateau regime is much smoother and rounded. As the concentration decreases, the plateau disappears with an inflexion point as the only reminiscence. This regime corresponds to a progressive and homogeneous orientation of the micelles submitted to shear. This type of behaviour is observed in the curves of Figs. 12a and 12b.

No model has been developed to describe the non linear flow behaviour of hydrophobically modified polymers. Both our results and those of Aubry and Moan show the existence of an intermediate regime between the Newtonian one and the shear stress plateau, likely associated with stretching and orientation of the chains (cf. Fig.1).[5] The shear stress plateau might still be the signature of a shear banding instability. In order for the instability to occur, the crosslinks between the associative units must be broken, and therefore the limiting step in the process will be controlled by the lifetime of the junction points, in agreement with the conclusions of Aubry and Moan.[5] The non linear rheology of the mixtures of EHAC and hm-HPG systems presents qualitatively the same features as those of hm-HPG polymers. It should be noted that the occurrence of a stress plateau was also recently reported by English et al. for hydrophobically modified alkali-swellable emulsion (HASE) polymers.[61] Contrary to the systems investigated here, addition of a high HLB surfactant tends to progressively diminish the shear-induced structuring.

Turning back to the synergistic effect, both linear viscosity and flow experiments show that for an overall concentration $C_M \approx$ 0.35wt% and T=25°C, the synergy is optimal for a composition of R = 0.2, as revealed by the maximum in T_R and η_0. Such a maximum can result from an increase of the micellar length, of the number and/or the lifetime of the temporary crosslinks, or also from both effects.

The normalized amplitude and the position of the dip of $G''(\omega)$ given in Table 2 exhibit a minimum for R = 0.2. However, the comparison of Tables 2 and 3 shows that for all systems, except the one with the composition R = 0.2, $\omega_m << \dot{\gamma}_c$, so that the validity of Eqs.(1) and (2) is questionable. Still, these results confirm the specific behaviour of the mixture with R = 0.2.

As for the variation of the critical shear rate with R reported in Table 3, it exhibits a minimum for the composition R = 0.2, suggesting a maximum of the lifetime of the crosslinks at this composition. As for the temperature dependence of $\dot{\gamma}_c$, it follows an Arrhenius behaviour (results not shown here) from which an activation energy E_a can be determined. This activation energy is found to be E_a=24k_BT for R=0 (hm-HPG), E_a=26.7k_BT for R=0.2 and E_a=12.1 k_BT for R=0.43 (determination from two data points). This result shows an enhancement of the activation energy for the lifetime of the associations at the synergistic composition R=0.2.

Three interaction mechanisms between micelles and associating polymers can be envisioned:

i) The presence of surfactant produces a strengthening of the hydrophobic interactions through a non-cooperative bonding. Recent studies have shown that the viscosity enhancement mostly results from a process where the surfactant decorates the pre-existing crosslinks and increases their lifetime.[34] However, this effect occurs for surfactant concentrations close to the *cmc* and disappears in the presence of an excess of surfactant. In the latter limit, it is generally believed that the hydrophobic sequences are singly solubilised by the spherical surfactant micelles.

ii) The incorporation of hydrophobic sequences within the wormlike micelles produces a micellar growth, thus increasing the viscosity of the system.

iii) Bridges are formed between the wormlike micelles and the hydrophobic sequences of the polymer to build a temporary network.

Considering the very large excess of surfactant concentration with respect to the hydrophobic sequences, a contribution arising from a decoration by the surfactant of pre-existing crosslinks must be ruled out. On the other hand, the formation of an interpenetrated network of wormlike micelles and hydrophobically modified chains, as schematized in Fig.13 might explain the viscosity enhancement. In such a scheme, most

of the hydrophobic sequences are embedded within the wormlike micelles and possibly some binary (or multiple) crosslinks are still present with also some free stickers. The scheme of Fig.13 represents a situation of entangled chains corresponding to an overall concentration C_M significantly larger than C^*_M.

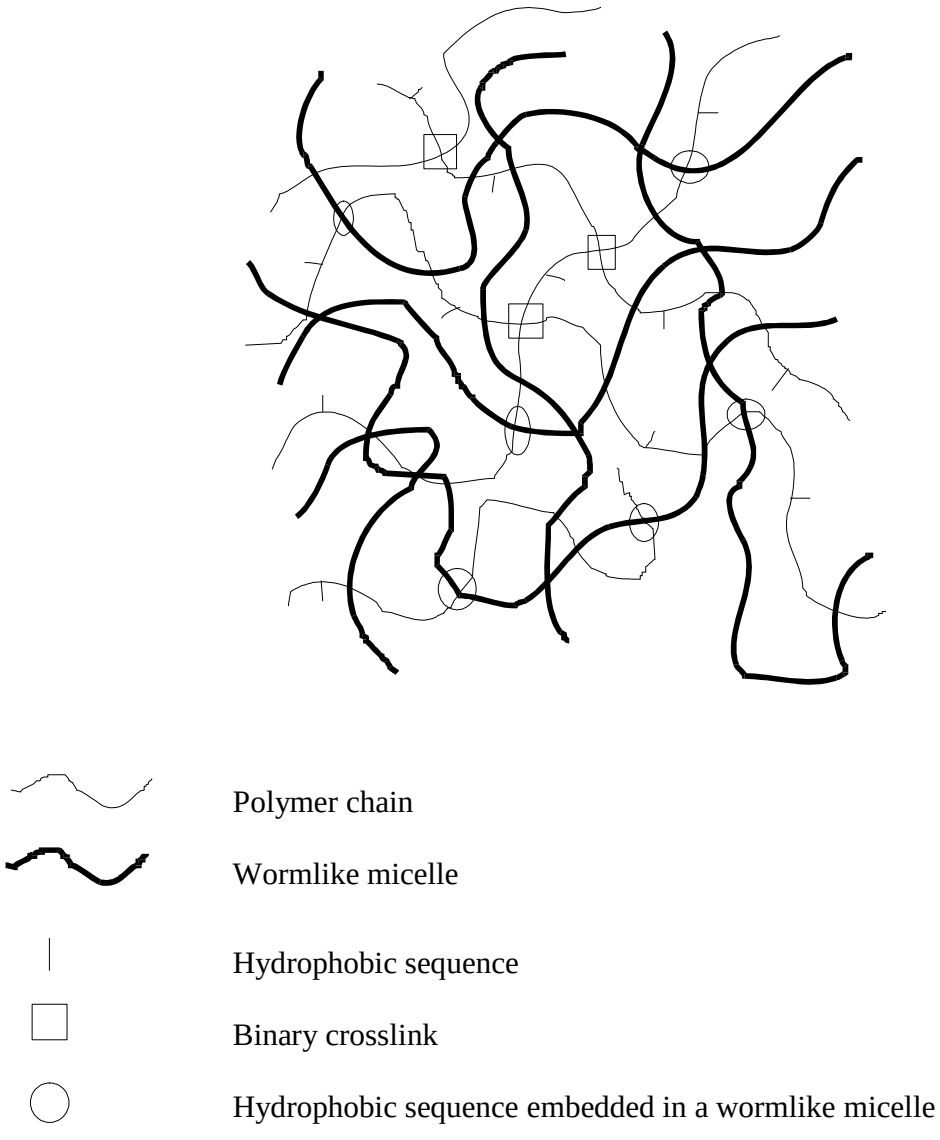

Figure 13: *Interpenetrated network of wormlike micelles and hydrophobically modified chains of hm-HPG.*

The coupled motion in such systems can be described by the sticky Rouse model in the vicinity of C^*_M or by the sticky reptation model in the entangled state.[11,62] The latter case is illustrated by the scheme 14, which represents one associating chain and one wormlike micelle in their respective tubes whose diameter is given by the average mutual entanglement length. Some stickers of the polymer chain are embedded in the wormlike micelle. In its reptation motion, the wormlike micelle can diffuse more or less freely within its tube despite the stickers, as the surfactant molecules can move without dragging the sticker. On the other hand, the polymer motion is somewhat hindered by the residency time of the sticker within the micelle, which is likely dependent on the micelle lifetime.

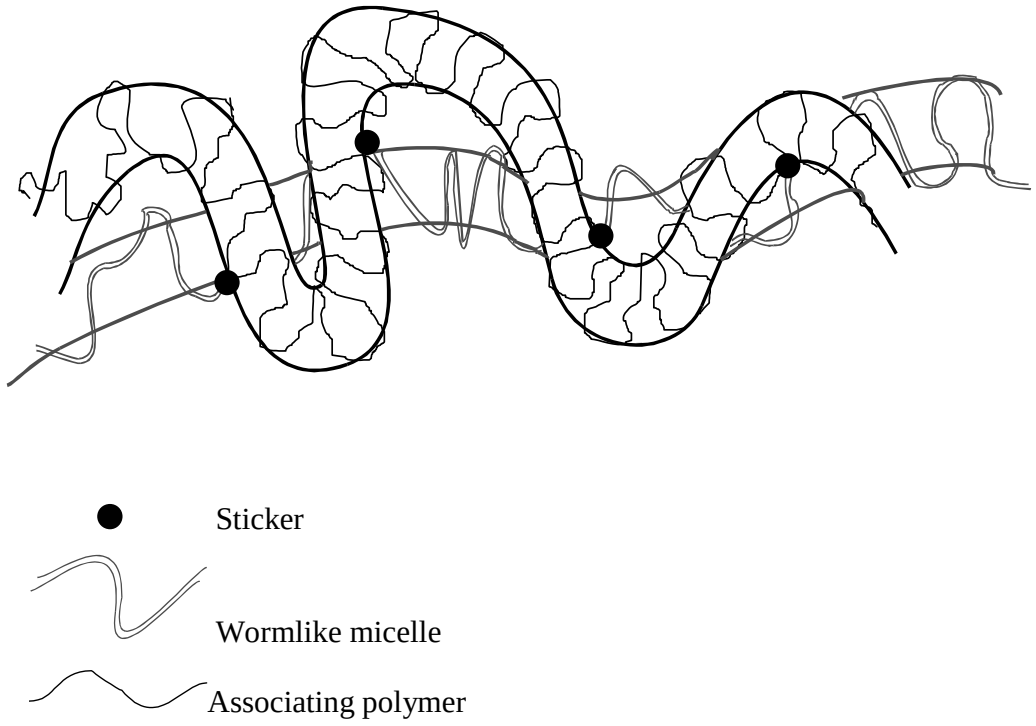

Figure 14: *Representation of an associating polymer chain and a wormlike micelle in their respective tubes.*

Experimentally, one observes a lesser or suppressed synergy at high concentration or at high temperature. In the high concentration regime, one might expect that the density of crosslinks between the stickers increases. The effect of these crosslinks possibly overcomes that of the stickers embedded in the micelle. Also, there may be some intermicellar branching that reduces the viscosity.[63] At high temperature, the micelles become much shorter. Therefore, the contribution to the viscosity from the wormlike micelles is decreased. Moreover, at high temperature, the micelles might become short enough not to make any longer efficient bridges between the polymer chains. In this limit, the surfactant will only decorate the hydrophobic sequences and the viscoelastic behaviour should tend to that of the unmodified polymer at the concentration of the modified polymer in the mixture.

Conclusion

This is the first report, to our knowledge, of synergystic effects in mixtures of hydrophobically modified polymers and wormlike micelles. The synergy manifests itself both in the linear and non linear properties of the systems. In particular, the zero-shear viscosity of the mixtures is significantly increased with respect to that of each component in an overall concentration range extending from 0.07wt% to 1wt% and for temperatures up to 60°C.

The combination of linear and non linear rheological measurements allowed us to show that the synergy results from an increase of the lifetime of the crosslinks, which suggests the formation of crosslinks between the micelles and the polymer chains. These results open new prospects both from fundamental and applied points of view. For thickening applications, the curves of Figs.7 and 8 and the comments given in the same section clearly show that it might be advantageous to replace the wormlike micellar systems or the modified polymers by a lesser amount of a mixture of these two components. This is reflected by the viscosity behaviour at both low and high shear rates. Of particular interest is the presence of a maximum in the curves of Fig.11. This maximum shows that even at T= 80°C and $\tilde{\dot{\gamma}} = 100 s^{-1}$, an appreciable viscosity of about 0.05Pa.s can be

obtained with an appropriate mixture, which make these systems useful as fracturing fluids.

Several issues concerning the fundamental properties are still open. The schemes proposed to explain the rheological behaviour of these systems are very qualitative and a real model describing the coupled flow of wormlike micelles and hydrophobically modified polymers is lacking. The experimental observation that the synergy takes place in a limited range of overall concentrations is not easily explainable. More results on both linear and non linear properties of another modified polymer- wormlike micelle system will be presented in a forthcoming paper.

Acknowledgements:

The authors wish to thank J.S. Candau (ULP, Strasbourg) and J. Selb (ICS, Strasbourg) for helpful discussions.

References

(1) *Polymers in Aqueous Media: Performance through Association,* Ed.: Glass, J. E.; Advances in Chemistry Series 223, American Chemical Society, Washington, DC, **1989**.

(2) *Hydrophilic Polymers: Performance with Environmental Acceptability*, Ed.: Glass, J. E.; Advances in Chemistry Series 248, American Chemical Society, Washington, DC, **1996**.

(3) Winnik, M. A.; Yelta A. *Curr. Opin. Colloid Interface Sci.* **1997**, *2*, 424.

(4) *Associative Polymers in Aqueous Solution,* Ed.: Glass, J. E.; Advances in Chemistry Series 765, American Chemical Society, Washington, DC, **2000**.

(5) Aubry, T.; Moan, M. *J. Rheol.* **1994,** *38*, 1681.

(6) Nyström, B.; Kjoniksen, A. L.; Iversen, C. *Adv. Colloid Interface Sci.* **1999**, *79*, 81.

(7) Jimerez Regalado, E.; Selb, J.; Candau, F. *Macromolecules*, **1999,** *32*, 8580.

(8) Candau, F.; Selb, J. *Adv Colloid Interface Sci* **1999,** *79*, 149.

(9) Rubinstein, M.; Dobrynin A.V. *Curr. Opin. Colloid Interface Sci.* **1999,** *4*, 83.

(10) Leibler, L.; Rubinstein, M.; Colby, R.H. *Macromolecules* **1991**, *24*, 4701.

(11) Rubinstein, M.; Semenov, A.N. *Macromolecules* **2001**, *34*, 1058.

(12) Caritey, J.-P. *Relation entre la modification chimique de précurseurs hydrophiles d'origine naturelle et leurs propriétés en solution diluée et semi-diluée*, Thèse Université de Rouen, **1994.**

(13) Aubry, T.; Moan, M. *J. Rheol.* **1996,** *40*, 441.

(14) Chase, B.; Krauss, K.; Lantz, T.; Chmilowski, W.; *Oilfield Review*, Autumn **1997**, 20.

(15) Sullivan P.F.; Huang H.; Nelson E.; The Society of Rheology, Paper SM43, 75th Annual Meeting, Oct **2003**.

(16) Maitland, G.C. *Curr. Opin. Colloid Interface Sci.* **2000**, *5*, 301.

(17) Qu, Q.; Nelson, E. ; Willberg, D.; Samuel, M.; Lee, J.; Chang, F.; Card, R.; Vinod, P.; Brown, J.; Thomas, R. ; U.S. Patent 6 435 277, **2002**.

(18) Raghavan, S.R.; Kaler, E. *Langmuir* **2001**, *17*, 300.

(19) Croce, V.; Cosgrove, T.; Maitland, G.; Hughes, T.; Karlsson, G. *Langmuir* **2003**, *19*, 8536.

(20) Couillet, I.; Hughes, T.; Maitland G.; Candau, F.; Candau S.J. *Langmuir* **2004**, *20*, 9541.

(21) *Interactions of Surfactants with Polymers and Proteins*, Eds.: Goddard, E.D.; Ananthapadmanabhan, K. P.; CRC Press, Boca Raton, FL, **1993**.

(22) Hansson, P.; Lindman, B. *Curr. Opin. Colloid Interface Sci.* **1996**, *1*, 604.

(23) Winnik, F.M.; Regismond, S.T.A. *Colloids Surf. A, Physicochem. Eng. Aspects* **1996**, *118*, 1.

(24) *Polymers-Surfactants Systems*, Ed.: Kwak, J.C.T.; Surfactant Science Series, 77, Dekker, New York, **1998**.

(25) Sau, A.C.; Landoll, L.M. In *Polymers in Aqueous Media: Performance through Association*, Ed.: Glass, J. E.; Advances in Chemistry Series 223, American Chemical Society, Washington, DC **1989**, p.343.

(26) Tanaka, R.; Meadows, J.; Phillips, G. O.; Williams, P. A. *Carbohydr. Polym.* **1990**, *12*, 443.

(27) Iliopoulos, L.; Wang, T.K.; Audebert, R. *Langmuir* **1991**, *7*, 617.

(28) Biggs, S.; Selb, J.; Candau, F. *Langmuir* **1992**, *8*, 838.

(29) Chang, Y.; Lochhead, R. Y.; McCormick, C. L. *Macromolecules* **1994**, *27*, 2145.

(30) Nyström, B.; Thuresson, K.; Lindman, B. *Langmuir* **1995**, *11*, 1994.

(31) Xie, X.; Hogen-Esch,T.E. *Macromolecules* **1996**, *29*, 1734.

(32) Panmai, S.; Prudhomme, R. K.; Peiffer, D.G. *Colloids Surf. A., Physicochem. Eng. Aspects* **1999**, *147*, 3.

(33) Piculell, L.; Guillemet, F.; Thuresson, K.; Shubin, V.; Ericsson, O. *Adv. Colloid Interface Sci.* **1996**, *63*, 1.

(34) Jimenez Regalado E.; Selb J.; Candau F. *Langmuir* **2000**, *16*, 8611.

(35) Peiffer D.G.; *Polymer* **1990**, *31*, 2353.

(36) McCormick, C.L.; Nonaka, T.; Johnson, C.B. *Polymer* **1988**, *29*, 731.

(37) Zhang, Y. X.; Da, A. H.; Butler, G. B.; Hogen-Esch, T.E. in *Journal of Polymer Science,* Polymer Chemistry Edition, **1992**, *30*, 1383.

(38) Hwang, F.S.; Hogen-Esch, T.E. *Macromolecules* **1995**, *28*, 3328.

(39) Biggs, S.; Selb, J.; Candau F. *Polymer* **1993**, *34*, 580.

(40) Caputo, M.R.; Selb, J.; Candau, F. *Polymer* **2004**, *45*, 231.

(41) Volpert, E.; Selb, J.; Candau, F. *Polymer* **1998**, *39*, 1025.

(42) Berret, J.F.; Roux, D.C.; Porte, G. *J. Phys. II France* **1994**, *4*, 1261.

(43) Grand, C.; Arrault, J.; Cates, M.E. *J Phys. II France* **1997**, *7*, 1071.

(44) Oda, R.; Narayanan, J.; Hassan, P.A.; Manohar, C. ; Salkar, R.A.; Kern, F.; Candau, S.J. *Langmuir* **1998**, *14*, 4364.

(45) Klucker, R.; Candau, F.; Schosseler, F. *Macromolecules* **1995**, *28*, 6416.

(46) de Gennes, P.G. *Scaling Concepts in Polymer Physics*; Cornell University Press, London, **1979**.

(47) Graessley, W.W. *Polymer* **1980**, *21*, 258.

(48) Colby, R.H.; Rubinstein, M.; Daoud, M. *J. Phys. II (Paris)* **1994**, *4*, 1299.

(49) *Statistical Physics of Macromolecules,* Eds.: Grosberg, A.Y.; Khokhlov, A.R.; A.I.P. Press: New York, **1994**.

(50) Adam, M.; Lairez, D.; Raspaud, E. *J. Phys. II France* **1992**, *2*, 2067.

(51) Kavassalis, T.A.; Noolandi, J. *Phys. Rev. Lett.* **1987**, *59*, 2674.

(52) Granek, R. *Langmuir* **1994**, *10*, 1627.

(53) Annable, T.; Buscall, R.; Ettelaie, R.; Whittlestone, D. *J. Rheol.* **1993**, *37*, 695.

(54) *The structure and rheology of complex fluids*, Ed.: Larson, R. G.; New York: Oxford University Press, **1999**.

(55) *Polymers as Rheology Modifiers*, Eds.: Schulz, D.N.; Glass, J.E.; ACS Symp. Series 462, American Chemical Society, Washington, DC **1991**.

(56) Tam, K.C.; Jenkins, R.D.; Winnik, M.A.; Bassett, D,R. *Macromolecules* **1998**, *31*, 4149.

(57) Morris, E.R.; Cutler, A.N.; Ross-Murphy S.B.; Rees, D.A.; Price, J. *Carbohydr. Polym.* **1981**, *1*, 5.

(58) *The Theory of Polymer Dynamics*, Eds.: Doi, M.; Edwards, S.F.; Clarendon Press: Oxford, **1986.**

(59) Cates, M.E. *Macromolecules* **1987**, *20*, 2289.

(60) Spenley, N.A.; Cates, M.E.; McLeish, T.C.B. *Phys. Rev. Lett*. **1993**, *71*, 939.

(61) English, R. B.; Laurer, J. H., Spontak, R. J.; Khan, S.A. *Ind. Eng. Chem. Res.* **2002**, *41*, 6425.

(62) Rubinstein, M.; Semenov, A.N. *Macromolecules* **1998**, *31*, 1386.

(63) Lequeux, F. *Europhys. Lett.* **1992**, *19*, 675.

Appendix III.1

Effect of temperature on the zero-shear viscosity of HPG and hm-HPG solutions

Figures 1 and 2 show the variation of the steady-state values of the relative viscosity η/η_s where η_s is the solvent viscosity, as a function of the shear rate $\dot{\gamma}$ for HPG samples at two different concentrations, C=2wt% (Fig.1) and C=3wt% (Fig.2), at various temperatures ranging from 25° C to 80° C. These results confirm the behaviour reported in the article for a HPG solution with a concentration C=1wt%, namely a decrease of the relative low-shear viscosity upon increasing temperature.

Figures 3 and 4 show the variation of the steady-state state values of the relative viscosity η/η_s where η_s is the solvent viscosity, as a function of the shear rate $\dot{\gamma}$ for hm-HPG samples at two different concentrations, C=2wt% (Fig.3) and C=3wt% (Fig.4) at various temperatures ranging from 25° C to 80° C. Again, the results confirm those reported in the article for a solution with a concentration C=1wt%.

We can thus conclude that the same temperature effect is observed for both HPG and hm-HPG samples for all the investigated concentrations. This is also illustrated by the results of the zero-shear viscosity reported in table 1 that gives the values of the ratio $\eta_0(80°C)/\eta_0(25°C)$ for various samples of HPG and hm-HPG at different concentrations.

$\eta_0(80°C)/\eta_0(25°C)$	**1wt%**	**2wt%**	**3wt%**
HPG	0.21	0.23	0.25
hm-HPG	0.06	0.13	0.20

***Table 1** : $\eta_0(80°C)/\eta_0(25°C)$ values of HPG and hm-HPG samples at different concentrations.*

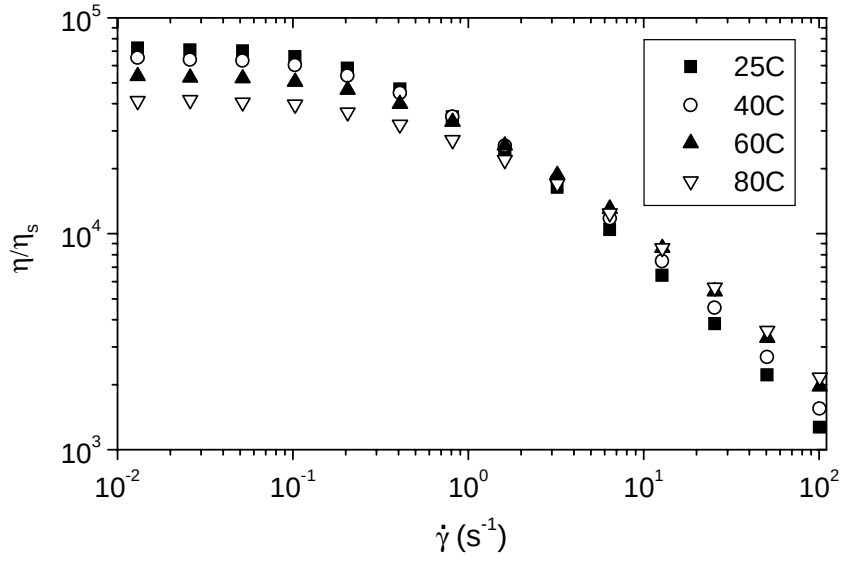

Figure 1: *Relative steady-state viscosity versus shear rate for a 2wt% HPG solution in the presence of 0.4M KCL, at various temperatures.*

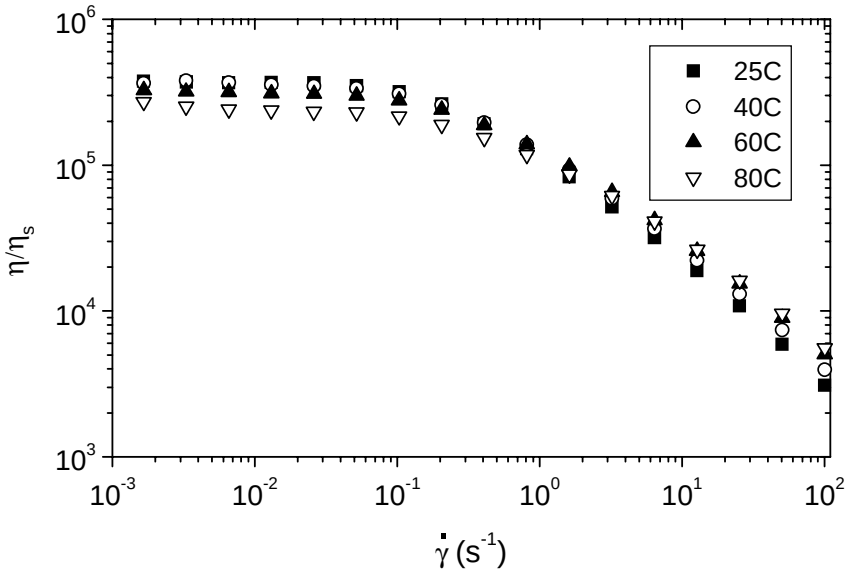

Figure 2: *Relative steady-state viscosity versus shear rate for a 3wt% HPG solution in the presence of 0.4M KCL, at various temperatures.*

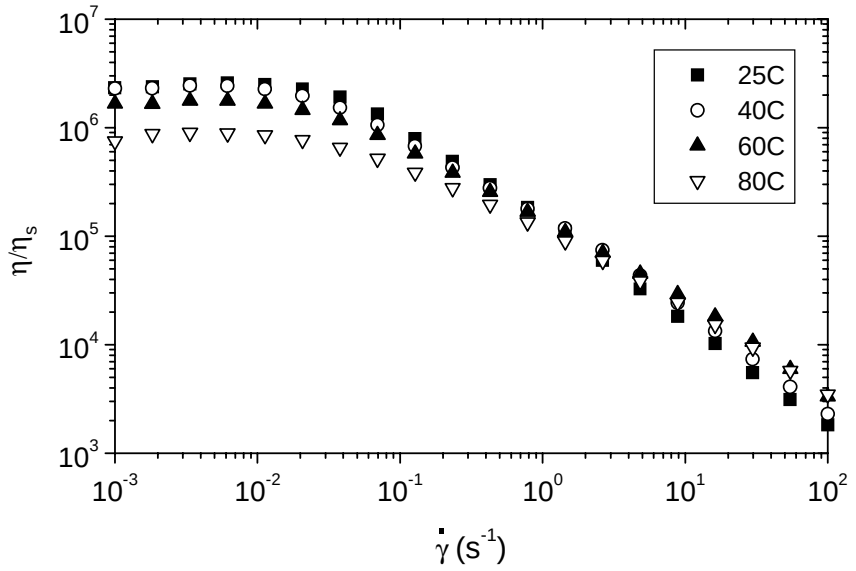

Figure 3: *Relative steady-state viscosity versus shear rate for a 2wt% hm-HPG solution, in the presence of 0.4M KCL, at various temperatures.*

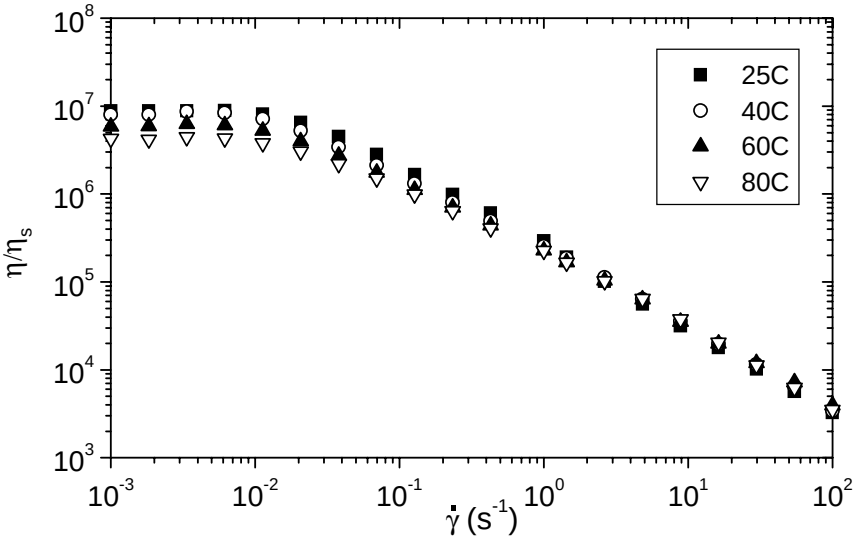

Figure 4: *Relative steady-state viscosity versus shear rate for a 3wt% hm-HPG solution, in the presence of 0.4M KCL, at various temperatures.*

We observe that the ratio $\eta_0(80°C)/\eta_0(25°C)$ increases with the polymer concentration, both for the modified and non modified HPG, which shows that the polymer solution becomes less sensitive to temperature with concentration due to the highest number of effective entanglements that compensate the solvent effect discussed in the paper responsible of the temperature variation of η_{0HPG}/η_s. This effect is much more pronounced for the hm-HPG than for the HPG polymer solution. According to the sticky reptation model developed by Leibler et al.[1], the zero-shear viscosity of associating polymers is found to be proportional to the polymer concentration as well as the average fraction of stickers engaged in an association and the average lifetime of a sticker in a crosslink (cf. Eq.(14) of the paper). By increasing the hm-HPG concentration, the number of associated stickers increases, that reduces the sensitivity of the polymer solution to temperature.

Figure 5 gives the semi-log plot of the ratio $\eta_{0hm\text{-}HPG}/\eta_{0HPG}$ as a function of $10^3/T$ for various polymer concentrations. By considering this ratio, one expects to eliminate the solvent effect discussed in the paper, responsible of the temperature variation of η_{0HPG}/η_s and thus to describe the combined behaviours of the lifetime of the stickers, the molar ratio of stickers with respect to the total number of monomers and the average fraction of stickers engaged in an association (cf. Eq.(14) of the paper).

As shown in Fig.5, the variation of $\eta_{0hm\text{-}HPG}/\eta_{0HPG}$ is non Arrhenian, which reflects a quite complex effect of the above parameters. It decreases upon increasing the temperature, which is most likely due to a decrease of the lifetime of the associations. The latter effect was also shown in the paper by the temperature dependence of the critical shear rate $\dot{\gamma}_c$ (cf. Table 3 of the article).

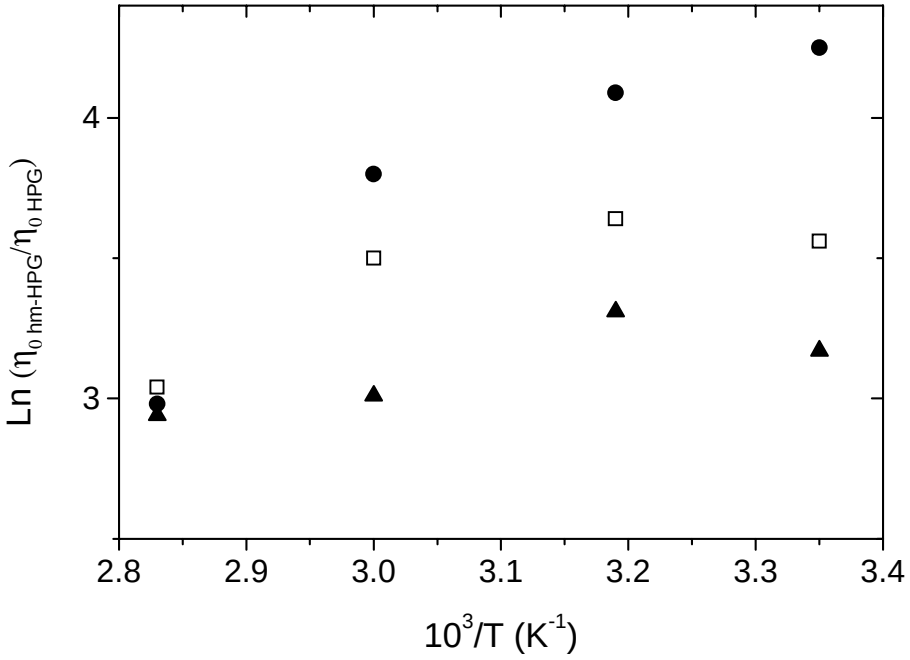

Figure 5: *Variation of $\eta_{0hm\text{-}HPG}/\eta_{0HPG}$ as a function of $10^3/T$ for various polymer concentrations (● 1wt%; □ 2wt%; ▲3wt%).*

REFERENCES

(1) Leibler, L.; Rubinstein, M. ; Colby, R.H. *Macromolecules* **1991**, *24*, 4701.

Appendix III.2

Non linear rheological properties of hm-HPG solutions

Figures 1-4 show the variation of the steady state viscosity versus the shear stress for hm-HPG solutions at various concentrations, in the presence of 0.4M KCl and at various temperatures.

For all the hm-HPG samples investigated, except for the less concentrated one at high temperature, one observes the behaviour characteristic of associating polymers: a Newtonian plateau followed by a gradual shear-thinning regime, then an abrupt drop of the viscosity. The latter occurs at a critical shear stress σ_c to which corresponds a critical shear rate $\dot{\gamma}_c$.

The variation (Fig.5a) of the critical shear stress σ_c with concentration can be fitted at T= 25°C by a power law $\sigma_c \approx C^{1.62}$ in agreement with the previous findings of Aubry and Moan in the salt-free systems: $\sigma_c \approx C^{1.7}$ [1]. As the temperature increases, the exponent of the power law of σ_c versus C tends to increase (1.67 at 40°C and 2.14 at 60°C). Also deviations from the power law appear in the high concentration range (Figs.5b and 5c).

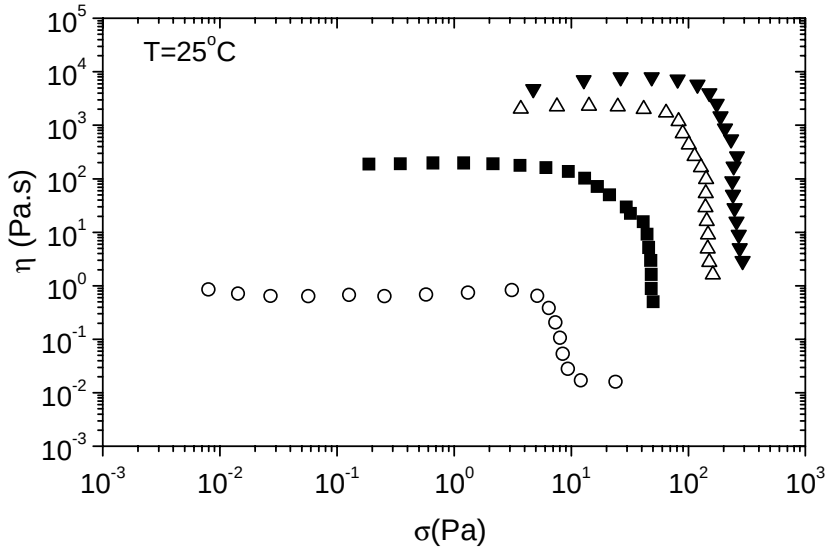

Figure 1: *Steady-state shear viscosity versus shear stress for hm-HPG solutions at various concentrations (○ 0.35wt%, ■ 1wt%, Δ 2wt%, ▼ 3wt%) in the presence of 0.4M KCl, at 25℃.*

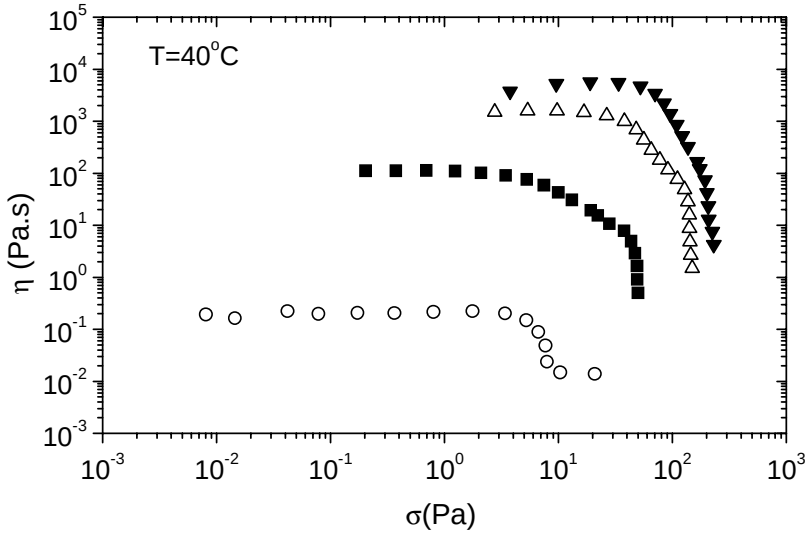

Figure 2: *Steady-state shear viscosity versus shear stress for hm-HPG solutions at various concentrations (○ 0.35wt%, ■ 1wt%, Δ 2wt%, ▼ 3wt%) in the presence of 0.4M KCl, at 40℃.*

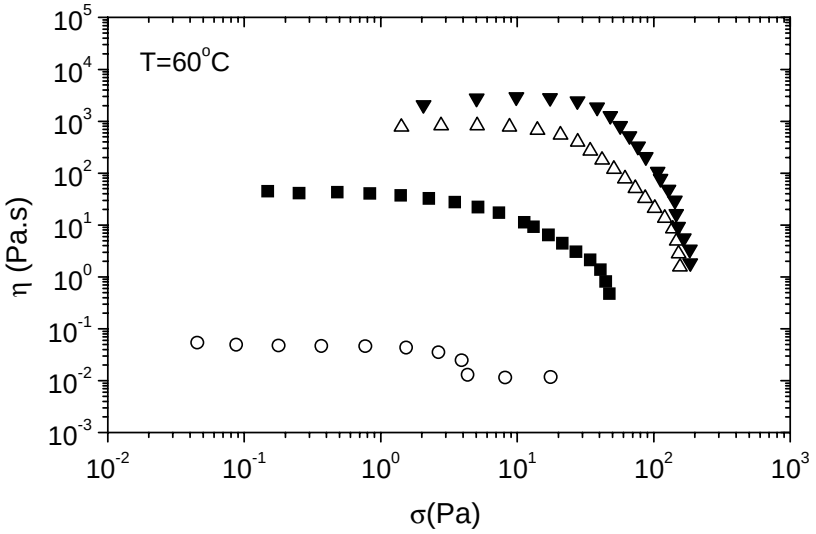

Figure 3: *Steady-state shear viscosity versus shear stress for hm-HPG solutions at various concentrations (○ 0.35wt%, ■ 1wt%, Δ 2wt%, ▼ 3wt%) in the presence of 0.4M KCl, at 60℃.*

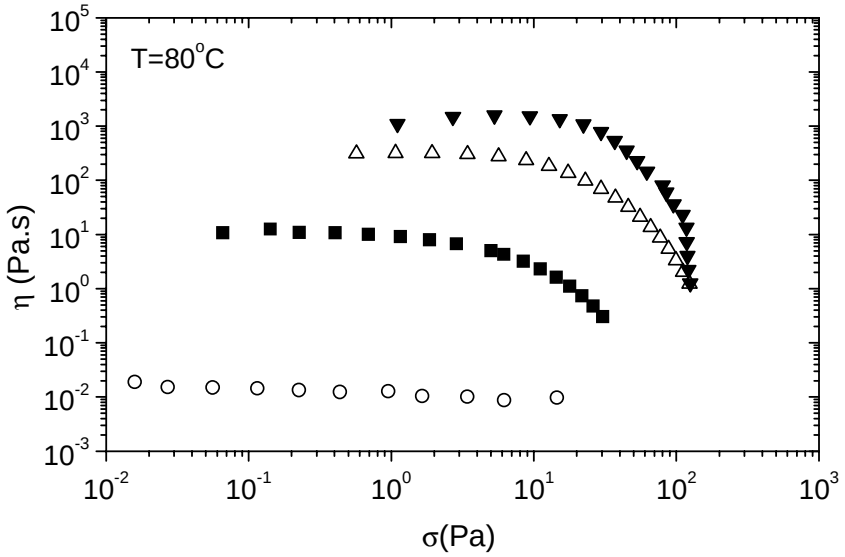

Figure 4: *Steady-state shear viscosity versus shear stress for hm-HPG solutions at various concentrations (○ 0.35wt%, ■ 1wt%, Δ 2wt%, ▼ 3wt%) in the presence of 0.4M KCl, at 80℃.*

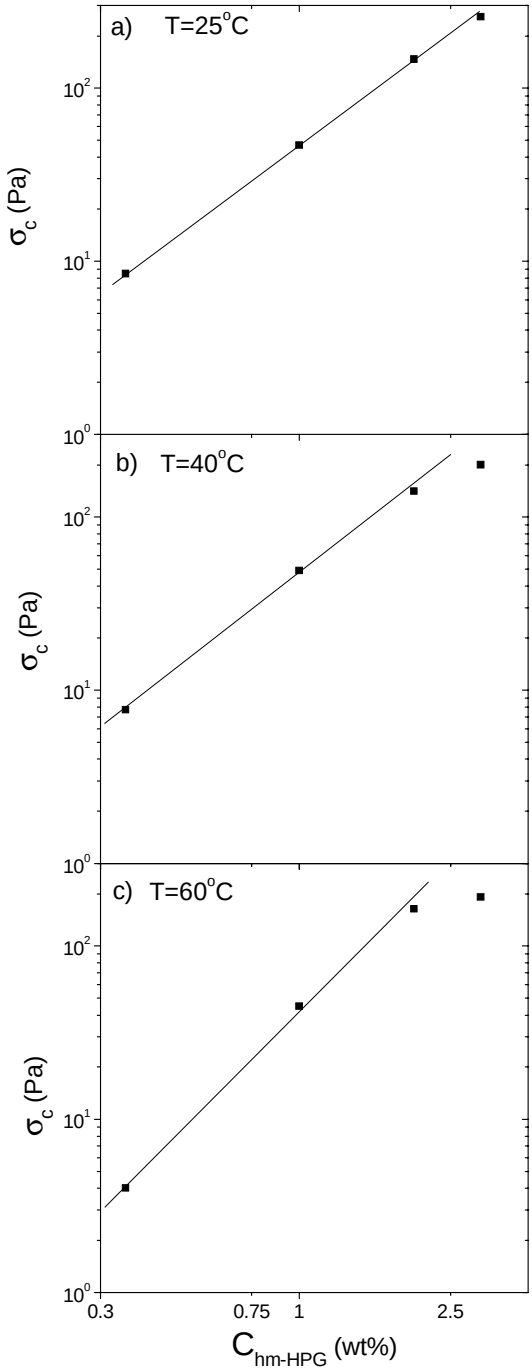

Figure 5: *Variation of the critical shear stress σ_c as a function of the hm-HPG concentration at various temperatures.*

At 25°C, the critical shear rate $\dot{\gamma}_c$ decreases upon increasing the concentration (Fig.6) with a trend to a plateau at concentrations $\geq$2wt%). The same effects are observed at 40°C and 60°C. This indicates that the lifetime of the hydrophobic crosslinks increases with the polymer concentration, thus suggesting that the fraction of stickers engaged in an association also increases with this parameter, with however a saturation at high concentration.

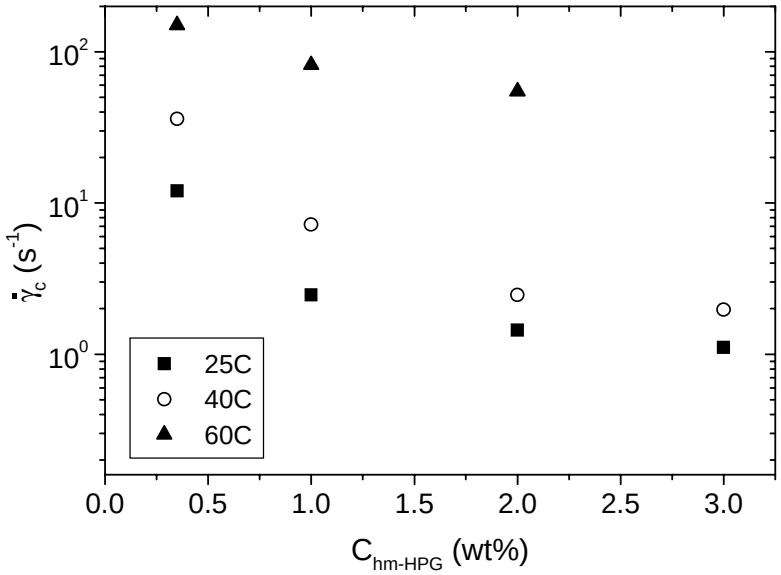

Figure 6: *Variation of the critical shear rate $\dot{\gamma}_c$ as a function of the hm-HPG concentration at various temperatures.*

Note that this result is at variance with the Aubry and Moan's observation[1] that $\dot{\gamma}_c$ is independent on concentration for salt-free systems in the concentration range 0.75wt%-1.5wt%.

The temperature dependence of $\dot{\gamma}_c$ for various hm-HPG concentrations is represented in Fig.7. For a concentration of hm-HPG equal to 0.35wt%, the temperature dependence of

$\dot{\gamma}_c$ follows an Arrhenius behaviour from which an activation energy has been determined: E_a=24k_BT (Fig.7). The activation energy for the lifetime of the associations increases with the hm-HPG concentration; for C=1wt%, E_a=33.6 k_BT. At higher concentrations, the behaviour of $\dot{\gamma}_c$ with temperature becomes more complex.

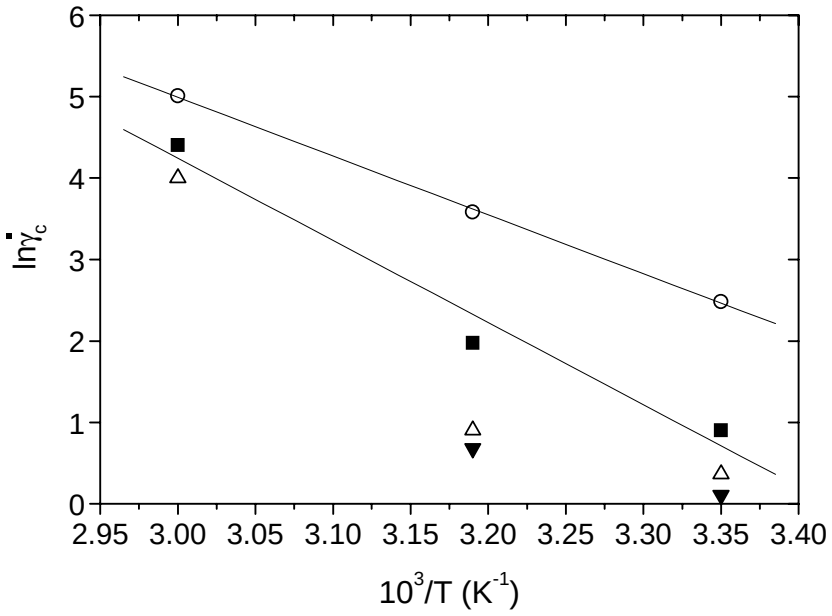

Figure 7: *Variation of the critical shear rate $\dot{\gamma}_c$ as a function of the temperature for hm-HPG solutions at various concentrations (○ 0.35wt%, ■ 1wt%, Δ 2wt%, ▼ 3wt%) in the presence of 0.4M KCl.*

REFERENCES

(1) Aubry, T.; Moan, M. *J. Rheol.* **1994**, *38*, 1681.

Appendix III.3

Rheological properties of hm-HPG/EHAC mixtures

III 1. Linear viscoelastic properties of the hm-HPG/EHAC mixtures

Figures 1-5 show the comparison of the variations of the shear modulus with the circular frequency for systems with various values of the mixture composition R previously defined in the paper ($R=C_{EHAC}/(C_{EHAC}+C_{hm\text{-}HPG})$).

One observes qualitatively the same behaviour for all the systems, with in particular a well marked dip at high frequency. As pointed out in the paper, the dip position ω_m and amplitude go through a minimum for R=0.2. If the Granek's equations (Eqs.(1) and 2 in the article) apply to the associating polymers and to the mixtures, then the above observation indicates that at R=0.2, the reptating entities are longer. As the length of the hm-HPG polymer cannot change, this would imply a micellar growth. Such an effect is not unlikely, considering that the hydrophobic groups are embedded in the micelle. Theoretical developments aiming at describing the high frequency viscoelasticity behaviour of associating polymers would be desirable.

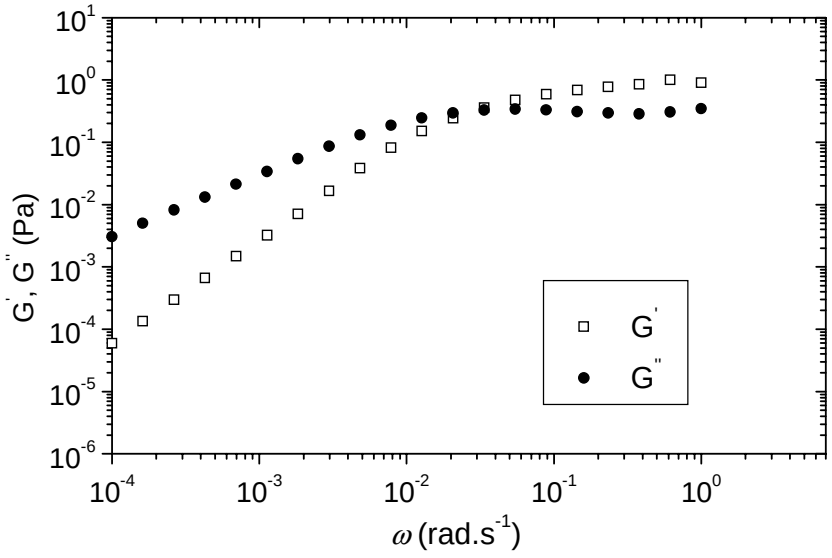

Figure 1 : *Storage ($G^{'}$) and loss ($G^{''}$) moduli as a function of frequency at 25°C for a solution of 0.35wt% hm-HPG, and 3wt% KCl (R=0).*

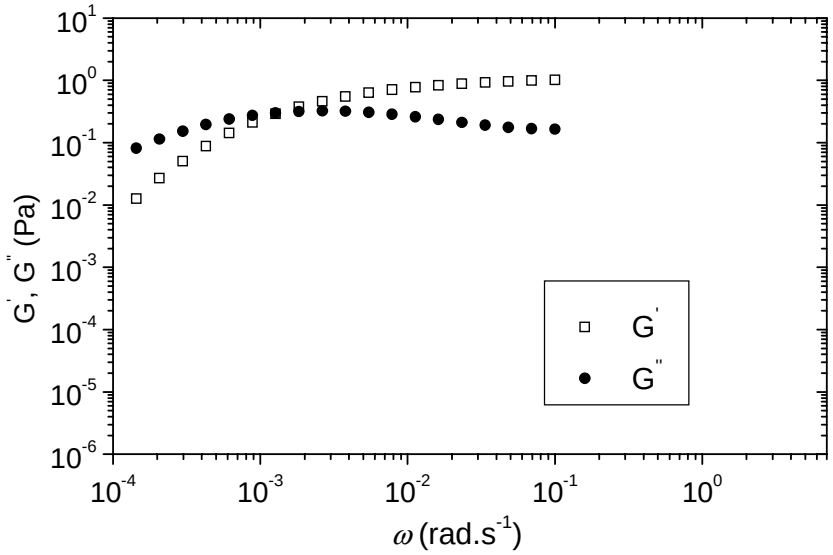

Figure 2 : *Storage ($G^{'}$) and loss ($G^{''}$) moduli as a function of frequency at 25°C for a solution of 0.3wt% hm-HPG, 0.075wt% EHAC and 3wt% KCl (R=0.2).*

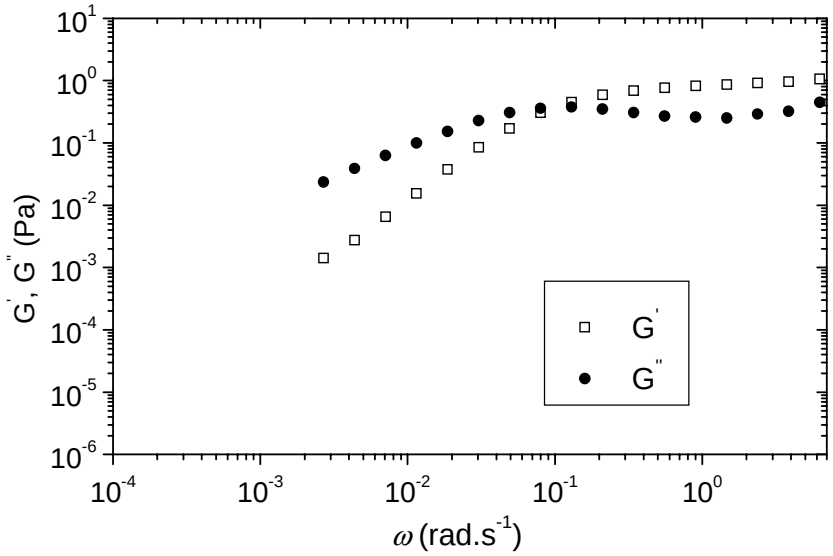

Figure 3 : *Storage ($G^{'}$) and loss ($G^{''}$) moduli as a function of frequency at 25°C for a solution of 0.2wt% hm-HPG, 0.15wt% EHAC and 3wt% KCl (R=0.43).*

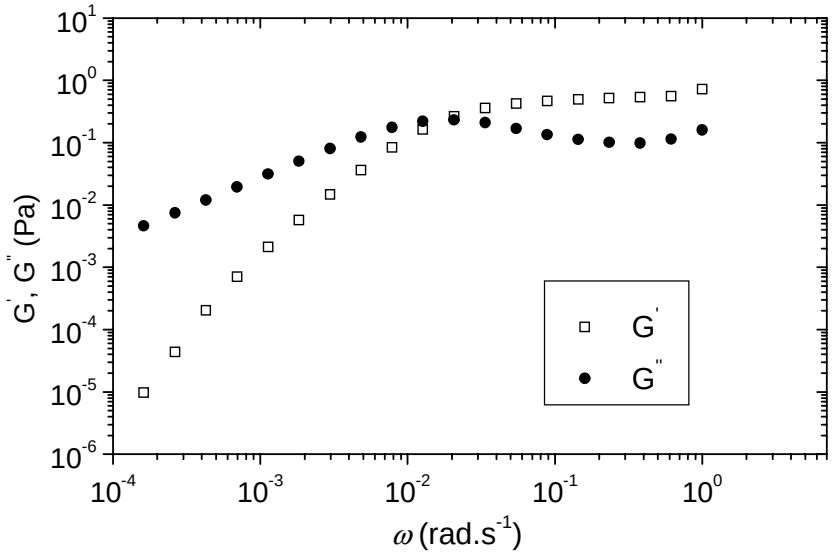

Figure 4 : *Storage ($G^{'}$) and loss ($G^{''}$) moduli as a function of frequency at 25°C for a solution of 0.1wt% hm-HPG, 0.225wt% EHAC and 3wt% KCl (R=0.69).*

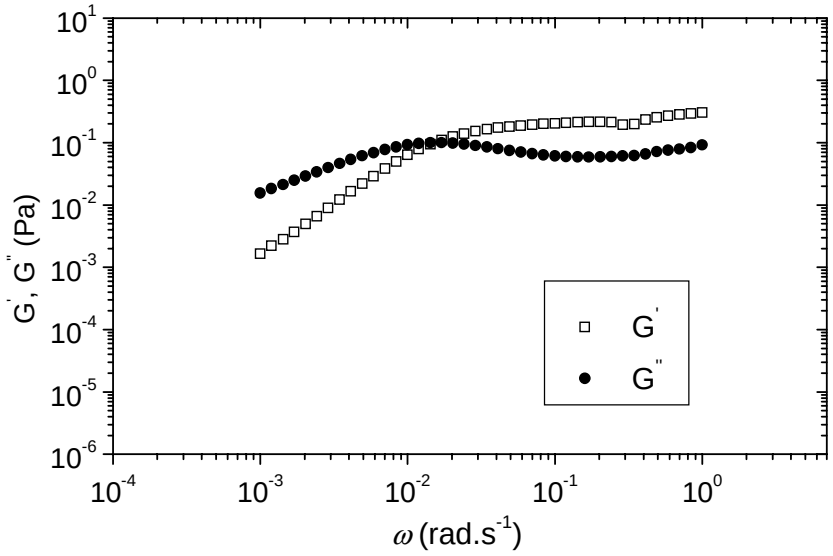

Figure 5 : *Storage ($G^{'}$) and loss ($G^{''}$) moduli as a function of frequency at 25°C for a solution of 0.375wt% EHAC and 3wt% KCl (R=1).*

III.2. Non linear rheology of the hm-HPG/EHAC mixtures

Figures 6 and 7 show the variation of the steady state viscosity versus the shear stress for a system with an overall concentration C_M≈0.35wt% for various compositions, at T=40°C and 80°C (the curves corresponding to the temperatures T=25°C and 60°C are reported in the paper).

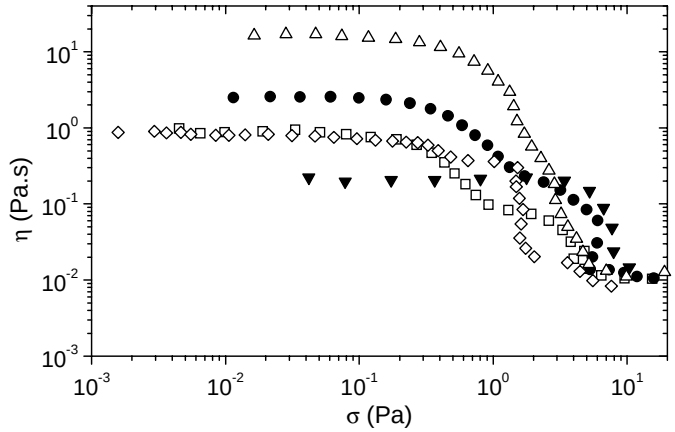

Figure 6: *Variation of the steady shear viscosity as a function of shear stress for different R values (▼ R=0, Δ R=0.2, ● R=0.43, □ R=0.69, ◊ R=1) with C_M≈0.35wt% at 40 °C.*

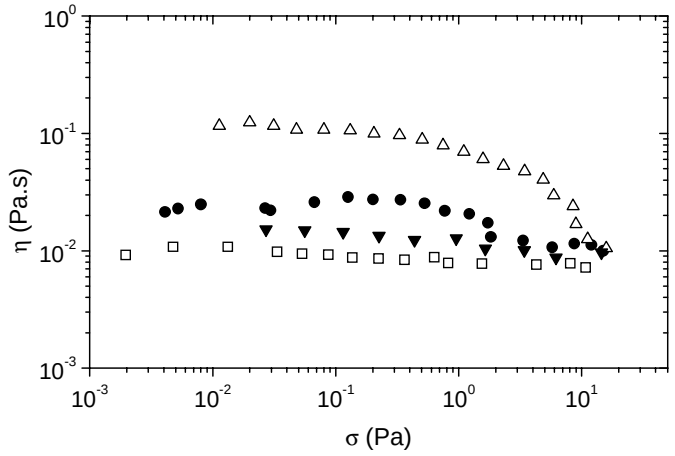

Figure 7: *Variation of the steady shear viscosity as a function of shear stress for different R values (▼ R=0, Δ R=0.2, ● R=0.43, □ R=0.69, ◊ R=1) with C_M≈0.35wt% at 80 °C.*

The behaviour of the blends is more complex than for the single component EHAC or hm-HPG solutions. The high shear viscosity of mixtures still exhibits a more or less sharp drop, depending on the composition and the temperature. For systems with a well defined plateau, the values of both σ_c and $\dot{\gamma}_c$ have been determined and reported in the Table 3 of the paper. It was observed that the critical shear stress $\dot{\gamma}_c$ present a minimum for a composition R=0.2 for all the temperatures investigated, that reveals a maximum of the lifetime of the associations. The behaviour of σ_c is more complex.

The temperature dependence of $\dot{\gamma}_c$ for a system with an overall concentration C_M≈0.35wt% for various mixtures compositions is represented in Fig.8. It follows an Arrhenius behaviour from which an activation energy has been determined: E_a=24 k_BT for R=0, E_a=26.7 k_BT for R=0.2, E_a=12.1 k_BT for R=0.43 (determination from only two data points). This result shows an enhancement of the activation energy for the lifetime of the associations at the synergistic composition R=0.2.

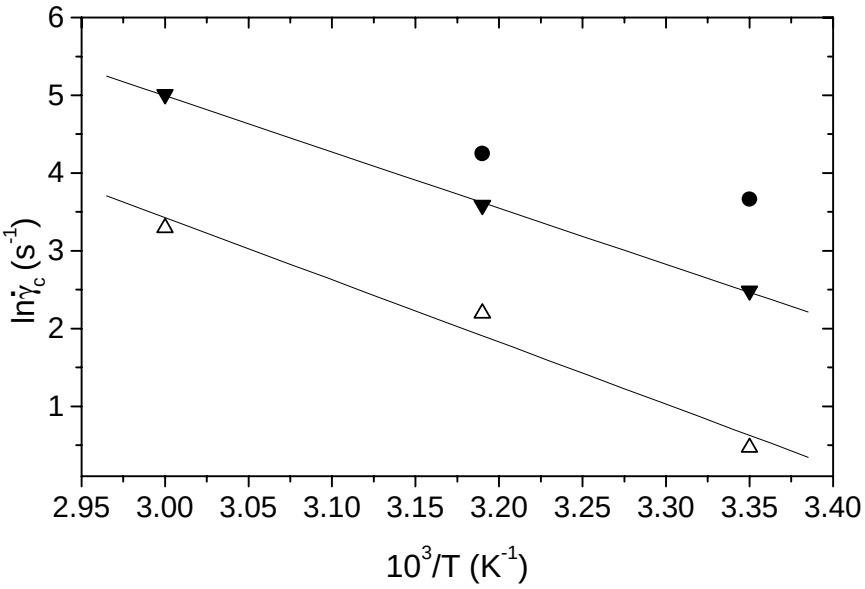

Figure 8: *Variation of the critical shear rate $\dot{\gamma}_c$ as a function of the temperature for different R values (▼ R=0, Δ R=0.2, ● R=0.43) with C_M≈0.35wt%.*

Chapter IV

SYNERGISTIC EFFECTS IN 0.4M KCl SOLUTIONS OF HYDROPHOBICALLY MODIFIED CHITOSAN/ ERUCYL BIS-(HYDROXYETHYL)METHYLAMMONIUM CHLORIDE MIXTURES

INTRODUCTION

Chitosan and modified-chitosan solutions have been extensively studied during the past few years. Chitosan is a water-soluble natural polymer obtained by deacetylation of chitin, a linear polysaccharide. When the average degree of acetylation of chitin becomes lower than 50% (DA expressed as molar percentage), the product is called chitosan and becomes soluble in acidic conditions due to the protonation of the $-NH_2$ group of the glucosamine unit. The chitosan is a polycation in neutral and acidic solutions (pKa=6.0)[1,2] and therefore can be used in a broad variety of industrial and biomedical applications[3-12].

The conformation and the size of chitosan chains in dilute solutions are strongly dependent on the degree of acetylation (DA) and the ionic strength[13-21]. The effect of the DA on the chain stiffness has been assessed from the molecular weight dependences of the intrinsic viscosity, $[\eta]$, and of the radius of gyration, R_G, through the Mark-Houwink-Kuhn-Sakurada relationship, $[\eta]=KM^{\alpha}$, and the relation $R_G=K'M^{\nu}$, respectively. Many authors found an increase of the α coefficient with DA and concluded that the acetyl groups induce some stiffness to the chains[16-18], whereas the dependence of ν on DA is less significant[14,18,20]. Some authors have determined the values of the persistence length L_p in order to show the effect of an increase of the acetyl content on the chain conformation. For several commercial chitosans, Terbojevich et al.[21] found L_p=22 nm for both DA=15% and DA=42%. For heterogeneously acetylated chitosan Brugnerotto et al.[14] found L_p =11nm independent on DA in the range $0 \leq DA \leq 25\%$.

Shaltz et al.[15] defined three domains of DA corresponding to different behaviours of chitosan: (1) a polyelectrolyte domain for DA below 20%, (2) a transition domain between DA=20% and 50% where chitosan loses its hydrophilicity, (3) a hydrophobic domain for DA over 50% where polymer associations can arise.

Contrary to hm-guar polymer, modified chitosan is not commercially available. The substituted derivative is obtained by reductive amination[22-24], leading to the grafting of the hydrophobic alkyl chains along the hydrophilic macromolecular chain. The resulting compound is an amphiphilic polymer whose hydrophobicity may be adjusted by variation of the length of the grafted alkyl chain (from 6 carbon atoms to 14) or the degree of

substitution of the amine functions. The length of the amine groups as well as their concentrations have a significant impact on the rheological properties of the modified chitosan[22,25,26]. An adequate length of the grafted chain is necessary for chitosan derivatives to present hydrophobic characteristics and self-association[22]. The role of temperature on the rheological behaviour of the modified chitosan was investigated and was found to be strongly dependent on both the length and the concentration of the amine groups[23,26]. The study of the aggregation phenomena in aqueous solutions of modified and unmodified chitosans by a fluorescent probe interacting with hydrophobic regions, revealed the formation of intermolecular aggregates in the unmodified chitosan[27]. The authors tried to elucidate the nature of these aggregates by different ways, such as addition of urea and ethanol, increase of temperature, and variation of ionic strength. They concluded that neither H-bonds nor hydrophobic interactions were responsible for the aggregation of chitosan. Two types of hydrophobic domains exist in the modified chitosan, one inherent to the chitosan itself, the other one typical for polymers with hydrophobic side chains.

The most detailed study of the concentration regimes of hm-chitosan was performed by Esquenet et al.[28,29] on samples with a molecular weight M_w=195,000g/mol, a substitution of hydrophobic units with various lengths (from C6 to C14) and a degree of substitution of 2%. These authors studied the aggregation process in the dilute regime using light scattering and viscometry. A behaviour similar to that of the telechelic polymers was observed (Fig.1). At low concentration, i.e., at concentrations below the critical aggregation concentration (c.a.c.), the supernatant phase corresponds to free isolated hm-chitosan polymer chains dissolved in the solvent, that are called unimers. The intermediate hm-chitosan contents (c.a.c.<c<c^*) correspond to the formation of micellar aggregates (associations of unimers) that do not enhance the solution viscosity. These micelles are not connected and are diluted in the solvent. They can be viewed as an assembly of spherical “flowerlike” micelles where polymer chains are “cross-linked” through alkyl associations. At higher polymer concentrations (c>c*), the system exhibits a large increase of the solution viscosity and a gel-like behaviour. This behaviour is likely to be due to the weak degree of substitution (2%). For higher degrees of hydrophobic substitution, one might expect to recover the behavior of the hm-guar.

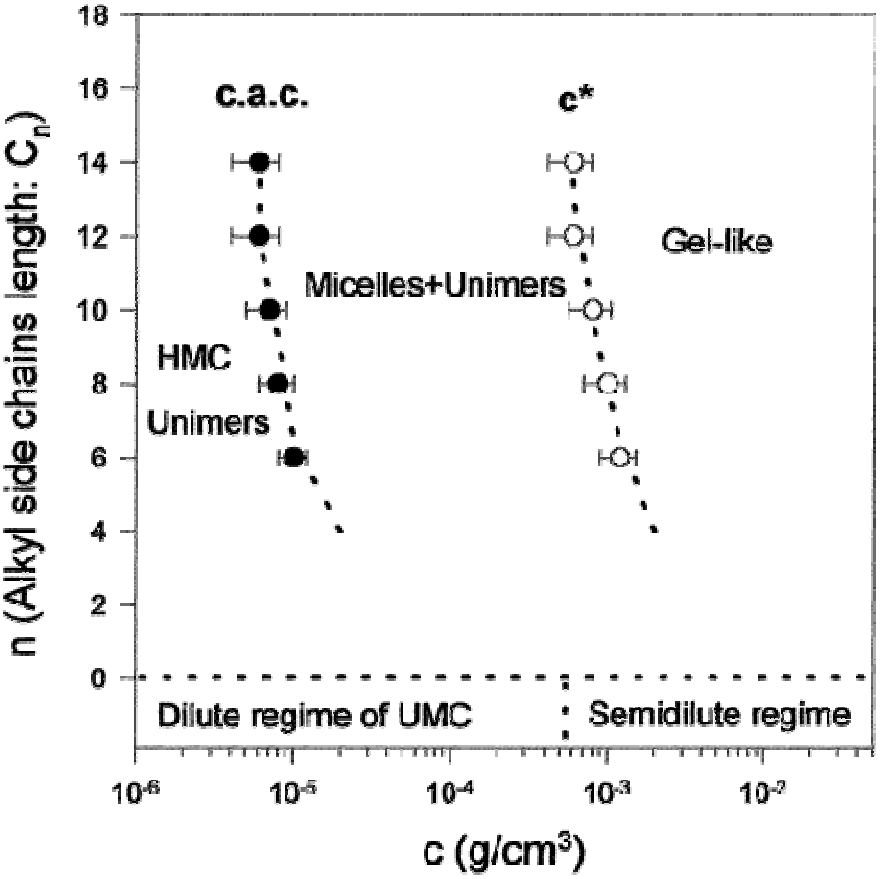

Figure 1: *Phase diagram in the alkyl side chains length-polymer concentration plane at a fixed temperature T = 25 °C. The points (•) represent the unimers-micelles transition (i.e., the c.a.c. deduced from static light scattering measurements), and the points (○) represent the micelles-gel transition (i.e., the concentration c* deduced from viscosity measurements). The degree of alkylation is equal to 2%. The length of the alkyl side chains is defining by C_n, with n varying from 6 to 14. The phase behavior of the analogue unmodified chitosan (i.e., C0) is also represented. (from refs. 28, 29)*

In most of the studies, the procedures for determining the rheological parameters and more specifically the zero-shear viscosity are not detailed. In fact, as discussed later, the transients when establishing a steady shear-stress or a shear-rate are very long and with large amplitude. This makes the determination of the equilibrium parameters very time

consuming. Moan and Aubry[30] already stressed this issue for hydrophobically modified hydroxypropyl guars. For this reason, some results reported in the literature might be erroneous.

The present study does not aim at giving a full description of the hydrophobically modified chitosan polymers, but rather at selecting a few samples and studying possible synergistic effects with wormlike micelles. Only few authors have reported studies on chitosan derivative/surfactant mixtures. Nystrom et al.[31-34] focused their studies on the rheological behaviour of one particular chitosan derivative (C12 aldehyde), and its interactions with the cationic CTAB (cetyl trimethyl ammonium bromide) surfactant. They studied the effect of pH, temperature, polymer concentration and addition of surfactant on the linear viscoelastic properties of chitosan samples having different degrees of hydrophobicity. Recently, Lee et al.[35] studied the effect of adding a modified chitosan to vesicles or wormlikemicelles of surfactant. Adding a modified chitosan to a solution of vesicles results in an elastic gel. The likely structure of these gels is a network of vesicles connected by associating polymer chains, with the hydrophobes of the polymer embedded in vesicle bilayers. The rheology of the modified chitosan/wormlike micelle mixture is very different. In that case, a non-permanent gel is obtained due to the formation of a transient network by junctions of a finite timescale.

The main goal of this chapter is to demonstrate the generality of the synergistic effects which may occur in mixtures of hydrophobically modified polymers and wormlike micelles, as already revealed in Chapter III for EHAC/hm-HPG mixtures. In this respect, we have studied the linear and non-linear rheological properties of aqueous solutions of another associating polymer, hydrophobically modified chitosan (hm-chitosan) and erucyl bis-(hydroxyethyl)methylammonium chloride (EHAC) surfactant (see Chaps. II and III).

An hm-chitosan with a lower molecular weight than that of the hydrophobically modified hydroxypropyl guar (hm-HPG) previously studied in Chapter III was chosen. A detailed study was carried out on the effect of the mixture composition and its overall concentration on the synergy of the system. The aim of comparing hm-chitosan with hm-

guar/derivative is to conclude if the use of the lower molecular weight polymer chitosan could conduct to a similar or more/less efficient system. This is an important issue from the applications point of view as it is thought that a lower molecular weight polymer may help to reduce formation damage.

I. SYNTHESIS AND CHARACTERISATION OF CHITOSAN AND HM-CHITOSAN SAMPLES

I.1. Synthesis of hm-chitosan

The original chitosan sample was obtained from Aldrich. The reported degree of deacetylation was about 80%, which has been verified by NMR[36]. The molecular weight of the sample, determined by capillary viscosimetry, was found to be around 90,000g/mol. The details of its determination are reported in the next paragraph.

The chitosan backbone is composed of D-glucosamine [β-(1,4)-2-deoxy-2-amido-D-glucopyranose] sugars, with a small fraction of N-acetyl-D-glucosamine [β-(1,4)-2-deoxy-2-acetamido-D-glucopyranose] sugars as well (Fig.2).

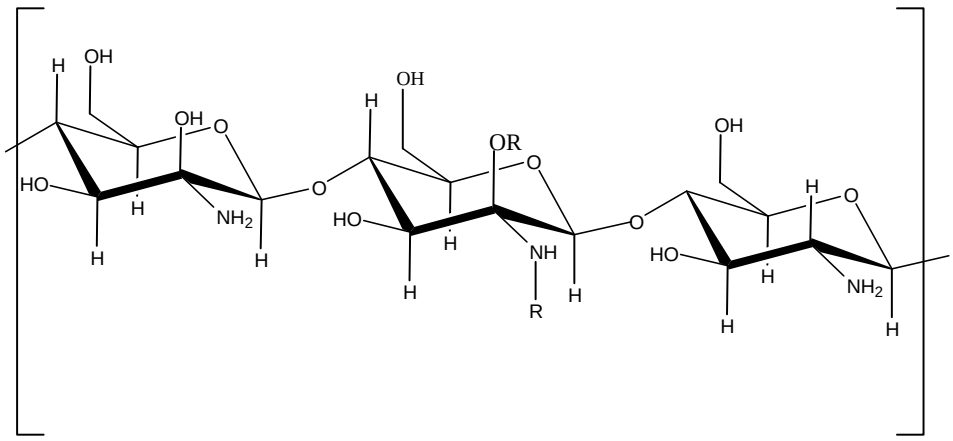

R=H or R= -CO-CH_3

Figure 2: *Structure of chitosan*

The chitosan derivative was obtained by reductive amination following the procedure described by Yalpani[24] (Fig.3). The alkylation reaction was processed as follows: 10 grams (62 mmol) of chitosan were dissolved in 800ml of 0.2M acetic acid, then 350 ml of ethanol were added to allow the aldehyde used for the alkylation to be in a solvating medium. After complete dissolution the pH was adjusted to 5.1 in order to avoid the precipitation of the macromolecules, the optimal reaction pH being between 4 and 8. An amount of 0.484grams (3.1 mmol, corresponding to a substitution degree of 5mol%) of decyl aldehyde in solution in ethanol was then added, followed by the addition of an excess of sodium cyanoborohydrate (11.69 grams, 186 mmol). The mixture was stirred during 24h at room temperature and the alkylated chitosan was precipitated with ethanol. The pH was adjusted to 7 with a sodium hydroxide solution and the precipitate was washed with ethanol/water mixtures with increasing ethanol contents from 70% v/v to 100%.

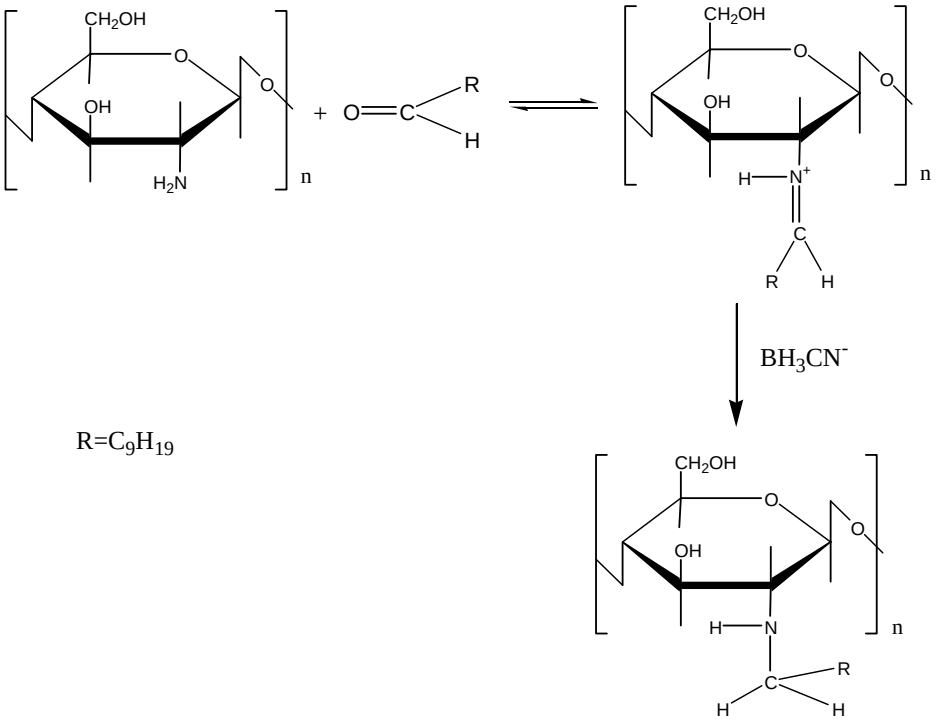

Figure 3: *Synthesis of hm-chitosan by reductive amination.*

The degree of acetylation (DA) as well as the degree of alkylation were checked by NMR[36]. The samples were dissolved at a concentration of 10mg/ml in D_2O in the presence of HCl (pH 4) and freeze-dried three times to exchange labile protons for deuterium atoms. The spectra were performed at 353K.

I.2. Determination of the molecular weight of the chitosan sample

The molecular weight of the chitosan sample was obtained by measurement of its intrinsic viscosity $[\eta]$. The intrinsic viscosity is related to the viscosity average molecular weight of the polymer through the Mark-Houwink-Sakurada relationship[37]:

$$[\eta] = KM_v^{\alpha} \quad (1)$$

where K and α are constants, both related to the stiffness of the polymer. For flexible polymer coils, α is 0.5 in a θ solvent and 0.8 in a good solvent. Brugnerotto et al.[14] determined the K and α constants values for samples of chitosan as a function of their degree of acetylation (DA). Using gel permeation chromatography (SEC) coupled with a multi-angle laser light scattering detector equipment, they obtained the variations of the radius of gyration R_G with the molar mass M_w of the sample. They also determined experimentally the intrinsic viscosity of the chitosan samples. In the dilute range, the viscosity of the solution can be represented by a power series of the polymer concentration C_p

$$\eta = \eta_s(1 + [\eta]C_p + k_H[\eta]^2 C_p^{\,2} + ...) \quad (2)$$

where η_s and k_H represent the solvent viscosity and the Huggins coefficient respectively. The intrinsic viscosity can be determined by measuring the viscosity of solutions at low concentrations and extrapolating to infinite dilution, according to the Huggins or Kraemer relationships, respectively[38]

$$\eta_{sp} / C_p = [\eta] + k_H [\eta]^2 C_p \quad (3)$$

$$\ln(\eta_r) / C_p = [\eta] - k^{"} [\eta]^2 C_p \quad (4)$$

where η_r is the relative viscosity, defined as the ratio of the solution viscosity and the solvent viscosity η/η_s, and η_{sp} is the specific viscosity (η_r-1).

Using the Mark-Houwink relation, Brugnerotto et al. could calculate the *K* and α constants for different DAs of chitosan samples (see Table 1).

DA (mol%)	***K***	α
0-3	0.079	0.796
12	0.074	0.8
22-24	0.070	0.810
40	0.063	0.83
56-61	0.057	0.825

Table 1: *Mark-Houwink parameters determined from the SEC analysis and [η] measurement (from Ref.14).*

The viscosities of dilute solutions of chitosan were determined using a capillary viscometer, at 25°C. The solutions were prepared by dissolution of chitosan in a 0.3M acetic acid (AcOH)/ 0.05M sodium acetate (AcONa) in order to screen the electrostatic repulsions without favouring hydrophobic interactions promoted by electrolytes. Figure 4 shows the variation of the reduced viscosity η_{red} (=η_{sp}/C) as a function of chitosan concentration. Taking the values of the Mark-Houwink parameters determined by Desbrieres for DA=20 (*K* =0.07; α=0.81) and the value of the intrinsic viscosity determined from Fig.4 ([η]=729mL/g), the weight average molecular weight was calculated from Eq.(1) and found to be equal to 90,000g/mol.

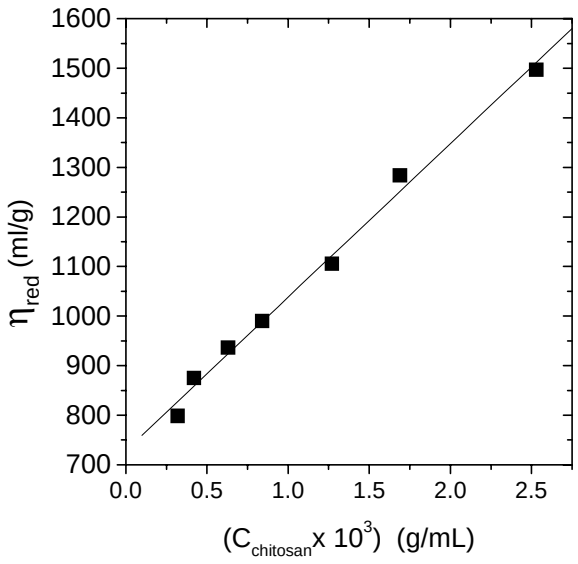

Figure 4: *Variation of the reduced viscosity η_{red} versus chitosan concentration.*

II. EXPERIMENTAL PROTOCOL

To take into account the evolution of the chitosan solution properties at rest as a function of time as well as the long equilibrium time required to reach a steady-state value of the shear viscosity, an experimental protocol was established in order to insure the reproducibility of the experimental results.

II.1. Evolution of the properties of chitosan and hm-chitosan solutions with time

The viscosity of aqueous polymer solutions can decrease gradually with time[39,40]. There is still much debate regarding the explanation of this viscosity decrease. It may be due to:

1. a change of the polymer conformation due to the breaking of inter and/or intra molecular hydrogen bonding.

2. a degradation of the polymer chains by micro organisms such as bacteria.

Our main concern was to insure good reproducibility of the results rather than to perfectly understand the mechanism involved in the viscosity decrease of chitosan solutions with time. We have therefore performed a preliminary study of the evolution of the viscosity of a chitosan solution with time, to get an estimate of the kinetics of the destabilisation process.

The results for a 1.2wt% unmodified chitosan in 1wt% acetic acid solution are reported in Fig.5. A decrease of 10% of the initial solution viscosity is observed after 24 hours, of 20% after 48 hours and 34% after 168 hours. The viscosity of a 0.5wt% hm-chitosan in 1wt% acetic acid solution was also measured over time. Figure 6 shows the variations of the decrease of viscosity (in %) with time for the chitosan and hm-chitosan samples. One can note that the ageing process of the hm-chitosan solution is slightly slower than that of the chitosan.

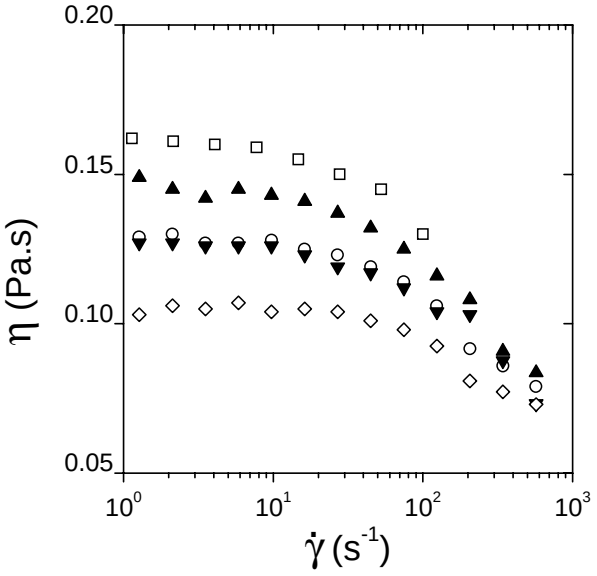

Figure 5: *Variations of the steady-state shear viscosity vs shear rate of a 1.2wt% chitosan solution at different aging times (□ t=0, ▲ t=24h, ○ t=48h, ▼ t=72h, ◊ t=168h).*

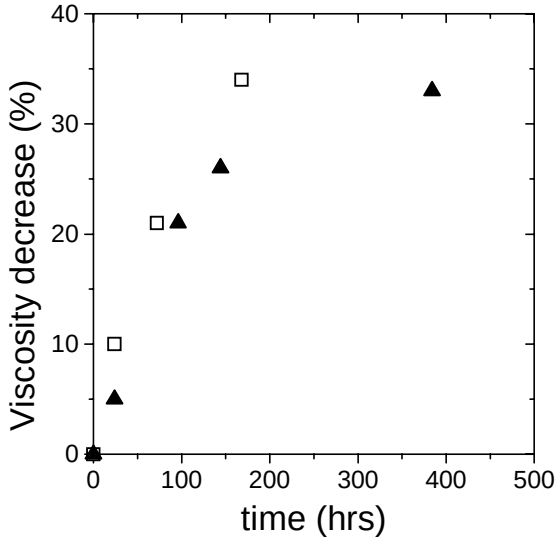

Figure 6: *Viscosity decrease (%) with aging time for a 1wt% chitosan solution (□) and a 0.5wt% hm-chitosan solution (▲) in 1wt% acetic acid, at 25°C.*

So, as describes later, the different chitosan, hm-chitosan, EHAC/hm-chitosan solutions were used immediately after preparation in order to avoid any ageing effect.

II.2. Equilibrium time for the establishment of the steady-shear viscosity of hm-chitosan solutions

As previously observed with the hm-HPG polymer (see Chapter III), the response of the hm-chitosan solutions to a shear stress was found to be time dependent. Previous studies on hm-chitosan do not mention this important feature nor the detailed procedures used to determine the rheological parameters and more specifically the zero-shear viscosity. Figure 7 shows the variation of the viscosity versus shear rate for a 2.5wt% hm-chitosan solution. The rheograms have been produced for different values of the time used for taking each data point. Under non equilibrium conditions (Fig.7: ○ t=80s, ▼ t=25s), an apparent Newtonian plateau, followed by a shear thinning regime is observed, whereas when the measurements are made under equilibrium condition (Fig.7: ■ t=4060s) no Newtonian plateau can be observed in the used shear rate range. As a result, particular

attention was paid in determining the equilibrium time for all hm-chitosan and EHAC/hm-chitosan solutions, before measuring the steady-shear viscosity.

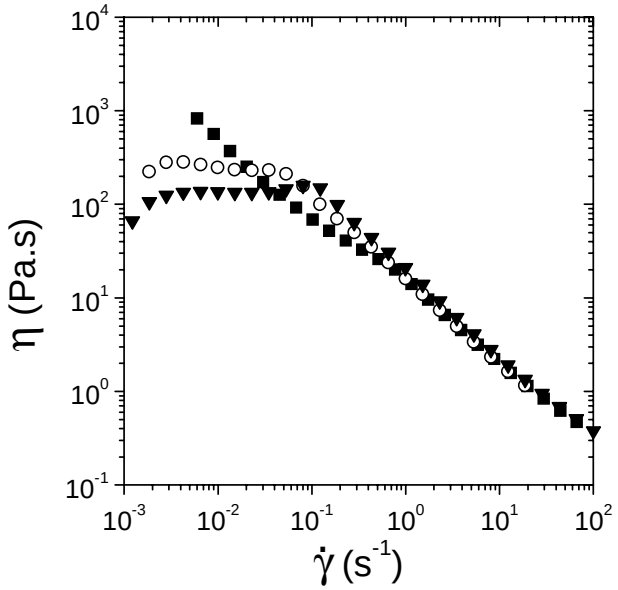

Figure 7: *Variations of the steady-state shear viscosity vs shear rate of a 2.5wt% hm-chitosan solution using different values of the time of measurement of each data point (■ t=4060s, ○ t=80s, ▼ t=25s).*

In our study, we have adopted the following experimental protocol. The chitosan was dissolved, at a convenient concentration, in a 1wt% acetic acid solution for 24 hours, at 25°C, under mechanical stirring (1000rpm, blade stirrer). An excess of salt (3wt% KCl) was then added to all the polymer solutions that were kept under stirring for another 4 hours. EHAC surfactant was added for the preparation of the polymer/surfactant mixtures. The solution was centrifuged to remove air bubbles and then was immediately used.

The equilibrium time for the establishment of the steady-shear viscosity was evaluated for each sample prior to steady-shear viscosity measurements.

III. COMPARISON OF THE FLOW RHEOLOGY OF CHITOSAN AND HM-CHITOSAN: DETERMINATION OF THE OVERLAP CONCENTRATION C^*

Compared studies of the flow rheology of chitosan and hm-chitosan have been reported in the literature[22,26,27,31,32]. Our main interest was to study the synergistic effects with wormlike micelles. That is the reason why this part of the study only focused on the determination of the overlap concentration C^* between the dilute and semi-dilute regimes of the hm-chitosan and of its non-modified equivalent.

Figure 8 shows the comparison between the variations of the zero-shear viscosity versus polymer concentration measured at T=25°C for the chitosan and hm-chitosan samples respectively.

For the unmodified polymer, one observes the classical behaviour of conventional polymers, as previously observed with the hydroxypropyl guar (see Chap. III), that is, a first break at the concentration C^* (0.2wt%) at which the chains start to overlap and a second break at a higher concentration C_e (1.1wt%) corresponding to the onset of entanglements. The ratio C_e/C^* is of the order of 5.5 that is in the range generally observed for other systems (between 5 to 10)[41-44]. Surprisingly, the concentration C^* of the chitosan polymer is closed to that of the HPG polymer presented in Chap. III (C^*=0.15wt%), although the molecular weight of the former is 20 times lower ((90,000g/mol for the chitosan as compared to 1.8x 10^6g/mol for the hm-HPG). This result suggests a larger expansion of the chitosan chains, due in part to a higher value of its persistence length ($L_{p\ chitosan}$ = 11-22nm[14,21], compared to $L_{p\ guar}$ = 4nm[45]).

In the entangled regime, the exponent of the dependence of the zero shear viscosity η_0 on the polymer concentration should be equal to 15/4[43]. In the present case, this exponent is found to be much larger (5.5), as already observed by Desbrieres[46]. The high value of the exponent may be linked to the presence of specific interchain interactions, as already mentioned by Amiji[47] and Anthonsen et al.[48], and discussed later on by Philippova et al.[27]. Chitosan is able to form hydrophobic intermolecular domains at concentrations

larger than the overlap concentration. This was shown by static[48] and dynamic[49,50] scattering experiments. Using these more sensitive techniques than rheology, the presence of aggregates was observed even in the dilute regime. These domains are stable and only weakly affected by heating or by the addition of salt, urea or ethanol, which suggests that neither hydrogen bonds nor hydrophobic aggregation are responsible for the aggregation of chitosan. The nature of the aggregates is still under discussion.

The rheological behaviour of the modified chitosan is quite different, as has been observed in the previous chapter for hm-HPG. The viscosity of the solution rises steeply beyond a concentration which is of the same order of magnitude as the crossover concentration C^* of the unmodified polymer. In this regime, the viscosity of the hm-chitosan is much larger than that of the unmodified analogue, which reflects the occurrence of intermolecular associations.

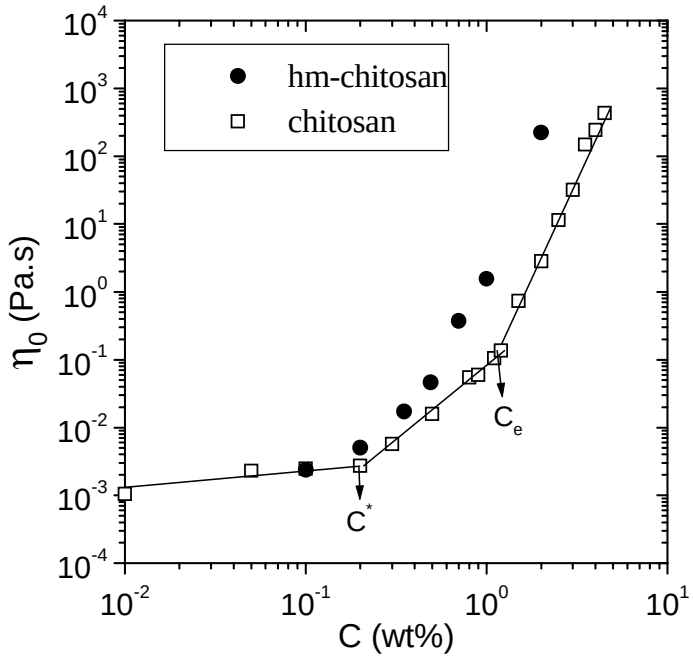

Figure 8: *Variations of the zero-shear viscosity with concentration for solutions of chitosan and hm-chitosan in the presence of 3wt% KCl at 25°C.*

IV. RESULTS AND DISCUSSION

IV.1. Effect of the composition of EHAC/hm-chitosan mixtures on the non linear rheological behaviour

We have investigated the rheological behaviour of EHAC/hm-chitosan mixtures with different compositions, first at an overall concentration C_M=0.35wt%, which was in the concentration range that appeared to give the maximum synergy for the EHAC/hm-HPG system. We have carried out subsequently the same experiments at a higher overall concentration C_M=0.7wt%.

The composition of the mixture was defined by the ratio $R=C_{EHAC}/(C_{EHAC}+C_{hm\text{-}chitosan})$ where the concentrations of the components are expressed in wt%.

IV.1.a. Effect of the EHAC/hm-chitosan composition at C_M = 0.35wt%

Figure 9 shows the flow curves obtained for different ratios of EHAC/hm-chitosan in mixtures with an overall concentration C_M=0.35wt% at 25°C.

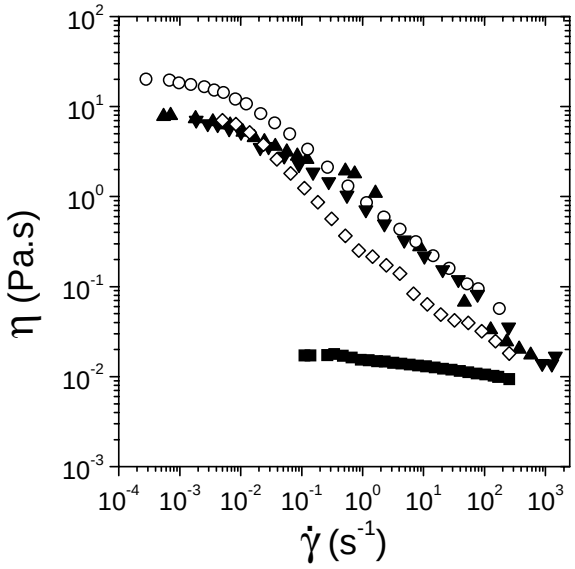

Figure 9: *Variations of the steady-state shear viscosity vs shear rate for different R values (■ R=0, ▲ R=0.2, ○ R=0.43, ▼ R=0.69, ◊ R=1) with C_M=0.35wt% at 25°C.*

A synergistic effect clearly appears in the Newtonian plateau. This synergy is also reflected by the behaviour of $\tilde{\dot{\gamma}}$ that corresponds to the onset of the shear thinning and is of the order of T_R^{-1} (see Chap.III).

Figure 10, showing the variation of the zero-shear viscosity versus the mixture composition *R*, is another illustrative description of this synergy. A maximum in the zero-shear viscosity is observed between *R*=0.2 and *R*=0.43, a similar range to that observed for the EHAC/hm-HPG system (around *R*=0.2). The amplitude of this maximum is higher than that obtained with the EHAC/hm-HPG mixtures when referenced to the viscosity of the pure polymer (*R*=0) (3 orders of magnitude increase from R=0 to R at the maximum compared to 2 for the EHAC/hm-HPG mixtures). However the maximum is lower when referenced to the viscosity of the pure surfactant (*R*=1) (less than one order of magnitude as compared to more than one order of magnitude for the EHAC/hm-HPG mixtures). Moreover, the zero-shear viscosity observed at the maximum is lower than that observed with the EHAC/hm-HPG system (η_0 = 20 Pa.s compared to η_0 = 100 Pa.s).
The variation of the high shear rate ($\dot{\gamma}$=100 s^{-1}) viscosity versus *R* (Fig.11) shows that the composition dependent synergistic effects are maintained at least up to $\dot{\gamma}$=100 s^{-1}, which is an important result from the point of view of the potential application of such fluids. At $\dot{\gamma}$=100 s^{-1}, the maximum is also observed around *R*=0.43.

Figure 12 shows the same flow curves as those of Fig.9 in the representation $\eta = f(\sigma)$. The solutions exhibit a shear thinning behaviour that depends on the sample composition. As discussed before (Chap.III) Moan and Aubry[30] reported a drastic shear drop of the viscosity at a shear stress σ_c. The shear rate $\dot{\gamma}_c$, measured just before the sharp drop was assumed to be the inverse of the lifetime of the associations. For *R*=0.43 and *R*=0.69, the viscosity decreases monotonically in the shear-thinning regime with two inflection points as observed by Jenkins et al. for the HEUR[51] and HASE[52-54] polymers. These results suggest the existence of two critical stress levels whose values depend on the mixture composition.

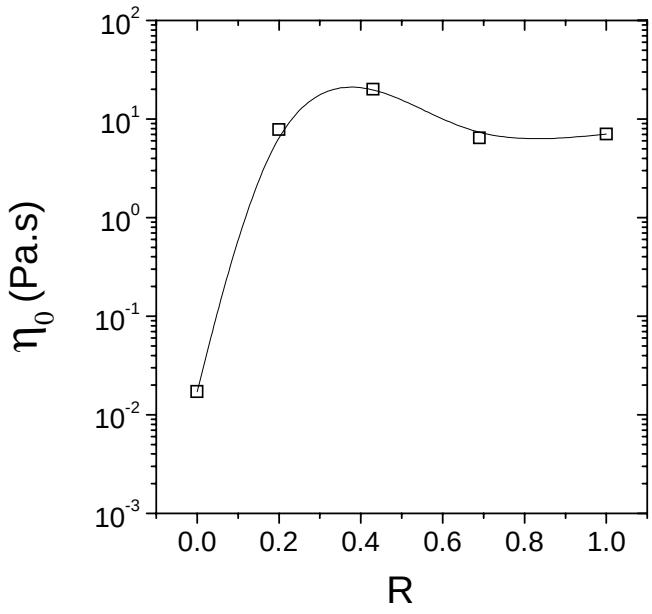

Figure 10: *Zero-shear viscosity versus R for systems with C_M=0.35wt% at 25℃*

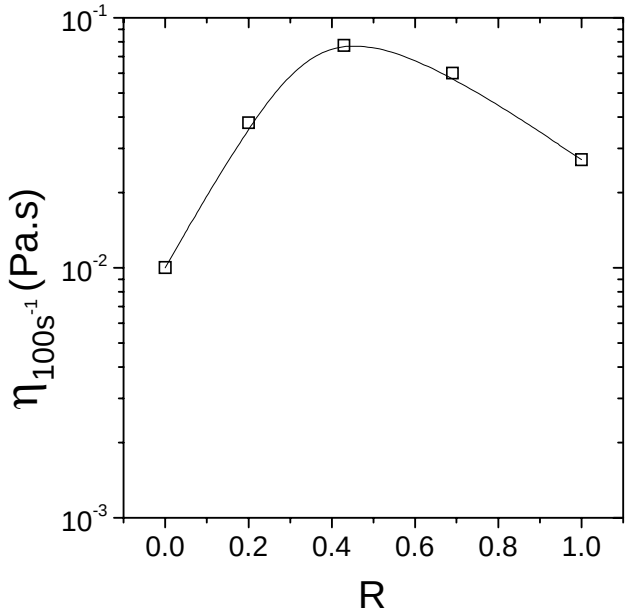

Figure 11: *High shear-rate viscosity versus R for systems with C_M=0.35wt% at 25℃*

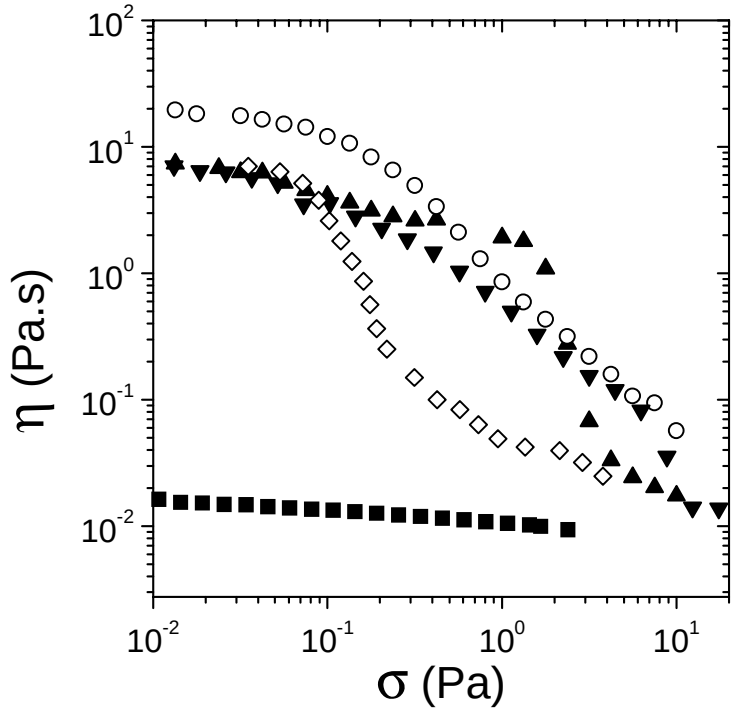

Figure 12: *Variations of the steady-state shear viscosity vs shear stress for different R values (■ R=0, ▲ R=0.2, ○ R=0.43, ▼ R=0.69, ◊ R=1) with C_M=0.35wt% at 25°C.*

IV.1.b. Effect of the EHAC/hm-chitosan composition and of the temperature at C_M=0.7wt%

Figure 13 shows the variation of the steady shear viscosity versus shear rate for solutions of EHAC/hm-chitosan mixtures having different compositions, with C_M=0.7wt%, at various temperatures. Again, a synergy with an amplitude similar to the one observed for C_M = 0.35wt%, is revealed in the Newtonian plateau.

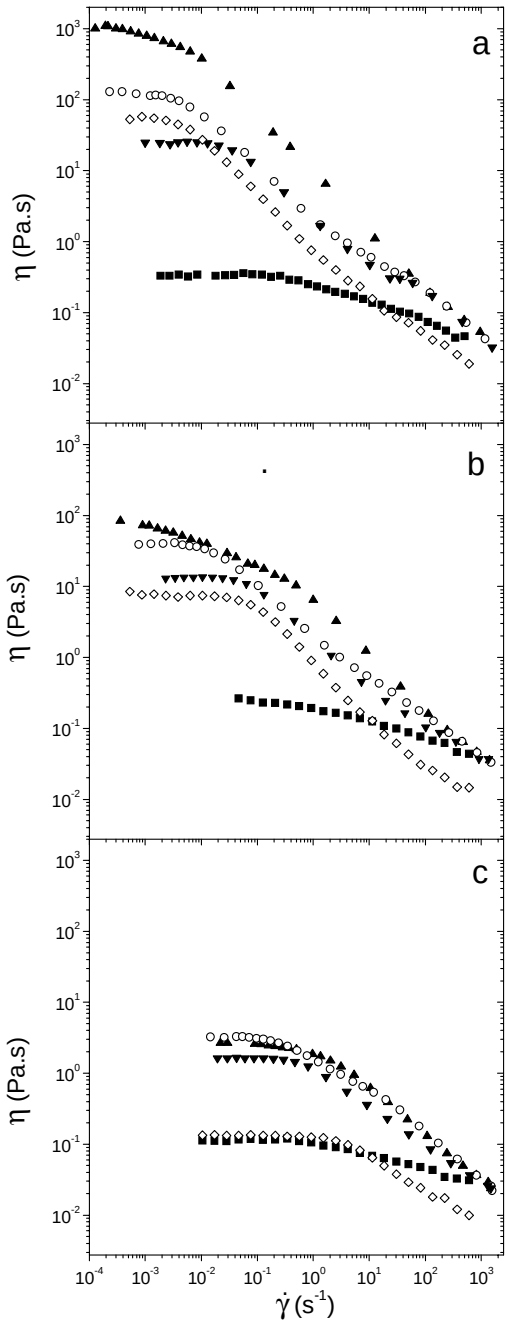

Figure 13: *Variations of the steady-state shear viscosity vs shear rate for different R values (■ R=0, ▲ R=0.2, ○ R=0.43, ▼ R=0.69, ◊ R=1) with C_M=0.7wt% at 25℃ (a), 40℃ (b) and 60℃ (c).*

Figure 14, another illustrative representation of the synergy, shows a maximum around R=0.2, similar to that observed at C_M = 0.35wt%. At 25°C, the zero-shear viscosity at the maximum is about 100 times larger than that of the mixture at C_M = 0.35wt% (cf. Fig.10). The amplitude of the maximum decreases upon increasing the temperature. It seems that the temperature dependence of the zero-shear viscosity of the mixtures in the range 0.2 < R < 0.69 follows qualitatively the behaviour of the EHAC (R=1) rather than that of the hm-chitosan (R=0).

Figure 15 shows that the composition dependent synergistic effects are maintained at high shear rate (at least up to $\dot{\gamma}$=100 s^{-1}) and that, in contrast to the zero-shear viscosity, the viscosity at $\dot{\gamma}$=100 s^{-1} is only weakly temperature dependent, whatever the composition of the system, as previously observed with the EHAC/hm-HPG mixtures.

Figure 16 shows the same flow curves as those of Fig.13 in the representation $\eta = f(\sigma)$. The flow curves display again a bimodal shape, more or less pronounced depending on the composition and on the temperature. The system with R=0.2, that corresponds to the maximum synergy, exhibits a steeper drop in the viscosity at a particular stress level. The determination of the values of both σ_c corresponding to the shear stress of the sharp viscosity drop, and $\dot{\gamma}_c$ measured just before the sharp drop, appears to be more delicate for these systems than for the EHAC/hm-HPG mixtures.

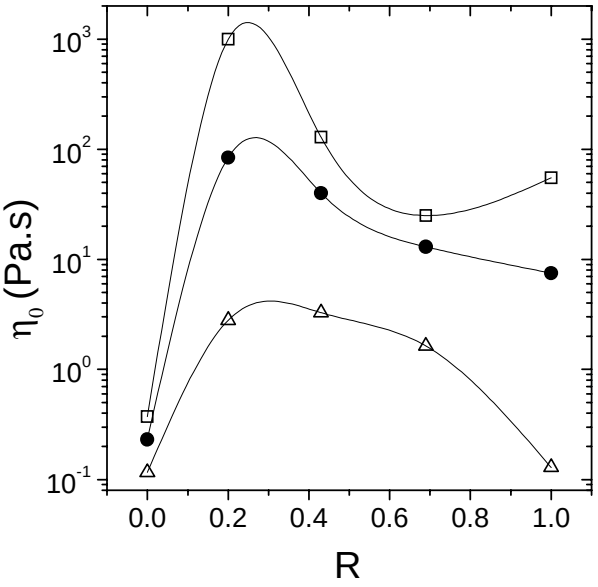

Figure 14: *Zero-shear viscosity versus R at various temperatures, □ 25℃, ● 40℃, Δ 60℃, for systems with C_M=0.7wt%.*

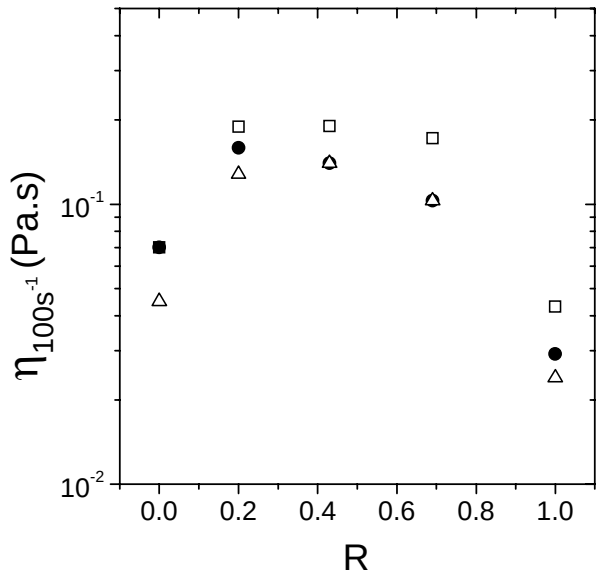

Figure 15: *High shear-rate viscosity versus R at various temperatures, □ 25℃, ● 40℃, Δ 60℃, for systems with C_M=0.7wt%.*

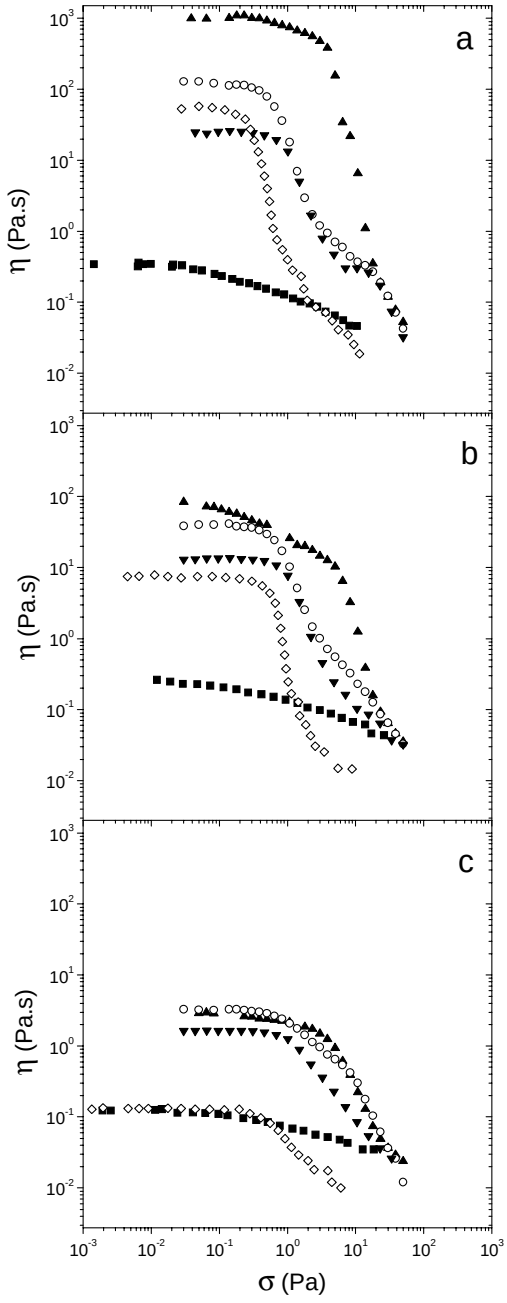

Figure 16: *Variations of the steady-state shear viscosity vs shear stress for different R values (■ R=0, ▲ R=0.2, ○ R=0.43, ▼ R=0.69, ◊ R=1) with C_M=0.7wt% at 25 ° (a), 40 ℃ (b) and 60 ℃ (c).*

To summarise, the results obtained for systems with overall concentrations C_M = 0.35wt% and C_M = 0.7wt% show that there is an optimal synergy for a certain composition range corresponding to a polymer concentration around 70-80% of the overall mixture concentration. So, the addition of a small amount of wormlike micelles to an entangled network of semi-rigid hm-chitosan chains leads to a huge increase of the viscosity. The wormlike micelles whose diameter ($d \approx$ 2nm) is 10 times higher than that of the hm-chitosan ($d \approx$ 0.2nm) occupy a larger volume than the polymeric chains. Moreover, for the same volume fraction of polymer and surfactant, the total length of the polymeric chains is much higher than that of the micellar chains. In addition to the hm-hm polymer interactions, some crosslinks are created between the polymeric chains and the micelles through the embedding of the polymer hydrophobic moities inside the wormlike micelles. As discussed before, the dynamics of the VES/hm-polymer system depends on the coupled VES/hm-polymer chains motion. The latter is governed by the reptation hindered by the polymer/polymer hydrophobic interactions, that depends on the concentration and the lifetime of the tie-points but also by the reptation hindered by the VES/hm-polymer crosspoints controlled by the concentration and the residency time of the sticker within the micelle. This might explain the two critical stress levels observed in the representation $\eta = f(\sigma)$.

A comparison of the above results with those discussed in Chap.III indicates that the synergy observed between the EHAC surfactant and the associating polymers appears to be stronger for hm-chitosan than for the hm-HPG as revealed by the larger amplitude of the maximum in the zero-shear viscosity as a function of R. However, the absolute values of zero-shear viscosity at the maximum are lower for the hm-chitosan system compared to the hm-HPG system.

These results are quite important from an applications point of view as they show that the molecular weight of the polymer does not alone control the amplitude of the synergy. Further studies are requested to determine the most adequate system based on either a high molecular weight polymer that is damaging for the formation or a low molecular

weight polymer that might require a higher concentration to reach the same viscosity, so increasing the fluid's cost.

IV.2. Effect of the overall concentration C_M on the rheological behaviour of the EHAC/hm-chitosan mixtures

We have investigated the effect of the overall concentration C_M on the rheological behaviour of two mixtures having compositions equal to R=0.43 and R=0.2, that is in the range of maximum of synergy. We have performed both steady-state and oscillatory experiments.

IV.2.a. EHAC/hm-chitosan mixtures with R=0.43

Figure 17 shows the steady shear viscosity versus shear rate for hm-chitosan/EHAC mixtures at different overall concentrations C_M, from 0.35wt% to 2wt%. As expected, the viscosity of the mixture increases with the overall concentration. For the lowest C_M values (0.35wt% and 0.7wt%), a Newtonian plateau is observed for the lowest shear rate, followed by a shear thinning behaviour above a certain shear. For the highest concentrations (1wt% and 2wt%), the Newtonian plateau is outside the shear rate range of the rheometer. The shear-thinning regime is again characterized by a bimodal shape. The representation $\eta = f(\sigma)$ is given in Fig.18. For the two lowest overall concentrations C_M (0.35wt% and 0.7wt%), two inflection points appear in the flow curves, similar to the findings of Jenkins and coworkers[51-54]. At higher concentrations, one observes a much steeper drop of the viscosity, followed by a small plateau then by a second shear thinning regime. These results once again indicate that the behaviour of the mixtures under shear is complex, due probably to some successive rearrangements of the transient physical network. The two sharp drops of the viscosity observed in the flow curves, whose steepness depends on the mixture composition, might correspond to the breaking of different kinds of associations (polymer/polymer, or polymer/VES). The shear rates at which the sharp drops in the viscosity occur increase with the overall concentration C_M.

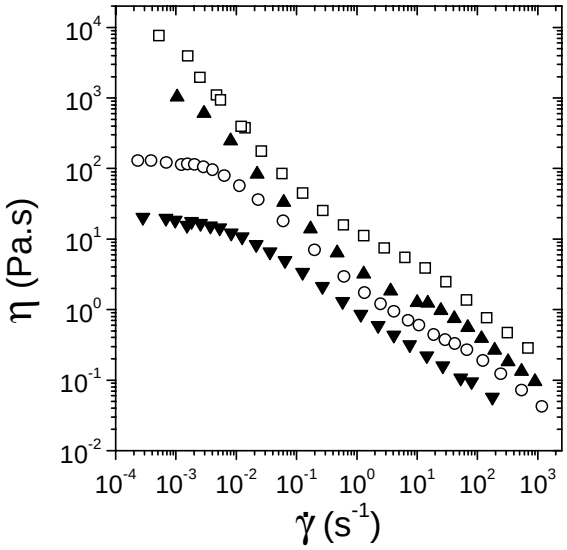

Figure 17: *Variations of the steady-state shear viscosity vs shear rate for different C_M values (□ C_M =2wt%, ▲ C_M =1wt%, ○ C_M =0.7wt%, ▼ C_M =0.35wt%) with R=0.43 at 25℃*

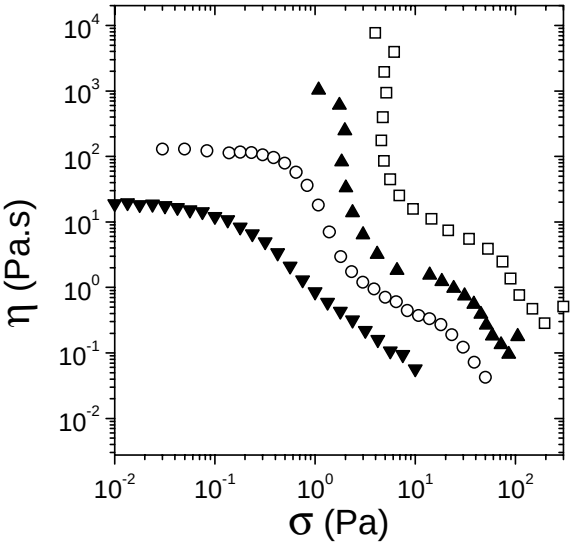

Figure 18: *Variations of the steady-state shear viscosity vs shear stress for different C_M values (□ C_M =2wt%, ▲ C_M =1wt%, ○ C_M =0.7wt%, ▼ C_M =0.35wt%) with R=0.43 at 25℃*

Oscillatory flow measurements were conducted on the same solutions. In Figs.19-22 are reported the steady-state viscosity $\eta(\dot{\gamma})$ and the dynamic complex viscosity $\eta^*(\omega)$ as functions of shear-rate or frequency. According to the the Cox-Merz rule[55], these two functions were found to coincide for entangled solutions of polymers. In the present case, the $\eta(\dot{\gamma})$ and $\eta^*(\omega)$ curves coincide only in the Newtonian regime. In the shear thinning regime, significant deviations occur. Such deviations were also observed for viscoelastic surfactant systems and were attributed to the occurrence of a shear banding instability and/or an isotropic nematic transition induced by the flow[56]. A deviation from the Cox–Merz rule has also previously been observed with HASE polymers in aqueous medium which was ascribed to the formation of shear-induced structures[57,58]. Tanaka and Edwards were able to predict the unusual deviation from the Cox-Merz rule behaviour, using a transient network theory[59].

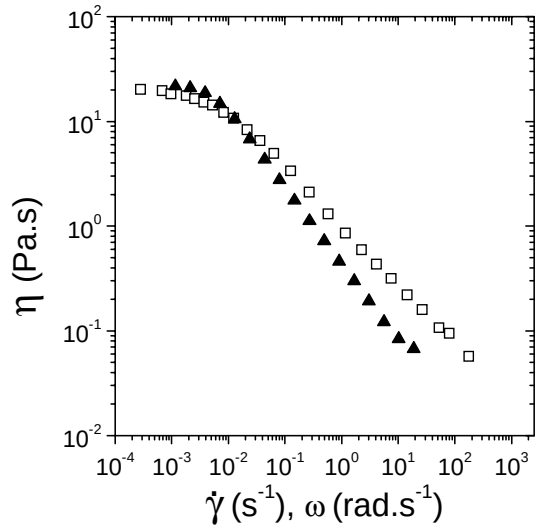

Figure 19: *Variations of the steady state shear viscosity η vs shear rate (□) and of the magnitude of the complex viscosity η^* vs the angular frequency (▲) for C_M = 0.35wt%, with R=0.43 at 25°C.*

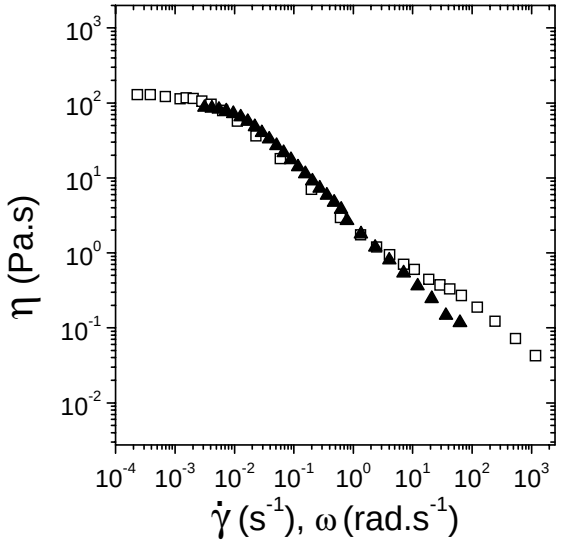

Figure 20: *Variations of the steady state shear viscosity η vs shear rate (□) and of the magnitude of the complex viscosity η^* vs the angular frequency (▲) for C_M = 0.7wt%, with R=0.43 at 25℃.*

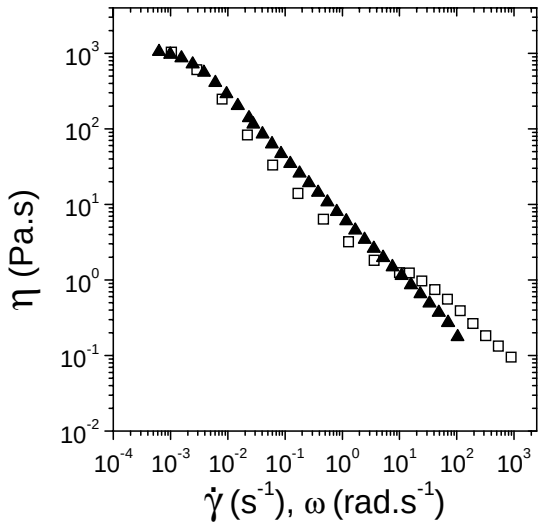

Figure 21: *Variations of the steady state shear viscosity η vs shear rate (□) and of the magnitude of the complex viscosity η^* vs the angular frequency (▲) for C_M = 1wt%, with R=0.43 at 25℃.*

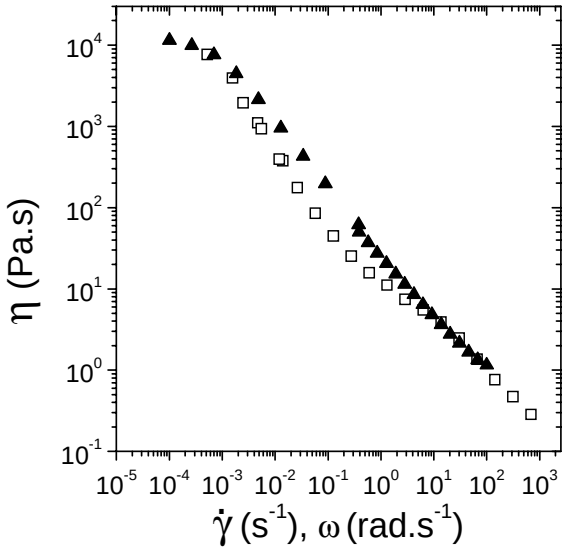

Figure 22: *Variations of the steady state shear viscosity η vs shear rate (□) and of the magnitude of the complex viscosity η^* vs the angular frequency (▲) for C_M = 2wt%, with R=0.43 at 25°C.*

In Fig.23 are represented the variation of the zero-shear complex viscosity as well as the variation of the low shear rate (10^{-3} s^{-1}) steady-shear viscosity as a function of the overall concentration C_M. The obtained values are in satisfactory agreement.

The mixtures maintain a viscosity at least 10000 times higher than that of water even at the overall concentration C_M=0.35wt%, that is just above the overlap concentration of the hm-chitosan (0.2wt%). The concentration dependence of the viscosity follows a power law with an exponent of the order of 3.5 that is much lower than that observed for the pure chitosan and the hm-chitosan solutions (5.5) (see paragraph III) but closer to the values obtained for both associating and non-associating flexible polymers (~4)[41,60,61].

Even at high shear rate ($100s^{-1}$), the viscosity of the mixture is at least 80 times higher than that of water, even at very low overall concentration, and keeps increasing with C_M (cf. Fig.24).

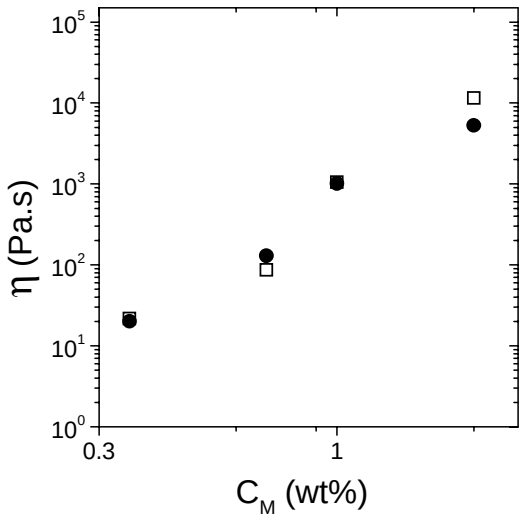

Figure 23: *Variations of the zero-shear complex viscosity (□) and low shear rate viscosity ($10^{-3}s^{-1}$) (●) vs C_M values for R=0.43 at 25 ℃.*

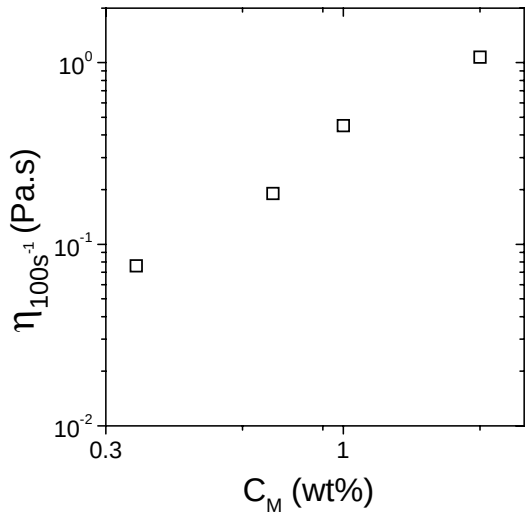

Figure 24: *Variation of the high shear rate viscosity vs C_M values for R=0.43 at 25 ℃.*

Rheological experiments performed in the oscillatory linear regime allow the determination of the frequency dependences of the storage (G') and loss (G'') moduli. Typical variations for mixtures at various overall concentrations, from 0.35wt% to 2wt%, and with R=0.43 are represented in Figs.25-28. One observes qualitatively the same behaviour in the whole concentration range, that is a crossing of the $G'(\omega)$ and $G''(\omega)$ curves and a more or less marked dip at high frequency depending on the value of C_M. A well defined plateau modulus G_0 at high frequencies cannot be observed, as was the case with the EHAC/hm-HPG systems. This may be associated with a higher polydispersity of the chitosan sample.

Values of $G_0 = 2G''_{max}$ are reported in Table 2. The terminal relaxation time T_R, determined from the crossing point of the curves $G'(\omega)$ and $G''(\omega)$, according to $\omega_{max}T_R$ =1, exhibits a minimum for C_M=0.7wt% (Table 2). The minimum which is observed for G'' at the circular frequency ω_m (Figs.25-28) corresponds to the crossover between the reptation controlled stress relaxation and the Rouse modes (cf. Chap.III). Its location goes through a maximum at C_M=0.7wt%. Such a non monotonic behaviour reflects the complex interplay of the concentration and composition effects in the mixtures. However, it must be noted that the values of T_R determined from the relation $\omega_{max}T_R$ =1, do not correspond to the terminal relaxation time because of polydispersity effects. Also, the characteristic frequency ω_m is not well defined, considering the smoother shape of $G'(\omega)$ and $G''(\omega)$ as compared to that of the EHAC/hm-HPG system.

On the other hand, the plateau modulus increases monotonically with the concentration, according to a polymer law with exponent close to the theoretical value of entangled polymers ($G_0 \sim C^{9/4}$)[61] *(Fig.29).*

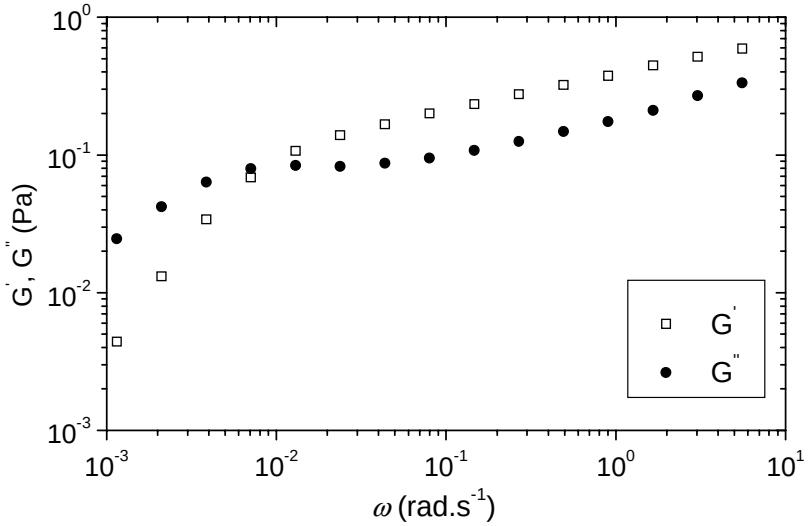

Figure 25: *Storage ($G^{'}$) and loss ($G^{''}$) moduli as a function of frequency for C_M=0.35 wt%, R=0.43, at 25 ℃.*

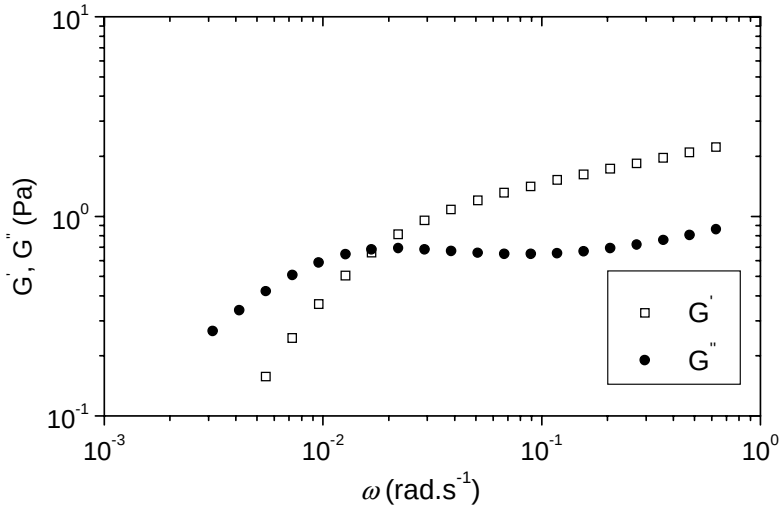

Figure 26: *Storage ($G^{'}$) and loss ($G^{''}$) moduli as a function of frequency for C_M=0.7 wt%, R=0.43, at 25 ℃.*

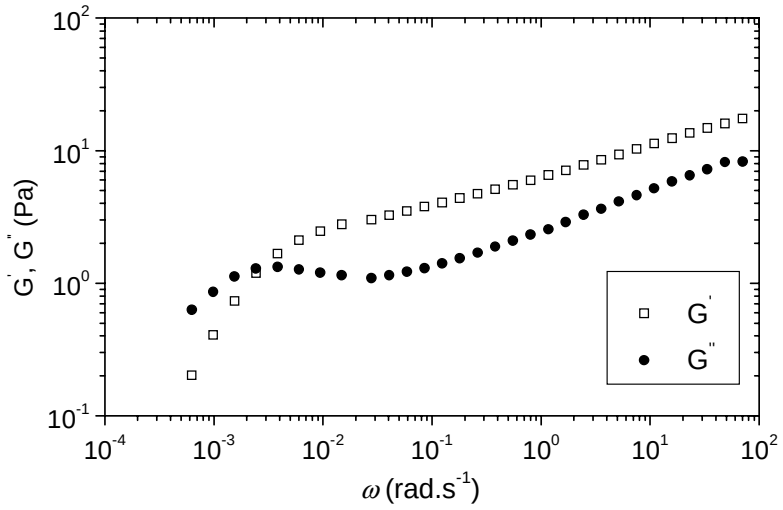

Figure 27: *Storage ($G^{'}$) and loss ($G^{''}$) moduli as a function of frequency for C_M=1 wt%, R=0.43, at 25 ℃.*

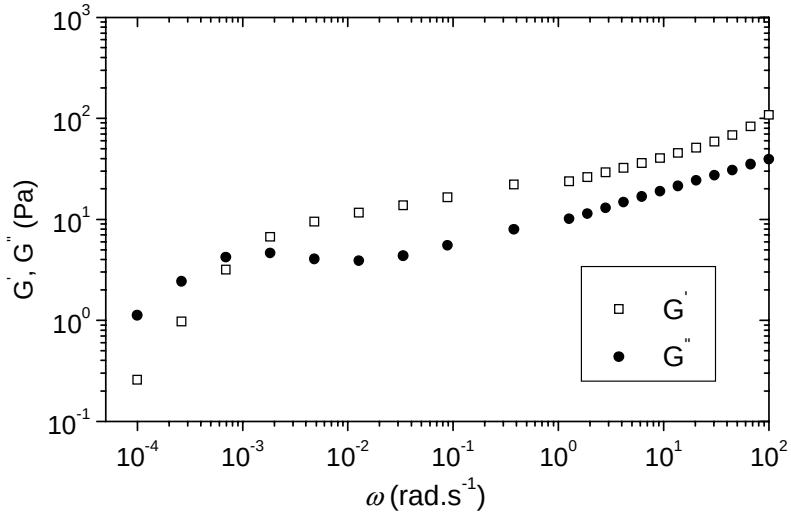

Figure 28: *Storage ($G^{'}$) and loss ($G^{''}$) moduli as a function of frequency for C_M=2 wt%, R=0.43, at 25 ℃.*

C_M	0.35wt%	0.7wt%	1wt%	2wt%
T_R (s)	121	60	380	983
ω_m (rad.s^{-1})	0.024	0.060	0.020	0.0127
$G_0=2G''_{max}$ (Pa)	0.16	1.362	2.64	8.82

Table 2: *Effect of the overall concentration C_M of the mixture on the terminal relaxation time T_R, the dip location ω_m and the modulus at the crossing point for solutions with a ratio R=0.43.*

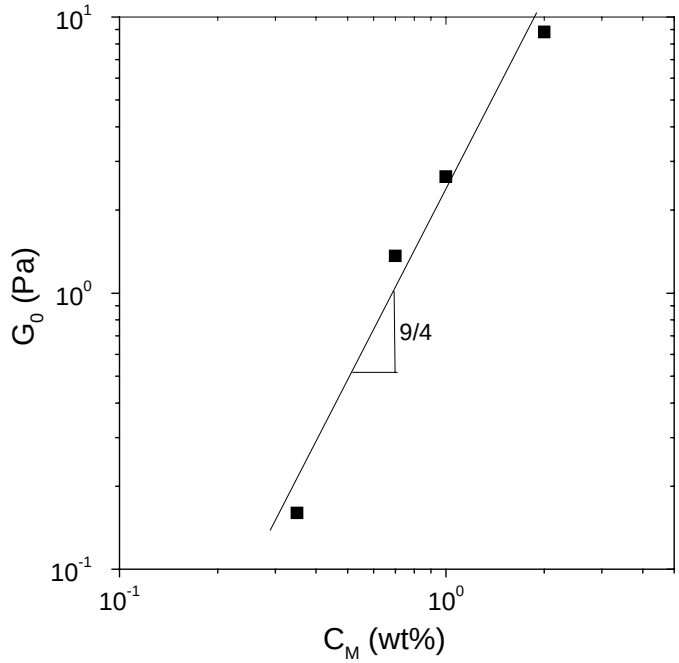

Figure 29: *Modulus G_0 versus C_M for systems with R=0.43.*

IV.2.b. EHAC/hm-chitosan mixtures with R=0.2

Figure 30 shows the steady shear viscosity versus shear rate for hm-chitosan/EHAC mixtures at different overall concentrations C_M, from 0.35wt% to 2wt%. Again, an increase of viscosity is observed with the overall concentration C_M. The flow curves of Fig.30 plotted in the representation $\eta = f(\sigma)$ (Fig.31) present a well-pronounced sharp drop of viscosity at a shear stress σ_c that increases with the overall concentration C_M.

The low shear viscosity and the high shear viscosity obtained for R=0.43 and R=0.2 (that is in the range of optimal synergy) versus the overall concentration C_M are reported in Figs.32 and 33. The overall variations follow the same trend for both R=0.2 and R=0.43. Moreover, the zero-shear viscosity of the mixtures is much larger than that of the hm-chitosan solutions (R=0) in the whole concentration range. However, the viscosity ratio $\eta_{0\ \text{mixture}}/\eta_{0\ \text{hm-chitosan}}$ tends to decrease upon increasing the overall concentration, indicating a progressive decrease of the synergy. The same behaviour was observed for the hm-HPG based mixtures (cf. Chap.III).

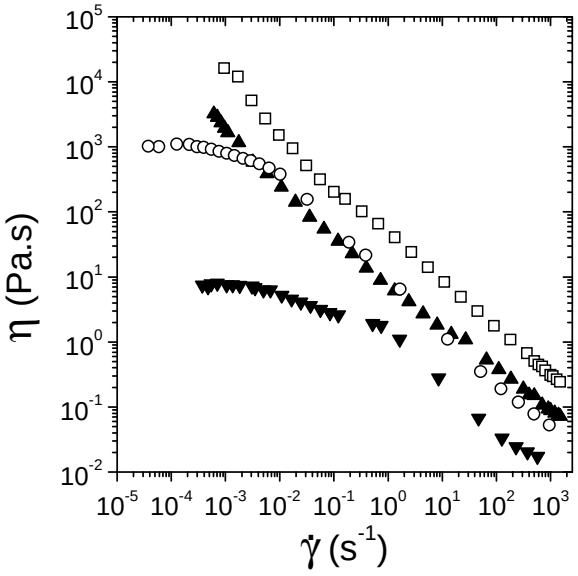

Figure 30: *Variations of the steady-state shear viscosity vs shear rate for different C_M values (□ C_M =2wt%, ▲ C_M =1wt%, ○ C_M =0.7wt%, ▼ C_M =0.35wt%) with R=0.2 at 25℃*

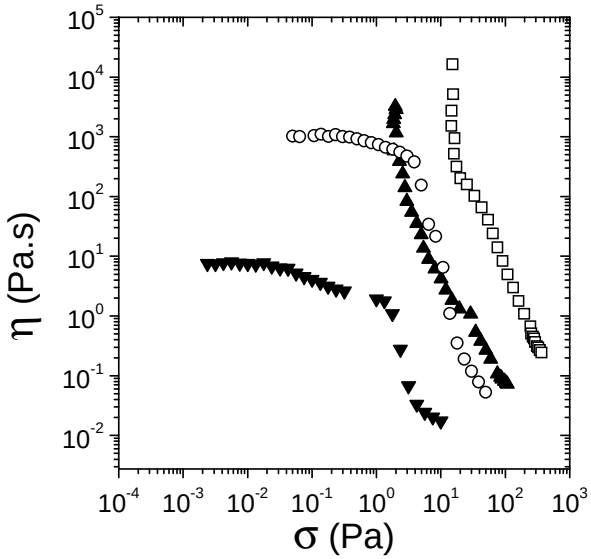

Figure 31: *Variations of the steady-state shear viscosity vs shear stress for different C_M values (□ C_M =2wt%, ▲ C_M =1wt%, ○ C_M =0.7wt%, ▼ C_M =0.35wt%) with R=0.2 at 25℃*

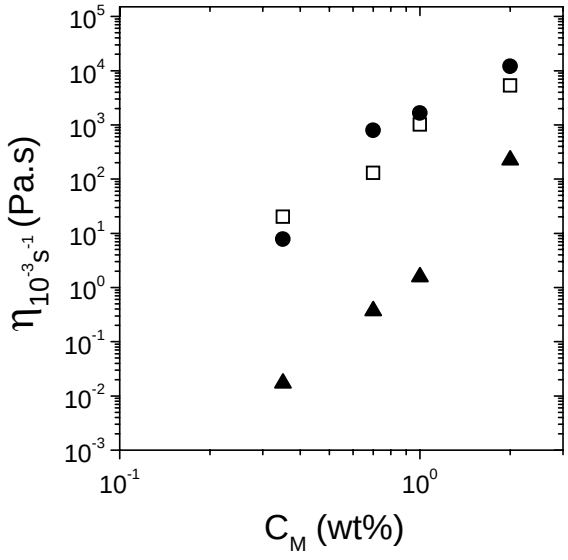

Figure 32: *Variations of the low shear rate viscosity ($10^{-3}s^{-1}$) vs C_M for R=0.43 (□), R=0.2 (●) and R=0 (▲), at 25℃.*

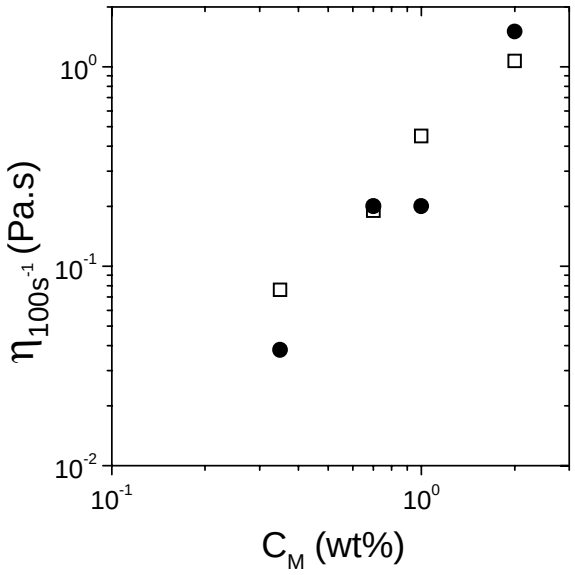

Figure 33: *Variations of the high shear rate viscosity ($100s^{-1}$) vs C_M for R=0.43 (□) and R=0.2 (●), at 25°C.*

CONCLUSION

This study has allowed us to show the generality of the synergistic effect that occurs in mixtures of hydrophobically modified polymers and wormlike micelles. This conclusion is also supported by another recent report on EHAC/hm-polyacrylamide[62].

The synergy is optimal for a composition range $0.2 \leq R \leq 0.43$, which corresponds to systems containing about 70-80% (in wt%) of hm-polymer. The synergy is maintained upon increasing the concentration at least up to an overall concentration C_M=2wt%, but tends to vanish at high concentration as in the case of the EHAC/hm-HPG mixture.

The comparison between the results obtained for the EHAC/hm-HPG and EHAC/hm-chitosan mixtures respectively shows that the latter is more efficient to enhance the zero-shear viscosity, as shown by a larger ratio of the zero-shear viscosity $\eta_{0\ \text{mixture}}/\eta_{0\ \text{hm-polymer}}$ at the optimal composition. Nevertheless, the zero-shear viscosity at the maximum is lower than that of the EHAC/hm-HPG system. These results are quite important from an applicative point of view, as discussed before.

The shapes of the flow curves of most of the mixtures indicate a complex rheological behaviour with two characteristic critical shear rates, probably reflecting successive rearrangements of the transient physical network under shear.

Contrary to the commercialised hm-HPG, the hm-chitosan was synthesized from a chitosan precursor, thus providing a large number of degrees of freedom regarding the choice of the length of the hydrophobic chain as well as its concentration. In this work, we did not study the interplay between these parameters and we only investigated the C_{11} n-alkyl-chitosan having a concentration of 5% molar alkyl chains. Various options remain open for further investigations of these complex systems and to optimize, from an applications point of view, the properties of the mixtures.

REFERENCES

(1) Rinaudo, M.; Pavlov, G.; Desbrieres, J. *Polymer* **1999**, *40*, 7029.

(2) Rinaudo, M.; Pavlov, G.; Desbrieres, J. *Int. J. Polym. Anal. Charact.* **1999**, *5*, 267.

(3) Rha, C. K.; Rodriguez-Sanchez, D.; Kienzle-Sterzer, C. in *Biotechnology of Marine Polysaccharides*, Eds.: Colwell, R.R.; Parisier, E.R.; Sinskey, A.J.; Washington, DC: Hemophere **1984**, p.283.

(4) Hirano, H. in *Chitin and Chitosan*, Eds.: Skjak Braek, G.; Anthonsen, T.; Sandford, P.; Essex: Elsevier **1989**, p.37.

(5) Tasi, G. J.; Su, W. H. *J. Food Protect* **1999**, *62*, 239.

(6) *Chitin Chemistry*, Ed.: Roberts, G. A. F.; London: MacMillan **1986**.

(7) Knorr, D. *Food Technol.* **1991**, *45*, 114.

(8) Sandford, P. A.; Hutchings, G.P., *Industrial Polysaccharides Genetic Engineering, Structure/Property Relations and Applications.* Ed.: Yalpani, M.;. Amsterdam: Elsevier **1987**, p.363.

(9) Mi, F. L.; Her, N. L.; Kaun, C. Y.; Wong, T.; Shyu, S. *J. Appl. Polym. Sci.* **1997**, *66*, 2495.

(10) *Encyclopedia of Polymer Science and Engineering*, Eds.: Mark, H. F.; Bikales, N. M.; Overberger, C. G.; Menges, G., John Wiley and Sons, N.Y., **1985**, *1*, 20.

(11) Hirano, H. in *Chitin and Chitosan*, Eds.: Skjak Braek, G.; Anthonsen, T.; Sandford, P.; Essex: Elsevier **1989**, p.713.

(12) Dutta, P. K.; Ravi Kumar, M. N. V. in *Textile Industries: Safety, Health and Environment.* Eds.: Trivedy, R.K.; Advance in Wastewater Treatment Technologies. India: Global Science **1998**, p.229.

(13) Buhler, E.; Guetta, O.; Rinaudo, M. *Int. J. Polym. Anal. Charact.* **2000**, *6*, 155.

(14) Brugnerotto, J.; Desbrieres, J.; Roberts, G.; Rinaudo, M. *Polymer* **2001**, *42*, 9921.

(15) Schatz, C.; Viton, C.; Delair, T.; Pichot, C.; Domard, A. *Biomacromolecules* **2003**, *3*, 641.

(16) Anthonsen, M. W.; Varum, K. M.; Smidsrod, O. *Carbohydr. Polym.* **1993**, *22*, 00.

(17) Wang, W.; Bo, S.; Li, S.; Qin, W. *J. Biol. Macromol.* **1991**, *13*, 281.

(18) Brugnerotto, J.; Desbrieres, J.; Heux, L.; Mazeau, K.; Rinaudo, M. *Macromol. Symp.* **2001**, *168*, 1.

(19) Berth, G.; Dautzenberg, H.; Peter, M. G. *Carbohydr. Polym.* **1998**, *36*, 205.

(20) Berth, G.; Dautzenberg, H. *Carbohydr. Polym.* **2002**, *47*, 39.

(21) Terbojevich, M.; Cosani, A.; Conio, G.; Marsano, E.; Bianchi, E. *Carbohydr. Res.* **1991**, *209*, 251.

(22) Desbrieres, J.; Martinez, C.; Rinaudo, M. *International Journal of Biological Macromolecules* **1996**, *19*, 21.

(23) Holme, K. R.; Hall, L. D. *Macromolecules* **1991**, *24*, 3828.

(24) Yalpani, M.; Hall, L. D. *Macromolecules* **1984**, *17*, 272.

(25) Desbrieres, J.; Rinaudo, M.; Chtcheglova, L. *Macromol. Symp.* **1997**, *113*, 135.

(26) Desbrieres, J. *Polymer* **2004**, *45*, 3285.

(27) Philippova, O. E.; Volkov, E. V.; Sitnikova, N. L.; Khokhlov, A. R.; Desbrieres, J.; Rinaudo, M. *Biomacromolecules* **2001**, *2*, 483.

(28) Esquenet, C.; Buhler, E. *Macromolecules* **2001**, *34*, 5287.

(29) Esquenet, C.; Terech, P.; Boue, F.; Buhler, E. *Langmuir* **2004**, *20*, 3583.

(30) Aubry, T.; Moan, M. *J. Rheol.* **1994**, *38*, 1681.

(31) Kjoniksen, A.-L.; Nystrom, B.; Iversen, C.; Nazkken, T.; Palmgren, O.; Tande, T. *Langmuir* **1997**, *13*, 4948.

(32) Nystrom, B.; Kjoniksen, A.-L.; Iversen, C. *Advances in Colloid and Interface Science* **1999**, *79*, 81.

(33) Iversen, C.; Kjoniksen, A.-L.; Nystrom, B.; Nazkken, T.; Palmgren, O.; Tande, T. *Polym. Bull* **1997**, *39*, 747.

(34) Lauten, R. A.; Marstokk, O.; Kjoniksen, A.-L.; Nystrom, B. *Polym. Bull* **2002**, *49*, 281.

(35) Lee, J.-H.; Gustin, J. P.; Chen, T.; Payne, G. F.; Raghavan, S. R. *Langmuir* **2005**, *21*, 26.

(36) Rinaudo, M.; Le Dung, P.; Gey, C.; Milas, M. *Int. J. Biol. Macromol.* **1992**, *14*, 121.

(37) Tanford, C. *Physical Chemistry of Macromolecules*, Ed.: Wiley, N.Y., **1961**.

(38) *Introduction to Polymers*, Eds.: Young, R. J.; Lovell, P. A.; Chapman and Hall: New York **1991**.

(39) Kulicke, W. M., *Unusual Instability Effects Observed in Ionic and Non-Ionic Water-Soluble Polymers*, Makromol. Chem. Macromol. Symp. **1986**, 2, p.137.

(40) Caulfield, M. J.; Qiao, G. G.; Solomon, D. H. *Chem. Rev.* **2002**, *102*, 3067.

(41) Graessley, W. W. *Polymer* **1980**, *21*, 258.

(42) Colby, R. H.; Rubinstein, M.; Daoud, M. *J. Phys. II (Paris)* **1994**, *4*, 1299.

(43) Adam, M.; Lairez, D.; Raspaud, E. *J. Phys. II France* **1992**, *2*, 2067.

(44) Kavassalis, T. A.; Noolandi, J. *Phys. Rev. Lett.* **1987**, *59*, 2674.

(45) Cheng, Y.; Prud'homme, R. K.; Chik, J.; Rau, D. C. *Macromolecules* **2002**, *35*, 10155.

(46) Desbrieres, J. *Biomacromolecules* **2002**, *3*, 342.

(47) Amiji, M. M. *Carbohydr. Polym.* **1995**, *26*, 211.

(48) Anthonsen, M. W.; Varum, K. M.; Hermansson, A. M.; Smidsrod, O.; Brant, D. A. *Carbohydr. Polym.* **1994**, *25*, 13.

(49) Buhler, E.; Rinaudo, M. *Macromolecules* **2000**, *33*, 2098.

(50) Wu, C.; Zhou, S.; Wang, W. *Biopolymers* **1995**, *35*, 385.

(51) Tam, K. C.; Jenkins, R. D.; Winnik, M. A.; Basset, D. R. *Macromolecules* **1998**, *31*, 4149.

(52) Tirtaatmadja, V.; Tam, K. C.; Jenkins, R. D. *Macromolecules* **1997**, *30*, 1426.

(53) Tirtaatmadja, V.; Tam, K. C.; Jenkins, R. D. *Macromolecules* **1997**, *30*, 3271.

(54) Seng, W. P.; Tam, K. C.; Jenkins, R. D. *Colloids Surf. A* **1999**, *154*, 365.

(55) Cox, W. P.; Merz, E. H. *J. Polym. Sci.* **1958**, *28*, 619-622.

(56) Berret, J. F.; Roux, D. C.; Porte, G. *J. Phys. II France* **1994**, *4*, 1261.

(57) English, R. J.; Gulati, H. S.; Jenkins, R. D.; Khan, S. A. *J. Rheol.* **1997**, *41*, 427.

(58) English, R. J.; Raghavan, S. R.; Jenkins, R. D.; Khan, S. A. *J. Rheol.* **1999**, *43*, 1175.

(59) Tanaka, F.; Edwards, S. F. *J. Non-Newtonian Fluid Mech* **1992**, *43*, 247.

(60) Jimenez-Regalado, E. J.; Selb, J.; Candau, F. *Macromolecules* **1999**, *32*, 8580.

(61) de Gennes, P. G. *Scaling Concepts in Polymer Physics*, Cornell University Press, London **1979**.

(62) Shashkina, J. A.; Philippova, O. E.; Zaroslov, Y. D.; Khokhlov, A. R.; Pryakhina, T. A.; Blagodatskikh, I. V. *Langmuir* **2005**, *21*, 1524.

GENERAL CONCLUSION

This work was focused on the determination of the structural and dynamic properties of two hydrophobically modified natural polymers, one having a low molecular weight, the other having a much higher one, a viscoelastic surfactant and more specifically mixtures of both types of components. The aim was to develop a greater in-depth understanding, at the molecular level, of the interactions between the hydrophobic groups on the polymer and the surfactant micelles and of the blend structure in order to help the formulation of a "hm-polymer/VES based fracturing fluid". This should have a greater ability than existing fluids to meet, at a low cost, the required characteristics: having a sufficient viscosity, having the ability not to enter too easily the pore throats of the subterranean formation so creating minimal damage to its permeability.

We first investigated the structural and dynamic properties of the micellar solutions of a cationic surfactant that has been shown to form efficient fracturing fluids, the erucyl bis-(hydroxyethyl)methylammonium chloride (EHAC), blended with 2-propanol in the presence of KCl, using light scattering and rheological experimental techniques. This surfactant is particularly interesting from an applications point of view as it has the property to self-assemble into giant wormlike micelles in the presence of salt, at very low concentration, giving rise to highly viscoelastic fluids in comparison with other conventional viscoelastic surfactants.

The viscoelastic data of EHAC performed in the linear regime, at high salt concentrations and at various temperatures, were analysed by means of three independent methods of measurement of its scission energy, using all the features of the complex shear modulus spectrum, including the Rouse modes. An inconsistency between the high value of the E_{sciss} determined by Raghavan and Kaler[1] and the lower values obtained in our study was explained by considering that the free energy of scission could contain a large entropic term, possibly associated with the rearrangement of counterions upon formation of an end-cap[2,3].

A light scattering study of the micellar growth induced by an increase of surfactant concentration was done comparing for the first time, quantitatively, the experimentally measured concentration dependence of the radius of gyration of the micelles with the mean-field and scaling models derived for linear micelles. The presence of large

aggregates, possibly rings or microgels, in the vicinity of C^* was concluded, as already observed for low-ionic strength micellar solutions of surfactants with a large scission energy[4,5].

The comparison between the zero-shear viscosity behaviours of the non-modified hydroxypropyl guar (HPG) and the corresponding hydrophobically modified hydroxypropyl guar (hm-HPG) shows a decrease of the intermolecular associations upon increasing the temperature.

The study of the linear and non-linear rheological properties of aqueous solutions containing both wormlike micelles of the EHAC surfactant and the hm-HPG polymer revealed a strong synergistic effect between both components at an overall concentration extending from 0.07wt% to 1wt%. This synergistic behaviour is the signature of strong interactions between EHAC wormlike micelles and hm-HPG associating chains. These interactions were confirmed by the fact that the increase of the zero-shear viscosity occurs at an overall concentration of the order of C^*_{EHAC} and, depending on the temperature, smaller or equal to $C^*_{\text{hm-HPG}}$. The synergistic effect is maintained at temperatures up to 60°C, and despite its shear dependency, sufficient viscosity from the applications point of view can be maintained up to a shear rate of $100s^{-1}$.

The combination of linear and non-linear rheological measurements allowed us to show that the synergy results from an increase of the lifetime of the crosslinks, which suggests the formation of crosslinks between the micelles and the polymer chains. A maximum of the viscosity is observed for a certain composition of the mixture, when the polymer concentration roughly represents 70-80% by mass of the overall mixture concentration. This result is particularly interesting from an applications point of view as the cost of the VES is 1.25 times higher than that of the polymer on a mass basis. Moreover, this maximum is independent of temperature and is still found at a shear rate of $100s^{-1}$.

No model has been developed to describe the non-linear flow behaviour of hydrophobically modified polymers. Both our results on the hm-HPG behaviour and those of Aubry and Moan show the existence of an intermediate regime between the Newtonian one and the shear stress plateau, probably associated with stretching and orientation of the chains[6]. The shear stress plateau might still be the signature of a shear

banding instability. In order for the instability to occur, the crosslinks between the associative units must be broken, and therefore the limiting step in the process will be controlled by the lifetime of the junction points, in agreement with the conclusions of Aubry and Moan[6]. The non-linear rheology of the mixtures of EHAC and hm-HPG systems presents qualitatively the same features as those of hm-HPG polymers alone.

The likely interaction mechanism between micelles and associating polymers might be the formation of an interpenetrating network of wormlike micelles and hydrophobically modified chains where most of the polymer hydrophobic sequences are embedded within the wormlike micelles. Possibly some binary (or multiple) crosslinks are still present and also some free "stickers". So in the entangled state the polymer motion, that is reasonably described by the sticky reptation model[7,8] ,is somewhat hindered by the residence time of the sticker within the micelle, which is likely to depend on the micelle lifetime.

A lesser or suppressed synergy was observed at high concentrations or at high temperature. In the high concentration regime, the density of crosslinks between the stickers might increase. The effect of these crosslinks possibly overcomes that of the stickers embedded in the micelle. Also, there may be some intermicellar branching that reduces the viscosity[9]. At high temperature, the micelles become much shorter. Therefore, the contribution to the viscosity from the wormlike micelles is decreased. Moreover, at high temperature, the micelles might become short enough to the point where they stop being efficient bridges between the polymer chains. In this limit, the surfactant will only decorate the hydrophobic sequences and the viscoelastic behaviour should tend to that of the unmodified polymer at the concentration of the modified polymer in the mixture.

The study presented in the last chapter on the rheological behaviour of the non-modified chitosan showed the classical behaviour of conventional polymers. Nevertheless, a difference was observed in the abnormally high value of the exponent of the dependence of the zero-shear viscosity η_0 on the polymer concentration, as already shown by other authors[10-12]. This effect may be related to the occurrence of specific interchain interactions leading to the formation of aggregates[13]. The rheological behaviour of the modified chitosan is similar to that observed with the hm-HPG.

The study on the linear and non-linear rheological properties of aqueous solutions of hm-chitosan and its mixture with erucyl bis-(hydroxyethyl)methylammonium chloride (EHAC) surfactant, has demonstrated the generality of the synergistic effects that exist in mixtures of hydrophobically modified polymers and wormlike micelles. Once again, a maximum of the synergy is observed for the same composition of the mixture, when the polymer concentration roughly represents 70-80% of the overall mixture concentration. The mixture composition at the maximum is independent of the overall concentration.
The synergy observed between EHAC surfactant and hm-chitosan appears to be stronger than that observed with hm-HPG. This is revealed by the larger amplitude of the maximum in the zero-shear viscosity. Nevertheless, the zero-shear viscosity at the maximum is lower than that measured for the EHAC/hm-HPG system.These results are quite important from an applications point of view. The choice of the system will be eventually dictated by the concern of the damaging produced in the formation by a high molecular weight polymer and the cost of the product.

The shapes of the flow curves of most of the mixtures have indicated that the behaviour of the mixtures under shear is really complex due probably to some successive rearrangements of the transient physical network. This is an area that carried benefit from further studies, linking rheological and structural characterisation techniques.

Several issues concerning the fundamental properties of the hm-polymer/VES mixtures are still open. The schemes proposed to explain the rheological behaviour of these systems are rather qualitative and a real quantitative model describing the coupled flow of wormlike micelles and hydrophobically modified polymers is still lacking. Some other visualisation and structure probing techniques, such as neutron scattering and CryoTEM, could bring further useful information on the structural and dynamical properties of the blends.
However, the present study must be considered as a starting point for further investigations of such systems. This work has therefore given considerable insight into the bulk and microstructural behaviour of hm-polymer/VES mixtures. It has also provided good guidelines for the design of such fluids for industrial applications, such as

oilwell fracturing. A lot of other parameters still need to be evaluated to fully understand the interaction mechanisms, such as the length, distribution and concentration of the hydrophobic side-chain of the polymer. From an oilfield applications point of view, hm-polymer/VES mixtures have shown some really interesting advantages compared to the pure polymeric or pure VES systems and various options remain open to continue to investigate these complex systems and to optimize their properties for different uses.

REFERENCES

(1) Raghavan, S. R.; Kaler, E. *Langmuir* **2001**, *17*, 300.

(2) Oelschlaeger, C.; Waton, G.; Candau, S.J. *Langmuir* **2003**.

(3) Kern, F.; Zana, R.; Candau, S. J. *Langmuir* **1991**, *7*, 1344.

(4) Cates, M. E. *Macromolecules* **1987**, *20*, 2289.

(5) Cates, M. E. *J. Phys (Paris)* **1988**, *49*, 1593.

(6) Aubry, T.; Moan, M. *J. Rheol.* **1994**, *38*, 1681.

(7) Rubinstein, M.; Semenov, A. N. *Macromolecules* **1998**, 1386.

(8) Rubinstein, M.; Semenov, A. N. *Macromolecules* **2001**, *34*, 1058.

(9) Lequeux, F. *Europhys. Lett.* **1992**, *19*, 675.

(10) Amiji, M. M. *Carbohydr. Polym.* **1995**, *26*, 211.

(11) Anthonsen, M. W.; Varum, K. M.; Hermansson, A. M.; Smidsrod, O.; Brant, D. A. *Carbohydr. Polym.* **1994**, *25*, 13.

(12) Desbrieres, J. *Biomacromolecules* **2002**, *3*, 342.

(13) Philippova, O. E.; Volkov, E. V.; Sitnikova, N. L.; Khokhlov, A. R.; Desbrieres, J.; Rinaudo, M. *Biomacromolecules* **2001**, *2*, 483.